UNIVERSITY OF SOUTHAMPTON

FACULTY OF ENGINEERING AND APPLIED SCIENCE

Department of Electronics and Computer Science

A STUDY OF FEASIBILITY OF IMPLIMENTING A DIGITAL LOUDSPEAKER ARRAY

by

Sangchai Monkronthong

A thesis submitted in partial fulfilment for the degree of Doctor of Philosophy

3 May 2018

UNIVERSITY OF SOUTHAMPTON

ABSTRACT

FACULTY OF ENGINEERING AND APPLIED SCIENCE

Department of Electronics and Computer Science

Thesis for the degree of Doctor of Philosophy

A STUDY OF THE FEASIBILITY OF IMPLIMENTING A DIGITAL LOUDSPEAKER ARRAY

Sangchai Monkronthong

The common method in audio player for sound generation with a loudspeaker is driving analogue electrical signals while this thesis will study an alternative method for application of a loudspeaker with digital signals. This thesis found feasibility of driving loudspeaker with digital pulses according to the concept of Multiple-level Digital Loudspeaker Array (MDLA) and discovered generation of sound from ultrasound with potential.

The concept of a MDLA can be applied as an alternative method to produce Amplitude Modulation (AM) sound. The new concept extends from Digital Loudspeaker Array (DLA) by application of Pulse Width Modulation (PWM). By Application-Specific Integrated Circuit system (ASICs), the clock speed would reach 1 GHz. With the chip, DLA will require only 7 speaklets for the reproduction of 16 bit audio.

A novel concept of sound generation from ultrasound originates from the concept of AM sound of Audio Spotlight technology. The new concept applies mechanical amplitude demodulation for improvement in efficiency of sound generation.

A rectifying loudspeaker is introduced for sound generation according to the concept. The loudspeaker uses a secondary source as the main source of sound generation, while vibration of the primary source is applied for speed control of air particles like a valve. The structure of the loudspeaker is adapted from the human voice system and can be fabricated by MEMs

Table of Contents

List of Tables

List of Figures

DECLARATION OF AUTHORSHIP

I, Sangchai Monkronthong declare that this thesis and the work presented in it are my own and has been generated by me as the result of my own original research.

A Study of the Feasibility of Implementing a Digital Loudspeaker Array .....

.....

I confirm that:

1. This work was done wholly or mainly while in candidature for a research degree at this University;
2. Where any part of this thesis has previously been submitted for a degree or any other qualification at this University or any other institution, this has been clearly stated;
3. Where I have consulted the published work of others, this is always clearly attributed;
4. Where I have quoted from the work of others, the source is always given. With the exception of such quotations, this thesis is entirely my own work;
5. I have acknowledged all main sources of help;
6. Where the thesis is based on work done by myself jointly with others, I have made clear exactly what was done by others and what I have contributed myself;
7. Parts of this work have been published as:
    - Monkronthong, S. White, N and Harris, N. “Multiple-Level Digital Loudspeaker Array”, the 28th European Conference on Solid-State Transducers, September 2014
    - Monkronthong, S. White, N and Harris, N. “A study of efficient speaklet driving mechanisms for use in a digital loudspeaker array based on PZT actuators”, the Sensors Application Symposium 2016, April 2016.

Signed: .....

Date: .....

Acknowledgements

Working in this thesis impresses me like an adventure in an unknown world; the exploration of electronic men in the acoustic world. I unintentionally stepped into the route even acoustic people might be not familiar, which is called a transient-state wave propagation. However I, as a scout, discovered “the promised land, a land flowing milk and honey” Through the way in years of work, I have been accompanied and supported by many people. It is with pleasure that I now take this opportunity to express my gratitude for all of them.

This work would not have been possible without the aid and guidance of my supervisor team of Prof. Neil White and Dr. Nicholas Harris. I thank Prof. Neil White especially for introducing me to this interesting topic of Digital Loudspeaker Array. When I was faced with dilemmas of research approaches, they were friendly prompt to give directions, advises and supports.

I would like to express my gratitude for Dr. Filiopo Fazi, Associate Professor in Institute of Sound and Vibration Research (ISVR). These are great opportunities for me as an electronic student to meet him as an acoustic examiner. He gave valuable comments and encouragements for this research in the couple times of oral examination.

I would like to thank Dr. Khemapat Tontiwattanakul, who was an acoustic PhD student. He is my friend and personal acoustic advisor. He dedicated his precious times for me. He gave a brief lecture and demonstrated programming and conduct of experiments in an acoustic domain several times. I acknowledge him that he expertizes a basis of acoustics I require for this research.

I would like to thank Ministry of Science and Technology of Thai government and Naresuan University in Thailand for the provision of scholarship for study in University of Southampton through the years of working.

I would like to dedicate my work as a sacrificial offering to the king of kings, who reigns over all Thai people’s hearts.

Nomenclature

a	area constant
A	Cross-section Area of flow
A_n	A-weighing value at frequency n Hz
A_h	The area of the neck of diffuser
A_a	Amplitude of audio
A_c	Amplitude of carrier
A_{core}	Cross-section area of core
A_{gap}	Cross-section area of air gap
B	Adiabatic bulk modulus
B_d	The damping constant
B_c	Magnetic flux density
c	Sound speed
C_{PZT}	Capacitance of a transducer
C_{BL}	Constant of coil
C_L	The life force constant
C_{pipe}	Pile constant
C_{priton}	Constant of piston
D	Diameter
D_c	Directivity constant
D_{core}	Diameter of core
D_{gap}	Diameter of flux at the gap
D_{magnet}	Diameter of magnet
d_r	Delay path
e	Induced voltage
f	frequency

f_0	The fundamental resonant frequency
f_B	The inertial force of damping
f_e	The external force
f_k	The inertial force of spring
f_m	The inertial force of mass
f_n	The natural frequency
f_s	Sampling frequency
f_u	Frequency of ultrasound
f_{mag}	Magnetic force
f_a	Frequency of audio
f_{coil}	The force from coil
f_c	Frequency of carrier
f_l	Life force
F_{mmf}	Magnetomotive force
F_v	Force density
g	Gravity
g_{array}	Interspacing
h	Thickness of diaphragm
H_p	Height of pile
Hz	Hertz, unit of frequency, cycles per second
H_n	Number of speaklets in a column
i	current
i_{PZT}	Current feeding in a transducer
k	Wave number
k_h	The ratio of specific heats
km	kilometre

K_q	The charge output per unit displacement
K_s	The spring constant
l_{air}	Length of the air gap
l_{coil}	Length of coil
L	inductance
L_x	Beam width
M	Weight of Mass
N	Coil turn
N_{core}	Number of core
p	Acoustic pressure
$p_<$	Acoustic pressure of wave incidence
$p_>$	Acoustic pressure of wave reflection
p_{rad}	Acoustic pressure of wave radiation
p_{ref}	Threshold of hearing
p_{rms}	the mean-square pressure
p_m	The power at the terminal of the coil
P	Pressure constant or Flow pressure
P_{pump}	A constant pressure of the air pump
q	Electrical charge
Q	Volume flow rate
r	Radius of sound source
r_{shape}	Shape constant
r_{path}	Path index
R	Distance from source
R_0	Location of source
R^2	the coefficient of determination

R_h	The ideal gas constant equal to 287 J/kg*°K
R_L	Resistant of Load
R_{PZT}	Resistance of a transducer
R_{rad}	Radiation resistance
R_c	Resistance of coil
R_{gap}	Reluctance of air gap
R_{tot}	Total reluctance
S_e	The electric sensitivity
SPL_n	Sound Pressure Level at a frequency of n Hz
t	time
T	A period of a cycle of the wave
u	Velocity
v	voltage
V_{pp}	Peak-to-peak voltage
w	Displacement
$\dot{w}$	The first derivation of displacement
$\dot{w}_{avg}$	The average velocity
$\ddot{w}$	The second derivation of displacement
w_g	The displacement of the gap
W_n	Number of speaklets in a raw
$\dot{W}$	A constant amplitude
W_0	Distance between the core and the weight
W_p	Width of the electrical pulse
W_{per}	The perimeter of the disc
W_p	Width of pile
x	Distance of the transverse of the wave

X_{rad}	Radiation reactance
Y	Young's modulus
z	The specific acoustic impedance
z_1	A level of flow
Z	Acoustic impedance
Z_0	Acoustic impedance at x = 0
Z_{rad}	Radiation impedance
α	Spreading angle
β_x	Beam angle
ρ	Density
J	Current density
du/dy	Velocity gradient
δ	Damping ratio
θ	The elevation angle
λ	Wavelength
ν	Poison's ratio
ξ	Proportional damping
π	Pi constant, the ratio of circle's circumference to diameter
τ	Shear stress
φ	The azimuthal angle
ω	Angular frequency
ϕ	Flux
∂	Partial derivation
ω_n	Angular natural frequency
$\in_0$	The dielectric of free space
$\in_t$	The relative dielectric constant

λ_m	Flux linkage
ω_d	The damped natural frequency
ω_f	Angular frequency of the external force
°C	Celsius, a unit of temperature
°K	Kalvin, a unit of temperature
μ	Viscosity
δ_d	The damping ratio

Chapter 1: Overview of the Research

This chapter is written for the purpose of understanding the essence of the whole thesis, and gives a guideline for navigation throughout the main body of the thesis. Due to this thesis evolving multidisciplinary sciences, such as acoustics, MicroElectroMechanical system (MEMs), telecommunication and fluid mechanics, some of the work is based on empirical approaches.

1.1 Research Inspiration

The common method in audio players for sound generation with a loudspeaker is by driving analogue electrical signals, which have waveforms similar to the recorded sounds. This thesis will study an alternative method for application of a loudspeaker using digital signals, which merely have on and off modes. This concept was first introduced as Digital Loudspeaker Array (DLA) by Busbridge *et al* and Diamond *et al* [1][2]. A few groups in academia have been involved in this field since 2002 (more detail in the introduction of Chapter 2). Most acoustic scientists and engineers might believe that it is impossible for DLA to produce as high quality sound as an analogue loudspeaker. The problems will be clarified in Section 1.4.Although research into DLAs might not be common, the creative inspiration comes from belief in changing to the digital era. Audio players used to be fully analogue devices, such as cassette tapes, but in the present day, audio players are digital devices such as iPods and stereo players. All components within the audio players, such as recorded data, data processors and circuits, are digital, except for the loudspeakers. These still require a Digital to Analogue Convertor (DAC). If the player's system became fully digital, what would the characteristics of sound of the array be, and what gap in sound quality would there be between an analogue loudspeaker and DLA? In addition, there is capital investment for application on this concept based on MEMs such as Audiopixels[3] and Usound[4] companies although they keep their productions secret. DLA is of interest here, to explore the possibility of implementation.

1.2 Big Picture of Work

This thesis will explore the feasibility of the generation of sound from ultrasound by driving with digital pulses, according to the concept of DLA, as described in Chapter2.3. The concept of sound generation of DLA is similar to the parametric array in that these reproduce sound from ultrasound, but they differ in electrical inputs. Digital signals are fed into a DLA, while analogue signals are applied to a parametric array. How the sound is generated, and brief details of parametric arrays, are described in Chapter2.2.3.

There are three main questions in the exploration of the feasibility of the implementation of DLA according to digital sound reconstruction of Diamond *et al* [2].

1.2.1 "If an ideal speaklet (a tiny loudspeaker) for DLA did exist, what would the characteristics of sound of the array be?", found in Chapter 3.

An ideal speaklet is mathematically simulated with Matlab for demonstration of its wave propagation. The 'ideal speaklet' means the speaklet has characteristics according to the requirements of digital sound reconstruction stated by Diamond *et al*, described in Chapter 2.3.3. In addition, 'the ideal' means simplification in order to easily understand its behaviours, similar to the study of the ideal spring or ideal gas.

The vibration and radiation of the speaklets are modelled as a Mass-Spring Dumper (MSD) and a point source, respectively. The wave propagation is simulated by the transient-state wave equation, because speaklets in DLA are driven by short discrete pulses. The wave propagation is transient, different from the steady-state propagation where speaklets are driven by a continuous analogue signal. The steady-state propagation is different from the transient-state propagation at the waveform of vibration. The waveform in transient-state is $e^{-t(\delta+j\omega)}$, while the waveform in steady-state is $e^{-j(\omega t)}$. The wave equation for transient state is based on the Helmholz steady-state equation (more detail in Chapter 2.4.2).

The ideal condition for high efficiency in sound generation from ultrasound is achieved by the directly proportional relationship between the acoustic pressure (p) and the displacement (w) of the surface of the acoustic source (pαw) when the multiplication of the square between the wave number (k) and the radius of the source (r) is significantly greater than 1 ($(kr)^2>>1$).This means the displacement is directly proportional to the velocity (u) of particles (uαw), and the velocity is directly proportional to the acoustic pressure (pαu). This condition can be applied with a large ultrasonic source diameter while the usual condition (low frequency) is directly proportional between acoustic pressure (p) and the second derivative of the displacement ($\ddot{w}$) of particles at acoustic surface(pα$\ddot{w}$) (more detail about the mathematical model in Chapter3.2).

The ideal condition of a source results in high efficiency in sound reproduction from ultrasound, because the sound level of the ideal speaklet directly affects the level of audio wave from the mechanical demodulation of Amplitude Modulation (AM) ultrasound, rather than relying only on acoustic non-linearity of the air medium, which is referred as a phenomenon of beat frequency. The waveform of the ultrasound generated by the ideal DLA becomes the half-wave Rectified Amplitude Modulation, because the condition enables the speaklet to ideally generate ultrasound with half waves, which only has a compression stage in the wave cycle but does not have a

rarefaction stage as the usual longitudinal wave does. The waveform can be seen in the acoustic response figures in Chapter3.3.2 and 3.3.3.7, for example Figure 3-10. According to telecommunication principles, the AM wave is demodulated by a rectifier to extract the audio wave.

A great advantage of sound generation from ultrasound is efficiency in controlling sound in a small boundary due to ultrasound traversing in far shorter distance than sound wave. The rectified sound, which has high frequencies, can be more highly attenuated than a normal sound, which has low frequencies. For example, the difference of attenuation between 1 and 40 kHz is from 5 to 1300 dB/km at 70% relatively humidity, as shown in Appendix A. The height of attenuation enables DLA to control the boundary of sound coverage for a small area (3-4 m^2).

The way a DLA works is that a loudspeaker is physically divided into a number of tiny, independent loudspeakers. These speaklets within a DLA can produce different sounds or ultrasounds, which are combined into one voice (a meaningful sound), similar to a choir, where singers make different sounds for a song in harmony.

This thesis will demonstrate four schemes of pulse assignment by raising all speaklet pulses at the same time.

It was found that although the sound fields of the patterns are different, the voice and sound directivity of the array are almost the same. The behaviour of directivity is similar to that of a normal loudspeaker where sound beams are formed when the frequency of the sound is higher (more details in Chapter3.3.3).

1.2.2 "If DLAs are applied in a real speaklet, what will its characteristics of sound be?"

In Chapter 4, experiments were conducted in order to test how well the characteristics of speaklet samples satisfied the requirements of digital sound reconstruction, involving the first and third requirements of emitting time, as defined in Figure 2-25, and linearity. The second requirement of uniformity of speaklets is omitted because of dependence on fabrication.

- The frequency response of the speaklet is tested by the frequency-sweeping method as the major feature for indication of samples. The details of the tests for the ideal and real cases are in Chapter 3.3.1, 3.3.2, 4.1.2.1 and 4.1.3.
- It was found that the pressure responses of real speaklets can meet the third requirement, but cannot meet the first requirement. The pressure response of a speaklet is maximized when the pulse rate driving into the speaklet is equal to its natural frequency.

Experiment 4.1.4 demonstrates application of DLA on real speaklets. Three samples of speaklets consisted of

- a magnetic buzzer,
- a Lead Zirconate Titanate (PZT) buzzer and
- an ultrasonic transduce.

It was found that the waveform of pressure responses of the samples were AM, but due to their frequency response some of the waveforms were not consistent. The best case of sound generation in the experiment was a 40-kHz ultrasonic transducer applied with a pulse rate of 40 kHz, as shown in Figure 4-17 . The case is a validation of sound generation from ultrasound while in the other cases, AM waves are formed but they do not generate sound from ultrasound.

Therefore, real case diaphragm-based speaklets can generate AM sound, but they cannot generate sound with a half-wave RecAM waveform similar to the ideal case. As a consequence, the speaklets in the array is required to have a very high intensity of ultrasound (more than 100dBSPL) in order to generate sound with reasonable loudness.

Another negative fact about ultrasonic transducers producing sound is that their sound beam is very narrow, while a common requirement for a loudspeaker is that it has a wide beam. The ideal speaklets in DLA should be as small as possible in order to expand the beam width, while emitting ultrasound intensity high enough for the frequency beat. In reality it might be impossible for common loudspeakers because the size and the intensity of speaklets are a trade-off. The details about the design of PZT-based speaklets is in Chapter 4.2.

1.2.3 "If a speaklet will generate rectified AM sound, what should its structure be?"

From this problem of a great gap between the ideal and reality we come to the final question in Chapter 5. To begin with, the reason a diaphragm-based speaklet cannot generate a rectifying sound is because the displacement of a diaphragm in a wave cycle has positive and negative or moves forward and backward (for more detail see Chapter 5.1.1).

Therefore, a pressure supply is introduced into the loudspeaker in order to rectify movement and velocity of air particles, and reinforce acoustic pressure. The air flows are designed to collide and rapidly change in direction and magnitude of velocity. These cause sound generation (for more detail see Chapter 5.1.1.1).

An FEM model is created for demonstration of the relationship between the velocity at orifice and the displacement of diaphragm, when the displacement is predefined (for more detail see Chapter 5.1.2).

Although the velocity is approximately directly proportional to the displacement because the relationship is the unsteady-state flow, their audible frequency components are not distorted (for more detail see Chapter 0).

Evidence to show that the beam width of the loudspeaker is far wider than the traditional ultrasonic transmitter is the small diameter of the opening - in the order of microns - and the fact that the direction of the velocity spreads according to the angles of the diffuser.

In addition to the AM sound becoming rectified AM sound, the structure enables the loudspeaker to have features similar to the ideal speaklet, which has a tiny diameter and high intensity of sound. Therefore, the rectifying loudspeaker is a wide-beam ultrasonic transducer (for more detail see Chapter 5.1.4).

In conclusion, an abstract landscape of this thesis is illustrated to show the coherence of the work. The fundamental differences between DLA and a normal loudspeaker are clarified. The intellectual challenges in the design of a rectifying loudspeaker are presented.

1.3 Goals of Thesis

- To derive acoustic impulse response of the ideal rectified sound source to show that the source can generate the rectified AM sound;
- To simulate a MDLA with rectified sources from the mathematical derivation as speaklets to investigate its temporal, spatial and spectral acoustic output as well as directivity;
- To implement the MDLA concept on real electro-acoustic transducers and investigate its characteristics according to the requirements of digital reconstruction;
- To design a potential structure for the rectified source with FEM software and show that it can produce acoustic pressure in a form of the rectified AM signal.

1.4 Statement of Problems, Proposed Solutions and Their Outcome.

The statement of problems can be divided into three parts. Each part identifies a problem in the implementation of DLA, a solution is proposed to deal with the problem, and the result of the application of the solution is evaluated.

1.4.1 Sound Quality

Low bit quality of sound is produced by DLAs due to the restriction in the number of speaklets. Firstly, a desktop-based application of a DLA may have approximately 32-128 speaklets within the array. As a result, the application can reproduce the acoustics output at a quality of 5 to 7 bits, while traditional audio systems have a sound quality of 16 bits PCM at 44.1 KHz. Therefore, in order to reproduce the sound at the same quality, at least 65,532 speaklets are required, which may be too many for implementation. However, in this research, around 70 speaklets within a digital transducer array can produce sound at a mere 6 bits. As a consequence, there is a difference of 10 bits between the bit quality of the input (16 bits) and the output sound (6 bits). Therefore, it is clear that there is a wide gap of quality between the input and output sounds in the desktop-based application.

A possible way for alleviating this problem is to enable speaklets within the DLA to emit sound at multiple levels by applying pulses with different widths of pulse. A pulse width represents a specific level of sound. The concept is referred to as a Multiple-level Digital Loudspeaker Array (MDLA). Each speaklet can produce different levels of clicks (short pulses). For this method, the quality of sound output is improved by using the same number of speaklets although this method may lead to sound reconstruction due to diffenrence in acoustic pulse shape[2] . The number of levels a speaklet requires for each bit quality is shown in Table 3-1 (for more detail see Chapter 3.1).

Table 1-1: Numbers of levels are required in sound reproduction with different qualities of PCM bits for a 70-speaklet DLA.

Number of bits	Audio resolution per speaklet
8	5
10	16
12	60
14	236
16	937

From the results of simulation and experiment, we see that the resolution of the sound level increases dramatically from one to hundreds because of the linear relationship between the maximum pressure (defined in Figure 2-25) and the pulse width. Although the relationship is in

fact non-linear, within a certain range of widths it becomes linear. The range depends on a pulse period (inverse of pulse rate feeding to a speaklet) and the resolution is computed from the range of linearity divided by a clock period (inverse of clock speed of digital pulse generator). In the mathematical model, a speaklet has 937 levels, while the ultrasonic transducer in the experiment has 1000 levels, as shown in Table 1-2. The details are found in Chapter 3.3.1 and 4.1.3.4.2. Because the computational logics of the digital pulse generator do not demand extensive computation, if it is designed and fabricated by the Application-Specific Integrated Circuit system (ASICs) the clock speed would reach 1 GHz. With the chip, the DLA will require only 7 speaklets for the reproduction of 16-bit audio.

Table 1-2: Summary of parameters and resolution of a speaklet

Speaklet Type	Clock speed (MHz)	Range of linearity (µsec)	Pulse rate/ Natural frequency (kHz)	Resolution / R^2 coefficient	Number of speakers for 16 bits
Ideal speaklet	200	4.685	44.1/44.1	937/0.9917	70
Ultrasonic transducer	100	10	40/40	1000/0.9626	66

However, this leads to another problem, because it is challenging for an MDLA's reconstruction of sound, which originates from the superposition of acoustic responses with different shapes and response times (defined in Figure 2-25). It is found, though, that the response time is linearly related to the pulse width. A time shift can be pre-calculated from the linear equation of the relationship in order that the click reaches the maximum pressure at the same time for different shapes. From the results of this technique, the sound reconstruction improved slightly from R^2coefficient 0.9917 to 1. Details are given in Chapter 3.3.2

1.4.2 Interference among Pressure Responses of Digital Electrical Pulses

The second problem is that the emitting time of the acoustic response of the general transducer is longer than the sampling period of 23 µs (44.1 kHz). When a digital pulse is feeding a normal speaker, acoustic output from the speaklet has a constant frequency (natural frequency), but the output consists of multiple cycles of the acoustic wave, which have gradually reducing amplitude. General acoustic or ultrasonic transducers have an emitting time far longer than the sampling period.The emitting time is approximately 2 ms (400 Hz) while the sampling period is 23 µs (44.1 kHz). Differing from the ideal case, a digital pulse generates a cycle of the acoustic wave. The ringing problem have been referred in ultrasonic imaging[5], it is less effect on it than DLA because the emitting time requires 33.3 msec or 30 frame per sec of frame rate in the imaging while the emitting time requires 22 usec or 1 period of 44.1 kHz. Dejaeger, R. et al refer it as pull-in limitation in DLA[6][7].

The root cause of the problem is the acoustic impedance of the transducer being far greater than the impedance of the air as the media, which causes ringing of the acoustic output. The ringing causes the emitting time to extend to a length greater than the sampling period, which conflicts with the first requirement of digital reconstruction. As a result, the acoustic response in the exceeding period interferes with the acoustic response of the electrical pulse of the successive sampling period. The interference results in the distortion of digital reconstruction.

The proposed method is to use double electrical pulses to stimulate a stroke of acoustic response. The two electrical pulses should create oscillations of acoustic responses with different phases of 180 degrees. Therefore the oscillation of the two pulses start to cancel each other out, since the phase of total acoustic output shifts 180 degrees, as shown in Figure 4-5. The amplitude of the total acoustic output, represented as the purple line in Figure 4-5, reduces dramatically since the second peak of oscillation of the response is similar to the ideal acoustic response of the DLA.

The driving speaklet pulses consist of two pulses of the same width. The first pulse is to stimulate a speaklet to emit a stroke of acoustic output; the other pulse is tostop the vibration of the diaphragm of the speaklet. The head-to head period of the pulse couple is adjusted in order to create the largest difference between the first peak and the second peak of the acoustic output for a certain pulse width. It was found that the period is equal to a half period of the natural frequency of the speaklet. However, this method can only be applied to a speaklet with a single frequency of free vibration (more details in Chapter 4.1.3.2 and 4.1.2.2.3).

In the experiment in Chapter 4.1.2.2.4, the results did not meet expectations, because the total response of the pulse couple were significantly attenuated. This results from the acoustic response of the transducer not reaching the maximum amplitude at the first cycle of the response, as shown in Figure 4-4. The acoustic responses of the pulse couple cancel each other.

Because the emitting time cannot be reduced, interference among the acoustic pulses is allowed. In other words, the first requirement is ignored. As a consequence of this, it is found that the amplitude of acoustic response of each frequency of pulse rate depends on the frequency response of the speaklet. The amplitude is maximized when the pulse rate is equal to the resonant frequency, as shown in the experiments in Chapter 4.1.3. This occurrence is similar to the application of the ordinary analogue electrical sinusoidal signal into a loudspeaker, but they are different in the shape of the waveform.

1.4.3 Efficiency in Sound Generation

Sound generation from ultrasound is based on the principle of frequency beat. The research involved in this area, uses a parametric array. The problem of sound generation is that loudness of sound relies on the non-linearity of an acoustic medium. As a result, the intensity of ultrasound is high enough for an ultrasonic transducer array to generate sound with reasonable loudness[8]. This is described in detail in Chapter 2.2.3 and 4.1.4.

Due to the fact that the sound, which is generated from ultrasound, is in an AM waveform, the sound can be considered according to the principle of telecommunication. This means that the

sound is the modulated wave. People would not hear the sound if the acoustic medium was linear (for more detail see Chapter 3.4.1 and 5.1.1).

From this point, in order to find a solution, the AM sound should be demodulated in order to extract the sound, which is a modulating wave, from its carrier. The demodulation can be performed by a loudspeaker, which is designed for the application of the condition of acoustic rectification.

Although there is no concrete evidence for the rectifying loudspeaker, there is good evidence from FEM simulation which shows that displacement is directly proportional to velocity (for more detail see Chapter 0).

Another problem of sound generation from ultrasound is that the width of the sound beam of an ultrasonic transducer is very narrow. The root causes are the flat diaphragm of the transducers and their large diameters compared to the wavelengths of ultrasound. These characteristics result in directional radiation of the transducers.

With the structure of the rectifying loudspeaker, there is clear evidence for a wide sound beam from FEM simulation. The diameter hole, which is the velocity transition surface and acts like a sound source, is tiny, at20 μm. The diaphragm of the loudspeaker vibrates at a frequency of 40 kHz. The beam width is 308 degrees (for more detail see Chapter 5.1.4.1).

In addition, the sound source of the loudspeaker is a secondary source, which is not a physical but a virtual acoustic surface. The acoustic surface is derived from the collision of a huge number of air particles and a rapid change in air velocity. The surface has a curved shape, as shown in Figure 5-10.

1.5 Scope of Work

This thesis is written to explore the feasibility of the implementation of a DLA, but not to design and fabricate the array. The work concentrates on sound generated from ultrasound. The method of exploration is quick observation of hearing on frequency only, and study focusing on conception, but with little detail on design and fabrication.

- Identifying whether DLA can reproduce sound or whether humans can hear it, because speaklets within the array generate sound from ultrasound. Normally sound humans can hear is identified by frequency and sound level, but frequency is the primary factor, because if the frequency of a wave is out of the audible frequency range, humans cannot hear it, however high the amplitude of ultrasound. Therefore, this research focuses only

on frequencies of emitted waves, while sound levels are ignored, because sound level is related to design and fabrication.

- Differentiating between a DLA and an analogue loudspeaker, and analysis of their advantages and disadvantages based on the concept of sound generation, not based on their structure or the fabrication of speaklets. Most of the work involved mathematical modelling and finite element modelling (FEM). Experiments were conducted to investigate the relationships between electrical inputs, pressure outputs and the frequency responses of speaklet samples. The samples are not prototypes but on-shelf transducers.

1.6 Contribution

In study about feasibility of implementing speaklets for DLA concept, we discover

1.6.1 Three Requirement of Digital Sound Reconstruction

Implementing speaklets within Digital Loudspeaker Array (DLA) is investigated by basing on the three requirement of digital sound reconstruction described in Section 2.3.3

- For the first requirement, due to the short emitting time of impulse responses in ten microseconds of the speaklet, Chapter 3 found that the dumping ratio of the speaklet requires 0.8 at 44.1 kHz to meet this requirement. Chapter 4 did not find a speaklet with the required dumping ratio from real electro-acoustic transducers and FEMs. Therefore, the speaklet for this requirement cannot be found in this study.
- Regarding the second requirement, the uniformity in the impulse response of the speaklet with the array cannot be investigated because this requirement has to be tested after fabrication process of speaklet.
- For the third requirement, the linearity in amplitude of impulse response, with MDLA concept, mathematical model speaklets, FEM speaklets and real transducers met this requirement.

1.6.2 MDLA.

- The concept of the Multiple-level Digital Loudspeaker Array (MDLA) is innovatively applied as an alternative method to produce amplitude modulation (AM) sound which is generated from the ultrasound. The concept of AM sound is developed from Audio Spotlight technology[9] which is the commercial name of a parametric array. The AM applies analogue electrical drive while MDLA applies digital one.

- The new concept is extended from Digital Loudspeaker Array (DLA) by the application of the Pulse Width Modulation (PWM) which is the fundamental technique for robots in motor speed control.

1.6.3 Rectifying loudspeaker

- A rectifying loudspeaker introduces a constant supply of air pressure into the sound generating system while the common loudspeakers have merely electrical supplies. A main goal of the loudspeaker is to produce half-wave rectified AM sound to improve the efficiency of sound generation. The word “rectifying” refers to the method of amplitude demodulation which is the original technique of radio broadcasting.
- The structure of the rectified loudspeaker is adapted from the human voice system, and can be fabricated by MEMs. A vibrating disc or diaphragm of the loudspeaker primarily applies as a valve for speed control of air particles from the pump to an air cone outlet.
- As a result, the air particles in front of a hole within the outlet of the loudspeaker move only in one direction, i.e. moving forwards and not going backwards. The air particles in front of diaphragms of common loudspeakers, on the other hand, move back and forth according to the movement of the diaphragms.

1.7 Document Structure

This thesis is divided into six chapters:

Chapter 2 provides a thorough background of acoustics, hearing and sound generation from loudspeakers, ultrasound and humans. It reviews the concept of DLA, which is the main topic of this thesis. It shows the fundamentals of the mathematical model of vibration and acoustic radiation. The radiation covers both steady-state and transient-state radiation.

Chapter 3-6 describes the original work:

Chapter 3 describes the mathematical model for speaklets within DLA, the conditions of acoustic rectification and application of the model, and the conditions according to the requirements of digital sound reconstruction.

Chapter 4 describes the experiments in application of the loudspeaker according to the concept of DLA. It also includes a study of the design of PZT- based transducers as DLA with FEM modelling.

Chapter 5 describes the principles and structure of a rectifying loudspeaker, and performs validation of the structure according to the conditions of acoustic rectification.

Chapter 6 summarizes the conclusion discussed in this thesis and provides recommendations for the design of the loudspeaker and future research for this area.

1.8 Publication

Monkronthong, S. White, N and Harris, N. “Multiple-Level Digital Loudspeaker Array”, *the 28th European Conference on Solid-State Transducers*, September 2014

Monkronthong, S. White, N and Harris, N. “A study of efficient speaklet driving mechanisms for use in a digital loudspeaker array based on PZT actuators”, *the Sensors Application Symposium 2016*, April 2016.

Chapter 2: A Review of Sound Generation and Digital Loudspeaker Array

The concept of a digital loudspeaker array (DLA) was first published in 2002 by Busbridge *et al* and Diamond *et al* [1][2]. The digital loudspeaker array consists of a number of speaklets (tiny loudspeakers), each of which is driven by a stream of rectangular pulses with constant width and amplitude in order to produce sound. Tatlas et al studied in topologies of speaklets effect on acoustic distortion in 2004[10]. Although, there were patents of digital loudspeakers, which consist of multiple piezoelectric transducers with different sizes in 1963 or multiple voice coils in 1977, they were not tiny loudspeakers and do not conform with the concept of DLA[11]. A few groups conduct experiment with available small loudspeakers[12][13]. In 2006, Audio Pixels Limited was founded. They employ the concept of DLA to generate sound by using low cost microelectromechanical systems (MEMs)[3].In 2012 Dejaeger et al started to fabricate 64-speaklet DLA and in 2015 they fabricated 256-speaklets of DLA with 2.6 mm diameter. They claim that it produces the sound level of 100 dBSPL at 13 cm from the array[6][7]. Throughout the past ten years, a very limited number of reseachers work in this area. This may be because the significant problem with the DLA is that the bit quality of the acoustic output depends on the number of speaklets. Typically, for conventional audio systems, this is 16 bits. Consequently, a DLA would require 65532 speaklets in order to reproduce the sound at the same quality as a conventional loudspeaker. We propose a concept of a multiple-level digital loudspeaker (MDLA) which increases the number of levels of sound that a speaklet can emit. The detail will be given in Chapter 3.

In order to investigate feasibility of implement of multiple-level digital loudspeaker array (MDLA), which is a technique of making sound from ultrasonic with digital voltage driver, this chapter gives background knowledge to the investigation. This chapter is divided into four main sections. The first section briefs on characteristics of sound and ultrasound waves. The wave behaviours such as attenuation and reflection are described in similarity and difference between sound and ultrasound. Effects of the waves on humans such as loudness of sound and risks are identified. This will give enough information to understand principles of sound and ultrasound waves for readers with no acoustic backgrounds. The second section investigates some available technologies, which are used for making loudspeakers and ultrasonic transducers, such as piezoelectric and electromagnetic technologies. Excitation force of each loudspeaker will be expressed in terms of specifications of the loudspeaker such as driving voltage, the inductance of a coil and the capacitance of piezoelectric transducer. The forces will be mathematically analysed

in Chapter 4 for digital voltage driver and evaluation of the technologies for MDLA. A parametric array is a technology for making sound from ultrasound, which is similar to MDLA but it feeds electrical analogue signal. It is interesting because this technology has launched some commercial products. The technology is referred as audio spotlight. The airborne output will be used as a reference to compare with the output of MDLA in Chapter 3 and 4. It will describe how the array makes sounds. Voice system of a human is another sound generator, which is basics of the new structure of loudspeaker proposed in Chapter 5. The third section reviews concepts of digital loudspeaker array (DLA) MDLA is developed from. The final section gives a detail about the mathematical model of vibration and wave radiation. The radiation model cover the steady state case, which is applied for normal (analogue) loudspeaker and the transient-state case, which are derived for a digital loudspeaker. The session prepares a basis for analysing the ideal model in Chapter 3.

2.1 Sound and Ultrasonic

Waves can be categorized into two types: mechanical and electromagnetic. Transverse electromagnetic waves do not need any medium, while transverse mechanical waves do need a medium. In other words, mechanical waves cannot propagate through a vacuum. Sound and ultrasound waves are mechanical waves and travel on a medium at the same speed. The speed of propagation of a mechanical wave is determined by the density and the stiffness of the medium it is travelling in. Sound and ultrasound are longitudinal waves, in which the vibration of the molecules in the medium is in the same direction as the propagation of the overall wave. A period of the longitudinal wave consists of one cycle of compression and rarefaction of atmospheric pressure. However, they are different in the range of frequencies. The range of frequencies of sound is between 20 Hz and 20 kHz, while the range of frequencies of ultrasound is above 20 kHz[14].

2.1.1 Wave Propagation

Sound and ultrasound waves can be generated from the movement of a piston or a diaphragm. They travel through the air with a constant speed. In order to understand the mechanism of propagation of an acoustic wave, which involves acoustic pressure and airflow rate, the process may be conceptually, but not actually described as a piston mounted in the end of a uniform square pipe.The air inside the pipe may be divided into cubes, which are linearly aligned. The air blocks are conceptually formed and their surfaces are joined together and bonded with a high damping spring. Similarly, the surface of the piston is attached to the surface of the air block, as shown in Figure 2-1.

For simplicity, the analogy are made on assumptions including

- Ignoring attenuation of the air medium;
- Laminar inflow profile without friction force on the surface of inner pipe;
- Linear constitutive relation between acoustic pressure and air particle velocity;
- Neglecting higher acoustic modes.

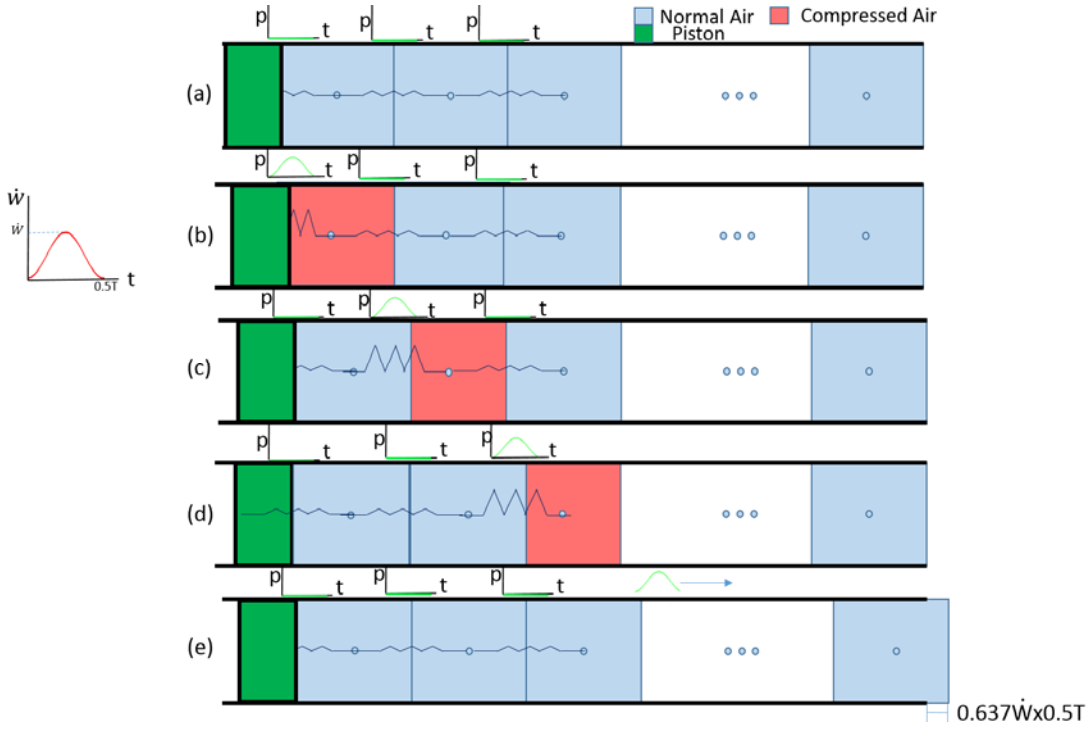

Figure 2-1: Schematic diagram of wave propagation.

Figure 2-1a-e shows the process of propagation. Figure 2-1a is the initial stage of the propagation. Pressure on the conceptual springs between air blocks and their consecutive blocks is equal to zero. When the piston moves forward and stops with simple harmonic motion, as shown on the velocity graph in Figure 2-1b, the boundary between the surfaces of the piston and the first air lump is shifted and the first lump is compressed. This causes pressure in the spring, as shown on the graph, over the boundary while the other side of the surface of the block stays still. This schematic diagram illustrates the case that pressure (p) is directly proportional to the flow rate ($\dot{w}$) at the boundary, which can be derived from the equation of momentum conservation or Euler's equation[14]:

$$\frac{\partial p(t)}{\partial x} = -\rho \ddot{w}(t) \tag{2.1}$$

where ρ and x are density of air. The wave speed (c), which is constant, is substituted in the equation and both sides of the equation are taken by the integral of dt The equation can be expressed as[14]:

$$p = \rho c \dot{w}(t) \tag{2.2}$$

If $\dot{w}(t)$ is the simple harmonic motion of the boundary, it is defined as:

$$\dot{w}(t) = \dot{W} e^{-j\omega t} \tag{2.3}$$

$\dot{W}$ is a constant amplitude of velocity and ω is the circular frequency in radians per second. It can be expressed as [14]:

$$\omega = \frac{2\pi}{T} \tag{2.4}$$

T is a repeating period of the simple harmonic. The next stage in Figure 2-1c, when the first block returns to its original shape, the boundary between the piston and itself stays still, but it pushes the boundary between itself and the second block, causing it to shift with velocity, as shown in the velocity graph. As a result of the boundary shifting with $\dot{w}$(t), pressure on the spring between the first and second blocks rises in direct relation to $\dot{w}(t)$, while pressure on the other spring of the first chunk drops to zero. This shows momentum energy transfer from the first lump to the second lump. In the next stage in Figure 2-1d, the process is similar to the previous stage but the forward movement of the boundary between the second and the third chunks results in the second chunk returning to its original shape, but the third chunk being compressed. This causes the acoustic pressure on the abstract spring to move from the spring between the first and second chunks to the spring between the second and third chunks. In Figure 2-1e, the acoustic pressure will travel through the train of chunks with a constant speed of c, while the air chunks in the flow move with a displacement of $\dot{w}_{avg} * T/2$. The average velocity $\dot{w}_{avg}$can be computed from:

$$\dot{w}_{avg} = \frac{\dot{W}}{\pi} \int_0^{\pi} \sin(t) dt = \frac{2\dot{W}}{\pi} = 0.637\, \dot{W} \tag{2.5}$$

2.1.2 Characteristics of Acoustic Wave

An acoustic wave is a wave derived from an oscillation of particles and transferring energy through a medium. There are four major characteristics of a wave: frequency, wavelength, speed and amplitude.

2.1.2.1 Frequency, Wavelength and Sound speed

The frequency (f) is the number of pressure variations per second and is measured in units of Hertz. Ultrasound, audible sound or infrasound can be distinguished by the range of frequencies. The frequency of a sound produces its distinctive tone. The human voice covers the 170 - 4000 Hz frequency range, while music sound has a range between 50 - 8500Hz [15]. The average adult male can produce sounds in the range 200-2500Hz, while a male opera singer might extend the range to 3500 Hz. Women and children's voices are higher frequency than the male voice, about 15-20% [16].

Wavelength (λ) is the distance a wave travels in the time it takes to complete one cycle. It can be measured between consecutive wave crests in units of metres (m) or millimetres (mm) and is inversely proportional to the frequency of the wave as expressed in the following equation [14]:

$$\lambda = \frac{c}{f} \tag{2.6}$$

where c is a constant of wave propagation speed or sound speed. The speed is defined as the rate at which a pressure pulse travels in a medium and is determined by the medium. It is related to density (ρ) and stiffness, or the adiabatic bulk modulus (B) of the material of the medium, as expressed in the following equation [14][17]:

$$c = \sqrt{\frac{B}{\rho}} \tag{2.7}$$

The density is measured in units of kg/m3 and stiffness is a measure of a material's resistance to deformation when a squeezing force is applied to it in units of Pa. In a material with low density and high stiffness the wave travels rapidly, while in a material with high density and low stiffness the wave travels slowly.

Temperature is a factor influencing a change in sound speed. The speed can be expressed by [18]:

$$c = \sqrt{k_h R_h T_h} \tag{2.8}$$

when the medium is an ideal gas. R_h and k_h and T_h are the ideal gas constants equal to 287 J/kg*K, the ratio of specific heats and temperature in Kelvin. For example, in acoustic measurement, the speed(c) is 344 m/s at room temperature in a medium of air with the ratio of the specific heat of gas at 1.4.

2.1.2.2 Amplitude and Sound Level

Amplitude of the wave is another main quantity affecting hearing. It is the size of the pressure fluctuation and is measured in pascals (Pa). The weakest sound pressure in a healthy human ear is 20 µPa, while a strong sound pressure might reach 20 Pa. Owing to the large pressure range, the logarithmic scale (dB) of pressure is used and referred to as sound pressure level (SPL). Due to sound in nature consisting of multiple frequencies, it is, therefore, convenient to use the mean-square value of the variation [19]:

$$p_{rms} = \sqrt{\lim_{T\to\infty} \frac{1}{T} \int_{t_1}^{T+t_1} p^2(t)dt} \tag{2.9}$$

in which t_1 is an arbitrary time. Consider a pure tone, which has only one frequency; it can be written as:

$$p(t) = Pcos(\omega t + \phi) \tag{2.10}$$

where P is the amplitude of pressure variation (p) and ϕ is the phase of the wave. The root mean square is [19]:

$$p_{rms} = \sqrt{\frac{1}{T}\int_0^T P^2 cos^2(\omega t + \phi)dt} = \frac{P}{\sqrt{2}} = 0.707P \tag{2.11}$$

The sound pressure level (SPL) in decibels (dBSPL) is defined by [19]:

$$SPL = 20\, log_{10}\left(\frac{p_{rms}}{p_{ref}}\right) \tag{2.12}$$

where p_{ref} is the threshold of hearing, 20 µPa.

2.1.3 Sound and Ultrasound with Wave Behaviours

Sound and ultrasound waves need a medium for propagation. The characteristics of a wave depend on the medium in which it travels. Depending on frequency or wavelength, wave behaviours differ in such things as attenuation, diffraction, reflection and refraction.

2.1.3.1 Attenuation

Attenuation is a decrease in the amplitude or intensity of a wave when it travels through the medium. This results from the conversion of sound to heat or the absorption of the medium. Attenuation increases with increase in frequency. This means a low frequency wave can travel through the medium farther than a high frequency wave. In air, the attenuation also varies with

temperature and humidity. Table A-1 shows attenuation in dB per km at 20°C and a pressure of 101.325 kPa with an uncertainty of ±10%. However, the attenuation with approximation is proportional to f^2.

2.1.3.2 Acoustic Impedance and Reflection

Acoustic impedance plays a major role in wave transmission and reflection. Acoustic impedance is an important characteristic of media. There are two meanings of acoustic impedance.

2.1.3.2.1 The specific acoustic impedance (z)

The specific acoustic impedance (z) is the ratio of acoustic pressure and the speed of particle vibration. It can be defined as [19]:

$$z = \frac{p(t)}{\dot{w}(t)} \tag{2.13}$$

From Eq. (2.2) acoustic impedance can be calculated as Eq. (2.14)[5] and its unit is rayls.

$$z(rayls) = \rho\left(\frac{kg}{m^3}\right) \times c\,(\frac{m}{s}) \tag{2.14}$$

The specific acoustic impedance is applied to the calculation of the wave transmission and refection when an ultrasound or sound wave travels in a perpendicular direction to the boundary between two media with different acoustic impedances. Some of the energy of the incident sound may move into the second medium with the same direction, while the remaining energy may be reflected back into the first medium, as shown in Figure 2-2.

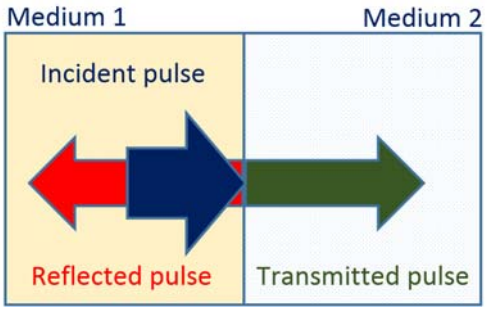

Figure 2-2: Transmission and reflection of a sound wave when its direction is perpendicular to a boundary of two media after Kremkau, F. [5].

The intensity of the transmitted and reflected sounds depends on the specific acoustic impedance of the two media, as in the following equations [5]:

$$intensity\ reflection\ coefficient = \left(\frac{medium\ 2\ impedance - medium\ 1\ impedance}{medium\ 2\ impedance + medium\ 1\ impedance}\right)^2 = \frac{reflected\ intensity(W/cm^2)}{incedent\ intensity(W/cm^2)} \tag{2.15}$$

$$intensity\ transmission\ coefficient = 1 - intensity\ reflection\ coefficient = \frac{transmitted\ intensity(W/cm^2)}{incedent\ intensity(W/cm^2)} \quad (2.16)$$

where intensity reflection coefficient is the fraction of the reflected intensity divided by the incident intensity and intensity transmission coefficient is the fraction of the transmitted intensity divided by the incident intensity.

From Eq. (2.15), the dB loss of energy can be obtained as Eq. (2.17) when the reflected intensity is considered as loss [5]:

$$acoustic\ loss = 10\ log_{10}(intensity\ transmittion\ coefficient) \quad (2.17)$$

From these equations, it can be seen that when sound travels from one medium to another with a different acoustic impedance, there will be loss of energy whenever it travels from high impedance to low impedance or from low impedance to high impedance.

2.1.3.2.2 The acoustic impedance (Z)

The acoustic impedance (Z) is defined as the ratio of acoustic pressure to acoustic volume flow (q) [19]:

$$Z = \frac{p(t)}{q(t)} = \frac{p(t)}{a\dot{w}(t)} = \frac{z}{a} \quad (2.18)$$

The volume flow q(t) depends on the shape of duct[19].

$$q(t) = a\dot{w}(t) \quad (2.19)$$

where (a) is the cross-sectional area of a duct. The relationship between acoustic impedance and the specific acoustic impedance is expressed in Eq.(2.18).

The acoustic impedance is applied to the calculation of the wave transmission and refection when an ultrasound or sound wave travels in the same medium but in different shape of duct. The size of the duct will affect the change in acoustic impedance. As a result, the effect on the reflected and transmitted waves at the boundary of change of size of duct is similar to a change in medium.

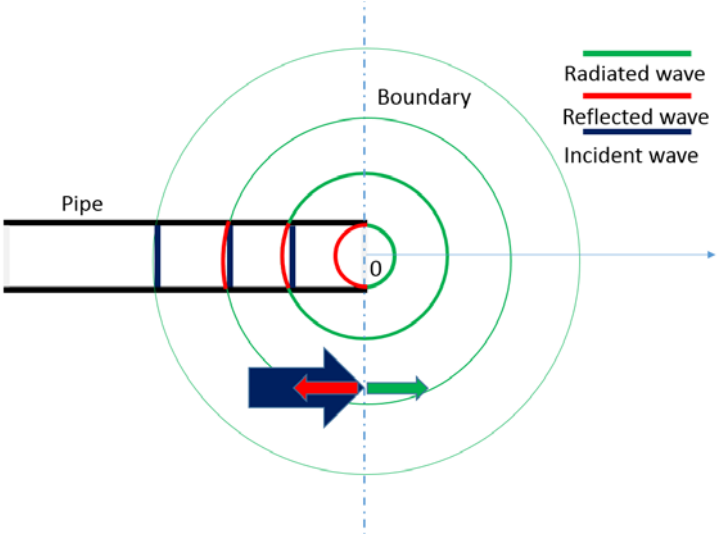

Figure 2-3: Wave front of transmission (or radiation) and reflection of sound wave when the wave travel out from a pipe.

Figure 2-3 shows a reflection at the open end of a pipe. At the boundary x= 0, the continuity of pressure and flow condition is satisfied [19]

$$p_{>}(t) + p_{<}(t) = p_{rad}(t) \tag{2.20}$$

and

$$q_{>}(t) - q_{<}(t) = q_{rad}(t) \tag{2.21}$$

where $p_{>}$, $p_{<}$ and p_{rad} are acoustic pressure waves of incidence, reflection and radiation respectively, while $q_{>}$, $q_{<}$ and q_{rad} are their flow rates. From the relationship of q and p from Eq.(2.18), Eq.(2.21) can be rewritten as [19]:

$$\frac{p_{>}(t)}{Z_0} - \frac{p_{<}(t)}{Z_0} = \frac{p_{rad}(t)}{Z_{rad}} \tag{2.22}$$

where Z_0 and Z_{rad} are acoustic impedance at x =0 and radiation impedance.

By substituting p_{rad} in Eq. (2.20) into Eq. (2.22) and rearranging terms $p_{<}$ and $p_{>}$, the reflection coefficient can be expressed as:

$$reflection\ coefficient = \frac{p_{<}(t)}{p_{>}(t)} = \frac{Z_{rad} - Z_0}{Z_{rad} + Z_0} \tag{2.23}$$

$$transmission\ coefficient = \frac{p_{rad}(t)}{p_{>}(t)} = 1 - reflection\ coefficient \tag{2.24}$$

The acoustic Impedance consists of mechanical impedance and radiation impedance. Mechanical impedance is derived from the source device which radiates the wave, such as string, tube or diaphragm, while radiation impedance (Z_{rad}) represents the impedance when the acoustic wave is propagated in air or a fluid. It can be expressed as [19]:

$$Z_{rad} = |Z_{rad}|e^{j\theta} = r_{rad} + jx_{rad} \tag{2.25}$$

where R_{rad} and X_{rad} are the radiation resistance and radiation reactance respectively.

Kensler, L. et al derive the radiation impedance for the circular piston and pulsating sphere with a radius (r). In the low frequency limit (kr<<1), for a circular piston, the radiation impedance is expressed as [19]:

$$Z_{rad} \cong 0.5\rho ca(kr)^2 + j(8/3\pi)\rho ca(kr) \tag{2.26}$$

where (a) is the cross-sectional area of radiation and k is the wave number and can be defined as:

$$k = \frac{2\pi}{\lambda} \tag{2.27}$$

In the high frequency limit (kr>>1) [19]:

$$Z_{rad} \cong \rho ca \tag{2.28}$$

The impedance is the pure real part. For the pulsating sphere, the radiation impedance for the high frequency limit (kr>>1) is the same as the piston but for the low frequency limit (kr<<1) [19]:

$$Z_{rad} \approx \rho ca(kr)^2 + j\rho ca(kr) \tag{2.29}$$

It can be roughly estimated as $Z_{rad} = jx_{rad}$, which is the pure imaginary part and neglects the real part.

2.1.3.3 Refraction

Refraction is the change in direction of a wave when it travels from one medium to another medium, which has a different acoustic impedance. In the atmosphere, sound and ultrasound rays can bend when they move between air with different temperatures or densities. The direction tends to bend from warm to cool air. The direction of the wave can be significantly bent by wind. It is a common experience to hear sound better downwind than upwind [15]. Therefore, wind direction is a major factor in considering wave propagation over long distances. However, this thesis will not consider the results of refraction but it has a major effect on distance of wave propagation for outdoors

2.1.3.4 Diffraction and Beam Width

Diffraction is a wave behaviour in which the wave encounters an obstacle or a slit. Diffraction is the bending of a wave around an object, or the spreading out of the wave through an aperture. If the object is smaller than the wavelength, the wave bends around the object but if the object is greater than the wavelength, the waves are blocked by the object [20]. In the case of a slit, if a aperture is smaller than the wavelength of a wave passing though the aperture, the wave spreads out, but if the aperture is greater than the wavelength, the wave travels in a direction perpendicular to the aperture and spreads relatively little [5]. Therefore, ultrasound, which has small wavelengths such as 8.625 mm for 40 kHz with sound speed of 345 m/s., is blocked by obstacles and if a aperture is smaller than the wavelength of the ultrasound, the spreading angle of the wave through the aperture is extended.

An acoustic wave, which is emitted by a diaphragm, spreads through different angles depending on the frequency of the wave and the diameter of the diaphragm as shown in Figure 2-4. The spreading angles can be approximated by:

$$sin\ (\alpha/2) = \frac{D_c \times c}{fD} \tag{2.30}$$

where (c) is the propagation speed in the medium and α is the angle between -6 dB points. D_c is the directivity constant, which is 0.514 for water as a medium [21] and 0.72 for gas [22]. D and f are the diameter of the transducer and the frequency of the emitting sound wave respectively. Variation of the directivity constant(D_c) may depend on the quality of the measuring instrument or the different materials of the ultrasonic transducers.

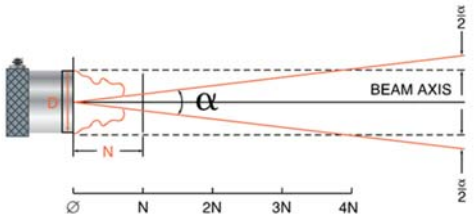

Figure 2-4: Beam Width of transducer after Olympus NDT [21]

2.1.4 Hearing, Hearing Criteria and Risk Caused by Sound and Ultrasound

This section prepares a brief about the concept of hearing and hazard of sound and ultrasound to the ears

2.1.4.1 Hearing

Any pressure variation in the air that the human ear can detect may be defined as sound, while ultrasound is also a pressure variation, but humans cannot perceive it because the frequencies are too high. Besides frequency, amplitude of sound pressure is another main factor in human hearing. The human ear is not equally sensitive at all frequencies. In order to give the same subjective loudness, different frequency tones must be produced at different sound levels, as shown in this set of equal loudness contours, Figure 2-5

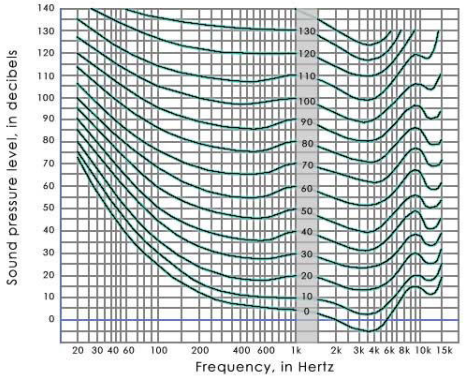

Figure 2-5: Robinson-Dadson curves are one of many sets of equal-loudness contours for the human ear after Gelfand, S.[23].

Loudness can be defined as the perceived sound level, while sound level can be defined as the magnitude of the sound exposure. In order to make loudness in all frequencies have the same or nearly the same values, the sound level in dBSPL is multiplied by A-weighting values (A_n), which match with the frequencies, as shown in Table B-1. Sound loudness level (SLL) in units of dBA can be computed by [24]:

$$SLL = 10\,log_{10}\left(\sum_{n\ for\ frequencies\ from\ 20\ Hz\ to\ 20k\ Hz} 10^{\frac{(SPL_n - A_n)}{10}}\right) \tag{2.31}$$

where all frequency is composed of the sound or noise. The A-weighting is commonly used as the weighting when referring to health and safety noise exposure levels. For example, sound sources and their common sound levels are shown in Table 2-1. Below 85 dBA for 8 hours is considered safe by Health and Safety Executives. However, A-weighting is not defined for frequencies over 20 kHz.

2.1.4.2 Hearing Criteria and Risk

Table 2-1: Typical Noise Levels [25]

Sound of source	Sound Level (dBA)	Perception
Jet plane at 30 m	140	Extreme pain
Threshold of pain	125	Pain
Pneumatic drill	110	Very loud
Siren at 30 m	100	
Car horn	90	Loud
Door slamming	80	
Dog barking	70	Noisy
Normal conversation	60	Moderate
Background TV or radio	40	Quiet
Quiet room or recording studio	20	Very quiet
Rustle of leaves	10	
Threshold of hearing	0	

Although ultrasound may have no effect on the hearing mechanism, exposure to ultrasound may cause health risks. Due to a huge difference in acoustic impedance between air and tissue, it is difficult for ultrasound to penetrate the body and to cause damage to the tissue. Ultrasound cannot be perceived in an audible sense, but it may be perceived as a kind of pressure in the ear. As a result, it might cause headaches or a feeling of dizziness and nausea when some people are exposed to a high intensity of ultrasound for a considerably long period[26].

AU weighting extends the A-weighing curve up to 40 kHz in order to consider both sound and ultrasound as a pressure wave potentially hazardous to health, as shown in Table B-1. Herbetz, who have proposed an 'AU-weighting curve', found that the tolerable sound pressure levels are 110 dB for 20 kHz, 125 dB for 25 kHz and 140 dB for 31.5-40 kHz.

2.2 Sound and Ultrasonic Generation

Loudspeakers and ultrasound transducers are devices which transform electrical signals into mechanical waves. The devices can be divided into two types: electro-mechanical transducers and acoustic drivers. The electro-mechanical transducer converts from electrical energy to mechanical energy, while the acoustic driver converts kinetic energy from surface vibration to acoustic energy in a form of pressure variation. Acoustic drivers are sources of sound, such as strings, bells and pistons but a diaphragm is the typical acoustic driver of a loudspeaker. For electro-mechanical transducers, there are two major technologies: piezoelectric and electro-magnetic.

2.2.1 Piezoelectric Technologies

Piezoelectric Technologies are commonly used for manufacture of ultrasonic transducers and buzzers, which emit sound at a certain frequency or a narrow range of frequencies. These transducers are made of piezo-ceramic, which is hard and has a narrow working bandwidth around its resonance frequency.

2.2.1.1 Piezoelectric Transducer

Piezoelectric transducers can be divided into two types; acoustic and ultrasonic transducers. Piezoelectric acoustic transducers are also called tone generators, or buzzers. They are typically suitable for producing a high frequency sound output with small power consumption. The conventional structure of the transducer consists of an acoustic diaphragm and a piezoelectric ceramic disk, as shown in Figure 2-6. Acoustic diaphragms are generally made of metal. In recent years, some diaphragms have been made of silicone rubber sheet [27] and some are made of polysilicon [6]. From the structure, sound can be produced by bending of the ceramic disk and acoustic diaphragms, which are bound together. The bending results from two bending moments, which have opposite directions when applying a voltage at the edge of the ceramic disk. From Bakke, T. et al.'s experiments and simulation [28], the materials and their characteristics are used as shown in Table 2-2

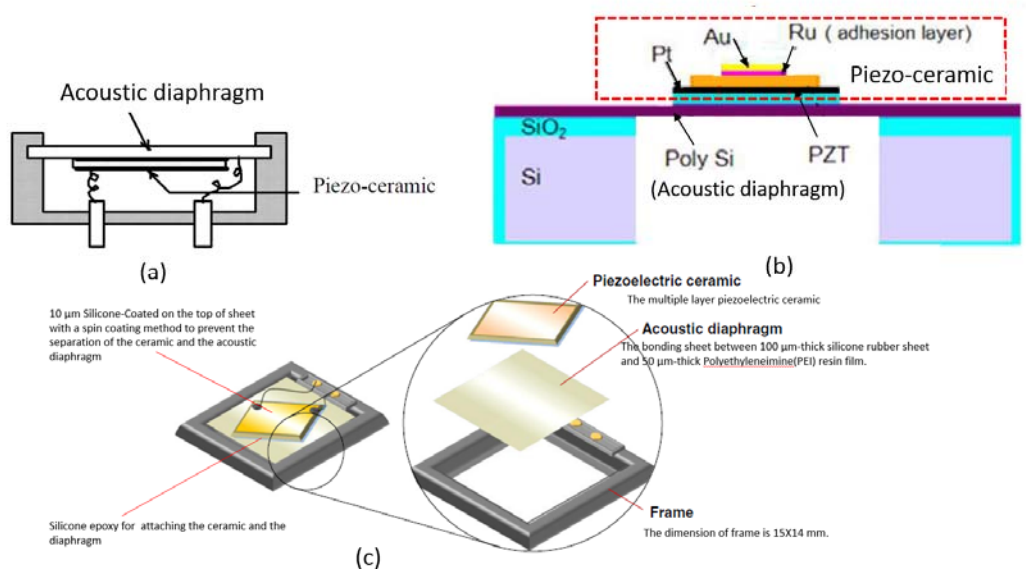

Figure 2-6:a) Typical acoustic transducer after Uchino, K.[29] b) MEMS Speaklet after Dejaeger, R. et al[6] c) piezoelectric acoustic actuator after Kim, H. et al [27].

Table 2-2: Material and their characteristics for acoustic transducers following Figure 2-6b [28]

Material	Thickness (nm)	Pre-stress (MPa)	Young's modulus (GPa)	Poisson ratio	Density $(kg/m)^3$
Au	214	282	78	0.44	19,300
PZT	1888[28], 360[6]	110	PZT-5A	PZT-5A	7,750
Pt	198	839	168	0.38	21,090
SiO_2	2319	-177	70	0.3	2,200
Si	7077	0	170	0.28	2,330

The vibration of the piezo-buzzer results from applying an alternating voltage to the electrodes of the transducer. The electrical alternation makes the transducer, which is attached to the diaphragm, extend and shrink. This causes bending of the diaphragm, both concave and convex. If the diaphragm vibrates rapidly, a sound wave will be generated.

The first natural frequency can be typically calculated by Eq.(2.32)[30][31]:

$$f_0 = r_{shape}\frac{h}{D^2}\sqrt{\frac{Y}{\rho(1-\nu^2)}} \tag{2.32}$$

where r_{shape} is a shape constant depending on the ratio of length to width. Constants of r_{shape} are 1.654 for a square diaphragm [30] and 1.648 for a circular diaphragm [31]. D is the diameter for a circular, or the length for a square diaphragm, while h is the thickness of the diaphragm. Y, ν and ρ are Young's modulus, Poisson's ratio and density of the ceramic material (kg / m).

For small microstructures, the surface and friction forces are additionally considered for the volume and inertial effects. Therefore, the first natural frequency is also affected by the compressive or tensile stress (T), which appears on the films, as shown in Eq.(2.33) [30]:

$$f_0 = r_{shape}\frac{h}{D^2}\sqrt{\frac{Y+T}{\rho(1-\nu^2)}} \tag{2.33}$$

Piezoelectric ceramics can consist of a single active layer (bending-mode) or multiple active layers (multilayer mode). Generally, a bending mode actuator produces a smaller force but a larger displacement than the multilayer mode actuator. Therefore, most acoustic applications are designed with the bending mode because it provides large displacement at low voltage. However, Kim, H. et al [27] proposed a multilayer mode actuator, which consists of three active multilayers of piezoelectric elements or multimorph, with larger displacement and larger generative force in 2014. They show that the serial multimorph in serial connection (SMS) and the parallel multimorph in parallel connection (PMP) configuration produce a large displacement and a large force. SMS consists of two tripled-layer multimorphs, which are serially connected during polarization and electric field drive. PMP consists of two triple-layered multimorphs, which are parallel connected during polarization and electric field drive, shown in Figure 2-7. The acoustic actuators fabricated with the configuration of SMS and PMP and assembled according to Figure 2-6c had high average sound pressure levels (SPLs) of 83.1 and 85.7 at a distance of 10 cm.

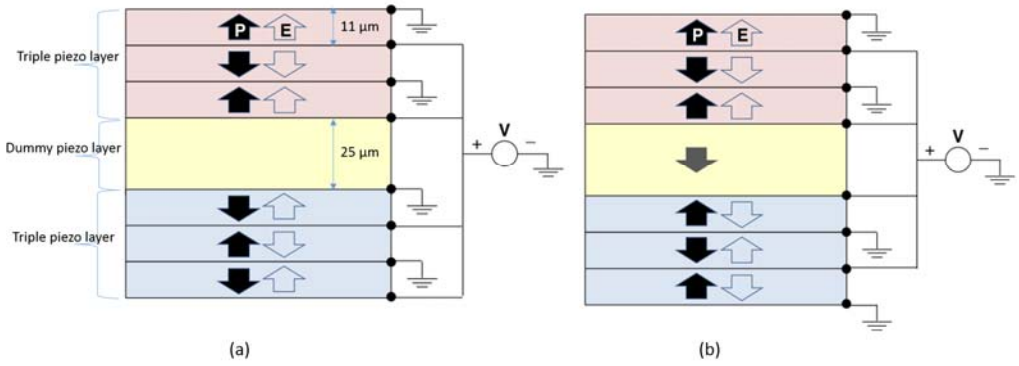

Figure 2-7: Schematic configurations a) SMS and b) PMP where P shows the polarization direction, while E shows applied electric field direction for each layer after Kim, H. et al [27]

Another type of acoustic transducer is an ultrasonic transmitter. Some ultrasonic transmitters use water as a medium but this thesis refers to ultrasonic transmitters which use air as a medium. Their application is mostly as distance sensors, which have a common working frequency of 40 kHz. Similar to the buzzer, the conventional structure of the transducer consists of an acoustic diaphragm and a piezoelectric ceramic disk. Different from the buzzer, the transmitter has a resonator, which is fixed at the centre of the diaphragm, and elastic material under the diaphragm. Their cases act to maximize the acoustic power and narrow the acoustic transmitting beam, as shown in Figure 2-8:

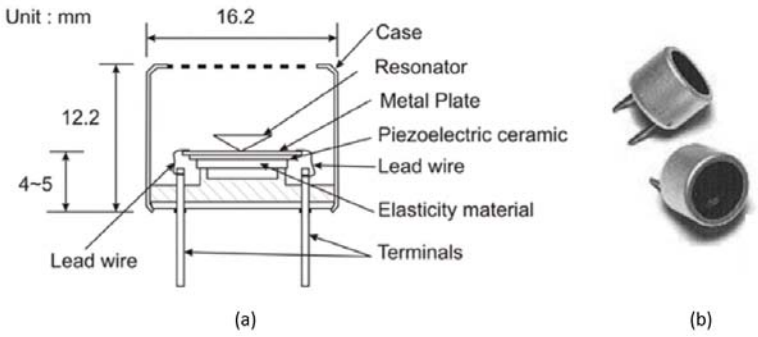

Figure 2-8: a) diagrammatic representation of an ultrasonic transducer and b) the transducers.after Senthilkumar and Vinothraj [32]

2.2.1.2 Excitation Force of Piezoelectric Transducer

In general, for the piezoelectric transducer, it is assumed that the relationship between electrical charge (q) and relative displacement (w) is linear. The relative displacement is expansion, compression or movement of a transducer for the original displacement while the electrical charge in the transducer changes. It is given by [33]:

$$q(t) = K_q w(t) \tag{2.34}$$

where K_q is the charge output of unit displacement. When differentiating both sides of the equation with respect to time, it can be expressed by [33]:

$$i_{PZT}(t) = \frac{dq(t)}{dt} = K_q \dot{w}(t) \tag{2.35}$$

where i_{PZT} is the current feeding the transducer. The analogous circuit of the transducer for the electrical subsystem is shown in Figure 2-9.

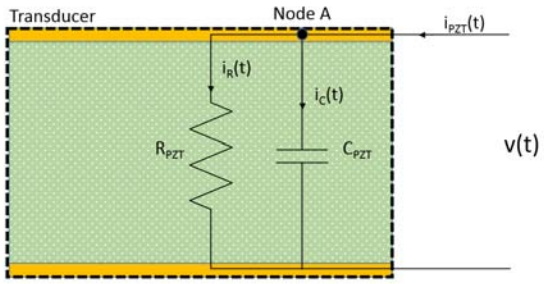

Figure 2-9: Analogous circuit of a piezoelectric transducer

where R_{PZT} and C_{PZT} are PZT resistance and capacitance, (which is the impedance of the transducer resulting from the leakage of current between both the electrodes of the transducer). In general, R_{PZT} is approximately $10^{11}\,\Omega$ [33], while C_{PZT} depends on the shape of the transducer and the dielectric constant of the piezoelectric material. It can be expressed by [31]:

$$C_{PZT} = \frac{\varepsilon_t \varepsilon_0 a_t}{h_t} \tag{2.36}$$

where a_t and h_t are the area and thickness of the transducer. The area is dependent on the shape of the transducer, for example a rectangle or circle. ε_t is the relative dielectric constant and ε_0 is the dielectric of free space(8.85×10^{-12} farad/m). The range of dielectric of PZT is between 1000 and 4000 [31].

Therefore, from the circuit, solving the relationship between the voltage feeding the transducer and the surface velocity of the transducer, by applying Kirchhoff's Current Law (KCL) at Node A, it yields:

$$i_{PZT}(t) = i_C(t) + i_R(t) \tag{2.37}$$

or

$$K_q \dot{w}(t) = C\dot{v}(t) + \frac{v(t)}{R} \quad (2.38)$$

when altering current form to voltage form and substituting Eq.(2.35) into (2.37). In order to find the force resulting from the change of voltage, differentiating both sides with respect to time and multiplying it by mass, the excitation force($f_e(t)$) is expressed as:

$$f_e(t) = M\ddot{w}(t) = \frac{MC}{K_q}\left(\ddot{v}(t) + \frac{\dot{v}(t)}{RC}\right) = \frac{M}{S_e}\left(\ddot{v}(t) + \frac{\dot{v}(t)}{\tau}\right) \quad (2.39)$$

where K_q is the charged output of unit displacement. M, R and C are weight, resistance and capacitance of the transducer, respectively. $\frac{K_q}{C}$ is defined as the electric sensitivity (S_e), and RC is the time constant (τ). This equation shows that the excitation force on the transducer exists when the excited voltage changes, the force becomes zero, and the voltage is constant.

2.2.2 Electro-magnetic technologies

Eletro-magnetic technologies are commonly used for manufacture of acoustic transducer such as loudspeaker and buzzer.

2.2.2.1 Magnetic Buzzer

A magnetic buzzer is the original small audio signalling device. It is commonly used in alarm devices. As shown in Figure 2-10, the structure of a typical buzzer mainly consists of a diaphragm, weight diaphragm and a pole wrapped with a winding coil, which acts as an electrical magnet. The diaphragm is vibrated by attraction of the pole with the magnetic field. When electrical pulses are applied through the coil, it produces a fluctuating magnetic field, which vibrates the diaphragm at a frequency equal to that of the drive pulse.

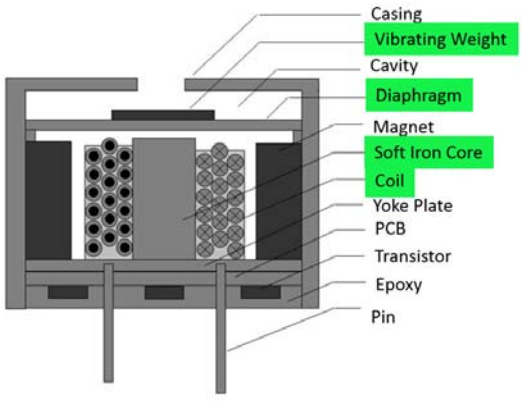

Figure 2-10: Schematic diagram of a buzzer

2.2.2.2 Excitation Force of Magnetic Buzzer

The calculation of the attractive force is not exactly determined by analytical theory because of the assumption that magnetic fluxes are uniform, as shown in Figure 2-11a, whereas in reality they are variably distributed. However, it enables us to understand the relationship between parameters in the model, such as force, voltage and the number of winding turns, before computation in FEM modelling or design and measurement from a device.

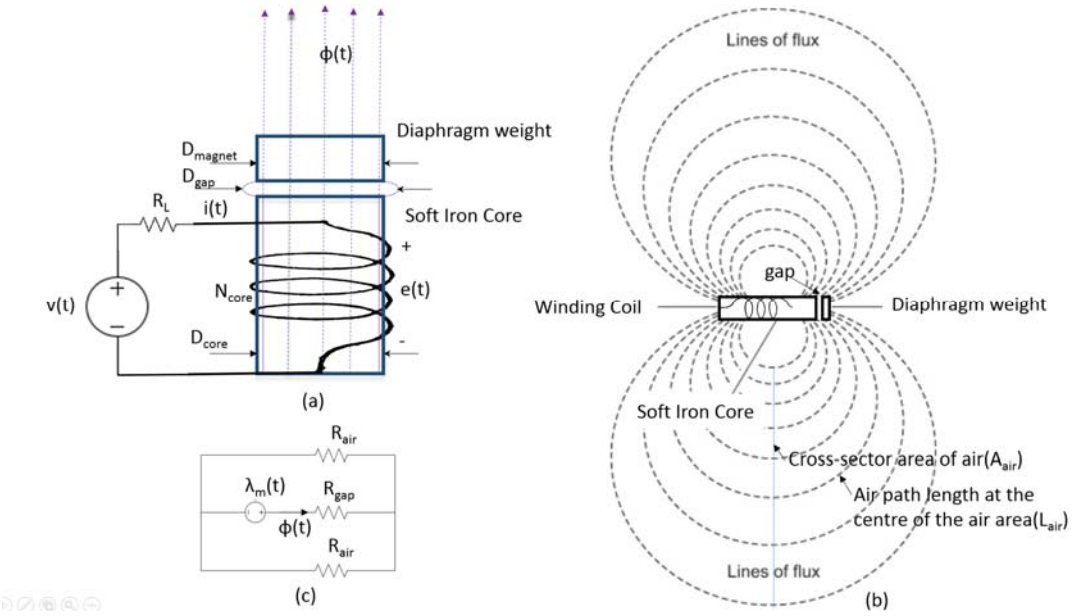

Figure 2-11:a) a) Magnetic flux within the core b) Magnetic flux outside the core c) Equivalent circuit after Fitzgerald, A. el at [34]

In order to calculate the exciting force, which vibrates the diaphragm, voltage is applied to the coil. It will generate a magnetic flux from the north pole (or the top) of the iron core through a thin air gap and iron or magnetic diaphragm weight as shown in Figure 2-11a and then the flux will bend and return to the south pole (or the bottom) of the core as shown in Figure 2-11b. The magnetic flux can be represented in the schematic equivalent magnetic circuit, as shown in Figure 2-11c. When the coil is induced with a voltage (e) it will produce a flux according to [34]:

$$e(t) = N\frac{d\phi(t)}{dt} = \frac{d\lambda_m(t)}{dt} \tag{2.40}$$

where λ_m is the flux linkage of the coil and is defined in units of weber-turns as [34]:

$$\lambda_m(t) = N\phi(t) \tag{2.41}$$

where $\phi(t)\ is$ the flux and N is the number of turns of the coil. The relationship between the linkage and the applied current(i) can be found from Eq. (2.41) to Eq.(2.43) the magnetomotive force (mmf) can be determined from the flux [34]:

$$F_{mmf} = \phi(t)R_{tot} \tag{2.42}$$

and the mmf can be determined from the current as [34]:

$$F_{mmf} = Ni(t) \tag{2.43}$$

Substituting the mmf from Eq.(2.43) into the flux Eq.(2.42) and then substituting the flux into Eq.(2.41), the relationship between the linkage and the current can be expressed as [34]:

$$\lambda_m(t) = \frac{N^2 i(t)}{R_{tot}} \tag{2.44}$$

The total reluctance R_{tot} of the equivalent circuit can be computed from R_{gap} in series with a parallel of R_{air}. R_{gap}, which is the reluctance of the gap between the core and the weight, which can be approximately computed by neglecting the fringe effect. The cross-sectional area of core (A_{core}) and the cross-sectional area of the air gap (A_{gap}) are assumed by neglecting that they are equivalent ($A_{gap} \approx A_{core}$) [34]:

$$R_{gap}(w_g) = \frac{w_g}{\mu_{air} A_{core}} \tag{2.45}$$

where μ_{air} is the air permeability, which is equal to $4\pi x10^{-7}$ in units of Henries per metre and w_g is the distance of the air gap. When the diaphragm vibrates it relates to the displacement (w) of the diaphragm weight as:

$$w_g = W_0 + w(t) \tag{2.46}$$

where W_0 is the distance between the core and the weight when the diaphragm is in the equilibrium position. R_{air} is difficult to compute because l_{air} and A_{air} are difficult to estimate.It needs to be done with FEM software. However, l_{air} and A_{air} can be written in terms of w_g in some ways. The total reluctance R_{tot} can be written as:

$$R_{tot}(w_g) = R_{gap}(w_g) + 0.5\, R_{air}(w_g) \tag{2.47}$$

The inductance L can be defined as [34]:

$$L = \frac{\lambda_m(t)}{i(t)} \tag{2.48}$$

Comparing Eqs (2.44) and (2.48), the inductance can be written in terms of w_g as [34]:

$$L(w_g) = \frac{N^2}{R_{tot}(w_g)} \tag{2.49}$$

The power at the terminals of the coil (p_m) can be computed from the product of current and voltage feeding to the coil, from Eq (2.40). It can be expressed as[34]:

$$\mathrm{p}_m = iv = i\frac{d\lambda_m(t)}{dt} \tag{2.50}$$

From Eq.(2.50), the change in magnetic stored energy (in units of watts or joules per second) in the circuit in the period between t_1 and t_2 is[34]:

$$\Delta W = \int_{t_1}^{t_2} p_m dt = \int_{\lambda_m(t_1)}^{\lambda_m(t_2)} id\lambda_m = \int_{\lambda_m(t_1)}^{\lambda_m(t_2)} \frac{\lambda_m}{L(w_g)} d\lambda_m = \frac{{\lambda_m}^2(t_2) - {\lambda_m}^2(t_1)}{2L(w_g)} \tag{2.51}$$

when substituting i from Eq(2.48) into it. After integration at the time (t1), the current is assumed as zero and the flux linkage is zero and the stored energy can be [34]:

$$\Delta W = \frac{{\lambda_m}^2(t_2))}{2L(w_g)} \tag{2.52}$$

Magnetic force (f_m) can be computed by the partial derivation of the stored energy by distance (w_g) while the linkage is constant and substitution of the linkage from Eq.(2.48) [34]:

$$\begin{aligned} \mathrm{f}_m(t) &= -\left.\frac{\partial W(\lambda_m, w_g)}{\partial w_g}\right|_{\lambda_m} = -\left.\frac{\partial W(\lambda_m, w_g)}{\partial L(w_g)}\frac{dL(w_g)}{dw_g}\right|_{\lambda_m} = \frac{{\lambda_m}^2(t)}{2L^2(w_g)}\frac{dL(w_g)}{dw_g} \\ &= \frac{i^2(t)}{2}\frac{dL(w_g)}{dw_g} = -\frac{i^2(t)}{2}\left|\frac{dL(w_g)}{dw_g}\right| \end{aligned} \tag{2.53}$$

From the common behaviour of magnets, the inductance reduces when the gap increases. The inductance changes rapidly when the gap is narrow, while the inductance changes gradually when the gap is wide. The inductance becomes zero if the gap is wide enough. As a result, the bigger the force is, the smaller the gap is, when the current is constant. $\frac{dL(w_g)}{dw_g}$ is always negative, which defines the pulse direction as out from the core. The direction of the force has only one way, which is attractive (negative) to the core, and the force varies as the square of the magnitude of the current. The electrical equation for this model is[34]:

$$\mathrm{v(t)} = i(t)R_c + \frac{d\lambda_m(t)}{dt} \tag{2.54}$$

where R_c is the electrical resistance of the coil. Substituting the linkage from Eq.(2.48) into Eq.(2.54) and differentiating it, it can be written as[34]:

$$\mathrm{v(t)} = i(t)R + \frac{dL(w_g)i(t)}{dt} = i(t)R_c + L(w_g)\frac{di(t)}{dt} + i(t)\frac{dL(w_g)}{dt} \qquad (2.55)$$
$$= i(t)(R_c + \frac{dL(w_g)}{dw_g}\frac{dw_g}{dt}) + L(w_g)\frac{di(t)}{dt}$$

2.2.2.3 Moving Coil Loudspeaker

The moving coil loudspeaker is a typical loudspeaker. There are three main parts: cone diaphragm, a metal coil and permanent magnet. The diaphragm is attached to the coil, which is called a voice coil, shown in Figure 2-12:

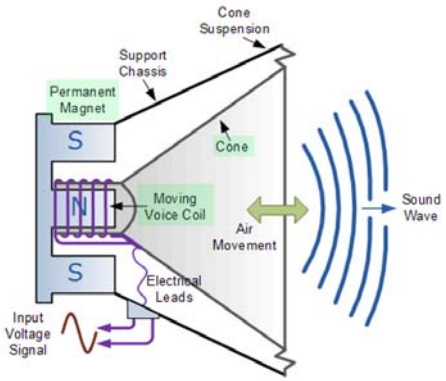

Figure 2-12: Moving coil loudspeaker

The cone is vibrated by force on the coil when an electrical pulse passes though the coil, which is placed within the magnet's magnetic field. This will induce the force pushing the coil in one direction, depending on the direction of the magnetic field and current flow and then vibrate the diaphragm. The force comes from the force on a particle of charge moving in the presence of the electric and the magnetic field.

From Weber, C. et al[35], another interesting acoustic actuator involves a microstructure and produces a high SPL, which is a good characteristic for a potential digital loudspeaker. Although these actuators are made with an inductive coil, which consume more electric power than piezoelectric ceramic, their microspeakers have a 2.5mm diaphragm and produce a maximum SPL at 80 dB. The MEMS speakers use a polydimetylsiloxane (PDMS) membrane as the acoustic diaphragm, which has a good SPL at low frequencies. The membrane is attached by a 5 turn coil at the centre of the 2.5mm diaphragm on the top of the Neodymium (NdFeB) hard magnet, which

has a thickness of 1.5mm and a diameter of 2mm on the bottom. The size and placement of the iron-nickel soft magnet and other details of the structure are shown in Figure 2-13:

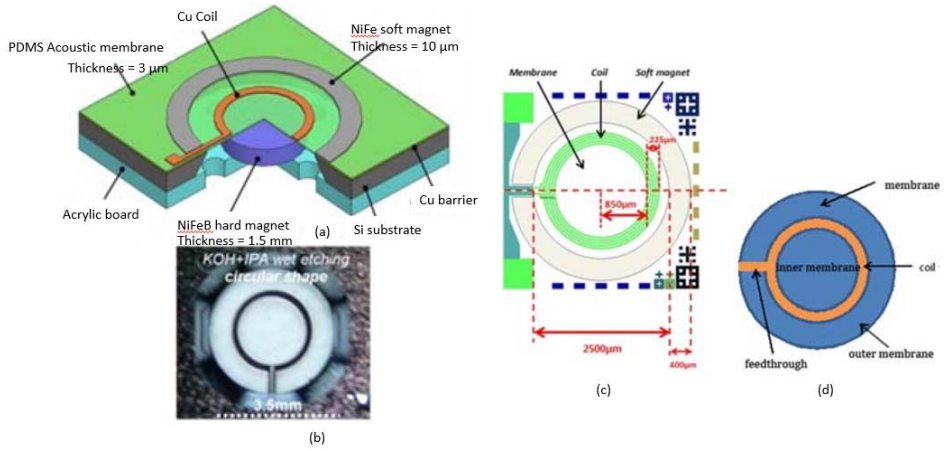

Figure 2-13: a) and b) fabricated microspeaker c) layout of microspeaker d) inner and outer part membrane placement after Weber, C. et al[35]

2.2.2.4 Excitation Force of Moving Coil loudspeaker

The force, which is called the Lorentz force, can be calculated by the product [34]:

$$F_v = J \times B_c \tag{2.56}$$

where $F_v$is force density in units of Newtons per cubic metre. J is the current density vector in units of amperes per square metre. B_c is the magnetic flux density vector of the permanent magnet, which is constant, in units of Teslas. Therefore, the magnitude of force depends on the magnitude of current in the coil, the volume of the coil in the presence of the magnetic field and the flux density of the magnet. The force (f_{coil}) will give the optimized value where the angle (θ) between the current and the magnetic field direction are perpendicular or 90°. The force on the coil in units of Newtons can be calculated by [34]:

$$f_{coil} = i(t)B_c l_c sin\theta = C_{BL} i(t) \tag{2.57}$$

The force from the coil varies according to the coil current, only when the length of the coil $l_c \ in\ units\ of\ metres$, is in the presence of the magnetic field, which is constant and we define a constant $C_{BL} = B_c l_c sin\theta$. The electrical equation for this model is [36]:

$$\mathrm{v(t)} = i(t)R_c + L_c \frac{di(t)}{dt} + C_{BL}\dot{w}(t) \tag{2.58}$$

where R_c and L_c are the resistance and the inductance of the voice coil and $\dot{w}$ is the velocity of vibration of the diaphragm.

2.2.3 Sound Generation with Ultrasound

This section will give a brief about how ultrasound can make sound and the structure of the loudspeaker.

2.2.3.1 Non linearity of acoustics

The study of the generation of sound with ultrasound relies on the non-linearity of acoustics. The study is referred to as a parametric acoustic array or parametric loudspeakers [8]. As a result of the non-linearity, the impression of air mass with increment and decrement in pressure are not equal. Figure 2-14a) shows the blue line is an assumption of acoustic linearity. In reality, the red line is a weakly non-linear relationship between pressure and specific volume ($1/\rho$), which is the inverse of density). Figure 2-14b shows an effect of the non-linearity of the medium on a pure sinewave. They found that the sinewave (blue line) become a saw-tooth wave (red line) when it travels in a non-linear medium. The sound consists of multiple tones rather than a single tone (frequency) of pure sinewave. The emerged tones from the fundamental frequency of the sinewave result from the sum and different tones among harmonics of the saw-tooth wave.

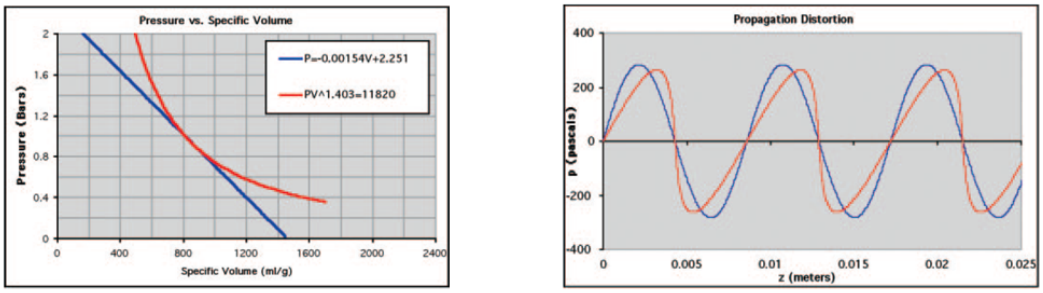

(a) (b)

Figure 2-14: a) Non-linear relationship between pressure and specific volume (red line) b) Distortion due to non-linearity of media (red line) after Croft, J.[9]

There are two common ways for sound generation from ultrasound: two transducers with different frequencies, or one transducer with amplitude modulation circuits.

- The pressure wave of the first way, two transducers with different frequencies can be expressed as:

$$\begin{aligned} \mathrm{p(t)} &= \mathrm{A}\cos(2\pi f_{u1}) + \mathrm{A}\cos(2\pi f_{u2}) \\ &= 2A\cos(2\pi(\frac{f_{u1}-f_{u2}}{2}))\cos(2\pi(\frac{f_{u1}+f_{u2}}{2})) \end{aligned} \quad (2.59)$$

where f_{u1} and f_{u2} are the wave frequencies from both transmitters. The wave is similar to that from an ultrasonic transmitter emitting a wave with amplitude modulation.

- The pressure wave of the second way, one transducer with AM can be expressed as:

$$p(t) = \left(A_c + A_a cos(2\pi f_a t)\right) cos(2\pi f_c t) = A_m(t)\, cos(2\pi f_c t) \quad (2.60)$$

where

$$A_m(t) = \left(A_c + A_a cos(2\pi f_a t)\right) \quad (2.61)$$

This equation is the same as for an electro-magnetic wave with amplitude modulation (the second way). The wave consists of audio frequency (or message) and carrier frequency. A_c and A_a are the amplitude of the carrier and the audio wave respectively, while f_c and f_a are the frequency of the carrier and the audio wave respectively. The carrier frequency is defined as a constant frequency in the ultrasonic range, while the audio frequency can vary within the audible band of frequencies. An example of $A_a = A_c$,f_c= 44kHz and f_a=2kHz is shown in Figure 2-15a. The case of two transmitters is considered as a case within modulating transmitter cases as the carrier frequency ($f_c = 0.5(f_{u1}+f_{u2})$), the audio frequency ($f_a = 0.5(f_{u1}-f_{u2})$), audio amplitude (A_a= 2A) and carrier amplitude (A_c =0), as shown is Figure 2-15b. It can be seen that all frequencies could be within the ultrasonic range if the air medium was linear between pressure and specific volume, as shown in frequency graphs in Figure 2-15:

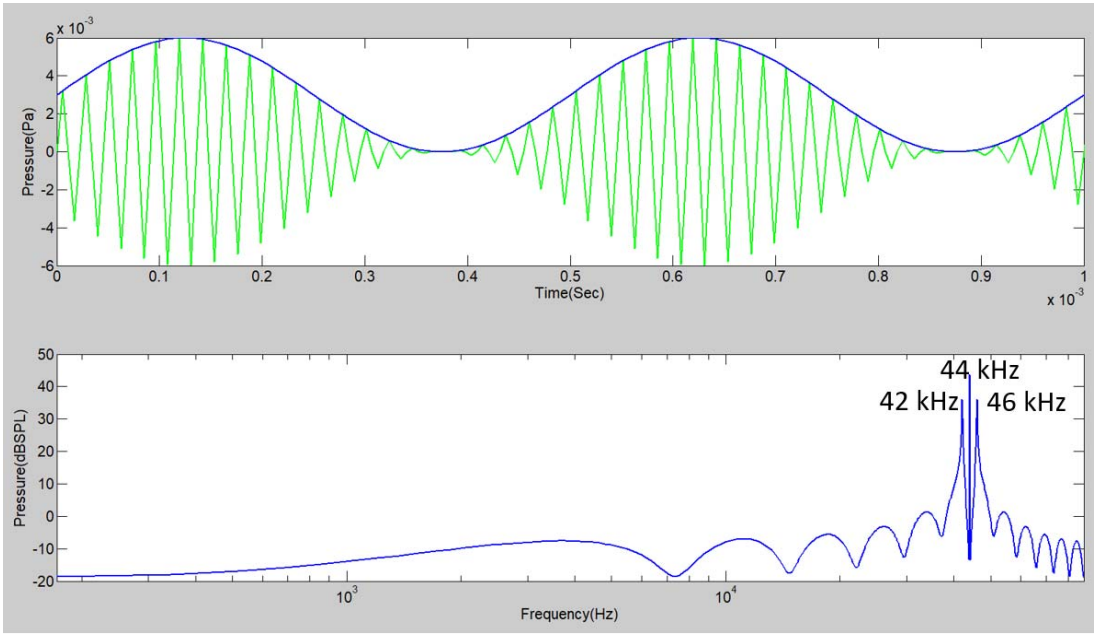

Figure 2-15: Temporal and frequency response of one transducer with amplitude modulation circuits for an audio frequency of 2 kHz and carrier frequency 44 kHz.

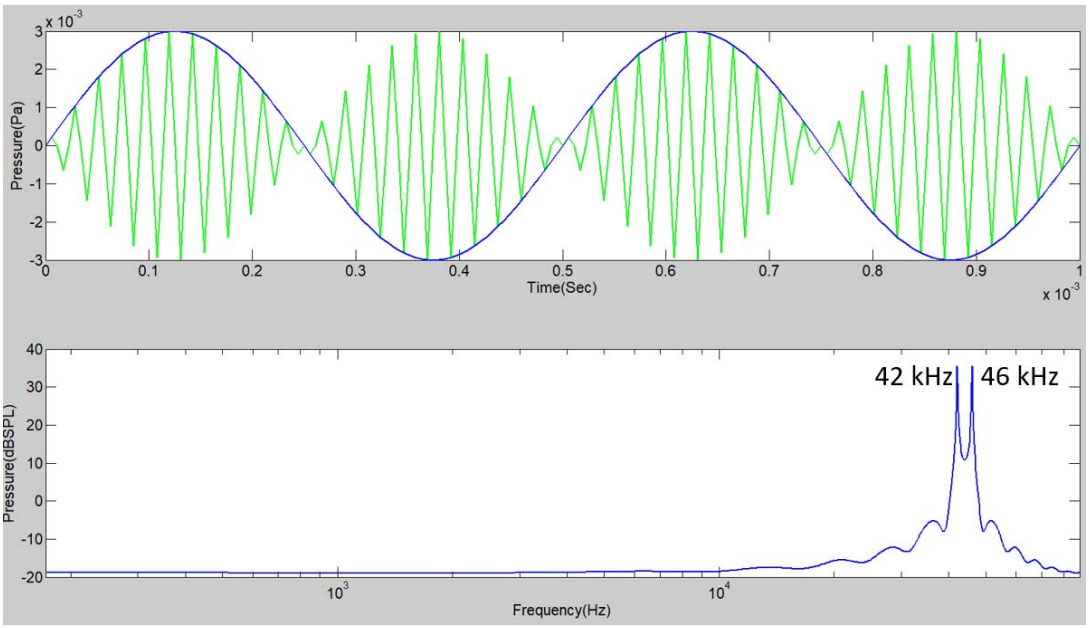

Figure 2-16: Temporal and frequency response of two transducers with different frequencies of f_{u1} and f_{u2} (42 and 46 kHz) (b)

With the non-linear effect in the medium, the waves of two different frequencies which interact, will produce two frequencies of the sum and difference frequency, which are referred to as beat frequencies, as shown in Figure 2-17. Calculation of beat frequencies from the non-linearity is discussed by Wetervet [37]and Joseph[38]:

Figure 2-17: Non-linear interaction process in air (frequencies in green font produced by non-linearity) after Wen-Kung,T [39]

2.2.3.2 Parametric Array

In their early state, parametric loudspeakers were developed from piezo-ceramic transducers. This made the loudspeaker reproduce sound in a very limited bandwidth. Based on polyvinylidenedifluoride(PVDF), a thin moving film, the bandwidth of the loudspeakers is extended to be able to reproduce broadband audio signals with reasonable loudness. Several patents have been granted and some commercial products based on parametric loudspeakers are available. It is referred as audio spotlight.

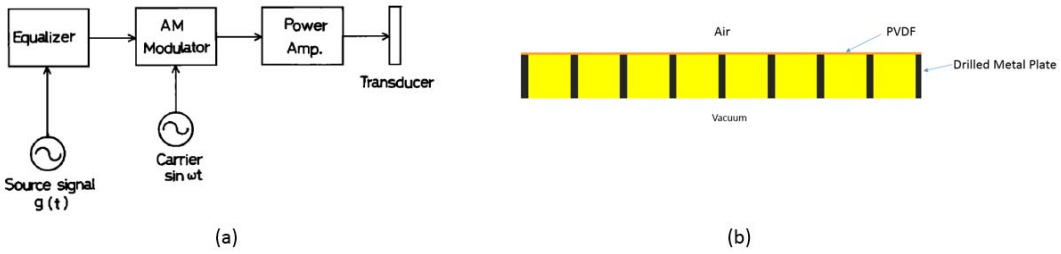

Figure 2-18: a) Structure of transducer after Yoneyama, M. and Fujimoto, J. [40]] and b) Construction of loudspeaker after Croft, J.[9].

The structure of the loudspeaker is shown in Figure 2-18a. The first loudspeaker was built with a diameter of 44.45 mm with 85 holes of a diameter of 3.57 mm. The holes were arranged in a tight hexagonal pattern with interspacing of 4.06 mm. The thickness of the film was 0.28 µm. Under the film was a nearly full vacuum in order to prevent sound radiation to the back. The resonant frequency was 37.23 kHz and the output was 136 dBSPL with 73.6 V_{pp}. Due to the considerately high voltage, the loudspeaker required a high power amplifier for feeding the modulated signal into the loudspeaker. Because the frequency response of transducers is quite steep, an equalizer was required to adjust the frequency response, as shown in Figure 2-18b.

Although a parametric array can produce audible sound, its beam width is very narrow because the wave frequencies, which are emitted with the amplitude modulation by the loudspeaker, are very high and within the ultrasonic frequency range, while the beam of sound from the transducer

normally emitting audible waves is omni-directional, as shown in Figure 2-19. This corresponds to the relationship between beam width and diameter, which have been discussed in Chapter 2.1.3.4.

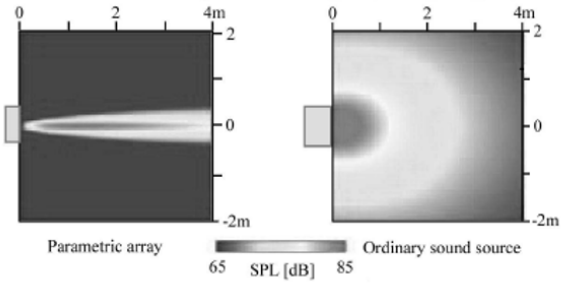

Figure 2-19: Difference of beam width of a 10 mm diameter transducer emitting sound at 2kHz between a parametric array and an ordinary sound source after Kamakura, T. and Aoki,K.[30.]

In addition to audio spotlight, Long-range acoustic device (LRAD) cooperation is a company producing the loudspeakers using in military[42] and Usound is a company, which is going to commercially produce the loudspeakers based on piezoelectric composition with MEMs[4].

2.2.4 The Voice as Bio-loudspeaker

The human voice system is considered as a sound generator, whose principle is applied for design a new structure of speaklet proposed in Chapter 5. There are three major parts in the system: lungs, larynx and vocal cavities. Sound is mainly generated by the vibration of the vocal cords in the larynx. The lungs, which act as an air pump, pass the air through the vocal cords, which are string-like membranes, in the larynx. The frequency of vibration is determined mainly by the muscular tension applied to the cords. Each time the cords vibrate, a sharp gust of air is emitted through the glottis, which is an air opening, into the vocal cavities[16]. As a result, the frequency of air gusts is synchronized with the frequency of cord vibration. Figure 2-20 shows a train of vibrations resulting from the gust, which are of two types: bright and dark tones. The bright tone, which is an overtone sound, is produced when the vocal cords completely close. The dark tone, which is a sound like a sine wave, is produced when the air can pass though the vocal cords because they do not completely close [16]. The vocal cavity, which extends from the larynx to the mouth and the nose, acts as an adjustable frequency filter. The simple airflow spectrum, which is provided by the vocal cords, is transformed into the recognizable patterns for making speech or song. The two main organs which transform the sound frequencies are the tongue and the lips. Each position produces a different sound. The spectrum of the voice consists of two or three

peaks, which are referred to as formants. For men, the first formant is between 150 - 850 Hz and the second formant is 500 - 2500 Hz [16].

.

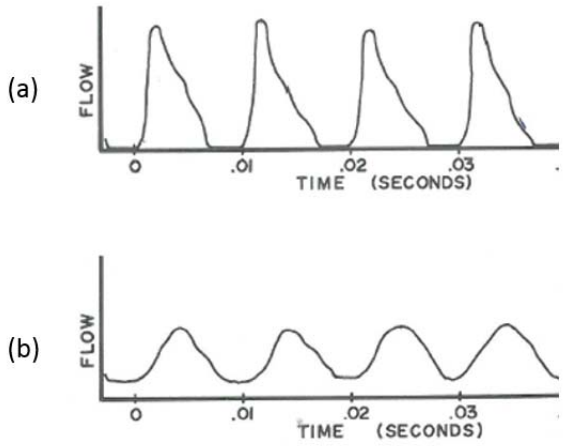

Figure 2-20: Air Flow Patterns from a Larynx a) bright tone b) dark tone after Arthur, B. [16]

Another creature, whose voice is in the ultrasonic range is the bat. Microbats produces ultrasound for echolocation with their larynx and project it through the mouth and the nasal opening, similar to the sound of humans or mammals. Due to an extremely thin vocal membrane, air pressure from the lungs and pressure fluctuation from the muscles of the chest and belly used for flapping their wings, bats produce a sound between 12-200 kHz [43].

The mechanism of sound generation of the larynx can be analogous, as shown in Figure 2-21. The vocal cord acts as a vertical spring mass system, which will close and open airflow from the lungs to the vocal tract, like a valve. When the mass vibrates up and down, a series of gusts of air are produced according to the frequency of the vibration.

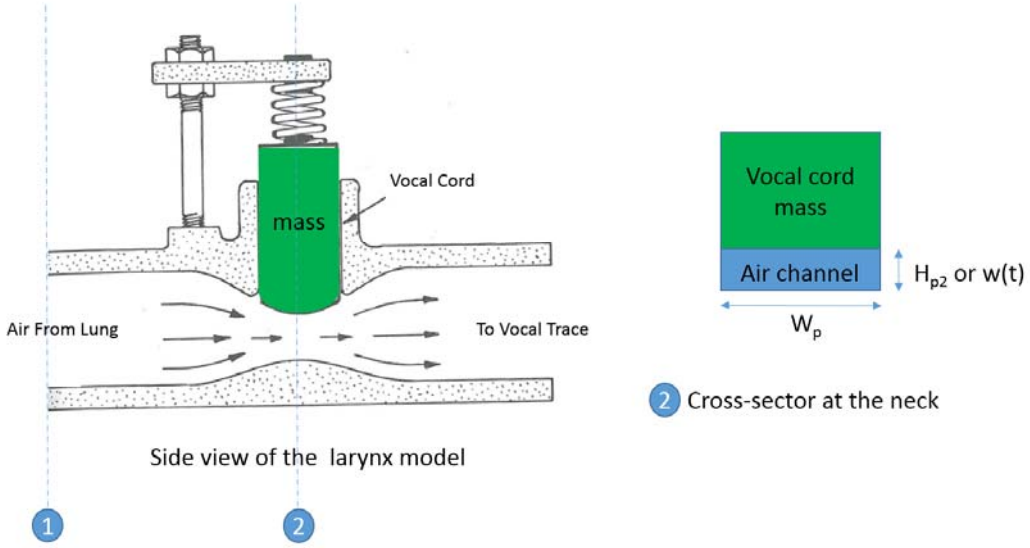

Figure 2-21: A mechanical analogous model of the larynx after Arthur, B. [16]

In order to understand this mechanism, there are six basic ideas of fluid mechanics:

- Air will flow from an area of high pressure (lungs) to low pressure (vocal tract)
- At a given spot airflow with high speed will have lower pressure than at another spot with low speed airflow when both spots are at the same height. Bernoulli's equation can be expressed as [44]:

$$\frac{P_1}{\rho g} + \frac{\dot{W}_1{}^2}{2g} + z_1 = \frac{P_2}{\rho g} + \frac{\dot{W}_2{}^2}{2g} + z_2 \qquad (2.62)$$

  where $\dot{W}_1$ and $\dot{W}_2$ are the average velocities in unit m/s at points 1 and 2 within the pipe. However, this equation is restricted to steady flow, no friction and laminar and incompressible flow. If it is assumed that the temperature of the whole system is equal, airflow can be considered as incompressible flow. Although in this case it is unsteady flow due to the moving of the vocal cords and Bernoulli's theorem does not hold true, the sine wave at the opening will lag behind in phase by a small amount due to the inertia of the flowing air.
- If a fluid flows with steady and continuous state, the velocity in any narrow part of the pipe will be higher. The continuity equation is derived from the volume flow rate (Q) which is equal at every spot within the pipe. The equation of volume flow rate can be expressed as [44]:

$$Q = A_1\dot{W}_1 = A_2\dot{W}_2 \qquad (2.63)$$

where $\dot{W}_1$ and $\dot{W}_2$ are the average flow rates in unit m/s at points 1 and 2 within the pipe. A_1 and A_2 are the cross-sectional areas at the spots

- Pressure at the narrow parts is lower than pressure at the broad parts of the pipe
- When the opening at the vocal cord is narrowed, the total volume of airflow is reduced due to an increase in viscous friction
- The viscosity of flow has an effect on the velocity in each layer. Viscosity (μ) is a measurement of a fluid's resistance to deformation under shear stress (τ). It is related to shear stress and velocity gradient (du/dy) as:

$$\mu = \frac{\tau}{du/dy} \tag{2.64}$$

when $\mu_1 < \mu_2$, the velocity gradient of fluid 1 is greater than the velocity gradient of fluid 2 under the same shear stress. The smaller the gap is in the velocity in each y layer, the lower the viscosity is as shown in Figure 2-22. The viscosity of air is $1.983X10^{-5}$ while the viscosity of water is 10^{-3} at room temperature.

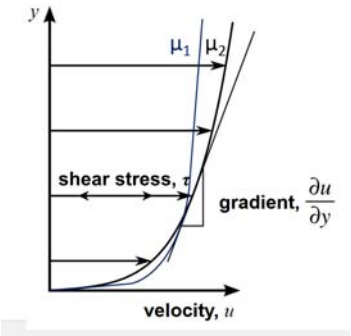

Figure 2-22 Velocity distribution next to a boundary after White, F.

Flow rate (Q) through the analogous vocal cord in Figure 2-21 might be estimated by assuming a steady state, incompressible air (constant air density), air with very low viscosity (inviscid flow) and laminar flow with negligible frictional losses and a small change in elevation due to low density of airflow. Therefore, relating the conservation of energy, the Bernoulli's equation (Eq.(2.62)) can be reduced to:

$$P_1 + \frac{\rho \dot{W}_1^{\,2}}{2} = P_2 + \frac{\rho \dot{W}_2^{\,2}}{2} \tag{2.65}$$

By substituting the continuity equation (Eq.(2.63)), the equation can be rearranged as:

$$P_1 - P_2 = \frac{\rho}{2}\left(\frac{Q}{A_2}\right)^2 - \frac{\rho}{2}\left(\frac{Q}{A_1}\right)^2 \tag{2.66}$$

Solving for Q, the equation can be rearranged into multiplication of 3 terms; area of the neck of the pipe, ratio of areas between the pipe and the neck and the pressure difference as shown in:

$$Q = A_2 \sqrt{\frac{1}{1 - \left(\frac{A_2}{A_1}\right)^2}} \sqrt{\frac{2(P_1 - P_2)}{\rho}} \tag{2.67}$$

If we define that the pipe is rectangular with height (H_p) and width (W_p) as shown in Figure 2-21, the area of the neck is dependent on the height of the neck (H_{p2}) when the width (W_p) of the whole pipe is the same and constant. The height of the neck varies according to the displacement of the vocal cord mass. If the height of the neck is far smaller than the height of the pipe and the change in displacement (of vibration of vocal cord) is very small compared to the height of the pipe, the second term can be approximately constant and equal to 1. If we define the pressure difference between the lungs (P_1) and the neck (P_2) as constant, the third term is constant. Therefore, the volume flow rate varies directly as the displacement of the vocal cord mass (w(t)) where C_{pipe} is a constant as shown in:

$$Q(t) = C_{pipe} w(t) = \sqrt{\frac{2(P_1 - P_2)}{\rho}} W_p w(t) \tag{2.68}$$

Although this equation is not exactly correct because Bernoulli's theorem does not hold true in unsteady flow from the vibration of the vocal cord, it is a good approximation for calculation in FEM modelling software.

A rapid change of the volume flow rate can generate sound with frequencies according to vibration of the air gate or the vocal cord.

2.3 Concept of Digital Loudspeaker Array

This section will review the principle of digital loudspeaker array and its related works

2.3.1 Concept of Digital reconstruction

The working principle of a digital loudspeaker array (DLA), or a digital transducer array (DTA) is the reproduction of acoustic sound by an array of speakers directly accepting a digital signal. Therefore, the acoustic sound is directly translated from a digital signal without digital to analogue conversion (DAC) [45]. In other words, the process of DAC is shifted to the very end of the audio reproduction. This reproduction results from the overlapping effect among steams of

discrete pulses (or clicks) of acoustic energy, which are reproduced from speakers or micro speakers, which are called speaklets, within the array. Therefore, for sound reconstruction, the loudness of sound is dependent on a number of speaklets emitting clicks, while the frequency is dependent on time-varying numbers of speaklets emitting clicks, as shown in Figure 2-23.

Contrary to the acoustic reproduction of a traditional analogue speaker, where the loudness of sound depends on the magnitude of motion of the diaphragm in the speaker and the frequencies of sound depend on time-varying motion magnitude, as shown in Figure 2 24, for the practical reconstruction of digital sound, each speaklet emits a train of pulses. The emitted pulses of all the speaklets at each point in time are combined to reconstruct the acoustic waveform.

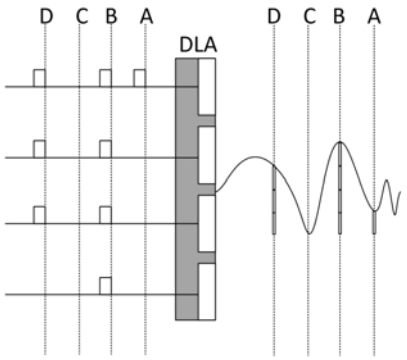

Figure 2-23 The acoustic sound is ideally reconstructed by 2-bit DLA (4 speaklets).Each speaklet is driven by a train of constant pulses in order to generate clicks. Different points (A, B, C and D) in wave are dependent on number of speaklet emitting the click.

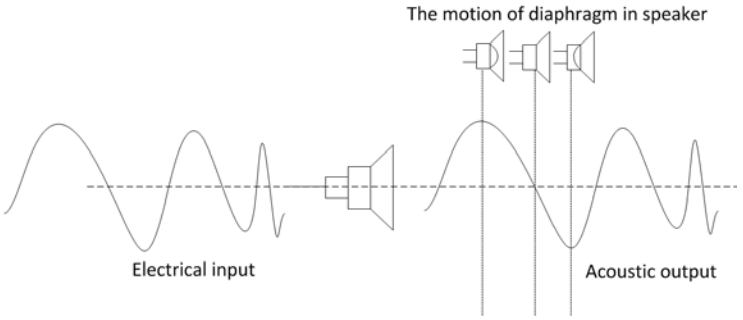

Figure 2-24: The reconstruction of a conventional analogue loudspeaker, which shows the relation between the positions of diaphagm and the positions in the the acoutic waveform. The movement of diaphagm are forced by the electrical input signal feeding the loudspeaker.

2.3.2 Terminology of Acoustic Response

There are three main parameters which characterize the acoustic response of speaklets. The first parameter is response time (RT) which can be measured from the start of the digital pulse

actuating a speaklet to the time the acoustic output of the speaklet reaches a peak. The magnitude of the peak, which can be measured from the reference point to the peak, is the second parameter, called maximum pressure (MP). The last parameter is the emitting time (ET) and can be measured from the start of the digital pulse to the acoustic output reducing to negligible levels, as shown in Figure 2-25. In addition, there are two main parameters of the pulses, which are used for actuating speaklets within DLA. The two parameters are pulse voltage (PV) and pulse width (PW), as depicted in Figure 2-25.

In order to combine acoustic response, there are three additional observed points. The first point is take-off time, which is the period between the time when the electrical pulse is raised and the time when the acoustic output starts raising. The turn-back time is the first time the acoustic response returns to zero. The minimum pressure time is the time the acoustic response reaches minimum pressure.

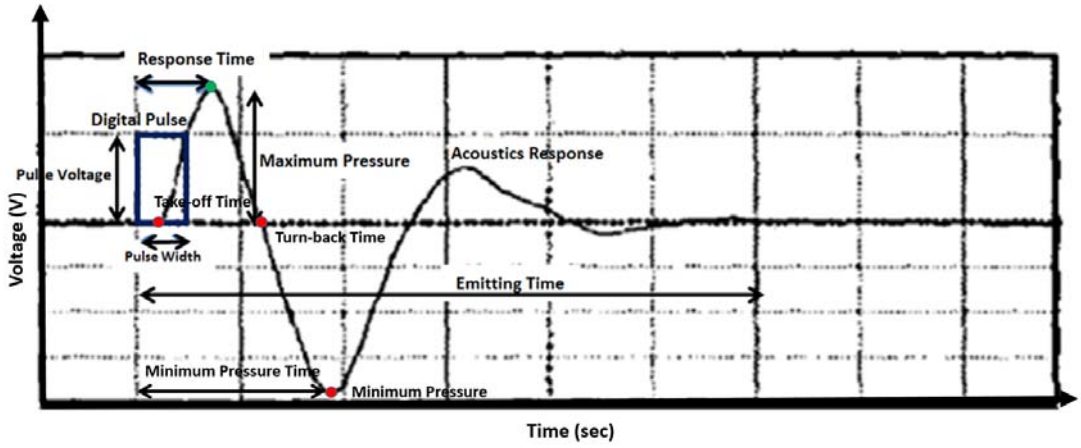

Figure 2-25: an acoustic output of a speaklet is driven by a discrete pulse after Diamond, B. M. et al.[1]

2.3.3 Requirement of Digital reconstruction

For the digital reconstruction of a DLA or a DTA, there are three basic requirements. Firstly, the emitting time should be in the order of tens of microseconds and equal to, or less than the sampling rate of digital audio information required to convert an analogue acoustic waveform [1]. Therefore, in order to reproduce sound at the quality of a typical commercial audio system, the emitting time of the speaklets must be equal to or less than 23 μs (44.1 kHz).

Secondly, all speaklets in the array must have uniform acoustic responses and every repeated response must be the same over time [1].

Finally, the steps of increase or decrease in the maximum pressure of the acoustic responses of multiple-level speaklets must be linear [1]. Not only is this requirement essential to digitally reconstructed sound, but it is also important in predicting the sound pressure level (SPL). Sound pressure depends on the number of speaklets.

2.3.4 Typical Structure of a Digital Loudspeaker Array

Typically, the system of a digital loudspeaker can be divided into three main parts: digital signal processing (DSP), digital audio amplifiers (AMPs) and the loudspeaker array (LA), as shown in Figure 2-26[13]:

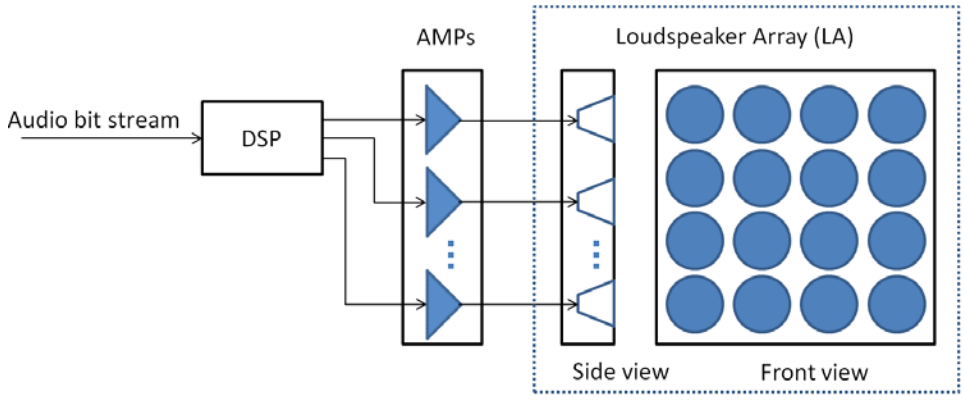

Figure 2-26: Typical structure of DLA system after Tatlas, N. [13].

For the DSP part, there are three main functions: conversion, bit assignment and digital filtering. The conversion of an input digital data stream to a digital format is appropriate to directly feeding the LA. Normally, the format is defined as pulse code modulation (PCM) or pulse width modulation (PWM), depending on the category of LA. For input digital format, the device may support serial digital formats, such as the sigma-delta modulation (SDM) format or compressed digital formats such as adaptive differential PCM (ADPCM) or MP3[46]. Bit assignment is used for assigning bit streams into the proper speakers, which reconstruct the acoustic sound from the bit streams.

Secondly, AMPs amplify bit streams, which are generated by DSP, before feeding the bit streams to speakers. The amplifiers reproduce the amplitude of pulse streams according to the voltage specification of a speaker for generating the sound.

Finally, the LA is fed with the amplified pulses. Shapes of speaker, such as circular, square or perpendicular are found to have an influence on the emitting acoustic signal, but the topology of the array has a considerable effect on signal distortion because of the path delay effect. However, topologies, which can minimize distortion, are symmetrical [10][47].

2.3.5 Design of Array and Sound Beam

Digital loudspeaker arrays (DLA), which are composed of one-dimensional or two-dimensional arrays of speaklets, are theoretically designed for controlling beam width and beam angle of the sound over a 180˚ arc [48]. The number of speaklets, the overall size of the array, the frequency response and the distance between consecutive speaklets are the main parameters affecting the performance of the DLA. The distance is referred to as interspacing (g_{array} metres) and shown in Figure 2-27:

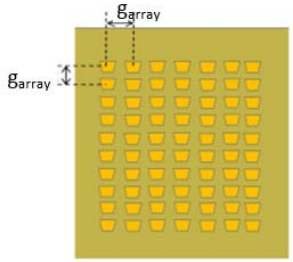

Figure 2-27: Interspacing (g_{array}) of a two-dimensional array

The overall size for a two-dimensional array can be calculated as shown in Eq. (2.69) and (2.70)[48]:

$$\text{Width of array} = (W_n - 1)g_{array} \tag{2.69}$$

where W_n is the number of elements in a row of the array.

$$\text{Height of array} = (H_n - 1)g_{array} \tag{2.70}$$

where H_n = number of elements in a column of the array.

Interspacing can be calculated as shown in Eq.(2.71) [48]. For digital loudspeakers, response frequency is equal to the natural frequency (f_n) of the speaklets, which results from the free vibration of the diaphragm of a speaklet within the array.

$$g_{array} \leq \frac{c}{2f_n} = \frac{\lambda}{2} \tag{2.71}$$

where c is the speed of sound in air (340 m/s at 20˚C) and λ is the wavelength of the response. If Eq. (2.71) is satisfied, a tightly directional beam will be produced as shown in Figure 2-28a. In contrast, if Eq(2.71) is not satisfied or one-half of the wavelength of the response is less than the

interspacing, the beam will be degraded or multiple lobes will be generated, as shown in Figure 2-28b, c and d.

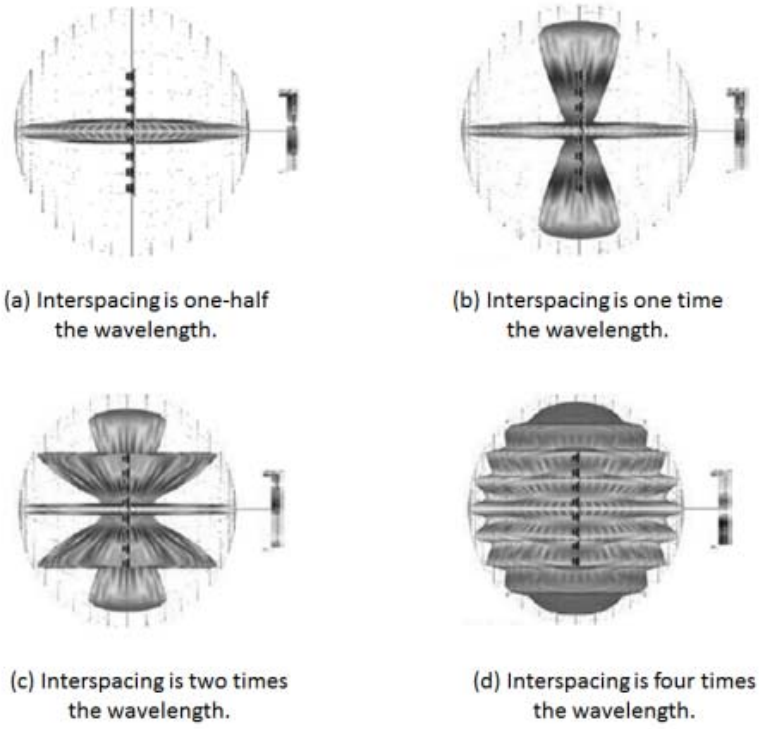

Figure 2-28 the relation between interspacing and wavelength after Ballou, G. [49].

Beam width as shown in Figure 2-29 can be controlled by the sampling frequency (f_s). The sampling frequency can be obtained from Eq.(2.72) [48]:

$$f_s = \frac{c}{\mathrm{g}_{array}\,\sin(L_x/2)} \tag{2.72}$$

where L_x is beam width in units of radians.

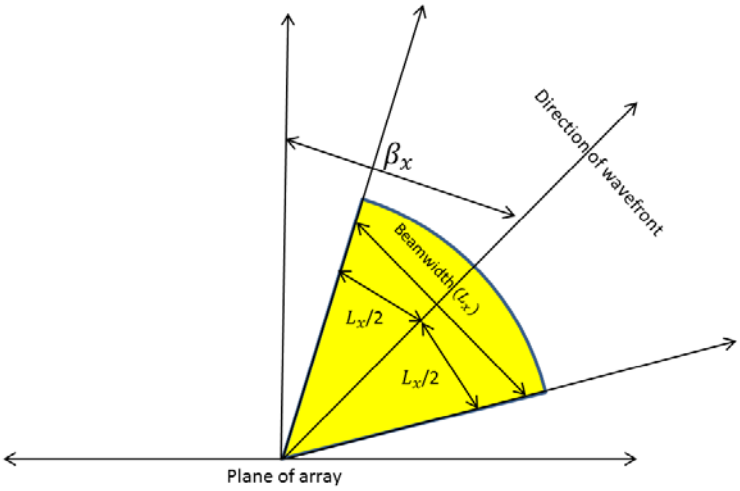

Figure 2-29: Far-field polar beam of width L_x with offset angle β_x after Hawksford, M. O. J. H [48].

Beam angle can be controlled by time delays corresponding to the delay paths (d_r). The delay paths of d_1 and d_2 means the first and second speaklets from the centre to the right-hand side while the delay paths of d_{-1} and d_{-2} means the first and second speaklets from the centre to the left-hand side, as shown in Figure 2-30. The time delay (T_r) in units of seconds can be obtained from Eq. (2.73) [48]:

$$T_r = \frac{g_{array}(0.5 + r_{path})\sin(\beta_x)}{c} \tag{2.73}$$

where r_{path} is the path index (…,-2,-1, 1, 2, …)

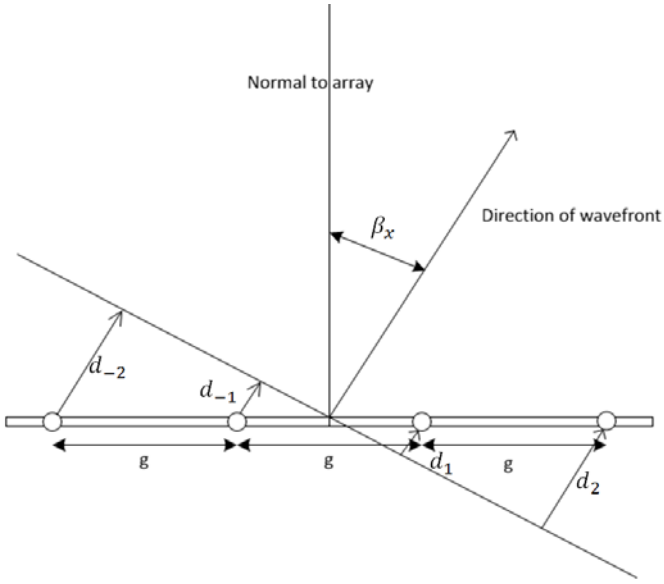

Figure 2-30: Delay paths for each speaklet for beam offset angle after Hawksford, M. O. J. H [48].

2.4 Mathematical Loudspeaker Model and Wave Propagation

This section shows derivation of vibration of a point mass and wave propagation of a point source, which are fundamentals of the mathematical model of speakets within a DLA in Chapter 3

2.4.1 Vibration for a Point Mass

The simplest way to start understanding the mechanism of a speaklet in vibration and radiation of its diaphragm is to treat the speaklet as in the mass-spring damper model. The model consists of an oscillating point mass attached to a spring and a damper, which has one degree of freedom. Such a system is schematically illustrated in Figure 2-31:

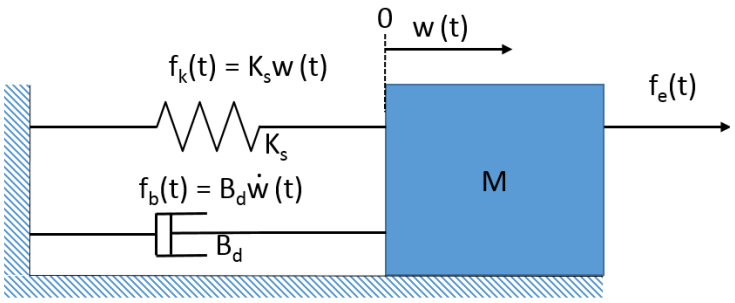

Figure 2-31: Mass-Spring damper Model

From the model, there are four forces that affect the vibration of the point mass. The first force is an inertial force generated by the mass according to Newton's second law of motion. The force can be expressed by [50]:

$$f_m(t) = M\frac{d^2w(t)}{dt^2} = M\ddot{w}(t) \tag{2.74}$$

where $\ddot{w}(t)$, f_m and M are the acceleration, the inertial force of the mass and its weight respectively. The second force is an inertial force produced by the spring. The force can be given by [1]:

$$f_K(t) = K_s w(t) \tag{2.75}$$

where $w(t)$, f_k and K_s are the displacement, the inertial force of the spring and the spring constant. The third force is an inertial force generated by the damper. The force can be expressed by [50]:

$$f_b(t) = B_d\frac{dw(t)}{dt} = B_d\dot{w}(t) \tag{2.76}$$

where $\dot{w}(t)$, f_B and B_d are velocity, the inertial force of the damper and the damping constant. The last force is an external force (f_e), which makes the mass move. Without other energy sources acting on the mass, the sum of the four forces will be zero. The equation of motion can be assembled by:

$$f_m(t) + f_b(t) + f_k(t) = f_e(t) \tag{2.77}$$

If Eq.(2.74), (2.75)and (2.76) are substituted in Eq.(2.77), the second order differential equation of motion can be obtained by [50]:

$$M\ddot{w}(t) + B_d\dot{w}(t) + K_s w(t) = f_e(t) \tag{2.78}$$

It can be rearranged as:

$$\ddot{w}(t) + 2\xi\omega_n\dot{w}(t) + \omega_n^2 w(t) = \frac{f_e(t)}{M} \tag{2.79}$$

where $\xi = \frac{B_d}{2\sqrt{K_s M}}$ and $\omega_n = \sqrt{\frac{K_s}{M}}$ [50]. ξ is defined as the proportional damping expressed as a percentage of critical damping and ω_n is defined as the angular natural frequency in units of radians/second. For more familiar units, ω_n is given by:

$$\omega_n = 2\pi f_n = \frac{2\pi}{T_n} \tag{2.80}$$

where f_n is the natural frequency in Hz and T_n is the period of one oscillation in seconds.

2.4.1.1 Free Vibration of a Point Mass

Considering the case of free vibration, there is no external force supplying the system ($f_e(t) = 0$). Therefore, Eq.(2.79) can be expressed as [50]:

$$\ddot{w}(t) + 2\xi\omega_n\dot{w}(t) + \omega_n^2 w(t) = 0 \tag{2.81}$$

This equation can be solved by a trial solution as shown in:

$$w(t) = We^{\vartheta t} \tag{2.82}$$

where W is a constant. After substituting the trial solution in Eq.(2.81) and differentiating it, the equation is reduced to simple algebra:

$$\vartheta^2 + 2\xi\omega_n\vartheta + \omega_n^2 = 0 \tag{2.83}$$

The roots of this equation will be:

$$\vartheta = \frac{-2\xi\omega_n \pm \sqrt{(2\xi\omega_n)^2 - 4\omega_n^2}}{2} = -\xi\omega_n \pm j\sqrt{\omega_n^2 - (\xi\omega_n)^2} = -\delta_d \pm j\omega_d \quad (2.84)$$

where the damping ratio (δ_d) is defined as [50] :

$$\delta_d = \xi\omega_n \quad (2.85)$$

and the damped natural frequency (ω_d) is defined as [50]:

$$\omega_d = \sqrt{\omega_n^2 - \delta_d^2} = \omega_n\sqrt{1 - \xi^2} \quad (2.86)$$

From this equation, the damping conditions can be defined by the magnitude of proportional damping (ξ). If $\xi < 1$, or an underdamped condition, the periodic oscillation will decay. If $\xi > 1$ or in an overdamped condition, the motion will decay, but not periodically. $\xi = 1$ causes a periodic and critically damped oscillation.

Therefore, the real solution of Eq.(2.81) is given by substituting (2.84) into the trial solution of (2.82):

$$w(t) = Ae^{(\delta_d + j\omega_d)t} + Be^{(\delta_d - j\omega_d)t} \quad (2.87)$$

where A and B are arbitrary constants. In order to make the whole expression real, constant B must be the complex conjugate of A because any complex number z, z + z* = 2 Re{z}. If the arbitrary constant A is defined as a complex number ($\alpha_A + j\beta_A$) and the complex notation is expressed by introducing Euler's Formula:

$$e^{jx} = \cos x + jsinx \quad (2.88)$$

$$e^{-jx} = \cos x - jsinx \quad (2.89)$$

the solution can be expressed as:

$$w(t) = 2Re\{Ae^{-t(\delta_d + j\omega_d)}\} = 2e^{-\delta_d t}Re\{(\alpha_A + j\beta_A)(cos\omega_d t + jsin\omega_d t)\} \quad (2.90)$$

C_d and D_d are defined as $2\alpha_A$ and $-2\beta_A$ respectively. This can be rearranged as[50]

$$w(t) = e^{-\delta_d t}\,(C_d cos\omega_d t + D_d sin\omega_d t) \quad (2.91)$$

This can also rearranged as:

$$w_{transient}(t) = E_d e^{-\delta_d t}\, cos(\omega_d t + \phi) = W_t Re\{e^{-t(\delta_d + j\omega_d)}\} \quad (2.92)$$

where E_d and W_t are constants. $E_d = \sqrt{C_d^2 + D_d^2}$, $\phi = -\arctan(D_d/C_d)$ and $W_t = E_d e^{-\phi}$. This solution might be referred to as transient-state representation. From the equation, the term δ_d causes exponential decay and emulates a damping effect, while ω_d has an effect on the condition of damping and period of oscillation.

2.4.1.2 Forced Vibration of a Point Mass

Considering the case of forced vibration, let us assume a harmonic force is supplied to the system. The force can be described as:

$$f_e(t) = \tilde{f}_e sin\omega_f t \tag{2.93}$$

where $\tilde{f}_e$ and ω_f are the amplitude of and the angular frequency of the external force. The time response resulting from this force can be calculated by substituting the force back to the second-order differential equation of motion (Eq.(2.79)). This can be expressed as:

$$\ddot{w}(t) + 2\xi\omega_n\dot{w}(t) + \omega_n^2 w(t) = \frac{\tilde{f}_e sin\omega_f t}{M} \tag{2.94}$$

For the steady-state assumption, the trial solution of this equation can be given by:

$$w(t) = A_f sin\omega_f t + B_f cos\omega_f t \tag{2.95}$$

where A_f and B_f are constants. If Eq.(2.95) is differentiated, the first and second derivatives are given as:

$$\dot{w}(t) = A_f\omega_f cos\omega_f t - B_f\omega_f sin\omega_f t \tag{2.96}$$

and

$$\ddot{w}(t) = -A_f\omega_f^2 sin\omega_f t - B_f\omega_f^2 cos\omega_f t \tag{2.97}$$

After substituting these equations into Eq.(2.94), two equations for solving A_f and B_f can be obtained from coefficients of cosine and sine terms.

This solution is not the general equation of motion but is only represented as the steady-state part. The solution from Eq.(2.95) can also be expressed in exponential terms similar to the rearrangement of Eq.(2.92):

$$w_{steady-state}(t) = E_f cos(\omega_f t + \phi_f) = W_f Re\{e^{-j\omega_f t)}\} \tag{2.98}$$

where E_f and W_f are constants. $E_f = \sqrt{A_f^2 + B_f^2}$, $\phi_f = -\arctan(A_f/B_f)$ and $W_f = E_f e^{-\phi_f}$.

However, the time response of this forced system consists of a transient part and a steady-state part. In other words, it is the sum of the transient and steady-state solutions, as shown in:

$$w(t) = w_{transient}(t) + w_{steady-state}(t) = W_t Re\{e^{-t(\delta_d + j\omega_d)}\} + W_f Re\{e^{-t(j\omega_f)}\} \quad (2.99)$$

2.4.2 Wave Propagation for a Point Source

This section shows derivation of steady-state and transient-state wave propagation of a point source. The function of $e^{-t(\delta+j\omega)}$ is represented as the waveform in transient-state, while $e^{-j(\omega t)}$ is the waveform in steady-state. The wave equation for transient state is based on the Helmholz steady-state equation.

2.4.2.1 Steady-State Plane Wave for one Dimension

For a study of the relationship between sound pressure on a medium and the vibration of a diaphragm surface, there are two major equations. This first equation is Euler's equation:

$$\frac{\partial p}{\partial z} = -\rho \frac{\partial^2 w}{\partial t^2} \quad (2.100)$$

where p is sound pressure, w is displacement of the diaphragm and ρ is the density of the acoustic medium. This equation shows the relationship between the sound pressure and the vibration while force components act on a volume element according to Newton's second law. From the equation, the pressure is only dependent on the z coordinate, which is perpendicular to the vibrating surface. The other equation is given by [51]:

$$p = -B \frac{\partial w}{\partial z} \quad (2.101)$$

or

$$w = -\frac{\int p \, \partial z}{B} \quad (2.102)$$

where B is the adiabatic bulk modulus. This equation shows the relationship between the sound pressure and the vibration resulting from the displacement of the diaphragm. Substituting

Eq.(2.102) into Eq.(2.1) and partially differentiating both sides of the equation with respect to z and moving it to the left, this can be obtained [51]:

$$\frac{\partial^2 p}{\partial z} - \left(\frac{\rho}{B}\right)\frac{\partial^2 p}{\partial t^2} = 0 \tag{2.103}$$

This equation shows the relationship between the temporal and spatial variation of the pressure field, which is referred to as the one-dimensional wave equation[51]. From this equation, sound velocity (c) can be derived as [51]:

$$c = \left(\frac{\rho}{B}\right)^{-\frac{1}{2}} \tag{2.104}$$

When a wave stays in the steady state, the harmonic solution of the wave equation can be assumed as [51]:

$$p(z,t) = Re[p(z)e^{-j\omega t}] \tag{2.105}$$

Substituting this equation into Eq.(2.103) and differentiating it, the wave equation becomes a second-order differential equation with spatial coordinates [51]:

$$\frac{\partial^2 p}{\partial z^2} + \left(\frac{\omega^2 \rho}{B}\right)p = 0 \tag{2.106}$$

This equation is denoted as the one-dimensional Helmholz equation, or the steady-state wave equation. It can be referred to as the Helmholz equation[51]:

$$\left(\frac{\partial^2}{\partial z^2} + k^2\right)p = 0 \tag{2.107}$$

where k is defined as the acoustic wave number [51]:

$$k = \sqrt{\frac{\omega^2 \rho}{B}} = \frac{\omega}{c} = \frac{2\pi}{\lambda} \tag{2.108}$$

when combining Eq.(2.104) into the equation. From the Helmholtz equation, the general solution can be assumed as [51]:

$$p(z) = A_+ e^{jkz} + A_- e^{-jkz} \tag{2.109}$$

where $A_+$and A_- are arbitrary constants. Substituting this equation back into Eq.(2.105), the equation is obtained as[51]:

$$p(z,t) = Re[A_+ e^{j(kz-\omega t)} + A_- e^{-j(kz+\omega t)}] \tag{2.110}$$

When the boundary between the diaphragm and the medium is defined as z= 0, a positive z direction means that sound waves, which are generated, travel away from the boundary. Therefore, if no other source and boundary is present, the pressure field of Eq.(2.110). is represented with only the positive exponent term of z as expressed in [51]:

$$p(z,t) = Re[A_+ e^{j(kz-\omega t)}] \tag{2.111}$$

The equation is referred to as the pressure of outgoing wave. A_+ can be rewritten in terms of $\dot{W}$, based on the fact that the velocity of vibration of particles in the medium at the boundary must equal the velocity of vibration of the diaphragm($\dot{w}(t)$),which is assumed as:

$$\frac{\partial w(t)}{\partial t} = \dot{w}(t) = \dot{W} e^{-j\omega t} \tag{2.112}$$

where $\dot{W}$ is the amplitude of the velocity of vibration. Substituting this equation into Eq.(2.100) and differentiating it, the equation can be expressed as:

$$\frac{\partial p(z,t)}{\partial z} = j\omega\rho\dot{w}(t) \tag{2.113}$$

This equation is equal to the partial differentiation with respect to z of Eq.(2.111), which can be expressed as:

$$\frac{\partial p(z,t)}{\partial z} = jkp(z,t) \tag{2.114}$$

Therefore, $p(z,t)$can be rewritten in terms of $\dot{w}(t)$:

$$p(z,t) = \frac{j\omega\rho\dot{w}(t)}{jk} = \rho c\dot{w}(t) \tag{2.115}$$

and $\frac{\partial p(z,t)}{\partial z}$ can be rewritten in terms of $\dot{w}(t)$ by substituting Eq.(2.115) into Eq.(2.114)[51]

$$\left.\frac{\partial p(z,t)}{\partial z}\right|_{z=0} = jk\rho c\dot{w}(t) \tag{2.116}$$

or

$$\left.\frac{\partial p(z)}{\partial z}\right|_{z=0} = jk\rho c\dot{W} \tag{2.117}$$

when dividing both sides of the equation by $e^{-j\omega t}$. This equation is satisfied when z is at the boundary condition. This shows relation between acoustic pressure and velocity of the air particles at the boundary between the source and the air.

2.4.2.2 Steady-State Wave for a Spherical Source in Three Dimensions

The previous section was about the relationship between sound pressure in a medium and vibration on the surface of a source for one-dimension, while a vibrating surface generates a pressure field in three orthogonal axes. Therefore, the two major equations (Eq.(2.1) and (2.101)) need to be rewritten in three dimensions. Euler's equation becomes [51]:

$$\nabla p = -\rho \frac{\partial^2 \boldsymbol{w}}{\partial t^2} \tag{2.118}$$

where

$$\nabla p = \frac{\partial p}{\partial x}\hat{x} + \frac{\partial p}{\partial y}\hat{y} + \frac{\partial p}{\partial z}\hat{z}$$

and **w** is a vector of displacement, while $\hat{x}$, $\hat{y}$ and $\hat{z}$ are unit vectors along axis x, y and z respectively. The expansion equation becomes [51]:

$$p = -B\nabla \mathbf{w} \tag{2.119}$$

The wave equation was constructed in one dimension (Eq. (2.103)), similarly, the wave equation in three dimensions can be obtained [51]:

$$\nabla^2 p - \left(\frac{\rho}{B}\right)\frac{\partial^2 p}{\partial t^2} = 0 \tag{2.120}$$

For steady-state conditions, the equation can be rewritten in the form of the three-dimensional Helmholtz equation [51]:

$$(\nabla^2 + k^2)p = 0 \tag{2.121}$$

Transforming the divergence of the equation in Cartesian coordinates to spherical coordinates, (r, θ, φ) can be obtained by [51]:

$$\nabla^2 \equiv \frac{\partial}{\partial R^2} + \frac{2}{R}\frac{\partial}{\partial R} + \nabla_\sigma^2 \tag{2.122}$$

where ∇_σ^2 is referred to as a two-dimensional or surface Laplace operator: [51]:

$$\nabla_\sigma^2 \equiv \frac{1}{R^2}\left[cot\theta\,\frac{\partial}{\partial\theta} + \frac{\partial^2}{\partial\theta^2} + \frac{1}{\sin^2\theta}\frac{\partial^2}{\partial\varphi^2}\right] \tag{2.123}$$

where $\theta$and φ are the elevation and the azimuthal angle.

Assuming that a speaklet shape is a sphere with radius (r) and has the centre at the origin and the surface of the sphere vibrates with uniform radial velocity, $\dot{W}e^{-j\omega t}$, the boundary condition from Eq.(2.117) becomes[51]:

$$\left.\frac{\partial p}{\partial R}\right|_{R=r} = jk\rho c\dot{W} = j\rho\omega\dot{W} \tag{2.124}$$

and

$$\nabla_{\sigma}^{2} p = 0 \tag{2.125}$$

Therefore, the Helmholtz equation in spherical coordinates from Eq.(2.121) reduces to [51]:

$$(\frac{\mathrm{d}^2}{\mathrm{dR}^2} + \frac{2}{R}\frac{\mathrm{d}}{\mathrm{dR}} + k^2)p(R) = 0 \tag{2.126}$$

The general solution of this equation can be given by [51]:

$$p(R) = Re[\frac{1}{R}\left(A_{+}e^{jkR} + A_{-}e^{-jkR}\right)] \tag{2.127}$$

If the sound pressure is derived from the outgoing wave, which is the first term of the equation similar to Eq.(2.111), the equation becomes [51]:

$$p(R) = Re[\frac{A_{+}e^{j(kR)}}{R}] \tag{2.128}$$

Differentiating this equation with respect to R and substituting R with the radius of the source (r) for the boundary condition gives [51]:

$$\left.\frac{dp(R)}{dR}\right|_{R=r} = \left(jk - \frac{1}{r}\right)\frac{A_{+}e^{jkr}}{r} \tag{2.129}$$

Solving A_{+} in terms of $\dot{W}$ by substituting (2.129) into the boundary equation Eq.(2.124) gives [51]:

$$\mathrm{A}_{+} = \frac{kc\rho r^2\dot{W}e^{-jkr}}{jkr - 1} \tag{2.130}$$

Substituting it into (2.128), it can be expressed as [51]:

$$p(R) = Re[\frac{kc\rho r^2\dot{W}e^{jk(R-r)}}{(jkr - 1)R}] \tag{2.131}$$

Multiplying Eq.(2.131) with $\frac{kr-j}{kr-j}$, the solution of sound pressure is expressed by [51]:

$$p(R) = Re[\frac{kc\rho r^2(kr-j)\dot{W}e^{jk(R-r)}}{((kr)^2+1)R}] \quad (2.132)$$

when kr is small. $(kr-j) \cong -j$ and$((kr)^2+1) \cong 1$ can be approximated as [51]:

$$p(R) \cong -Re[\frac{jkc\rho r^2\dot{W}e^{jk(R)}}{R}], kr \ll 1 \quad (2.133)$$

For the speaklet that is not on the origin, the solution can be obtained by replacing R with the absolute of ($R-R_0$), as shown in [51]:

$$p(R) \cong -Re[\frac{jkc\rho r^2\dot{W}e^{jk|R-R_0|}}{R-R_0}], kr \ll 1 \quad (2.134)$$

where R_0 is the location of the speaklet. Multiplying this equation with $e^{-j\omega t}$, the pressure field can be given by [51]:

$$p(R,t) \cong -Re[\frac{jkc\rho r^2\dot{W}e^{j(k|R-R_0|-\omega t)}}{R-R_0}], kr \ll 1 \quad (2.135)$$

The sound pressure becomes purely imaginary, which means the sound pressure lags in phase relative to the velocity by 90°. It can be rearranged into acceleration as:

$$p(R,t) \cong Re[\frac{\rho r^2\ddot{W}e^{jk(|R-R_0|-\omega t)}}{R-R_0}], kr \ll 1 \quad (2.136)$$

where

$$\ddot{W} = -jkc\dot{W} \quad (2.137)$$

Therefore, sound pressure is directly proportional to the derivative of the velocity.

For high frequency limit and $(kr)^2 \gg 1$, $(kr-j) \cong kr$ and$((kr)^2+1) \cong (kr)^2$ the sound pressure in Eq.(2.132) will become [51]:

$$p(R) \cong Re[\frac{\rho cr\dot{W}e^{jk(R-r)}}{R}], (kr)^2 \gg 1 \quad (2.138)$$

and by multiplying this equation with $e^{-t\omega}$ and substituting R with $|R-R_0|$ where the sound source is not located at the origin point .Sound pressure in terms of space and time can be expressed as:

$$p(R) \cong Re[\frac{\rho cr\dot{W}e^{jk(|R-R_0|-r-\omega t)}}{R-R_0}], (kr)^2 \gg 1 \quad (2.139)$$

Therefore, sound pressure is directly proportional to the velocity.

2.4.2.3 Transient-State Plane Wave for one dimension

The time response of a forced system of MSD consists of two solutions: the transient-state and steady-state as shown in Eq.(2.99)

Most research studies were carried out for wave propagation of continuously forced vibration in steady-state. In other words, the main interest is in the propagation of vibration after a transient or initial time when the effect of the transient-state is neglected or becomes zero.

Therefore, the solution of wave for a continuous force is in the term of steady-state($Re\{e^{-j\omega_f t)}\}$)as shown in Section2.4.2.1 and 2.4.2.2. The effect appears for only a short time. It is referred as the transient state.

In the case of DLA, the sound source is driven by short discrete forced pulses. The transient wave was assumed to be meant as a wave generated from free vibration of a simple point mass by a discrete force.

The solution of the wave for a short discrete force has only the term of an impulse response ($Re\{e^{-t(\delta_d+j\omega_d)}\}$) and no term for the steady-state, where ω_d can be derived from the natural frequency of the MSD model and $\delta_d$is a dumping term.

The transient state wave equation refers to the wave propagation equation of an impulse response.

When a wave stays in the transient state, the harmonic solution of the wave equation can be assumed as a general solution:

$$p(z,t) = Re[p(z)e^{-t(\delta+j\omega)}] \tag{2.140}$$

where δ is the damping ratio of the wave. Similar to the steady-state case, the wave equation in one dimension can be derived from Eq.(2.103). Therefore, substituting the transient solution of Eq.(2.140) into the equation and differentiating it:

$$\left(\frac{\partial^2}{\partial z^2} + k_t^2\right)p = 0 \tag{2.141}$$

where k_t is defined as :

$$k_t = \sqrt{\frac{-(\delta+j\omega)^2\rho}{B}} = \frac{\omega - j\delta}{c} = k - j\frac{\delta}{c} \tag{2.142}$$

Similar to the steady-state in Eq.(2.107) and (2.111), the outgoing wave of the general solution of Eq.(2.141):

$$p(z,t) = Re[A_+ e^{-\delta t + j(k_t z - \omega t)}] \tag{2.143}$$

Partial differentiation of this equation with respect to z of Eq.(2.111) can be expressed as:

$$\frac{\partial p(z,t)}{\partial z} = jk_t p(z,t) \tag{2.144}$$

The velocity of vibration of a diaphragm ($\dot{w}(t)$) at the boundary is defined as:

$$\frac{\partial w(t)}{\partial t} = \dot{w}(t) = \dot{W} e^{-t(\delta + j\omega)} \tag{2.145}$$

where $\dot{W}$ is the amplitude of the velocity of vibration. Substituting this equation into Eq.(2.100) and differentiating it, the equation can be expressed as:

$$\frac{\partial p(z,t)}{\partial z} = (\delta + j\omega)\rho \dot{w}(t) \tag{2.146}$$

In order to find the boundary condition, $p(z,t)$can be rewritten in terms of $\dot{w}(t)$ from Eq.(2.144) and (2.146) and substituting k_t from Eq.(2.142) as in:

$$p(z,t) = \frac{(\delta + j\omega)\rho \dot{w}(t)}{jk_t} = \frac{(\delta + j\omega)\rho c \dot{w}(t)}{j(\omega - j\delta)} = \rho c \dot{w}(t) \tag{2.147}$$

and $\frac{\partial p(z,t)}{\partial z}$ can be rewritten in terms of $\dot{w}(t)$ by substituting Eq.(2.147) into Eq.(2.144):

$$\left.\frac{\partial p(z,t)}{\partial z}\right|_{z=0} = jk_t \rho c \dot{w}(t) \tag{2.148}$$

or

$$\left.\frac{\partial p(z)}{\partial z}\right|_{z=0} = jk_t \rho c \dot{W} = (\delta + j\omega)\rho \dot{W} \tag{2.149}$$

when dividing both sides of the equation by $e^{-t(\delta + j\omega)}$and substituting k_t from Eq.(2.142) into it. This equation is satisfied when z is at the boundary condition. The boundary condition is similar to the steady state except k is replaced with k_t.in Eq (2.117).

2.4.2.4 Transient-State Wave for a Spherical Source in Three Dimensions

Similar to the steady-state plane wave, the wave equation in three dimensions can be derived from Eq.(2.120). Therefore, substituting the transient solution of Eq.(2.140) into the equation and differentiating it, the wave equation for the transient-state can be obtained as:

$$(\nabla^2 + k_t^2)p = 0 \tag{2.150}$$

It is assumed for a speaklet that its shape is a sphere with radius (r) and it has its centre at the origin of the coordinates and the surface of the sphere vibrates with uniform radial velocity $\dot{W}e^{-(\delta+j\omega)t}$, the boundary condition from Eq.(2.149) becomes:

$$\left.\frac{\partial p}{\partial R}\right|_{R=r} = jk_t\rho c\dot{W} = (\delta + j\omega)\rho\dot{W} \tag{2.151}$$

and

$$\nabla_\sigma^2 p = 0 \tag{2.152}$$

From this wave equation for the transient state and its boundary condition, it can be seen that the cases of the transient and the steady states are the same, except k is replaced with k_t from considering Eq.(2.121) and (2.150) for the wave equation and Eq.(2.117) and (2.149) for boundary conditions. The pressure fields in both cases are similar but the wave numbers are different. Therefore, from the pressure field of Eq.(2.132) for the steady state, the pressure field for the transient state will become, by substituting k with k_t:

$$p(R) = Re[\frac{k_t c\rho r^2(k_t r - j)\dot{W}e^{jk_t(R-r)}}{((k_t r)^2 + 1)R}] \tag{2.153}$$

For high frequency limitation, $k - j\frac{\delta}{c} \cong k$ or k_t is approximately equal to the wave number (k) because δ is the damping ratio, which is between 0 and 1 in the underdamping case. The imaginary term is far smaller than the real. Similar to the steady state in Eq(2.138), sound pressure can be approximated to:

$$p(R) \cong Re[\frac{\rho cr\dot{W}e^{jk_t(R-r)}}{R}], (kr)^2 \gg 1, k_t \cong k \tag{2.154}$$

For the speaklet not on the origin, the solution can be obtained by replacing R with the absolute of ($R-R_0$) as shown in:

$$p(R) = Re[\frac{\rho cr\dot{W}e^{jk_t(|R-R_0|-r)}}{|R - R_0|}] \tag{2.155}$$

where R_0 is the location of the speaklet. Multiplying this equation with $e^{-t(\delta+j\omega)}$ and conversing the term of (k_t) into term of $(\delta + j\omega)$ with Eq.(2.142), the pressure field can be given by:

$$p(R,t) = Re[\frac{\rho c r \dot{W} e^{(\delta+j\omega)\left(\frac{|R-R_0|-r}{c}\right)-t(\delta+j\omega)}}{|R-R_0|}] \quad (2.156)$$

Therefore, sound pressure is directly proportional to the velocity for high frequency limitation.

Chapter 3: Characterization of an Multiple-Level Digital Loudspeaker Array (MDLA) with Rectifying Speaklets

Chapter 3 will describe how an ideal MDLA can emit a sound. It is divided into 4 sections. The first section will explain the proposed concept of the MDLA. The second section will describe the mathematical model and the ideal conditions under which a speaklet can make a sound by the pressure response similar to a rectified amplitude modulation. The response will be shown in results of the simulation in the third section. The digital sound reconstruction of MDLA will be analysed according to the requirements in Chapter 2.3.3. The section studies effects of different locations of speaklets on sound fields, temporal responses, frequency responses, sound distortion, directivity through a study case of the 4 pulse assignment schemes, which will be described in Chapter 3.3.3.2 The final section will give a detail of application of amplitude modulation, which is a technique in telecommunication, in acoustic science. Major advantages of the technique are identified.

3.1 Concept of Multiple-Level Digital Loudspeaker Array

The concept of a multiple-level digital loudspeaker (MDLA) which increases the number of levels of sound that a speaklet can emit is proposed here and is considered as a novel approach to digital loudspeaker arrays. The nature of the pulses feeding the MDLA will thus differ from those used with a conventional DLA, where the width and amplitude of the pulses are uniform. An MDLA requires pulses of constant amplitude, but variable width, as shown in Figure 3-1, thereby maintaining the digital nature of the system:

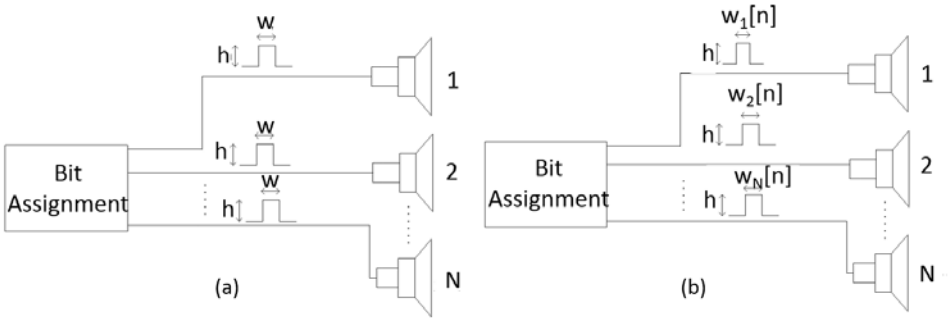

Figure 3-1 (a) Traditional DLA and (b) MDLA

3.2 Mathematical Model of Acoustic Response of the Ideal Rectifying Loudspeaker

A mathematical model of the ideal rectifying sound source which is used as a speaklet within a MDLA is developed in this section.

3.2.1 Physical Model of the ideal rectifying source

The ideal rectifying source is based onthe human voice system. This imitation is described in Section 2.2.4. There are three major components: an air pump as the lung, a vibrating gate in an air valve as the vocal cord and a spherical air outlet as the mouth. The air flows from the constant pressure pump to the air outlet through the air valve as shown in Figure 3-2. It is assumed that the air equally and omni-directionally blows out from the outlet.

The generation of the acoustic pressure wave of the rectifying source is different from the traditional spherical source as described in Table 3-1

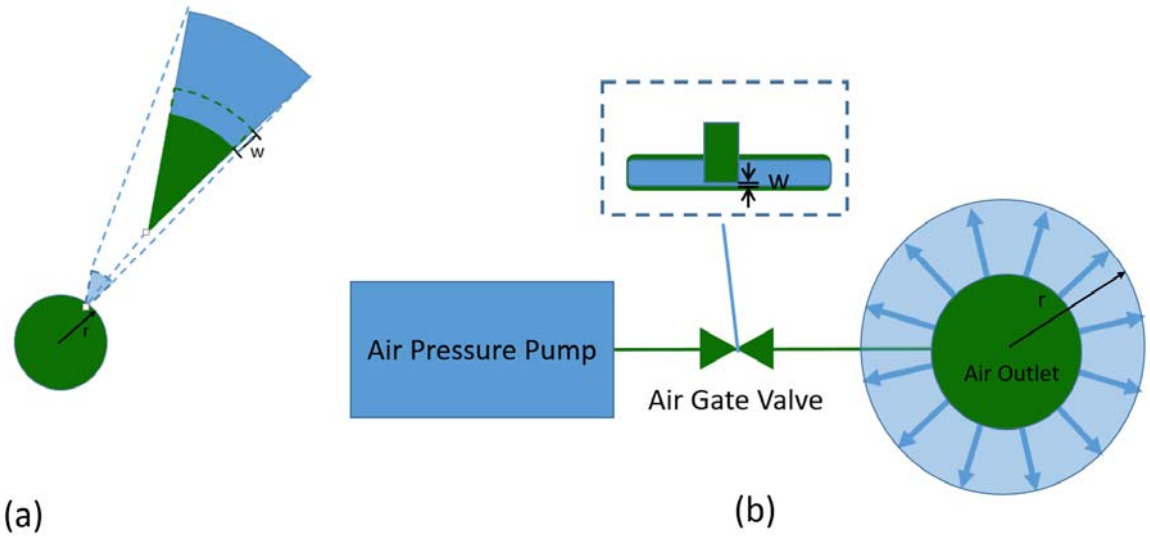

Figure 3-2 (a) a spherical source, (b) the ideal rectifying source

Table 3-1: Comparison of sound generation between a spherical source and a rectifying source

	Spherical source	Rectifying source
Primary vibrating source	The source surface	The gate in the air valve
Sound generation	Rapid movement of the air particles at the boundary between the sound source and the air result from caused by a the force in the movement of the source surface	Rapid movement of the air particles at the boundary of the outlet caused by the force in movement of the air flow blown from the pressure pump.
Derivation of the acoustic pressure	Velocity of the source surface of the source	Velocity of the air flow blown from the pressure pump
Sound generating boundary	The source surface of the source	The surface of an air volume blowing blown from the pressure pump
Relationship between the velocity of air flow at the boundary and the displacement of the primary vibrating source	According to the motion equation, the velocity linearly relates to the derivative of the displacement of the primary vibrating source f	According to Bernoulli's equation Eq.(2.68), the velocity linearly relate to the displacement of the primary vibrating source
Radius of the sound sources	Constant and equal to the radius of the physical source	Variable, depending on the air volume blown from the air outlet. The air volume is depended on the pressure in the air pump and the gap area of the gate in the air valve.
Direction of the air particles at the boundary of the source or outlet	Back and forth according to the compression and expansion of sound source	Forward only but the velocity of the air particles depended on the gap area of the vibrating gate in the valve.

3.2.2 Mathematical Model

A MATLAB simulation was developed to explore the acoustic behaviour of the proposed MDLA with an ideal rectifying sound sources. It is involved with the propagations of an impulse response

in the air. It is defined that the rectifying source, as shown in Figure 3-2, is a source of the impulse response. The primary source of the vibration of the rectifying source is the gate in the air valve. The vibration of the gate is mathematically modelled as the mass-spring-damper (MSD) systems by defining a discrete force with the constant width and the magnitude as the exciting force $f_e(t)$ in the system as shown in Figure 2-31.

This derivation will prove that the acoustic impulse response of the ideal rectifying spherical sound source is directly proportional to the movement of the vibrating gate in the air valve.

To simplify the model in Figure 3-2, in this simulation it is assumed that the force that excites the gate in the air valve, rather than the excited voltage can be controlled. The displacement of the gate in the air valve in the source (w(t)) can be expressed as Eq.(2.79).The exicited force $f_e(t)$ is the discrete mechanical pulse can be expressed as:

$$f_e(t) = \begin{cases} F, & 0 < t < W_p \\ 0, & otherwise \end{cases} \tag{3.1}$$

where F and W_p are the height and width of the force and are constant. The excited force can be expressed in terms of a unit step function u(t) as:

$$f_e(t) = F[u(t) - u(t - W_p)] \tag{3.2}$$

when taking a Laplace transform, it can be expressed as:

$$F_e(s) = \frac{F}{s}(1 - e^{-sW_p}) \tag{3.3}$$

From the MSD model in Eq.(2.79), taking a Laplace transform both sides of the equation:

$$s^2 w(s) + 2\xi\omega_n s w(s) + \omega_n^2 w(s) = \frac{F(1 - e^{-sW_p})}{sM} \tag{3.4}$$

when it defines the initial conditions that $w(t = 0) = 0$ and $\dot{w}(t = 0) = 0$. Taking w(s) out from the s terms, rearranging the s terms and moving to the right hand side of equation, it can be expressed as:

$$\begin{aligned} w(s) &= \frac{F(1 - e^{-sW_p})}{Ms(s + \sigma_d + \omega_d)(s + \sigma_d - \omega_d)} \\ &= \frac{F}{M}\left(\left(\frac{1}{s(s + \sigma_d + \omega_d)(s + \sigma_d - \omega_d)}\right)\right. \\ &\quad \left. - \left(\frac{1}{s(s + \sigma_d + \omega_d)(s + \sigma_d - \omega_d)}\right)e^{-sW_p}\right) \end{aligned} \tag{3.5}$$

where $\sigma_d = \omega_n \xi$ and $\omega_d = \omega_n \sqrt{\xi^2 - 1}$. The s terms can be written into the summation of three terms by partial fraction as:

$$\begin{aligned} &\frac{1}{s(s+\sigma_d+\omega_d)(s+\sigma_d-\omega_d)} \\ &\quad = \left(\frac{1}{\omega_n^2}\frac{1}{s} + \frac{0.5}{(\omega_d+\sigma_d)\omega_d(s+\sigma_d+\omega_d)}\right. \\ &\quad \left. - \frac{0.5}{(\sigma_d-\omega_d)\omega_d(s+\sigma_d-\omega_d)}\right) \\ &\quad = \frac{1}{\omega_n^2}\left(\frac{1}{s} + \frac{0.5}{(\xi^2-1+\xi\sqrt{\xi^2-1})(s+\sigma_d+\omega_d)}\right. \\ &\quad \left. + \frac{0.5}{(\xi^2-1-\xi\sqrt{\xi^2-1})(s+\sigma_d-\omega_d)}\right) \end{aligned} \tag{3.6}$$

After taking the $\frac{1}{\omega_n^2}$ terms out, it can been seen that the coefficients of the last two terms are a complex conjugation, when $\xi^2 < 1$. This means they are equal in real part and imaginary part in their magnitude, but the signs of the imaginary part are different. Taking an inverse Laplace transform of the s-terms, it can be written as:

$$\begin{aligned} &\mathcal{L}^{-1}\left\{\frac{1}{s(s+\sigma_d+\omega_d)(s+\sigma_d-\omega_d)}\right\} \\ &\quad = \frac{1}{\omega_n^2}\left(u(t) + \xi_d^* e^{-t(\sigma_d+\omega_d)} + \xi_d\, e^{-t(\sigma_d-\omega_d)}\right) \end{aligned} \tag{3.7}$$

where ξ_d^* is a complex conjugation of ξ_d and we define that:

$$\xi_d^* = \frac{0.5}{(\xi^2-1+\xi\sqrt{\xi^2-1})} = \frac{0.5}{2\xi^2-1} - \frac{\xi\sqrt{\xi^2-1}}{(2\xi^2-1)(\xi^2-1)} \tag{3.8}$$

It can be written as a complex number by multiplying $\left(\frac{\xi^2-1)-(\xi\sqrt{\xi^2-1})}{(\xi^2-1)-\left(\xi\sqrt{\xi^2-1}\right)}\right.$. As a result, the first term is the real part and the second term is the imaginary part when $\xi^2 < 1$.

From the vibration equation in Eq. (3.7), there is a summation of three terms. The first term is a unit step function. The step function of displacement is differentiated to solve its velocity equation and it becomes zero. This term can be ignored. For the case of the ideal rectified source, constitutive relationship among displacement and velocity and acoustic pressure becomes linear. Because a single force is considered in the equation, the step function exists. In reality of the discrete pulses, there are a couple of the forces occurring at the rising edge and falling edge of the pulse, which have the same magnitude but different in the sign. The step function will be cancelled with the step function from the opposite force. Generally, the width of the pulse is small comparing to the period of the vibration. Hence the step function could be neglected.

The other two terms of the vibration produce the transient-state waves of the impulse response. The second term of Eq. (3.7) produces a term of the outgoing wave, while the third term produces the incoming wave. For spherical sources, the outgoing wave is considered, but the incoming wave is omitted because only the outgoing wave travels across the space.

Eq.(3.5), which is composed of the s terms and the delay of the s term with W_p, can be inverse Laplace transformed by substituting the outgoing wave back into the equation. The displacement can be expressed as:

$$w(t, W_p) = Re[\frac{F\xi_d^*}{M\omega_n^2}(e^{-t(\sigma_d+\omega_d)} - e^{-(t+W_p)(\sigma_d+\omega_d)})] \quad (3.9)$$

From the equation it can be seen that two impulse responses are generated at both the rising and falling edge of a pulse with the width of Wp. It can be expressed in the lumped form of the transient vibrations as:

$$w(t, W_p) = Re[W(e^{-t(\sigma_d+j\omega_d)} - e^{-(t+W_p)(\sigma_d+j\omega_d)})] \quad (3.10)$$

where $W = \frac{F\xi_d^*}{M\omega_n^2}$ and re-defining $j\omega_d = \omega_n\sqrt{1-\xi^2}, \xi^2 < 1$.

For acoustic pressure of the ideal rectifying source, it is not considered at velocity of the air particles on the vibrating surface of the gate similar to the spherical source case, but the velocity of air particles flowing out from the air outlet through the controlled air flow valve. Hence, the velocity of the air flow at the outlet is linearly varied by the displacement of the gate in the valve according to Bernoulli's theorem. A possible evidence of the relationship is the human voice system, which is discussed in Section 2.2.4. Substituting Eq.(3.10) into w(t) in Eq.(2.68), the velocity of the air flow can be expressed as:

$$\dot{w}(t, W_p) = Re[\frac{WC_{pipe}}{a}(e^{-t(\sigma_d+j\omega_d)} - e^{-(t+W_p)(\sigma_d+j\omega_d)})] \quad (3.11)$$

where (a) is the cross-sectional area of the gap in valve the air pass through the gate. It notes that $\dot{w}$ is not derivative of the displacement term but it is represented as velocity of the air flow Therefore, the velocity can be rewritten in terms of movement of the vibrating gate by:

$$\dot{w}(t, W_p) = \frac{\dot{W}}{W} w(t, W_p) \quad (3.12)$$

where $\dot{W} = \frac{WC_{pipe}}{a}$

For radiation of an ideal rectifying source, it is assumed frequency of vibration of the gate is high in a ultrasonic range and $(kr)^2 >> 1$,where r is radius of the source as shown in Figure 3-2b. As a

consequence of the assumption, the acoustic pressure of a source is directly proportional to velocity of air particles at boundary of the source. In other words, the acoustic wave is in phase with variation of the velocity, or acoustic impedance of the source is a pure real number according to the transient-state wave propagation as discussed in Section 2.4.2.4. When $(kr)^2>>1$, the relationship between acoustic pressure of the source and velocity of the air flow blowing from the outlet can be rewritten by substituting $\dot{w}$(t,Wp) in Eq.(3.11) into $\dot{w}$(t) in Eq.(2.156) as:

$$p(R,t,W_p) = Re[\frac{\rho cr\dot{W}e^{(\sigma_d+j\omega_d)\left(\frac{|R-R_0|-r}{c}\right)}\left(e^{-t(\sigma_d+j\omega_d)}-e^{-(t+W_p)(\sigma_d+j\omega_d)}\right)}{|R-R_0|}] \quad (3.13)$$

where r, R and R_0 is the radius of the sound source, distance from the source and location of the source respectively. It can be lumped by terms of the radius, the distance and sound speed ($\frac{|R-R_0|-r}{c}$) as time shift due to distance (t_R) and the wave equation of the rectifying source can be rewritten as:

$$p(R,t,W_p) = P\dot{w}(t-t_R,W_p) \quad (3.14)$$

where

$$P = \frac{\rho cr}{|R-R_0|} \quad (3.15)$$

and

$$t_R = \frac{|R-R_0|-r}{c} \quad (3.16)$$

Therefore, the wave equation at a point location (R) can be written in terms of vibrating displacement by substituting Eq.(3.12) into (3.14)

$$p(t,W_p) = \frac{P\dot{W}}{W}w(t-t_R,W_p) \quad (3.17)$$

where t_R, P, W and $\dot{W}$ are constant and pure real numbers. This equation shows the acoustic pressure directly proportional to the displacement vibration with a time shift for the ideal sound radiation ($(kr)^2>>1$). Effect of a value of kr on the propagating wave is discussed in Section 3.3.3.9

3.2.3 Computation of Acoustic response for a MDLA

Acoustic responses of speaklets within MDLA can be computed by Eq. (3.13). There are three scenarios for computing the acoustic response

- Two discrete pulses are hitting a speaklet at time t_0 and t_1, respectively. A small microphone places at the observation point. The distance from the speaklet to the point is R metre. The acoustic response of the first pulse (t_0) or Signal 1 can be computed by substituting t with t- t_0 into Eq. (3.13). In the same way, the acoustic response of the second pulse (t_1) or Signal 2 can be computed by Substituting t with t- t_1 into Eq. (3.13). Therefore the acoustic response of the both pulse is the superposition between Signal1 and Signal2 as shown in Figure 3-3

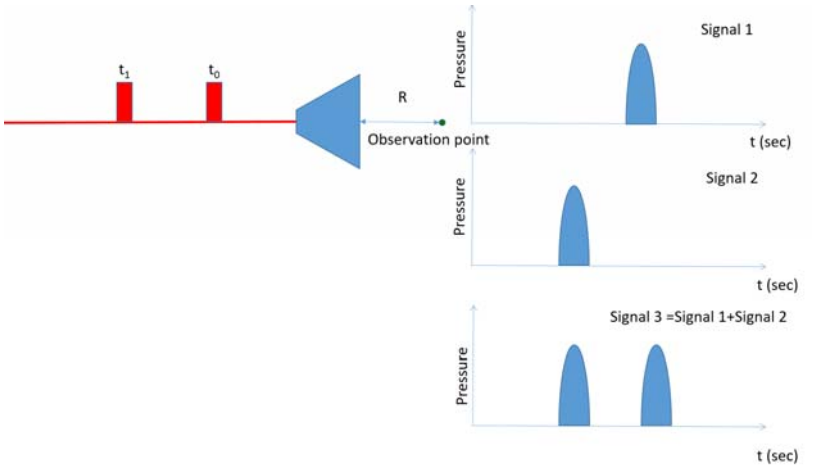

Figure 3-3: Acoustic response of two pulses feeding a speaklet with different time.

- Two speaklets are placed away from the observation point R1 and R2 metre. They are fed with a rectangular pulse at the same time t0. The acoustic response of the first speaklet or Signal 1 can be computed by substituting t with t- t0-R1/c into Eq. (3.13), where c is sound speed and R1/c is propagating time from the speaklet to the observation point. Similarly, the acoustic response of the second speaklet or Signal 2 can be computed by substituting t with t- t0-R2/c into (3.13). Therefore Signal 3 is the superposition between Signal1 and Signal2 as shown in Figure 3-4

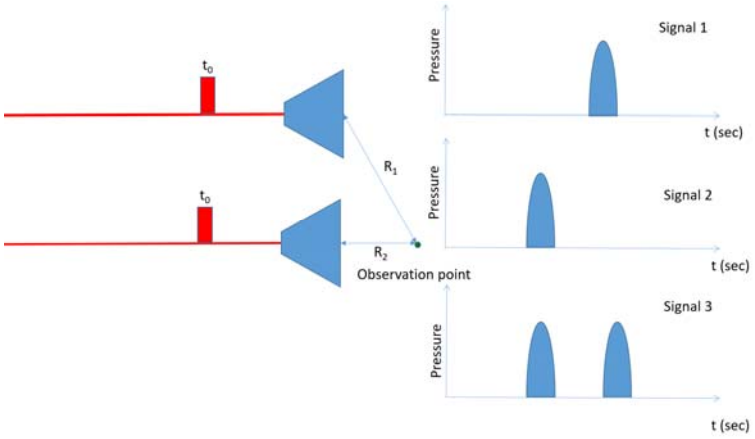

Figure 3-4: Acoustic response of driving two speaklets on different locations

- For spatial plot of the speaklet as shown in Figure 3-5, the acoustic response of the first pulse (t_0) or Signal 1 can be computed by substituting R with R- ct_0 into Eq.(3.13) where c is sound speed and ct_0 is a distance, which a wave travels before the first pulse (t_0) hits the speaklet. In the same way, the acoustic response of the second pulse (t_1) or Signal 2 can be computed by substituting R with R- ct_1 into Eq. (3.13). By superposition of both signals, the acoustic output can be plotted.

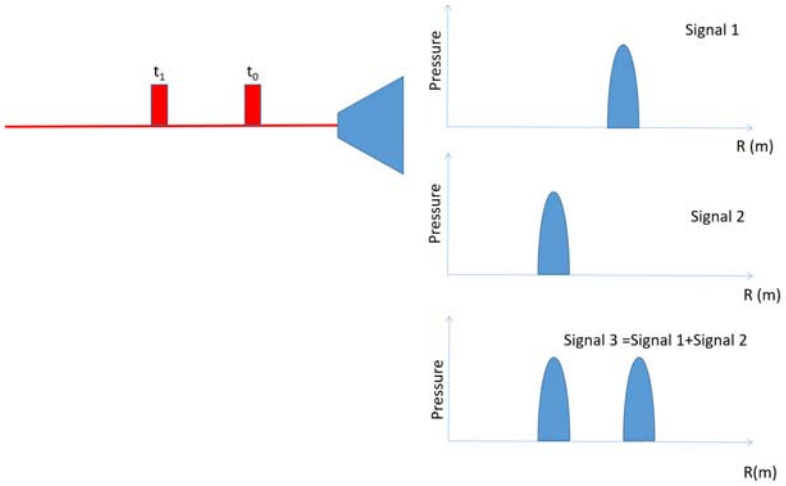

Figure 3-5: Spatial output of two pulses feeding a speaklet at a moment (t)

3.3 Assumptions and Results of Simulation of a MDLA

This section shows simulation, which is based on the mathematical model. The simulation includes test of fulfilment of digital reconstruction requirement and application of a MDLA.

3.3.1 Assumptions, Results and Fulfilment of Digital Reconstruction Requirement

Speaklets within the MDLA produce different acoustic pressures as they are driven by electrical pulses of different widths. In order that the acoustic response meets the requirement for digital reconstruction, the natural frequency (ω_n) and damping ratio (ξ) of the speaklets are set at 80 kHz and 0.7 respectively. The frequency of the clock generator, which is used for generating 1-Newton pulses, is set at 200 MHz which allows digital pulses with variable pulse widths of a minimum of 5 ns with a resolution of 5 ns.

Additionally, a speaklet is a spherical point source with a radius of 1mm and the distance from the speaklets is 1 metre and $\dot{W}$ is 1 and F is 1N.

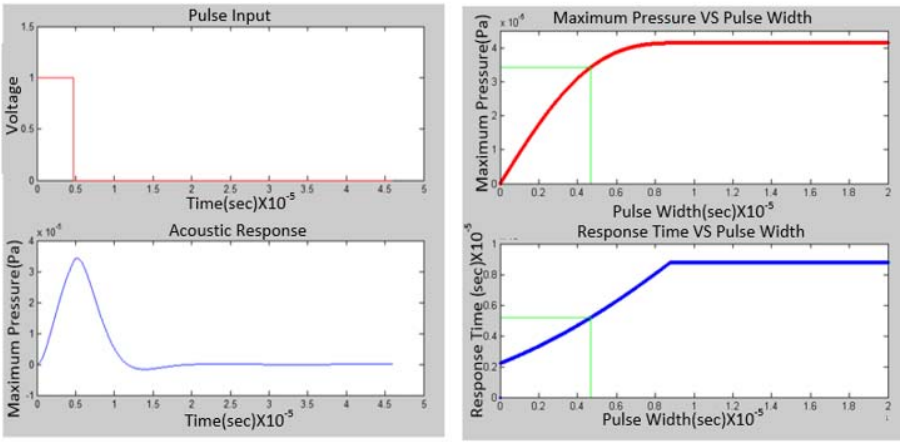

Figure 3-6: Graph of a mechanical pulse driving a speaklet with pulse width of 4.685 µs and its acoustic response. (b) The relationship between maximum pressure and pulse width and the relationship between response time and pulse width.

From the above assumptions, the acoustic output of a speaklet is related to the pulse width of the mechanical rectangular pulse in Eq. (3.13), as shown in Figure 3-6a. The pressure of the acoustic output reduces to 0 (or negligible) voltage in less than 22.3 µs. This means that the response can digitally reconstruct sound at a sampling rate of 44.1 kHz, in accordance with the first requirement mentioned in Section 2.3.3. In addition, the relationship between maximum pressure and pulse width, and the relationship between the response time and pulse width are not linear as shown in Figure 3-6b but are linear from 0 sec up to a pulse width of 4.685 µsec, with an R^2 coefficient of 0.9917 and 0.9967 respectively, within the green frame. The linear regression equations are shown in Table 3-2. Because the coefficient is greater than 0.95, this verifies that the multiple-level digital loudspeaker can meet the third requirement of digital reconstruction, i.e. that the step of increase or decrease in the maximum pressure of acoustic responses must be linear, which fulfils the third requirement in Section 2.3.3. Therefore, 937 different pulse widths are available for a speaklet, by varying the pulse width from 0 ns to 4.685 µs in steps of 5 ns. For a 16-bit resolution in a conventional audio system, this requires a speaklet array of 70 elements.

Table 3-2: Results of linear regression.

Relationship	R^2	Linear equation
maximum pressure VS Pulse width	0.9917	M_P=7.4483 W_p+ 1.6970 *10^{-6}
Response time VS Pulse width	0.9964	R_T=0.6523 W_p + 2.0838 * 10^{-6}

3.3.2 Response time and Improvement in Linearity

The principle of digital sound reconstruction is the superposition of the acoustic response in a DLA. Since acoustic responses with different values of maximum pressure have different response times, as described in the method of division of quantizing level, these acoustic responses can be combined to reproduce the reconstructed acoustic output with different levels by making the moment of every combined acoustic response reach maximum pressure at the same time. This combination can be achieved by delaying the start of the digital pulse actuating the speaklets by the reponse times obtained from the linear equation of response time in Table 3-1.

For Figure 3-6, when digital data of 2^{16} level or 16 bit PCM system for the level at 2100 arrives, three speaklets are driven by three pulses, which represents the levels at 937, 937 and 226. The last pulse is delayed by the time period derived from the linear equation of response time, as shown in Eq.2.5 in order that the acoustic response of all speaklets reaches the peak at the same time.

$$Time\ Delay = S\left(W_{pmax} - W_n\right) + X_0 \tag{3.18}$$

where W_n is the pulse width feeding the n^{th} speaklet and W_{pmax} is the maximum pulse width, where the relationship between maximum pressure and width becomes linear and S and X_0 are the slope and y-axis intersection of the linear equation between response time and pulse width.

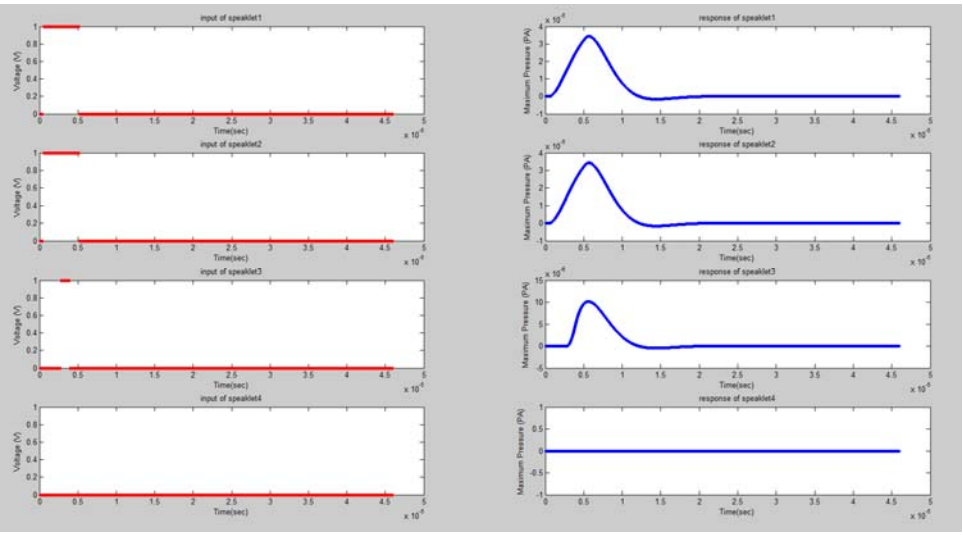

Figure 3-7: The digital reconstruction for level at 2100 , reproduced by 4 speaklets with different levels 937, 937,226 and 0, which are the sum of 2100 (937+ 937+226=2100).

In simulation for a series of data points, each data point generates a graph of response for two sampling periods. This is because the emitting time of a response may be more than one sampling period. This should result in the consecutive response. Therefore, two consecutive responses can

be linked by adding the last sampling period of a response to the first sampling period of the following response. For example, Figure 3-8 shows the reconstruction of a data series (from 935 to 940).

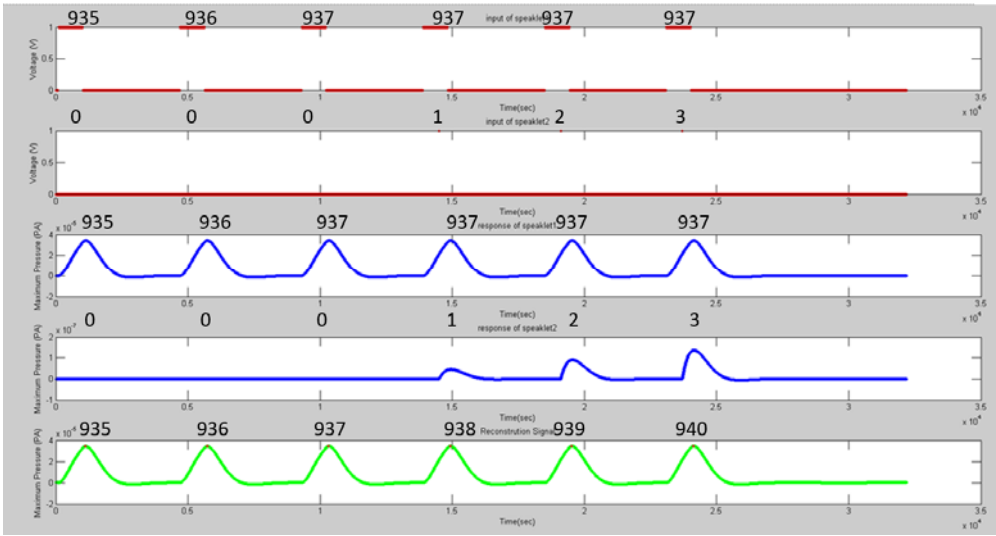

Figure 3-8: The digital reconstruction for levels from 935 to 940

If there are 70 speaklets with 937 levels of pulse widths, they can represent 16 bit or 216 or 65590 levels of a sample of digital audio PCM data. A specified delayed time is added into a specified pulse width so that the response of all pulse widths have similar response time. By applying the time delay, the relationship of 65590 levels generating by the 70 speaklets and their maximum acoustic pressures is plotted as a straight line with the R^2 coefficient equal to 1, as shown in Figure 3-9 by assuming that all speaklets are placed in the same area. This verifies that delay shift time can improve the linearity between maximum pressure and pulse width as shown in the increase of the coefficient from 0.9917 to 1.

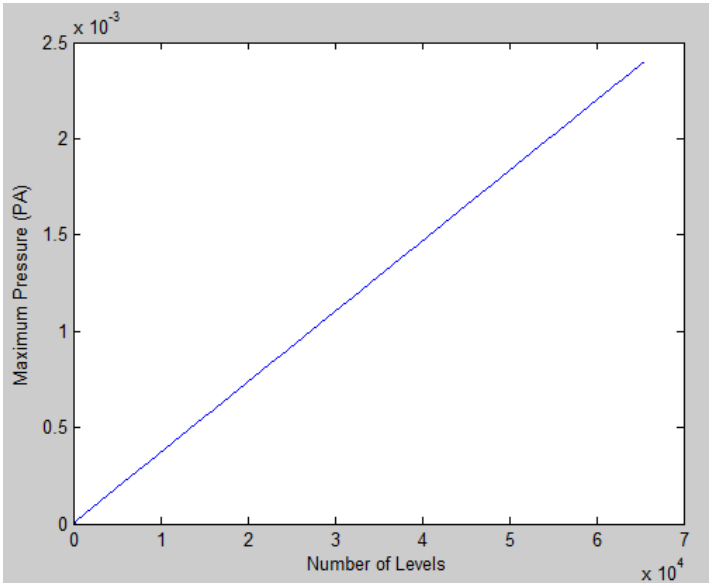

Figure 3-9: Maximum pressure for the acoustic response of all levels (65590 levels).

For the final results of the simulation, Figure 3-10 and Figure 3-11 show the digitally reconstructed signal of sine waves of 2.2 kHz and 200 Hz

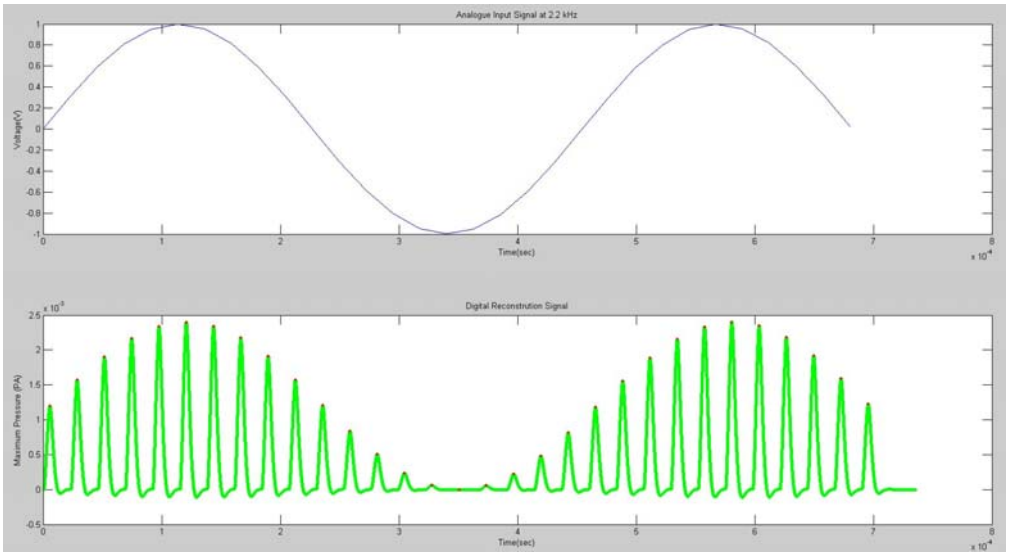

Figure 3-10: The sinusoidal input of 2.2 kHz and its digitally reconstructed output.

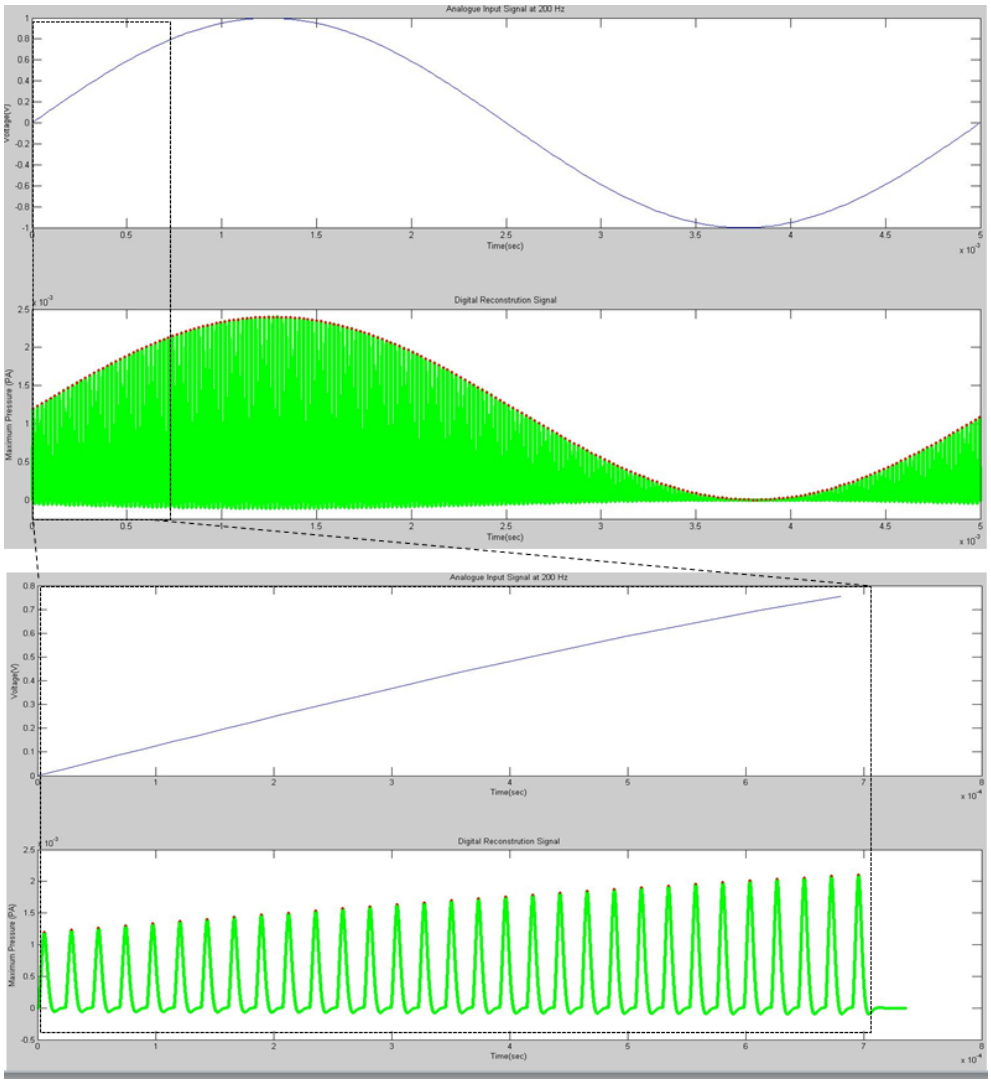

Figure 3-11: The sinusoidal input of 200 Hz and its digitally reconstructed output.

3.3.3 Assumptions and Results of Sound Field, Acoustic Output and Spectrum of MDLA

In previous section, it is assumed that speaklets within the array share the same location but, in this section, the speaklets are located in different positions. The effect of difference in the locations on the pressure response will be investigated.

3.3.3.1 Typical process of pulse assignment

To begin with the input of the system, as shown in Figure 3-12, the audio stream is a series of digital codes with entered pulse assignments. The serial codes are processed one by one to extract a set of combination codes, which are uniquely pre-defined audio codes. Each combination code in the set is particularly pre-assigned to a speaklet within the array. The pre-defining and pre-assignment is referred to as pulse assignment. For example, an audio code of 8

can be extracted to 4 combination codes of 2(2+2+2+2). The combination is assigned to the 3rd, 4th, 5th and 6th of an 8-speaklet array. From the example, it can be realized that for an audio code, there are many possible combination codes and many possible patterns of assignment. Each possible scheme might give different results of acoustic response. Some of the many possible schemes have been chosen in order to study this effect. These schemes will be discussed in the next section.

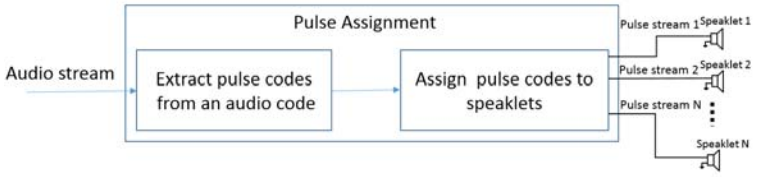

Figure 3-12: Typical system of pulse assignment

3.3.3.2 Schemes of Pulse assignment

Due to each speaklet having a different location, the pulse generator assigns digital pulses with different pulse widths to feed to different speaklets. In this simulation, four schemes are chosen from numerous schemes for pulse assignment as case studies in order to study the effect of the location of speaklets on acoustic response.

The four schemes of pulse assignment consist of minimization of sound levels among speaklets, minimization of the number of speaklets with inside-out symmetry, minimization of the number of speaklets with outside-in symmetry and minimization of the number of speaklets with asymmetry.

- The first scheme uses all speaklets within the array and balancing combination codes equally. This scheme gives effectiveness of beam control because all speaklets emit sound similar to the way a speaker within a traditional analogue array produces sound.
- The second scheme requires minimizing the number of speaklets by using speaklets one by one until they reach their maximum level, starting from the centre and moving to the edge of the array and balancing transmitting power between the left and right side of the array.
- The third scheme is similar to the second, except it starts from the edge and moves to the centre of the array.
- The fourth scheme requires minimizing the number of speaklets by using speaklets one by one until they reach their maximum level, starting from the right side and moving to the left side of the array.

An audio stream is processed into each of the four pulse assignments in order to understand the four schemes of pulse assignment. As an example, an audio code of 9 was assigned to 8 speaklets with a maximum of 3 levels. The first scheme of pulse assignment will compute the combination codes of 2,1,1,1,1,1,1,1. The second scheme will compute the combination codes of 0,0,2,3,3,1,0,0. The third scheme will compute the combination codes of 3,2,0,0,0,0,1,3.The fourth scheme will compute the combination codes of 3,3,3,0,0,0,0,0, as shown in Figure 3-13 . From Figure 3-9, examples of a simplified audio stream are operated with different pulse assignments. As an example, an audio code of 9 was assigned to 8 speaklets with a maximum of 3 levels. The first scheme of pulse assignment will compute the combination codes of 2,1,1,1,1,1,1,1 as shown in Figure 3-14. It shows an example of a simplified audio stream operated with the different pulse assignments.

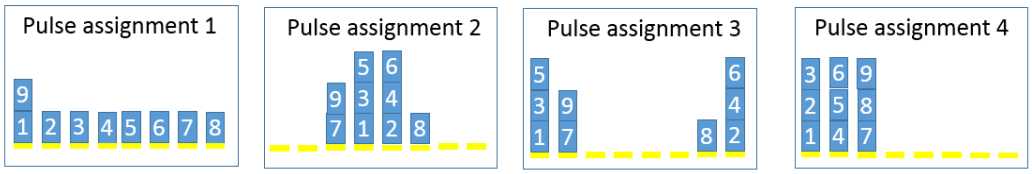

Figure 3-13: The combination codes of the four schemes of pulse assignment

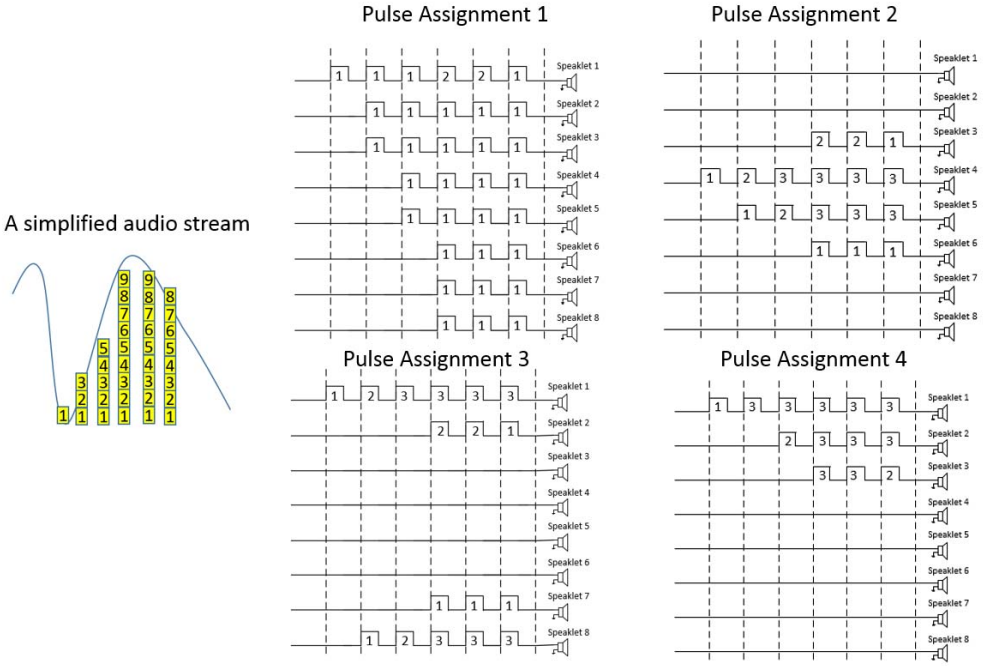

Figure 3-14: The pulse streams of the four pulse assignment for an audio stream.

3.3.3.3 Assumption of sound field and acoustic response of an MDLA

In order to study the effect of different locations of speaklets, which reproduce acoustic output with different magnitudes on the total acoustic output and spectrum within the array, the pulse assignment is simulated. It is assumed in the array that the speaklets are point sources, which can radiate sound omni-directionally, aligned on the *x*-axis. Their interspacing computed by Eq.(2.71) is 3.83 mm (a half of the sampling distance at 44.1 kHz) with sound speed(c =343 m/s). The array has different numbers of 4, 8 and 16 speaklets. The results of the MDLA are simulated by generating a digital audio stream of a pure sine wave with frequencies of 20 Hz, 2 kHz and 10 kHz. 20 Hz and 10 kHz are represented as low and high audio frequencies respectively, while 2 kHz is represented as a frequency within the human voice band. A sound field is simulated at the front of an array with dimensions of 20 cm x 20 cm. The points for observing the total acoustic response and spectrum are 40cm from the centre of the array, which is a distance greater than the array size, at angles of ±90, ±60, ±30 and 0 from the perpendicular to the array, as shown in Figure 3-15.

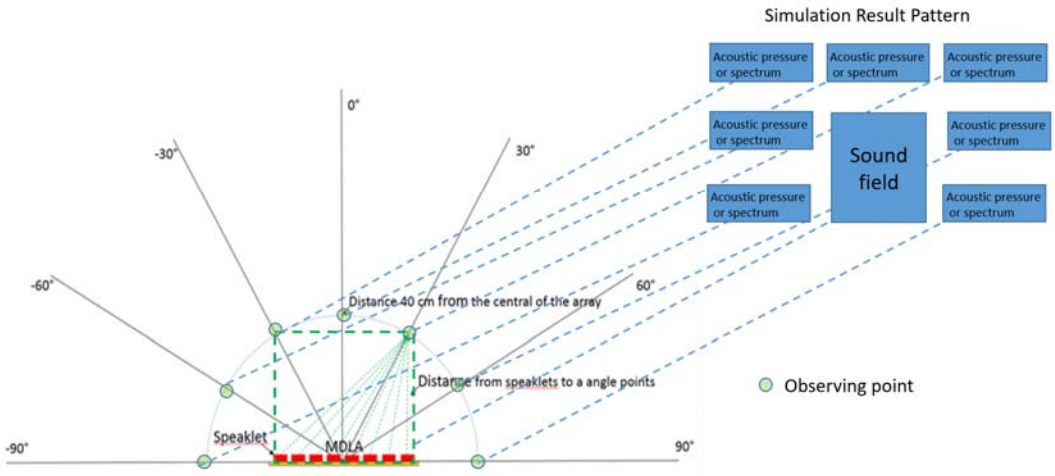

Figure 3-15: Speaklets in a linear array, the observing points and pattern in simulation result.

3.3.3.4 Reconstruction of Acoustic Response

In order to show reconstruction of the acoustic response of the four schemes, we assume that there are four speaklets within the array fed with a digital audio stream of a pure sine wave of 2kHz frequency. They can emit sound with 937 different levels. The acoustic response is observed at the angle of 0 or at the front of the array by separating the acoustic output from the four speaklets. The response output of each speaklet and the reconstructed output are shown in Figure 3-16 to Figure 3-19.

Figure 3-16 shows the acoustic output for pulse assignment 1. The acoustic output from the four speaklets is similar because they are stimulated by electrical pulses of almost equal width. From Figure 3-17 for pulse assignment 2, the acoustic outputs are symmetric between the left and right sides (speaklet 1and 2 and speaklet 3 and 4). Considering the speaklets on one side, when the audio level code is less than, or equal to 936, only speaklet 2 is fed with the pulses. When the code is greater than 936, speaklet 2 is fed with the pulses with the 936 width code, while speaklet 1 is fed with the pulses with a width code exceeding 936. For pulse assignment 3, shown in Figure 3-18, this scheme is similar to pulse assignment 2, but the combination codes of electrical pulses for the outer and inner speaklets are swapped. For pulse assignment 4, speaklets will be used one by one when reaching the maximum level (936), shown in Figure 3-19.

Finally, although the speaklets are fed with pulses with different schemes of pulse assignments, the reconstructed acoustic outputs at the angle of 0 for the four schemes is the same, as shown in the last graph in Figure 3-16 to Figure 3-19.

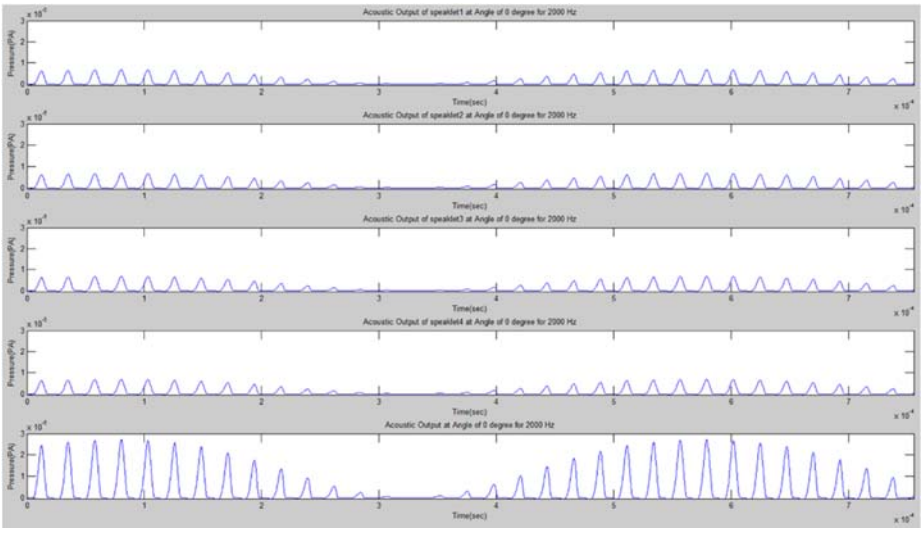

Figure 3-16: Acoustic response of 4 speaklet MDLA at the front of the array (0°)

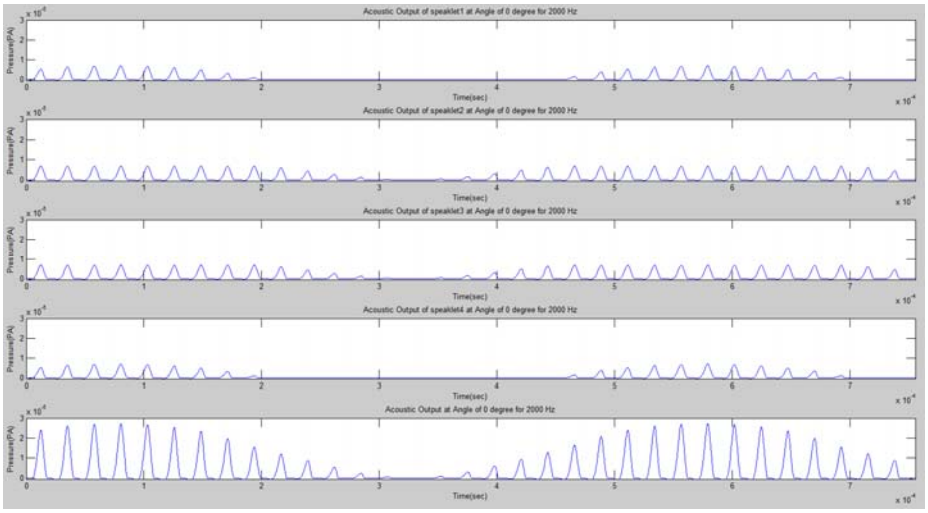

Figure 3-17: Acoustic response of 4 speaklet MDLA at the front of the array for pulse assignment 2.

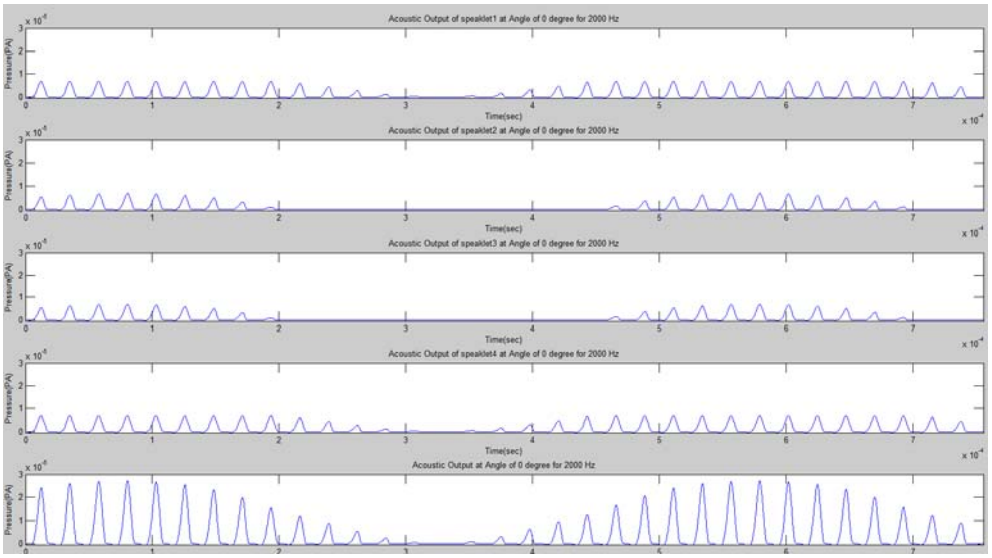

Figure 3-18: Acoustic response of 4 speaklet MDLA at the front of the array for pulse assignment 3.

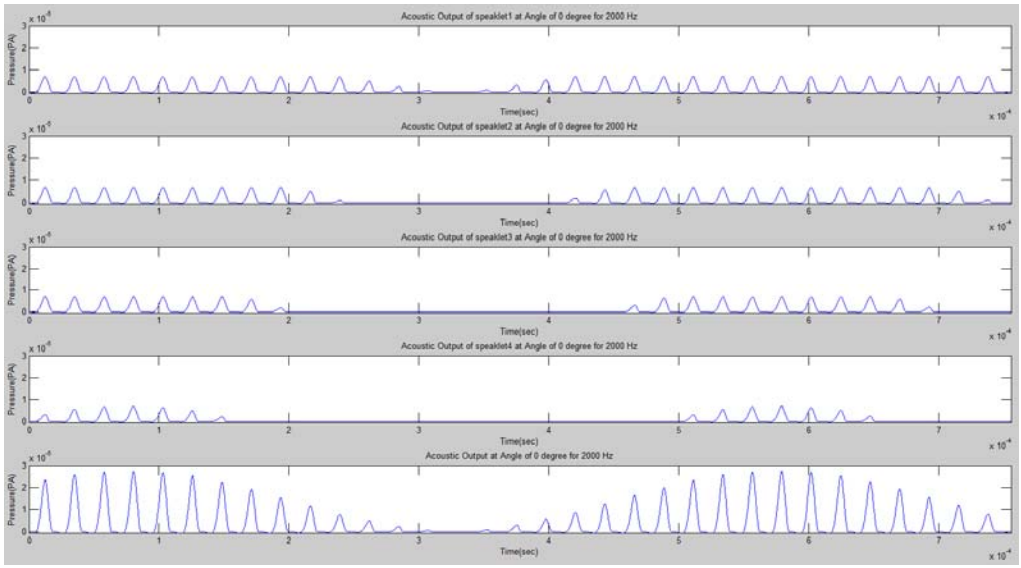

Figure 3-19: Acoustic response of 4 speaklet MDLA at the front of the array for pulse assignment 4.

3.3.3.5 Effects of Different Locations of Speaklet within the Array on Acoustic Response.

Due to the different distances between different locations of speaklets and the different angles around the centre of the array at a distance of 40 cm, as shown in Figure 3-15, the reconstructed acoustic outputs at different angles are different, as shown in the last graph of Figure 3-20 and Figure 3-21.

Figure 3-20 shows the time delays at angles of -90° (red line) and 0° (black line) degrees of arc. The 0° means the direction is at the front of the speaket array while -90° means the direction is the left of a speaklet array. The arrows point to an acoustic pulse of the sampling code in the audio stream. At the angle of 0°, the acoustic pulses of all four speaklets reach the observed point at almost the same time, while they reach the point at the angle of -90° at different times. As a result, the acoustic output is reconstructed at the angle of 0° without distortion, but not at the angle of -90°. From the first and second graphs, the acoustic pulse of the first (the left side of the array) and second speaklets reach the angle of -90 before the angle of 0 because the distance from the position of the first and second speaklets to the angle of -90° is shorter than the distance from the speaklet to the angle of 0. In the third and fourth graph, the acoustic pulse of the third and fourth (the right side) speaklets reaches the angle of -90° after the angle of 0°. It is 0° because the distance from the position of the third and fourth speaklet to the angle of -90° is longer than from the speaklet to the angle of 0°. In a similar way, the acoustic pulse is not reconstructed at the angle of 90°, as shown in Figure 3-21.

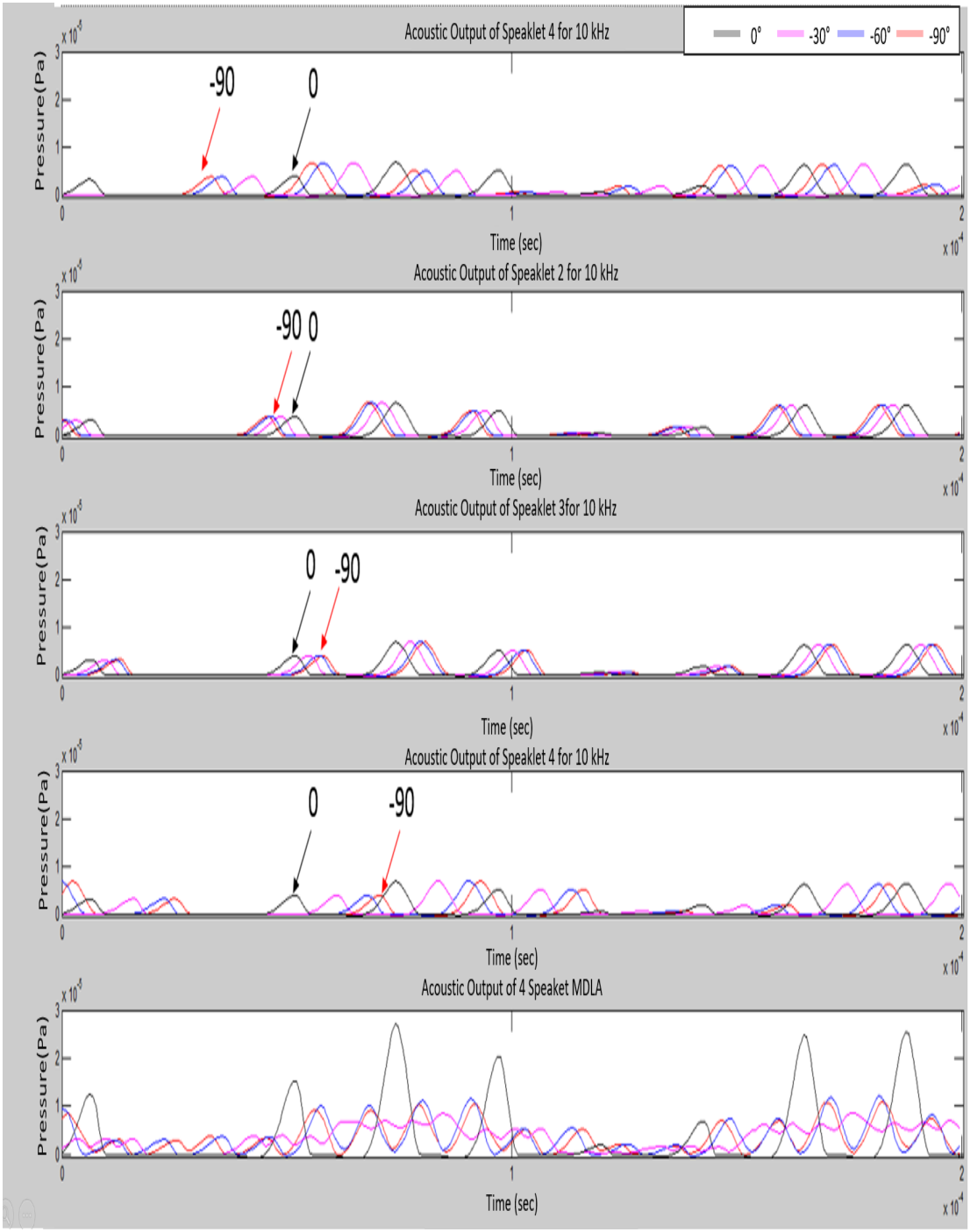

Figure 3-20: Acoustic response of 4 speaklet MDLA at different angles from -90 to 0 for pulse assignment1.

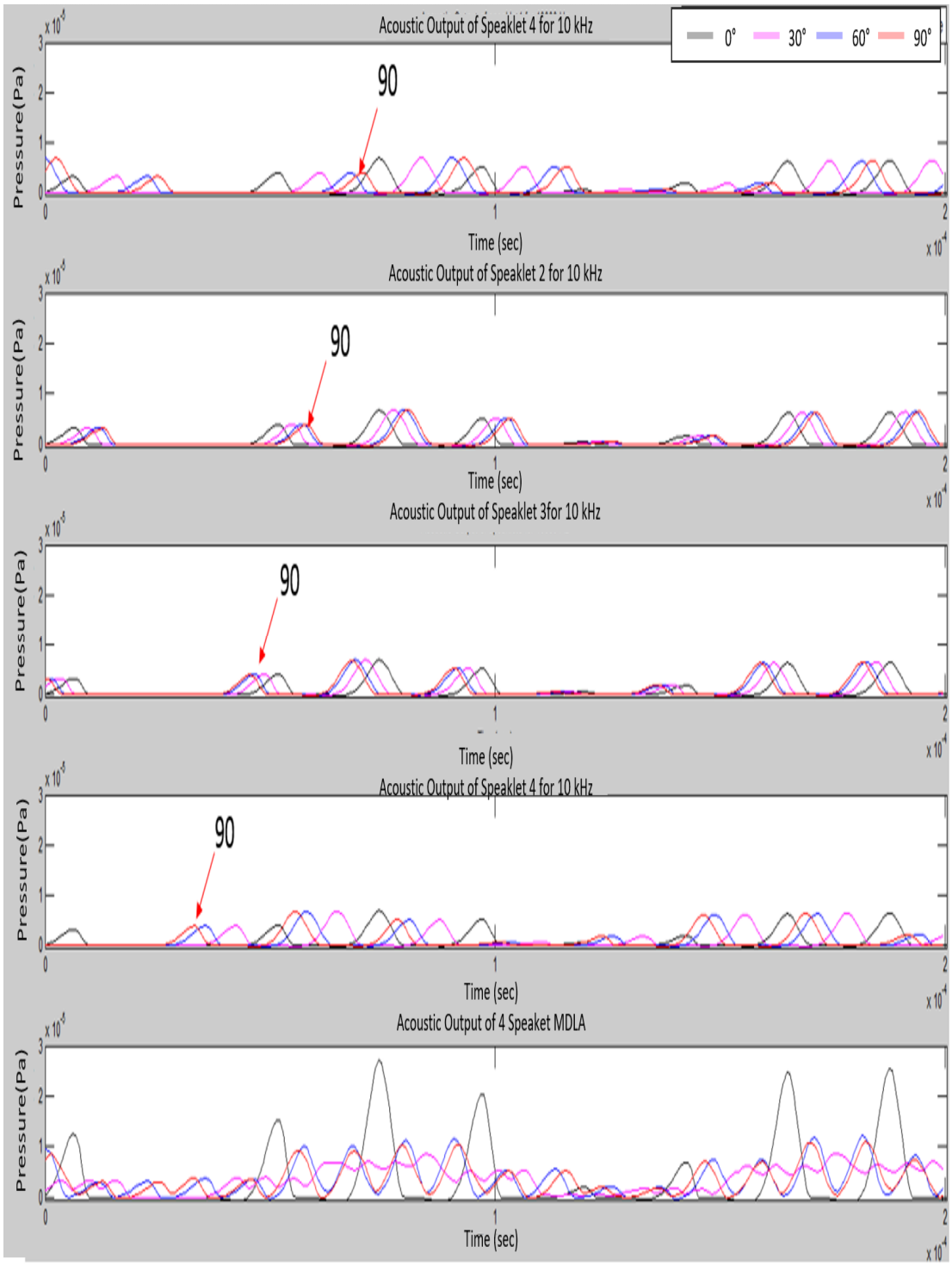

Figure 3-21: Acoustic response of 4 speaklet MDLA at different angles from 0 to 90 for pulse assignment 1.

3.3.3.6 Effects of Digital Circuit (DC)component

It can be clearly seen that the acoustic responses for the rectified source are the rectified AM sound from Figure 3-16 to Figure 3-21. A DC component appears. In other words, average pressure of the signal is not zero.

The DC components might increase the atmosphere pressure. This may cause the danger in the eardrums or in the hearing ability if the magnitude of DC component is too high. For digital transmission, a low frequency signal with a DC component cannot pass a low-pass filter. However, the ears can endure a small range of the variation of the atmosphere pressure.

The DC component of the pressure signal shows non-conservative circumstance. The air particles as a medium not only vibrate but also move from place to place. It is different from the acoustic response of a common sound which has not a DC component. The air particles vibrate at the same location.

3.3.3.7 Results of sound field and acoustic response

The results of the simulation are shown to present general characteristics of the acoustic response of the MDLA and its harmonic distortion. In order to investigate the spectrum of the acoustic response of the array, a Fast Fourier Transform (FFT) with a sampling rate of 160 kHz and 2000 data points of window size is applied. A finite impulse response (FIR) low pass filter with 256 taps is used for antialiasing.

For sound reconstruction within the MDLA, there are two additional points to consider: firstly, due to differences in pulse width, the response times of individual speaklets will be different. In order to ensure that the speaklets produce an acoustic response which reaches maximum pressure at the same time, the delay of sending electrical pulses needs to be calculated from the relationship between the response time and pulse width. Secondly, due to the acoustic output of the MDLA, resulting from a superposition of the response of the speaklets within the array, there are a variety of combinations of different levels of speaklets, allowing the same quantized level of output of the array. Therefore, a specific combination of levels is assigned for a specific quantizing level of output. This simulation will show temporal and frequency responses of the four schemes of the pulse assignment.

3.3.3.8 General Characters of Acoustic Response

The sound field intensity was also simulated, by assuming that the speaklets are point sources aligning on the x-axis and their interspacing is equal to 3.83 mm (half the sampling distance at 44.1 kHz), as shown in Figure 3-15. The sampling distance can be calculated by the multiplication

between the wave speed and the sampling period, which is the reciprocal of the sampling rate. The figure shows the spectral response from an array at a distance of 40cm from the centre of the array through different angles and acoustic outputs.

Figure 3-22 and Figure 3-29 shows both the temporal directivity response and the spectral content at that angle with a number of speaklets for an audio frequency of 10kHz. It can be seen that the outputs consist of three main components of frequency, especially at an angle of 0 degrees (i.e. directly in front of the element). The first component is the required audible frequency, which is reproduced by digital reconstruction. The second component depends on the natural frequency of the speaklets, which is around 44.1 kHz. The last component is a harmonic frequency of 71.9 kHz, which results from the sum of side bands of 44.1 kHz AM wave. However, the last two components have no effect on hearing because they are beyond the response of the human ear.

Different pulse assignments make different sound fields depending on the series of combination codes defined in the schemes of pulse assignment. The difference in the sound fields of different pulse assignments still results in a difference in acoustic response observed in all directions, except at the angle of 0 (at the front of the array), which have the same acoustic response, as shown from Figure 3-22 to Figure 3-29. In addition, symmetric pulse assignments have a direct effect in symmetric sound beams of the array, as with pulse assignments 1 to 3, which have the same acoustic response between the pairs of plus and minus angles (±30, ±60 and ±90). Asymmetric pulse assignments (pulse assignment 4) have different acoustic outputs in every direction, as shown in Figure 3-25.

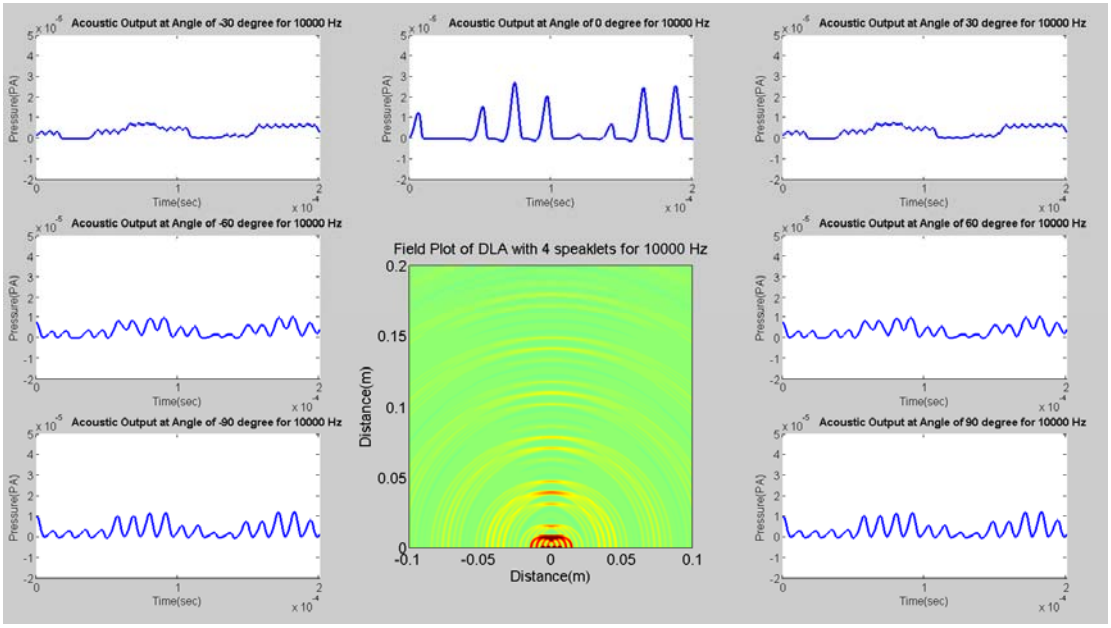

Figure 3-22: Sound field and acoustic response for pulse assignment 1. The main image of pulse assignment 1 shows sound field for 10 kHz with 4 speaklets while the satellite images show acoustic output with different angle of -90,60,-30, 0, 30, 60 and 90.

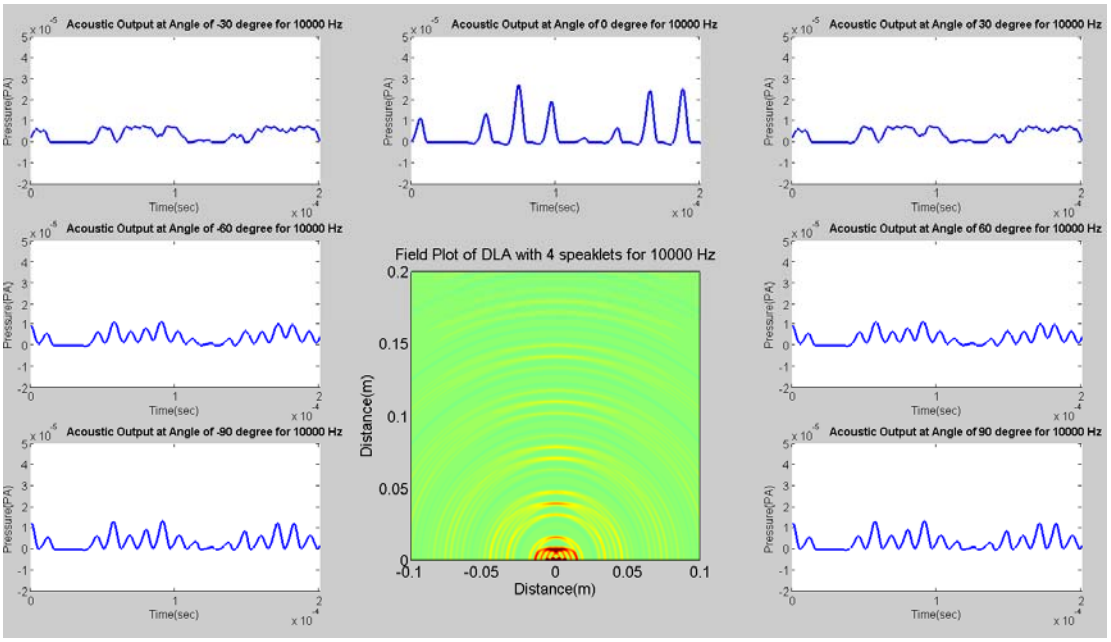

Figure 3-23 : Sound field and acoustic response for pulse assignment 2. The main image shows sound field for 10 kHz with 4 speaklets while the satellite images show acoustic output with different angle of -90,60,-30, 0, 30, 60 and 90.

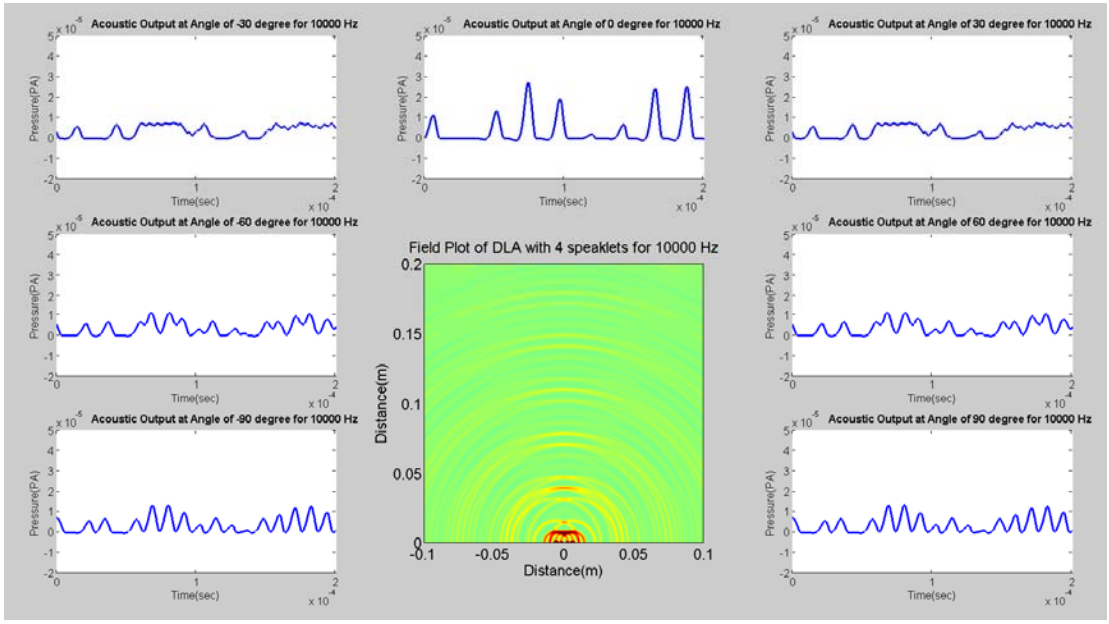

Figure 3-24: Sound field and acoustic response for pulse assignment 3. The main image shows sound field for 10 kHz with 4 speaklets while the satellite images show acoustic output with different angle of -90,60,-30, 0, 30, 60 and 90.

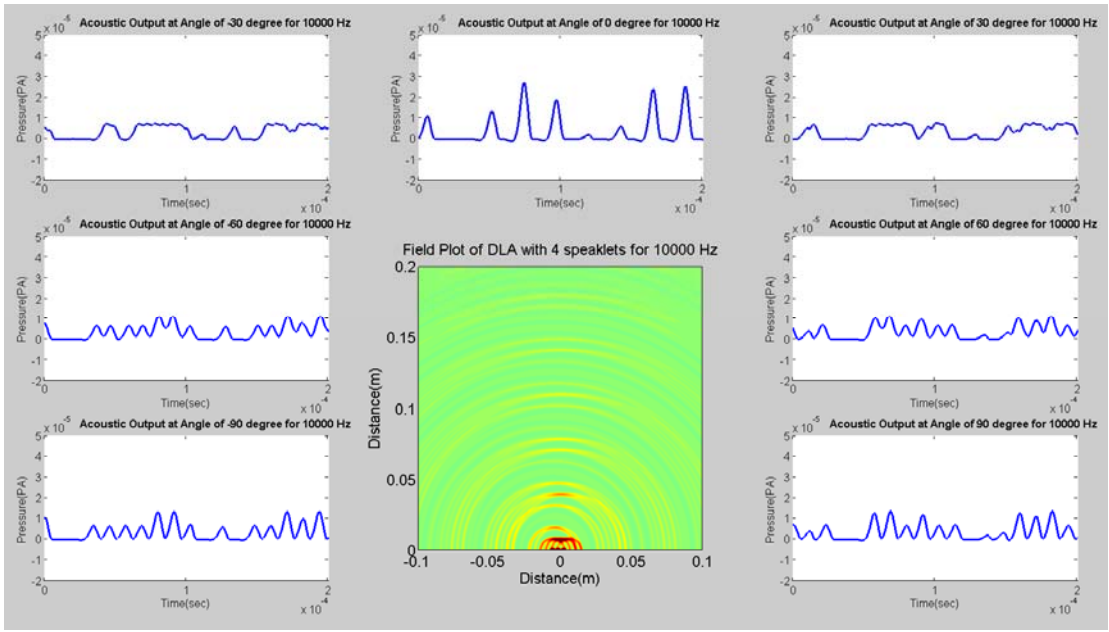

Figure 3-25 : Sound field and acoustic response for pulse assignment 4. The main image of shows sound field for 10 kHz with 4 speaklets while the satellite images show acoustic output with different angle of -90,60,-30, 0, 30, 60 and 90.

It can be found that the sound beam of the MDLA is formed in a sound field for every scheme of pulse assignment. The focus of the sound beam of the symmetric schemes of pulse assignments 1 to 3 is straight while the focus of the sound beam of the asymmetric schemes of pulse assignment 4 is bent according to the frequency of sound reproduction.

Although a beam of the MDLA is formed in the sound field, audible sound radiates in all directions for all schemes of pulse assignment.Figure 3-26 to Figure 3-29 for a 4-speaklet MDLA shows that at all angles the power spectrum of 10 kHz is equivalent. In addition, there is good evidence of omni-directional radiation from an MDLA in Chapter 3.3.3.8.2.

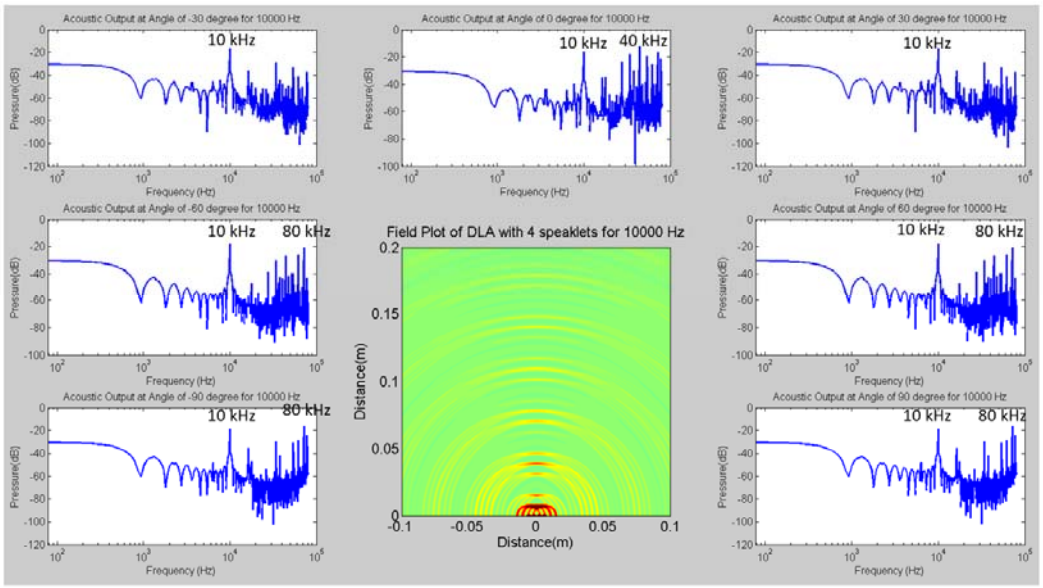

Figure 3-26: Sound field and acoustic spectrums for pulse assignment 1. The main image shows sound field for 10 kHz with 4 speaklets while the satellite images show acoustic spectrums with different angle of -90,60,-30, 0, 30, 60 and 90

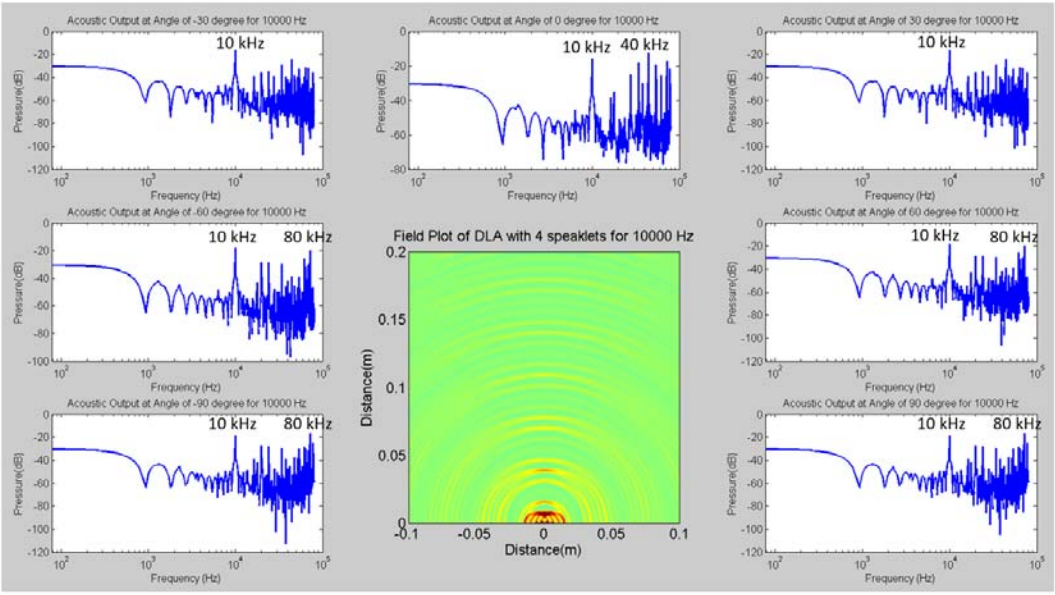

Figure 3-27: Sound field and acoustic spectrums for pulse assignment 2. The main image shows sound field for 10 kHz with 4 speaklets while the satellite images show acoustic spectrums with different angle of -90,60,-30, 0, 30, 60 and 90

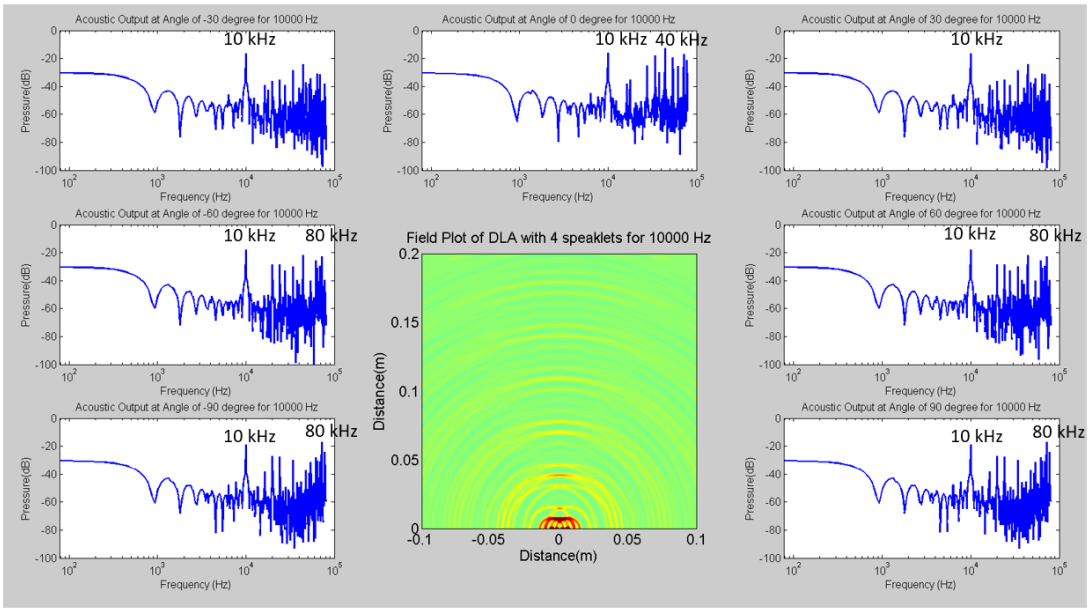

Figure 3-28: Sound field and acoustic spectrums for pulse assignment 3. The main image shows sound field for 10 kHz with 4 speaklets while the satellite images show acoustic spectrums with different angle of -90,60,-30, 0, 30, 60 and 90

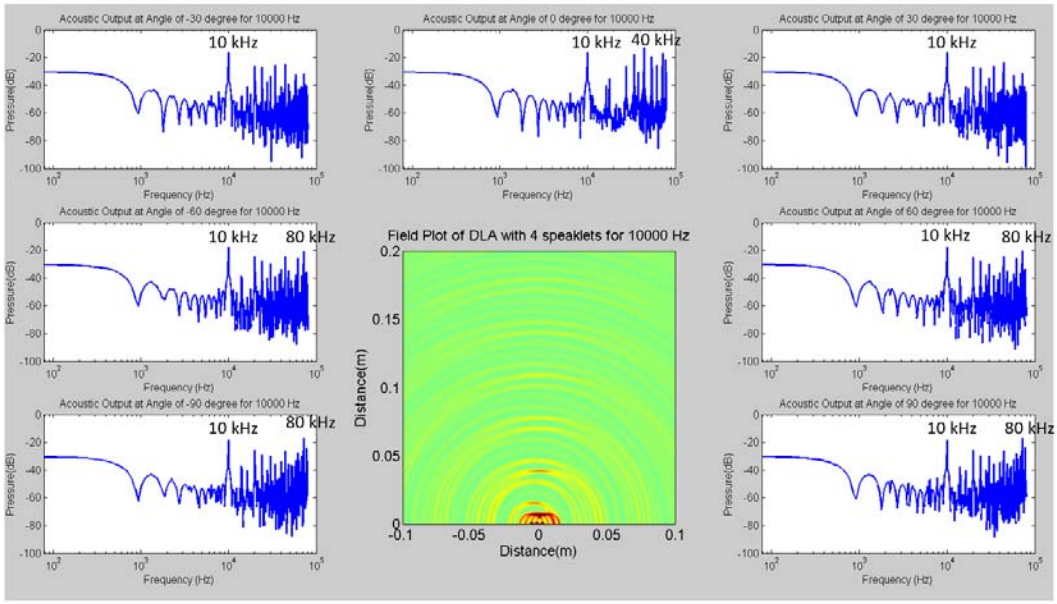

Figure 3-29: Sound field and acoustic spectrums for pulse assignment 4. The main image shows sound field for 10 kHz with 4 speaklets while the satellite images show acoustic spectrums with different angle of -90,60,-30, 0, 30, 60 and 90

3.3.3.8.1 Harmonic Distortion

There are two factors causing harmonic distortion in an MDLA: the size of array and the range of required audible frequencies. When the size of the array increases, harmonic distortion rises. Figure 3-30 to Figure 3-33 shows the different levels of harmonic distortion in a 16 speaklet MDLA for different pulse assignments (inside red circles), while a 4 speaklet MDLA has no distortion, as shown from Figure 3-26 to Figure 3-29 for every scheme. In addition, from Figure 3-30 to Figure 3-33, it is clear that the schemes of pulse assignment have an effect on the level of the distortion. Pulse assignment 4 in Figure 3-33, the scheme of minimizing the number of speaklets with asymmetry, has the highest level of distortion of the schemes. Pulse assignment 1 in Figure 3-30, the scheme of minimization of sound levels among speaklets, has no distortion in the audible range.

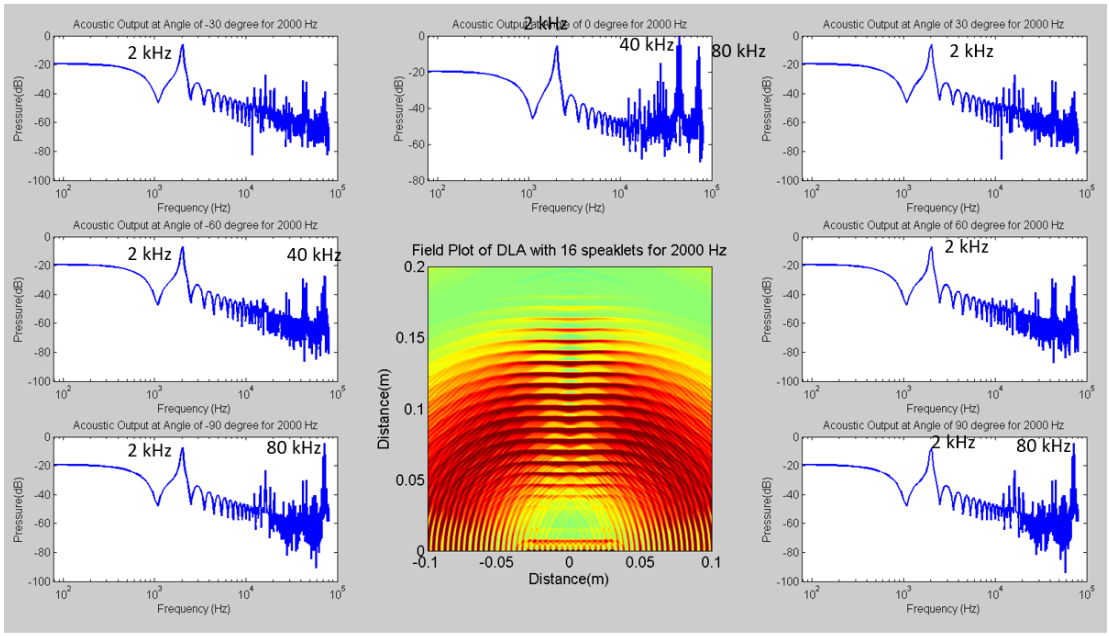

Figure 3-30: Sound field, the spectral response and sound distortion of a 16 speaklet DLA emitting a digital audio stream of 2 kHz for pulse assignment1.

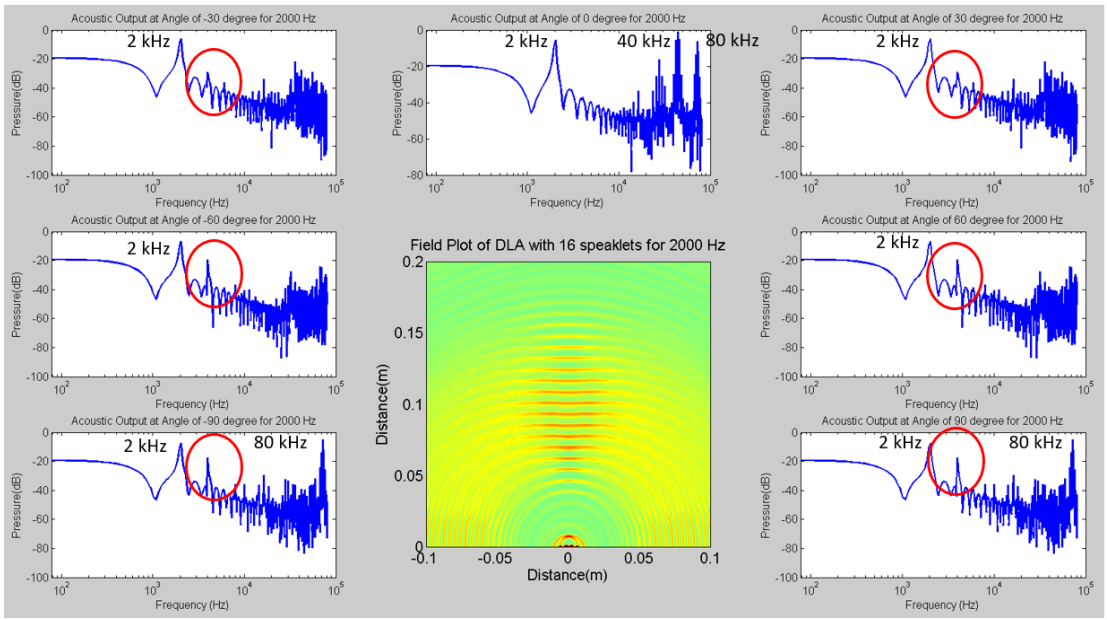

Figure 3-31: Sound field, the spectral response and sound distortion of a 16 speaklet DLA emitting a digital audio stream of 2 kHz for for pulse assignment2.

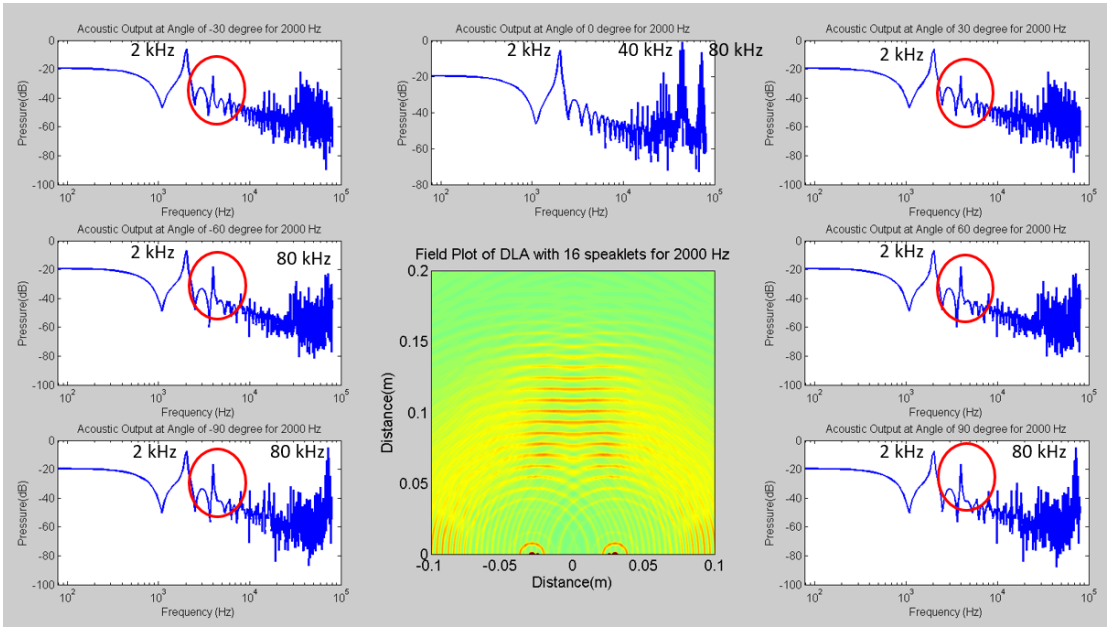

Figure 3-32: Sound field, the spectral response and sound distortion of a 16 speaklet DLA emitting a digital audio stream of 2 kHz for pulse assignment3.

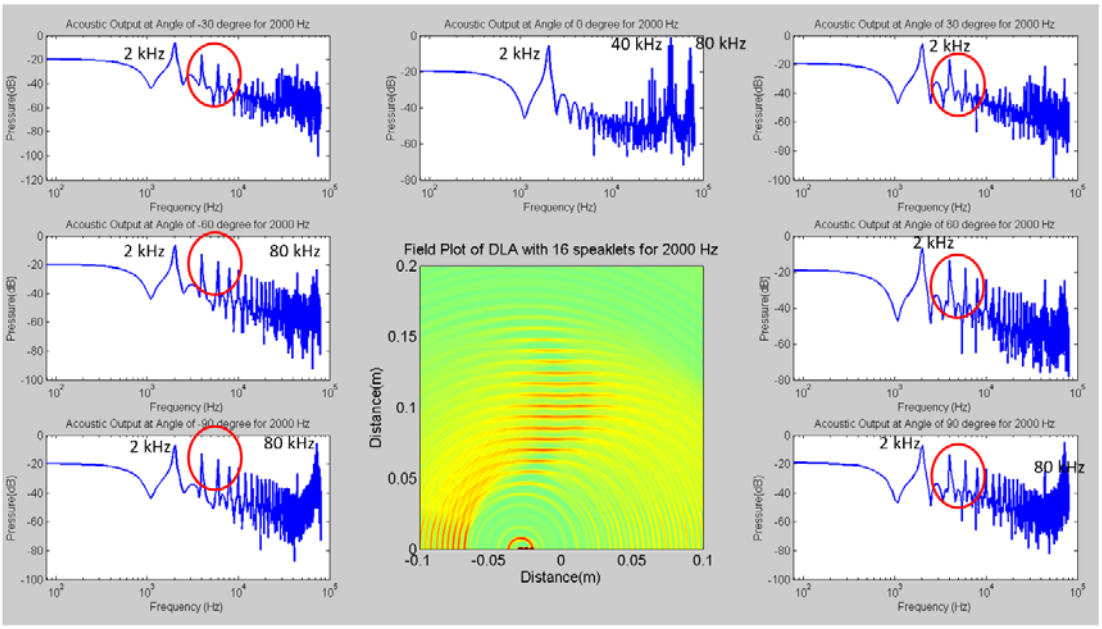

Figure 3-33: Sound field, the spectral response and sound distortion of a 16 speaklet DLA emitting a digital audio stream of 2 kHz for pulse assignment4.

From Figure 3-34 to Figure 3-29, a 8 speaklet array reproduces sound at 20 Hz and harmonic distortion is found at 20 kHz showing inside the red circles. In addition, every scheme has the effect of harmonic distortion when it produces audio sound at low frequency. The level of distortion depends on direction, especially at the front of the array, which has the highest level of distortion. However, it have high effect to human's hearing because frequency of the distortion is near limit of the hearing range.

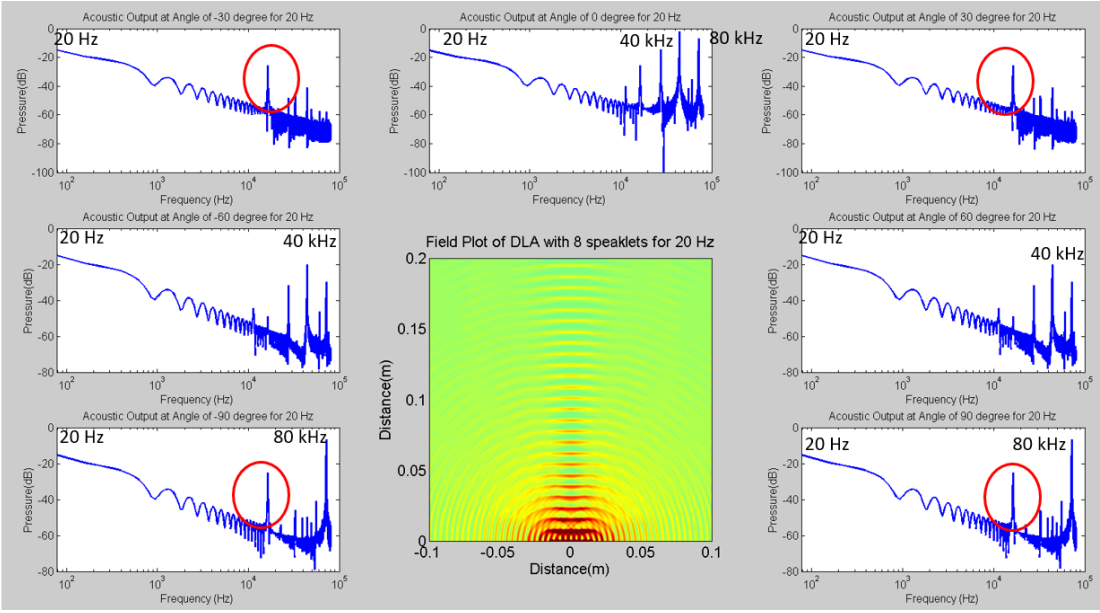

Figure 3-34: Sound field , the spectral response and sound distortion of 8 speaklets DLA emitting digital audio stream of 20 Hz for pulse assignment1.

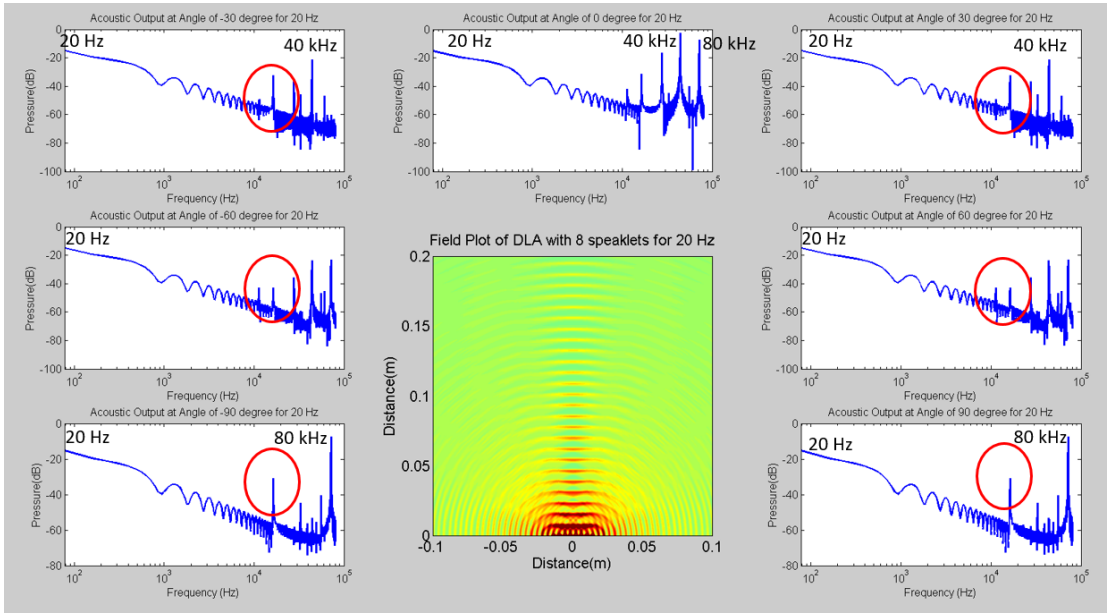

Figure 3-35: Sound field , the spectral response and sound distortion of 8 speaklets DLA emitting digital audio stream of 20 Hz for pulse assignment2.

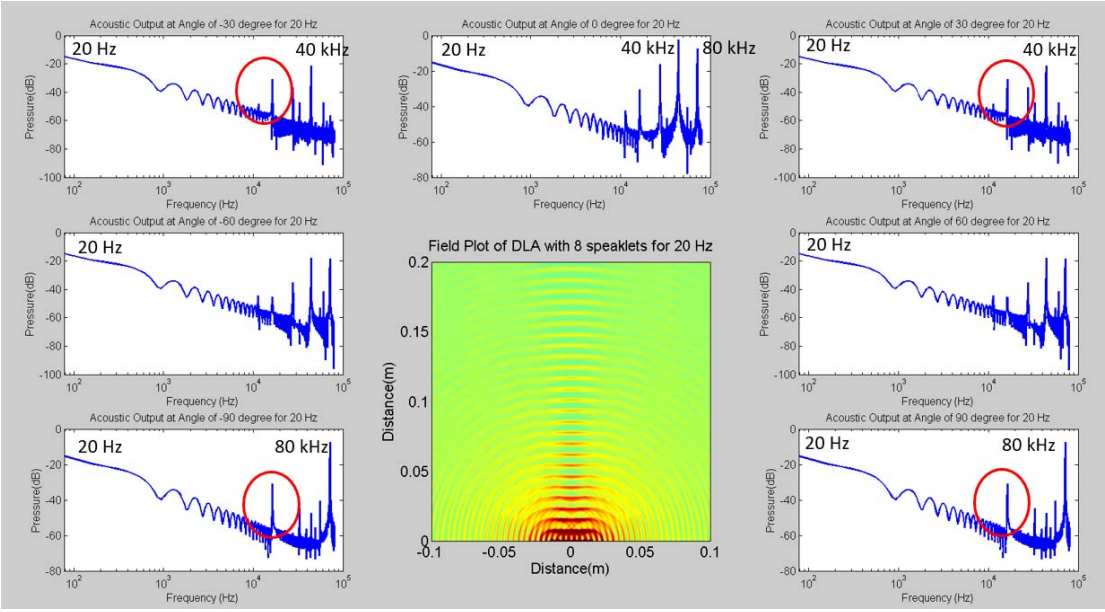

Figure 3-36: Sound field , the spectral response and sound distortion of 8 speaklets DLA emitting digital audio stream of 20 Hz for pulse assignment3.

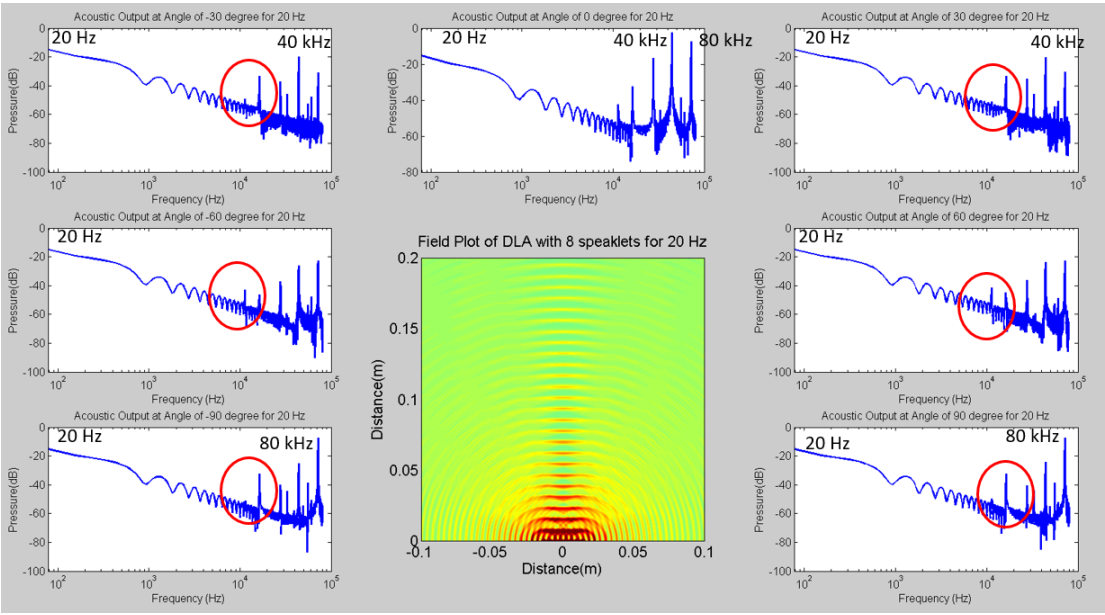

Figure 3-37: Sound field , the spectral response and sound distortion of 8 speaklets DLA emitting digital audio stream of 20 Hz for pulse assignment4.

3.3.3.8.2 Results of Directivity of MDLA

The directivity of an MDLA is plotted using three components: audible frequency, the natural frequency of the speaklet and the harmonic frequency, which is the sum of AM components. However, only the audible frequency is detectable by the human ear.

From Figure 3-38 to Figure 3-41, although the beams of the natural frequency (red curve) and harmonic frequency (green curve) are different for all schemes of pulse assignment, the beams of audible frequency (blue curve) are similar. The power of the audible frequency is equal to half the maximum power of the natural frequency of the speaklet.

The width of the sound beam depends on the frequency of the sound reproduced and the size of the array. When the frequency is high and the size of the array is large, a sound beam will be formed. When the frequency of the sound reproduced is low and the size of the array is small, sound will radiate in all directions. From the figures, the sound beam of a 4 speaklet MDLA reproducing sound with a high frequency of 10 kHz has a width of 180 degrees for all schemes of pulse assignment. The array with the size of 4, 8 and 16 can radiate omni-directionally when it reproduces sound with a low frequency of 2 kHz. However, with an array with a large size of 8 or 16 speaklets a beam is formed when it reproduces sound with a high frequency of 10 kHz

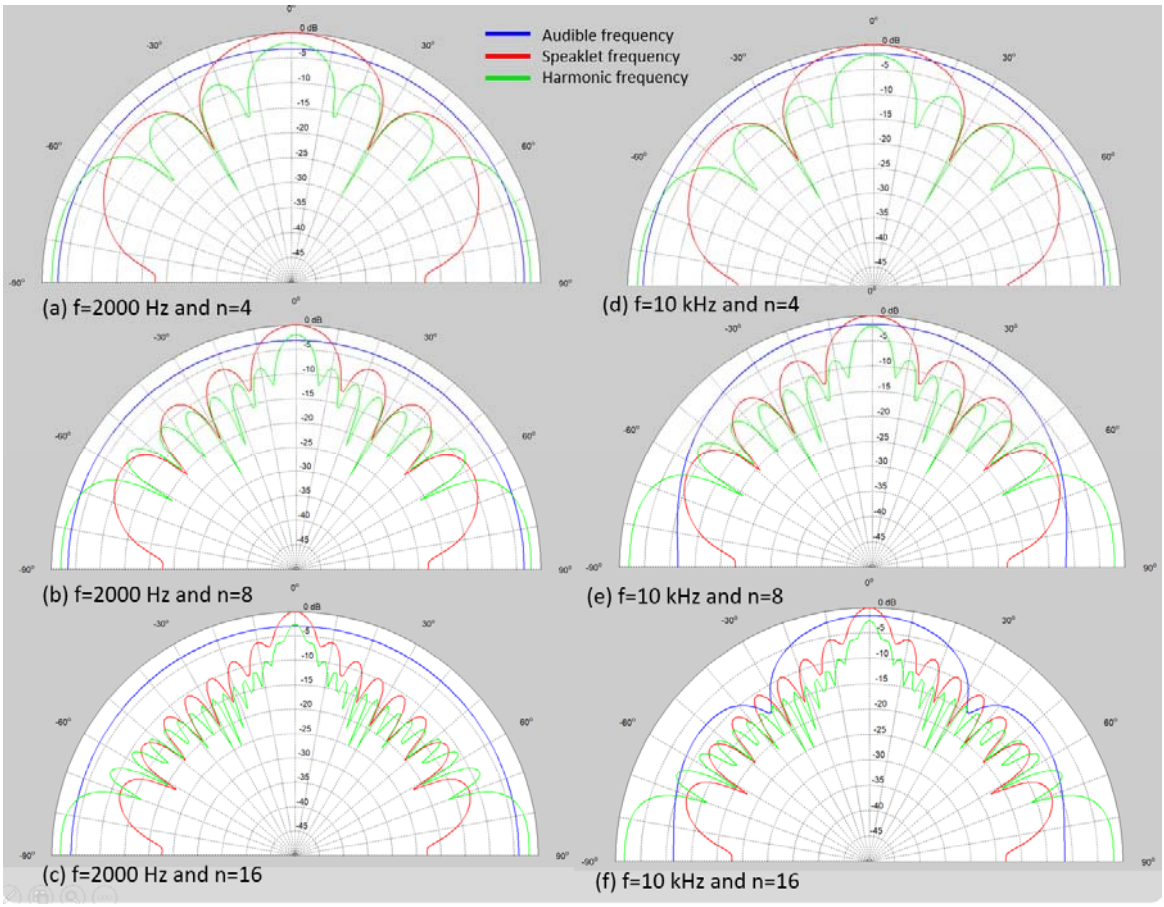

Figure 3-38: Directivity of audible frequency, natural frequency of speaklet and harmonic frequency for pulse assignment 1.

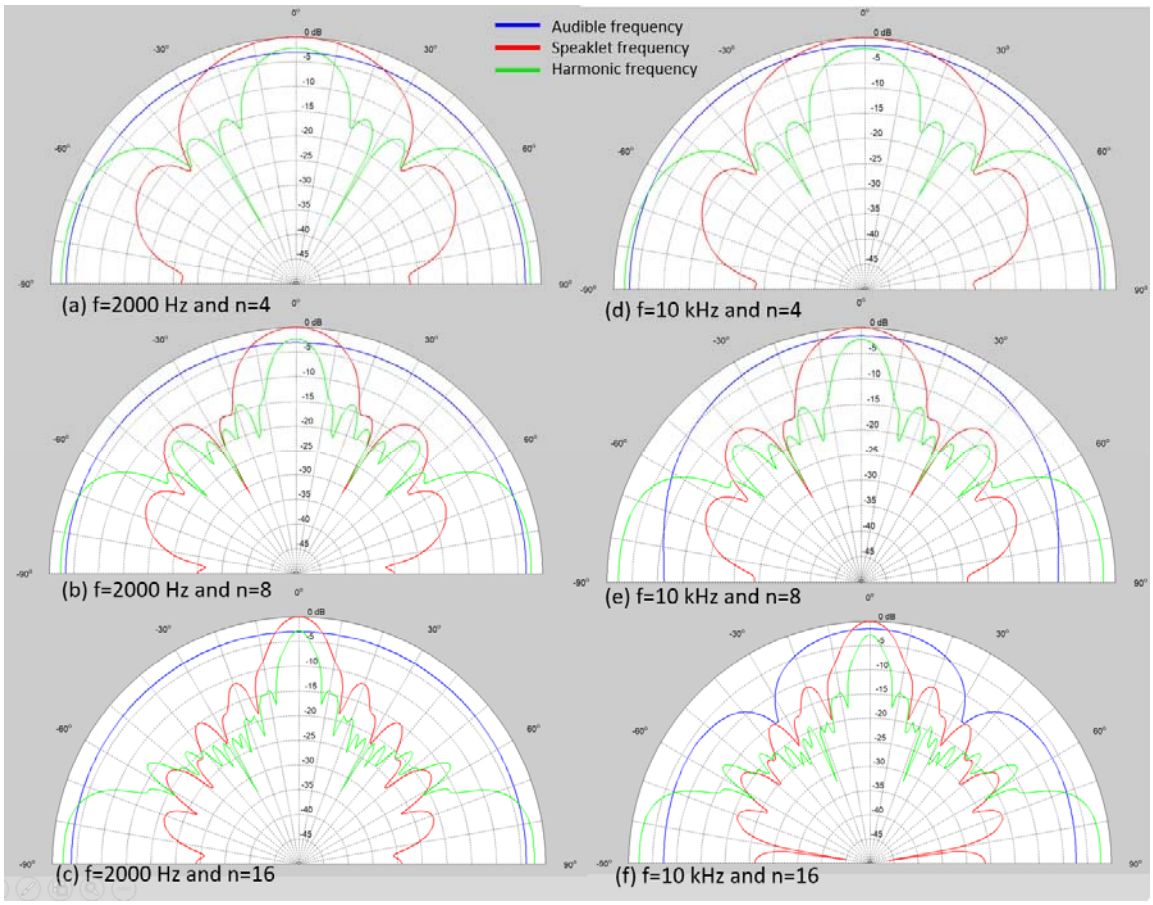

Figure 3-39: Directivity of audible frequency, natural frequency of speaklet and harmonic frequency for pulse assignment 2.

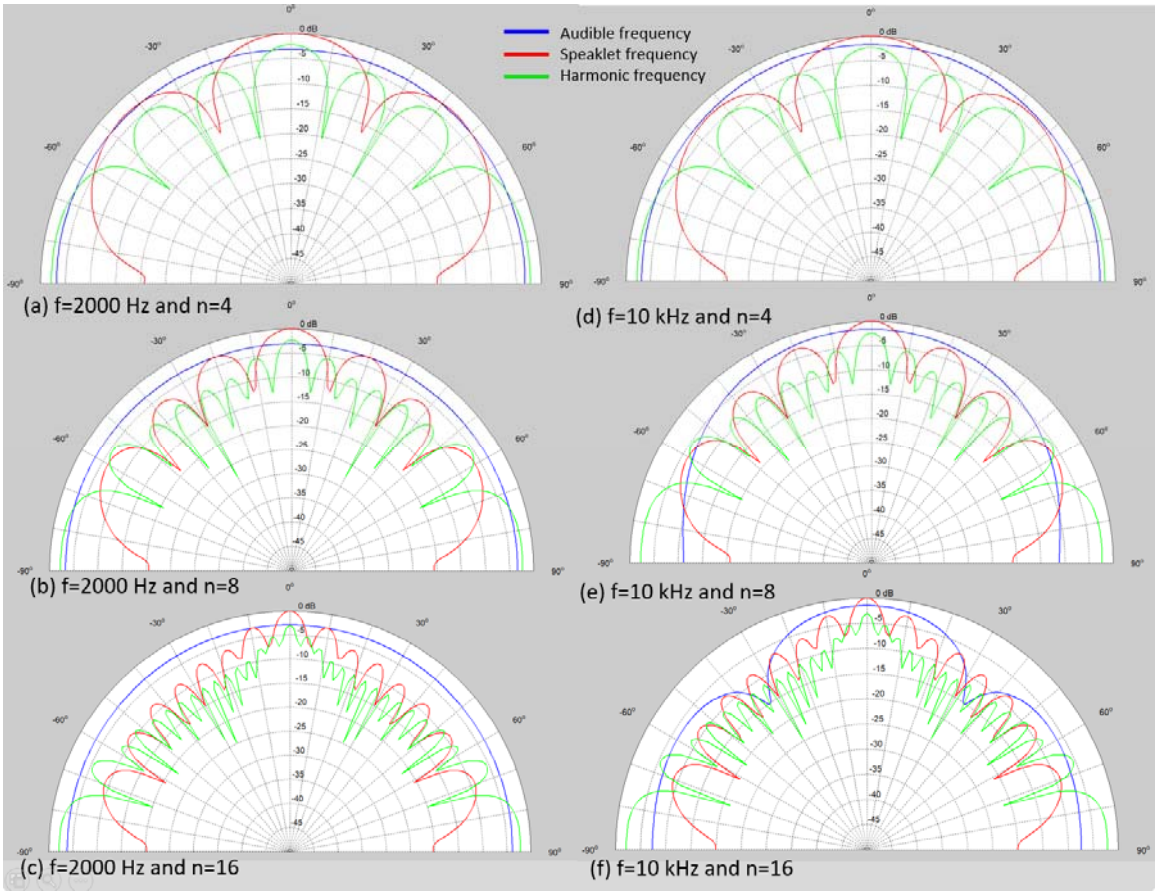

Figure 3-40: Directivity of audible frequency, natural frequency of speaklet and harmonic frequency for pulse assignment 3.

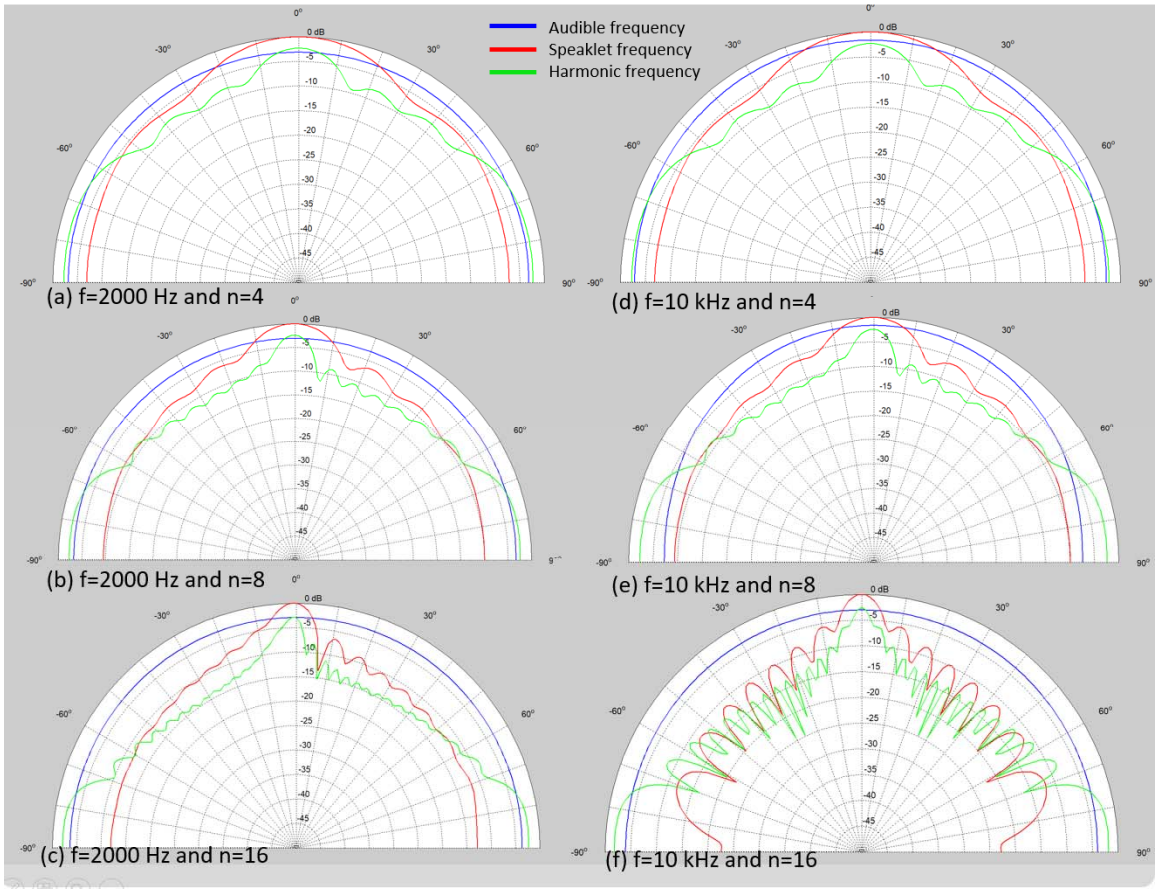

Figure 3-41: Directivity of audible frequency, natural frequency of speaklet and harmonic frequency for pulse assignment 4.

3.3.3.9 Acoustic Impedance of a Rectifying Sound Source

This simulation is based on the wave equation of a spherical sound sound in the transient state. Acoustic impedance is assumed as a real number under the condition of $((kr)^2>>1)$ or the phase angle of the acoustic impedance is equal to zero. However, the acoustic impedance is not a real number but a complex number. It can be expressed in Eq.(2.153) and can be rearranged in terms of p(R), $\dot{W}$(R) and acoustic impedance (z):

$$p(R) = z\dot{W}(R) \tag{3.19}$$

where

$$z = \frac{k_t c\rho r^2(k_t r - j)}{((k_t r)^2 + 1)R} \tag{3.20}$$

and k_t ,which is defined in Eq.(2.142), can be equivalent to the wave number (k) when the imaginary part is neglected and far less than 1.

Therefore, the polar angle (θ) of the acoustic impedance can be found by solving:

$$\tan(\theta) = \frac{1}{kr} \tag{3.21}$$

The angle causes phase difference between the velocity of air flow and the acoustic pressure. The difference results in negative pressure in the rectified sound.

For the natural frequency at 40 kHz, if the phase angle of acoustic impedance of the source is 9.46° degree or slightly more than 10 % of 90° degree, the radius of the source needs to be at least 8.19 mm as shown in Table 3-3.

However, the radius of the source is not depended on the physical structure of the rectifying sound source, but on the air volume blowing from the air outlet or the source as shown in Figure 3-2.

Therefore, rarefied or negative pressure of the rectified sound is reduced by increasing the pressure in the pump. As a result, the air volume from the outlet and the radius of the source(r) will increase, and the phase angle of acoustic impedance will decrease.

Table 3-3: Radius of sound source in millimetre (mm) for phase angles and frequencies

The phase angle of acoustic impedance z in degree		9.46°	5.7°	4.39°
Frequency	Wave number(k)	kr =6	kr =10	kr =13
40 kHz	732.7	8.19	13.6	17.74
65 kHz	1190.7	5.04	8.40	10.92
80 kHz	1465.5	4.09	6.82	8.87

3.4 Amplitude Modulation in Acoustics and Loudness

This section describes how to apply amplitude modulation in acoustics and identifies its advantages.

3.4.1 Amplitude Modulation in Acoustics

AM is a technique in telecommunication. A common application of AM is in radio broadcasting. It is a technique used to transmit analogue messages, such as audio waves, via a carrier wave. The carrier wave, which is a high frequency wave, is modulated to convey the audio wave, which is low frequency, from one place to another, by varying the amplitude of the carrier according to the audio wave. When it reaches its destination, the information signal is extracted from the modulated carrier by demodulation. This shows the demodulating process by rectifying the modulated wave to obtain audio frequency (4 kHz). The high frequency components can be removed by a low-pass filter before feeding the signal into a loudspeaker.

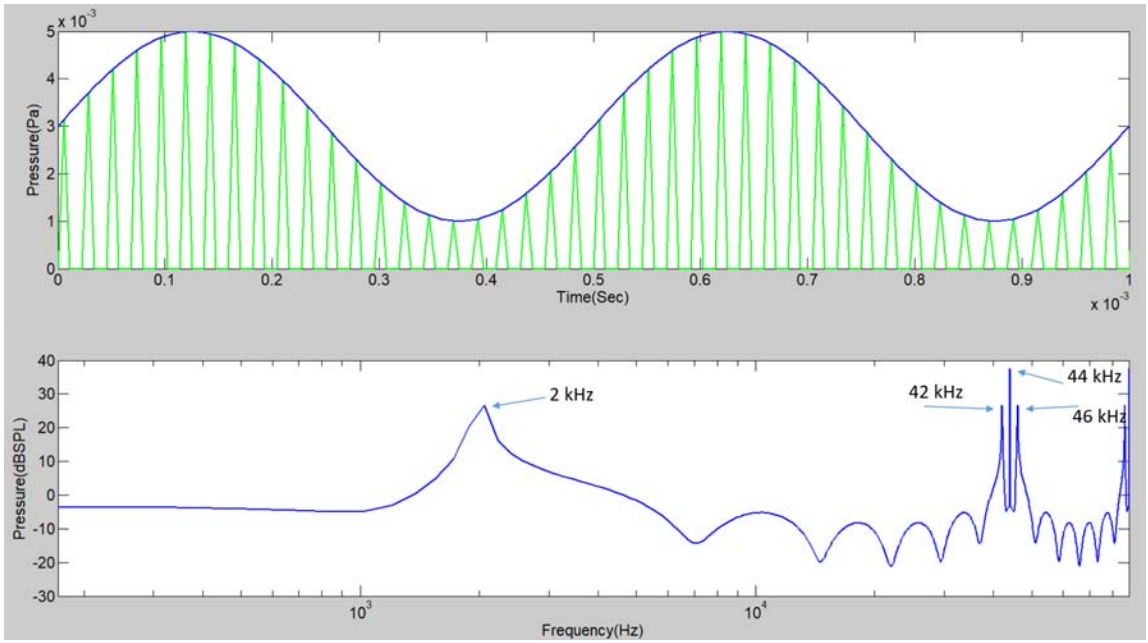

Figure 3-42: temporal and frequency of acoustic response of rectified amplitude modulation when frequency of audio (2 kHz) and carrier (44 kHz) are equal

The airborne response of an MDLA is similar to the rectified signal of amplitude modulation (AM). A train of electrical pulses feeding into speaklets of a MDLA relates to a rectified AM signal:

- The carrier frequency of the AM signal is equal to the pulse rate of a MDLA

- The audible frequency of the AM signal is equal to the audio frequency represented by variable pulse widths of MDLA. The maximum frequency of the audio signal is not over half of the pulse rate of MDLA according to the Nyquist criterion.

Therefore, a MDLA can generate the AM signal, which has audible frequencies less than half of the carrier frequency.

Considering the rectification of AM in Table 3-4, Rectifying source give high efficiency in sound generation more than the source generate AM wave because the rectification is the demodulation of audio signal of AM.

Table 3-4: Comparison between AM in telecommunication and in acoustics

	Acoustics	Telecommunication
Traversing energy	Acoustic pressure	Electro-magnetic energy
Medium	The air	None or no requirement
AM signal	Audible frequency components are found due to the beat effect. Loudness of the sound relies on non-linearity of the air media.	There is no audible frequency component.
Rectification of AM signal	Amplitude of audible frequency component of the rectified sound is higher than the amplitude of the AM sound. Loudness of the sound does not relies on non-linearity of the air media.	Audible frequency component can be detected.
Low pass filter	Although the acoustic wave consists of the frequencies in an audible range and in an ultrasonic range. Although the ear can hear sound in the audible range, the ultrasound has no effect on hearing	High frequency components are removed but Audible frequency components remain.

Another feature of AM is that audio will only be present when the carrier exists. Because the AM sound modulates or mixes ultrasound and audio sound together. Propagation of the wave should be similar to ultrasonic wave propagation. Therefore, the sound generated by an MDLA will be directional if speaklets within the array are common ultrasonic transducers, which have narrow

beam widths. In the simulation, it is assumed that speaklets are spherical sound sources, which radiate sound in all direction. As a result, the MDLA omni-directionally generates sound.as the ultrasonic sound.

3.4.2 Loudness of AM sound

Because the response of a DLA consists of frequencies within the audible range and frequencies outside the audible range (infrasound and ultrasound), loudness for hearing should be calculated from the intensity of the frequencies within the audible range as:

$$SLL = \ 10\ log_{10}\left(\sum_{n\ for\ frequencies\ from\ 20\ Hz\ to\ 20k\ Hz} 10^{\frac{(SPL_n - A_n)}{10}}\right) \qquad (3.22)$$

while the intensity of the response of the DLA can be calculated from Eq.(2.31).

3.4.3 Advantage of Rectified AM Sound

Sound modulated with ultrasonic sound using amplitude modulation has the following advantages:

- The sound generated by an MDLA is directional because speaklets within the array are common ultrasonic transducers, which have narrow beam widths. This enables the loudspeaker to control the boundary of the sound. It is difficult to control this with normal sound because low frequency sound can bend and is omni-directional. Although AM sound have high frequencies in a range of ultrasound but it can be heard the same as a normal sound
- The hearing boundary can be sharply defined by an MDLA with a spherical speaklet and a wave guide. Similar to the defining spotlight of a flashlight, the speaklet acts as a light bulb while the wave guide acts as the metal reflector cone. Because the attenuation of high frequencies is higher than low frequencies, as shown in Table A-1.
- The audio sound ideally generated by an MDLA has more intensity than the parametric loudspeaker. The sound of an MDLA is a rectified amplitude modulation. The sound relies on linear and nonlinear acoustics while the sound from a parametric loudspeaker relies on only non-linear acoustics.
- A MDLA or an AM loudspeaker array enables a small-diameter speaker to reproduce sound in low frequencies or bass sound better than high frequencies. Normally, a small loudspeaker have poor quality in reproduction of bass sound. A larger loudspeaker is required for the bass reproduction.

3.5 Discussion and Summary

A Multiple-Level Digital Loudspeaker Array (MDLA) generates sound by feeding a train of electrical rectangular pulses with constant pulse height but variable pulse widths into speaklets (tiny loudspeakers). This chapter studied the ideal case of an MDLA by assuming a speaklet as an MSD model, which does not take into consideration the details and limitations of the speaklets, such as their structure and driving circuits and assumes the speaklet is a spherical source driven by a discrete force. The force produces two transient responses at the rising and falling edges of a pulse. The conditions for the production of sound in this simulation are that the velocity of vibration is directly proportional to the displacement of vibration, as Eq.(3.11) and that the sound pressure is directly proportional to the velocity as Eq.(3.17). Sound pressure is computed by Eq. (3.13).

The ideal speaklet in a digital loudspeaker requires a high damping ratio (0.7 in this simulation) in order to meet the first requirement of digital reconstruction. The high damping of a speaklet makes its acoustic response short. The response has only one acoustic pulse or a second pulse significantly smaller in amplitude than the first one.

The relationship between maximum pressure and pulse width and the relationship between response time and pulse width are linear up to pulse widths of 4.685 μs, with R^2 coefficients of 0.9917 and 0.9967 respectively (fulfilling the third requirement). Therefore, 937 different pulse widths are available for a speaklet, by varying the pulse width from 0 ns to 4.685 μs in steps of 5 ns. For a 16-bit resolution in a conventional audio system, this requires a speaklet array of 70 elements.

The range of linear relationship between the amplitude of acoustic response and the pulse width of an electrical pulse can be approximately equal to a quarter of a period of the natural frequency of vibration of the speaklet (f_d=44.1 kHz), which is 5.668 μsec while the period of linearity is 4.685 μsec.

Due to feeding with different width pulses, the acoustic response time of each pulse width is different. However, the response time is linearly related to pulse width. The time shift can be calculated in order that acoustic pulses of different pulse widths can rise at the same time. The time shift can improve the linearity for a small angle of listening from 0.9917 to 1, but for a wide angle of listening, time shift might not help to improve the linearity.

The resolution of the sound of a speaklet within a DLA is dependent on the ratio between the range of linearity and the period of clock frequency of the electrical pulse generator. The clock speed of market Field-Programmable Gate Array (FPGA) boards is 50 or 100 MHz.

The sound field intensity was also simulated, by assuming that the speaklets are point sources aligned on the x-axis and their interspacing is equal to 3.83 mm (half the sampling distance at 44.1 kHz). The spectral response is observed for an array at a distance of 40 cm from the centre of the array through different angles and acoustic outputs. Four schemes of pulse assignment are assumed to study the effect of location of the speaklets on acoustic response. Both the temporal response and the spectral content are shown at different angles with different numbers of speaklets.

Due to the acoustic output of an MDLA resulting from a superposition of the response of the speaklets within the array, the scheme of pulse assignments needs to be pre-defined for a quantizing level of digital audio (16 bits or 65,536 levels) because there are various combinations, which assign different pulse widths to different speaklets to reconstruct the level. Different pulse assignment schemes give different acoustic responses, different distortion and different directivity. These differences result from the combination of acoustic pulses travelling from the different locations of the speaklets. Therefore, a specific combination of the levels is assigned for a specific quantizing level of the output. The best scheme for minimizing distortion from the four schemes in this study is bit assignment 1, which assigns pulse widths with minimization of sound levels among the speaklets.

The spectrum of acoustic response of an MDLA consists of three main components of frequency, especially at an angle of 0 degrees (i.e. directly in front of the element). The first component is the required audible frequency, which is reproduced by the difference in AM frequencies. The second component depends on the natural frequency of the speaklets, which is around 44.1 kHz. The last component is a harmonic frequency of 71.9 kHz, which results from the sum of AM frequencies. However, the last two components have no effect on hearing because they are beyond the response of the human ear. These three frequency components are plotted for directivity. For a frequency of 2 kHz, sound radiates omnidirectionally. For a frequency of 10 kHz, as the number of speaklets increases, the response is more directional for all schemes of pulse assignment. This behaviour is similar to the behaviour of analogue loudspeakers. The larger the diaphragm of the loudspeaker, the more directionally it reproduces sound. Although the response may be different at different angles, the power spectrums at the audio frequency of the response are the same. The response has high amplitude directly at the front of the array but the audible spectrums are the same in all directions.

The results of the simulation demonstrate that the MDLA can reproduce audio. However, the simulation has not taken into account some practical issues such as:

- Impedance mismatch and efficiency of the piezoelectric element

- The directivity of an individual speaklet within the array resulting from its shape and size
- Non-uniformity of acoustic outputs of the speaklets due to imperfections in the fabrication process
- Difference in delay time from the pulse generator to the different locations of speaklets
- Non-ideal shape of the rectangular pulse, because of the transition state limitations of transistors

The speaklets in the array are also linearly aligned in this simulation, while the array alignment will be square in the practical implementation.

In addition, the condition of kr >> 1 in the rectifying source is assumed because it constitutes the linear relation the acoustic pressure and the velocity of air flow from the air outlet. The radius (r) of the source include the radius of air outlet and air volume blown out from the outlet to push the air in atmosphere. Therefore, the radius varies by the air volume from the outlet. If pressure from the pump is high enough, the condition can be satisfied. However, in reality, it is difficult in measuring the radius of the source

Although the study of sound reproduction of an MDLA from the simulation is only for an ideal case, it indicates that people will be able to hear the sound reproduced by the MDLA, and gives confidence that good performance is possible from the concept, despite the presence of ultrasonic frequency components.

Chapter 4: Multi-Level Digital Loudspeaker Array Based on Piezoelectric

A multiple level digital loudspeaker array (MDLA), as mentioned in Chapter 3.1, is proposed for extending the audio resolution of the digital loudspeaker array (DLA), which is another concept of sound generation using ultrasound. There are two main sections in this chapter. One section describes the experiments used to investigate the fulfilment of the requirements for digital sound reconstruction, described in Chapter 2.3.3, for the MDLA. The other section studies the design of a speaklet within the DLA through finite element modelling software (Comsol). The study focuses on the relationship between the response of a speaklet to an electrical rectangular pulse and the diaphragm structure of the speaklet.

4.1 Experiments

Three experiments were conducted in order to test the requirements of digital sound reconstruction with a MDLA speaklet and their audio reproduction for pure tone. The first requirement, which is involved with the period of ringing of the pressure response of a speaklet, is considered for three types of speaklets in Experiment 4.1.2. The third requirement, which is related to the linearity between input pulse width and output pressure amplitude, is examined in Experiment 4.1.3. Experiment 4.1.4 shows audio reproduction of a MDLA speaklet for a pure sine wave. However, the second requirement, which is involved with uniformity among speaklets with the array, is not tested because the uniformity depends on technologies for fabricating speaklets with the array. The speaklets will have the same specification.

4.1.1 Setup of Experiments

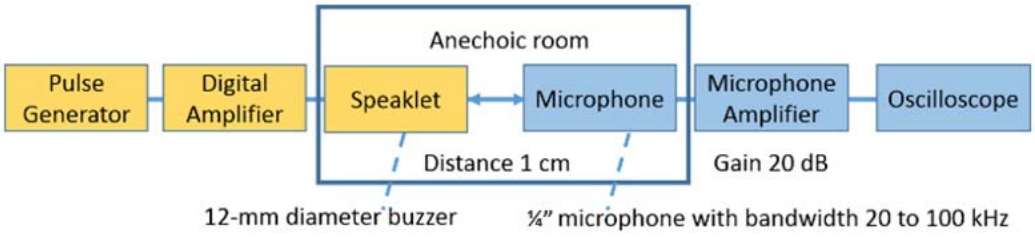

Figure 4-1: Configuration of Digitally-Driving Speaklet Experiment

The experimental set-up can be divided into two sides as shown in Figure 4-1: transmitting and receiving. The transmitting side consists of:

- A pulse generator producing a train of rectangular pulses with different widths but the same height. In this research, the generator implemented is DE2-115, which is an FPGA board having a 100 MHz oscillator clock and a PC connecting module with serial communication RS232.
- A digital amplifier, a simple high frequency switching circuit, which can be implemented with a transistor. In this research, the amplifier is implemented by L293D, which is a Darlington transistor integrated circuit (IC) designed to provide drive currents up to 600 mA at voltages from 4.5 to 36 V and a transition time faster than 330 nsec.
  The speaklets are tiny loudspeakers, the responses of which will be investigated when driven by digital pulses.

The main objective of experiments is to explore MDLA concept for sound reproduction. The proposed method is designed for driving a high number of speaklets within an array with digital signals. However, in this research, an array of speaklets have not been fabricated. The experiment with off-the-shelf electro-acoustic transducers is an alternative way for the proof, which is sufficient for characterising acoustic response from MDLA concept.

Three representative transducers of piezoelectric and electro-magnetic technologies for sound and ultrasound generators are described in Section 2.2.1 and 2.1.2.

- A piezoelectric buzzer has a structure as shown in Figure 2-6a similar to a real DLA, as shown in Figure 2-6b, but they are different in size and material. The buzzer has an aluminium diaphragm with 12 mm diameter and 250 µm thickness.
- An ultrasonic transducer has different structure from the buzzer as shown Figure 2-8The transducer has an aluminium diaphragm with 10 mm diameter and 300 µm thickness. It is designed from the transmitting ultrasonic signal at 40 kHz.
- Magnetic buzzer has electro-magnetic transducer as shown in Figure 2-10. operating in a low voltage range between 3 and 16 V and having an aluminium diaphragm with 10 mm diameter and 250 µm. With the electro-magnetic technology, an array of microspeakers is fabricated as shown Figure 2-13. It is used as a MDLA.

The receiving side consists of:

- A ¼ inch free-field microphone, type 4939, with a frequency response between 4 Hz to 100 kHz and a sensitivity of 4mV per Pa
- A microphone amplifier with a gain up to 50 dB and bandwidth up to 80 kHz

- An oscilloscope for measuring the electrical input to a speaklet, and the pressure output from the microphone

Driving electrical rectangular pulses to speaklets is controlled by Matlab-implemented programs on a PC connected with FPGA for charactertics of a pulse train. The program have three modes for generating pulse. Each mode has different main parameters but share the same FPGA-connecting parameters: serial port number, data transfer rate and CPU speed of FPGA. Experimental methodology is described in a procedure section in each experiment.

Mode 1: Single pulse generator has two major defining parameters of a pulse rate and a pulse width. This mode is used in Experiment 4.1.2.1 and 4.1.3. It generates a pulse with a defined constant width in a defined pulse period.

Mode 2: Double pulse generator has four parameters; a pulse rate, the first pulse width, the second pulse width and a pulse interval. It generates two pulses in a defined pulse period. This mode is used in Experiment 4.1.2.2. The widths of the first pulse and the second pulse are equally defined. The pulse interval is duration between the rising edges of the pulses.

Mode 3: MDLA generator has four parameters; a pulse rate, a pure tone frequency, minimum and maximum pulse widths. It generates a pulse in a defined period. The pulse width respresents a quatizing sound level of the pure tone. The minimum and maximum of widths are defined within the range of linearity between the pulse width of electrical input pulses and the amplitude of the pressures. This mode is used in Experiment 4.1.4.

4.1.2 Experiment Acoustic Response of Loudspeakers to digital pulse and attempt to stop to vibration

The experiments were conducted for testing satisfaction of the first requirement of digital sound reconstruction, which is involved with the interval of oscillation of pressure output.

4.1.2.1 Driving single pulse

The experiment investigates pressure response when a pulse feeds a speaklet.

4.1.2.1.1 Objective

- To study acoustic response and its spectrum when driving speaklets with a discrete pulse with a constant width and voltage.
- To investigate emitting time(ET) of the response

4.1.2.1.2 Expectation of Acoustic response for a DLA

According to the first requirement of digital sound reconstruction (Chapter 2.3.3) the emitting duration of pressure response of speaklets, is defined as the emitting time (ET) in Chapter 2.3.2 and is shorter than the sampling period of digital audio (22.67 μsec for 44.1 kHz).

4.1.2.1.3 Procedures

There are two methods of frequency response test for the three types of speaklets: a piezoelectric buzzer, a magnetic buzzer and an ultrasonic transducer.

For the first method, the pulse generator is set at a pulse rate of 400 Hz, which has a period wide enough for the pressure response of ringing to become zero, or the ignored level of pressure. The width and height of the pulses are 10 μsec and 10 V. A pulse is wide enough to show the different resonance frequencies of a speaklet. From the graphs, the electrical signal fed into a speaklet is shown in magenta, while the pressure response from a speaklet is shown in blue.

For the second method, a function generator is used to test the frequency response of a speaklet by sweeping a pure sine wave with a frequency step of 1 kHz. The amplitude is measured, normalized and plotted on graphs.

Each graph consists of two sub-graphs. The top sub-graph shows electrical input and pressure output in the time domain. The electrical input is the signal feeding the speaklet, while the pressure output is the signal from the microphone. Input and output are plotted in magenta and blue respectively. The bottom sub-graph shows the pressure output in frequency domain and the frequency response of the speaklet obtained from the second method of the tests. The output is plotted with a blue line and the frequency response is plotted with a green dashed line. Therefore, the bottom sub-graph shows the frequency response results from the two test methods.

4.1.2.1.4 Results

The signals of a piezoelectric buzzer, a magnetic buzzer and an ultrasonic transducer are shown in Figure 4-2 to Figure 4-4 respectively. Figure 4-2 shows that the pressure response of the piezoelectric buzzer has two resonant frequencies, 4 kHz and 22 kHz, from the pulse response test. The emitting time of pressure response is approximately 1.2 msec.

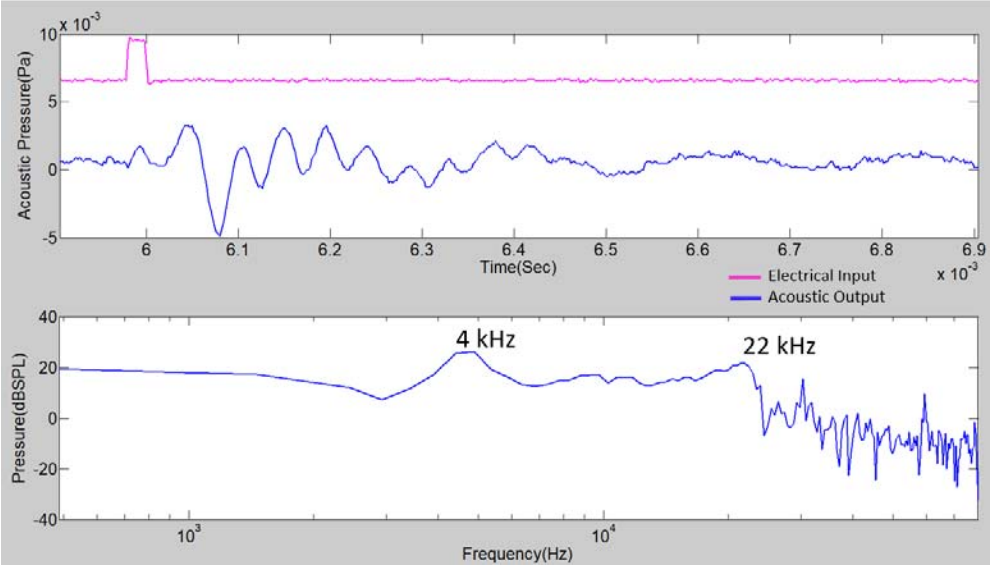

Figure 4-2: Pressure output of a piezoelectric buzzer.

The emitting time of pressure response is about 0.9 msec. The frequency response of the magnetic buzzer has two resonant frequencies at 8 and 15 kHz from the pulse response test, as shown in Figure 4-3.

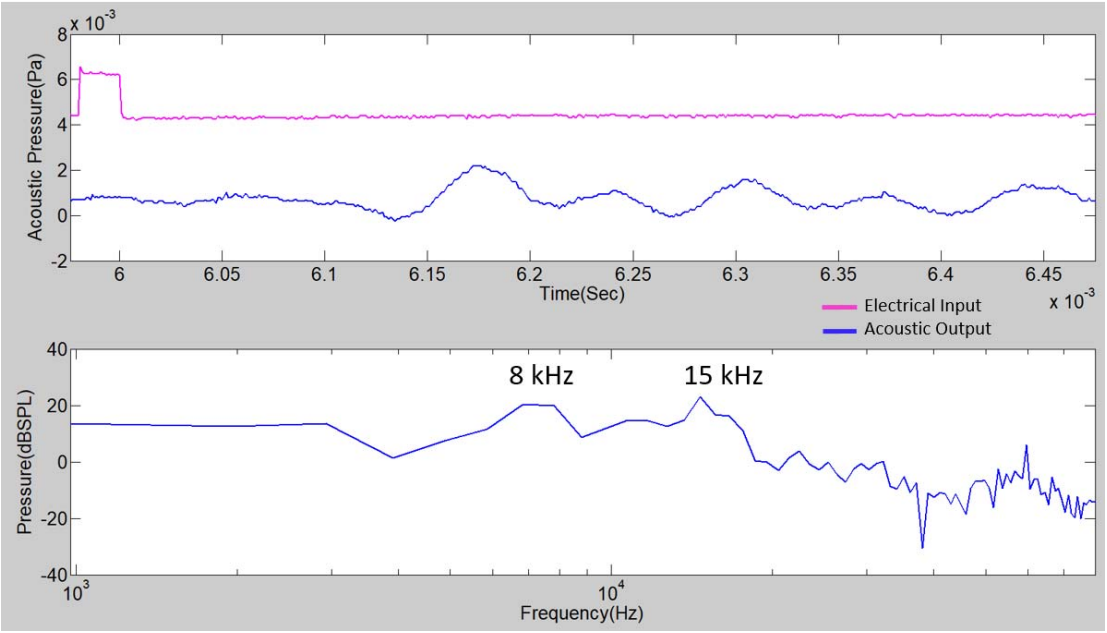

Figure 4-3: Pressure output of a magnetic buzzer

The emitting time of pressure response is approximately 0.8 msec. The frequency responses of an ultrasonic transducer from both methods are similar. They have the same single resonant frequency at 40 kHz. The time response of the transducer can be divided into two periods: an initial interval and a dissipated interval. The initial interval starts from the time the wave is formed until the amplitude of the wave reaches maximum pressure. The amplitude of the periods of

oscillation gradually increases within the initial period. The dissipated interval starts from the moment the wave reaches maximum pressure until the amplitude of the wave is equal to zero or a negligible level, as shown in Figure 4-4.

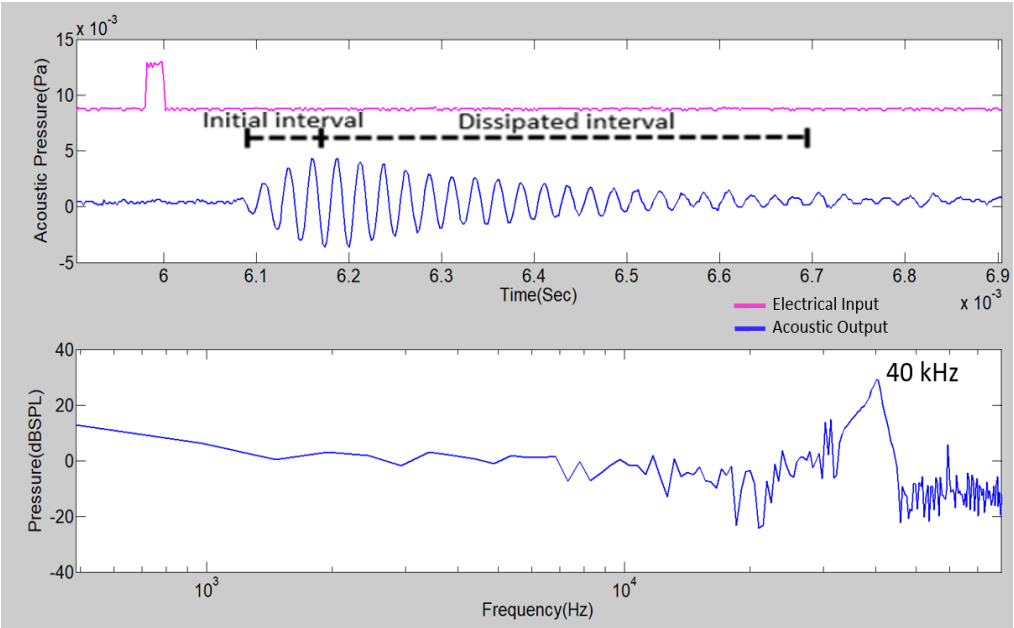

Figure 4-4: Pressure output of an ultrasonic transducer

4.1.2.1.5 Discussion

The results of pressure response in the experiment can be summarized in Table 4-1:

Table 4-1: Summary of acoustic response of speaklets to a short rectangular pulse

Speaklet Type	Emitting time (msec)	Resonant Frequency (kHz)
piezoelectric buzzer	1.2	4 and 22
Magnetic Buzzer	0.9	8 and 15
Ultrasonic transducer	0.8	40

Considering the emitting times of the speaklets' responses with the first requirement of digital sound reconstruction for 44.1 kHz (common sampling rate of digital audio), it is required to be faster than 22.67 µsec, while the emitting times of the speaklets are in the order of milliseconds. Therefore, it is clearly seen that the emitting time of the speaklets cannot meet the requirement.

The emitting time is longer than expected because of the problem of ringing, which implies that the vibrating system has a low damping ratio. Due to the low damping ratio, the surface of diaphragm of the speaklet vibrates freely more than one cycle as shown the pressure output of

speaklets in the temporal domain graphs of the figures in the previous section. In contract, a high damping ratio is defined as 0.8 in the ideal case of a MDLA, the duration of vibration of the response is a cycle of wave shown in Figure 3-2a.

Ringing is recognised as a problem in ultrasonic imaging instruments [5] because imaging speed depends on emitting time. Periods between pulses will prevent interference between a signal and its successive signal. The interference causes an error in the imaging.

The ringing pressure generated from feeding a short electrical pulse to the speaklet, results from the free vibration at the natural frequencies of the speaklets. The number of resonant frequencies depends on the number of vibrational modes. For example, the fundamental, 1 nodal circle and 1 nodal diameter modes of a circular diaphragm vibrate at f_0, 1.594 f_0 and 2.296 f_0 respectively [36]. The fundamental frequency (f_0) of a speaklet depends on the size and material of the speaklet's diaphragm and can be estimated by Eq.(2.32) or (2.33). From the experiment, the pressure responses of piezoelectric and magnetic buzzers are composed of two resonant frequencies, which imply that the diaphragm vibrates with two vibrational modes, the fundamental mode and 1 nodal circle or diameter mode. For the ultrasonic transducer, the free vibration has a single resonant frequency, or a single vibrational mode. The fundamental mode of an ultrasonic transducer is suppressed by the resonator, which is fixed at the centre of the diaphragm, as shown in Figure 2-8a. In other words, the diaphragm of the transducer vibrates in only 1 nodal circle mode.

In summary, the emitting time of the three speaklets in the experiment cannot meets the first requirement of digital sound reconstruction because of the ringing. The pressure response of both buzzers consists of the two resonant frequencies, while the pressure response of the ultrasonic transducer has a single resonant frequency. The next experiment will study the feasibility of a proposed method for suppressing the ringing in order to reduce the emitting time.

4.1.2.2 Driving double pulse Experiment

From the previous experiment, it is found that the emitting time (in the order of milliseconds) is far greater than the audio sampling period (in the order of ten microseconds). There are two types of resonance in speaklets: a single resonant frequency and multiple resonant frequencies. For multiple resonant frequencies, it is impossible to cancel the ringing with a pulse. Therefore, this experiment investigates pressure response when two identical pulses are fed into an ultrasonic transducer, which has a single resonant frequency, with an interval between the pulses equal to a half period of the resonant frequency of the speaklet.

4.1.2.2.1 Objective

- To study the feasibility of suppression of ringing with double pulse technique

4.1.2.2.2 Expectation of double pulse technique in suppression of ringing effect

Although the emitting time of a single resonant frequency speaklet with a low damping ratio vibrational system is longer than the period of the audio sampling rate, if the pulse response of the speaklet is expressed as the transient response in Eq.(2.140), a burst of two pulses of the response with an interval of a half period of the resonant frequency will suppress the ringing, as shown in Figure 4-5. It can be seen that the emitting time dramatically reduces and two successive pulses subtract from each other and leave the first crest of the precedent pressure wave, as shown with the purple line.

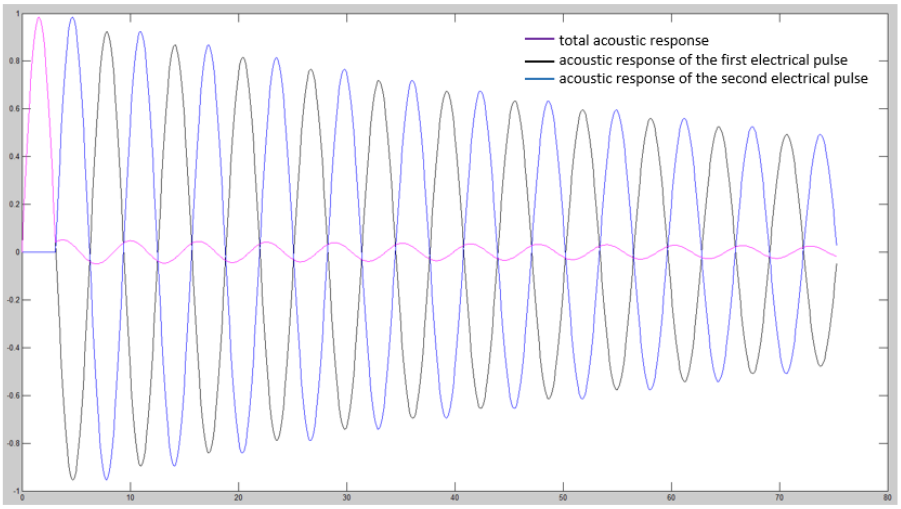

Figure 4-5: The conceptual result of the double pulse technique

4.1.2.2.3 Procedure

The pulse generator is set at a pulse rate of 400 Hz, a pulse width of 10 µsec and a pulse height of 10 V, similar to the previous experiment, but the generator emits two identical pulses with a head to head interval of 12.5 µsec, which is a half period of the resonant frequency of 40 kHz of the ultrasonic transducers.

4.1.2.2.4 Results

The pressure amplitude of the double pulse response reduces significantly from 8 to 0.8 mPa and the pressure at 40 kHz, which is the resonant frequency of the transducer, disappears, as shown in Figure 4-4.

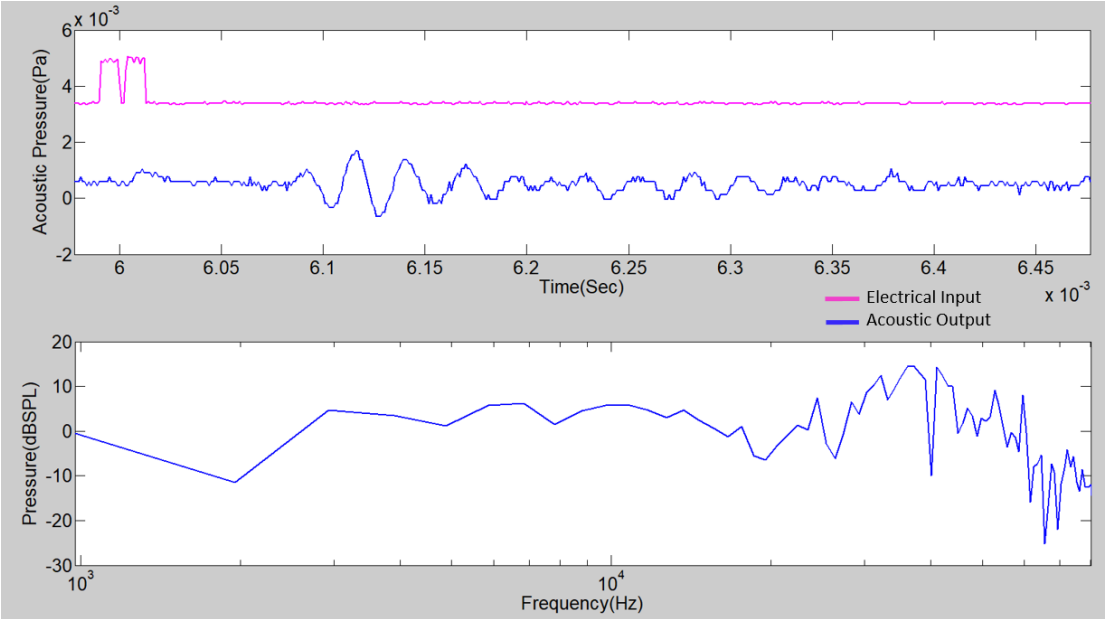

Figure 4-6: Pressure response of the ultrasonic transduce with double pulse technique

4.1.2.2.5 Discussion

The double pulse technique does not work for ringing suppression because the whole pressure response of the transducer is significantly attenuated. The magnitude of pressure outputs reduces dramatically from 20 to 10 dBSPL. This implies that the successive pulses can subtract from each other. Due to the initial interval of the transient response of the transducer, as shown in Figure 4-4, the response cannot reach maximum pressure in the first cycle of the transient wave as in the ideal transient response shown in Figure 4-5. Therefore, the amplitude of the first crest of the transient response of the transducer, which follows the subtraction, is small. It is almost as if the whole response is suppressed.

The duration of the initial interval may result from the hardness of the piezo ceramic layer, the active component attached to the diaphragm of the transducer, as described in Chapter 2.2.1.1. The hardness affects the vibration of the diaphragm. Other types of piezo layer, such as composite [6] [7] and PVDF, are alternatives [40], which are more flexible than the ceramic. The study in the effects of the flexibility of a piezoelectric layer in a transducer on the reduction in the initial interval of the transient response is interesting because the double pulse technique will work for ringing suppression if the initial interval is less than a period of the resonant frequency of the transducer.

However, the flexible piezoelectric materials have a lower d_{33} coefficient (a parameter of conversion between electrical and mechanical energy of piezo materials) than the ceramic. A higher voltage is required for excitation of the transducers.

4.1.3 Experiment to Determine the Relationship between Pulse Width of Driving Signal and Amplitude of Acoustic Wave

From the previous experiments, it is impossible for the three speaklets to meet the first requirement of digital sound reconstruction because their emitting time is far longer than the period of the audio sampling rate. In this experiment, the third requirement is tested when the pressure responses of pulses in a train interfere with each other due to ignoring the first requirement. The third requirement is that the relationship between pulse width and amplitude of acoustic response must be linear in Chapter 2.3.3.

4.1.3.1 Objective

- To study the relationship between pulse width and amplitude of acoustic response when the first requirement is ignored.
- To study the effects of change in pulse rate on the relationship between pulse width and amplitude of the airborne response.

4.1.3.2 Expectation of range of linear relationship

The pulse width of electrical rectangular pulses, which are fed into a speaklet, is linearly related to the amplitude of the airborne response of the speaklet in a certain range of widths. R^2, which is a statistical measure of how close the data are to the fitted regression line, is greater than 0.95 or 95%.

4.1.3.3 Procedure

The pressure responses of a piezoelectric buzzer and an ultrasonic transducer are tested for linearity. The pulse generator is set at a pulse height of 10 V, the pulse rate of electrical excitation to the speaklet is related to the frequency response of the speaklet (green line), which is measured from frequency response tests using frequency-sweeping method. Frequency-sweeping signal generator is used to produce sine sweep signal which its amplitude is invariant but its frequency is gradually changed. The transducers is fed to the generator, the amplitude of acoustic pressure of the transducer and the frequency are recorded from an oscilloscope which is connected to a measurement microphone.

The pressure response of the speaklets is measured according to the pulse rates and pulse widths shown in. Table 4-2. The amplitudes of the response are obtained from the magnitudes at given pulse rates on the frequency domain subgraphs, as shown in the red dot in the bottom graph of each response to different pulse widths in Figure 4-7, Figure 4-8,Figure 4-10 and Figure 4-11. The

amplitudes are plotted with the pulse widths for each pulse rate as shown in Figure 4-9 and Figure 4-12.

Table 4-2: Values of pulse rate and pulse width in experiments

Experiment	Speaklet Type	Resonant Frequency(kHz)	Pulse Rates	Pulse Width (µsec)
1	Piezoelectric buzzer	22	14,18,22,26 and 30	1,2,3,…,26 and27
2	Ultrasonic transducer	40	32,36,40,44 and 48	1,2,3,…,21 and22

4.1.3.4 Results

The results are divided into two parts: piezoelectric buzzer and ultrasonic transducer, which have different frequency responses.

4.1.3.4.1 PZT Buzzer

From Figure 4-7, it can be found that:

- Although the waveforms of the pressure output are not pure sine waves, the average frequency is at 22 kHz, which is equal to the pulse rate of the electrical input.
- An increase in the pulse width results in a growth in the amplitude of pressure output from 0.7, 2.25, 4.13 to 5.88 mPa for the pulse widths of 1, 5, 10 and 20 µsec respectively.

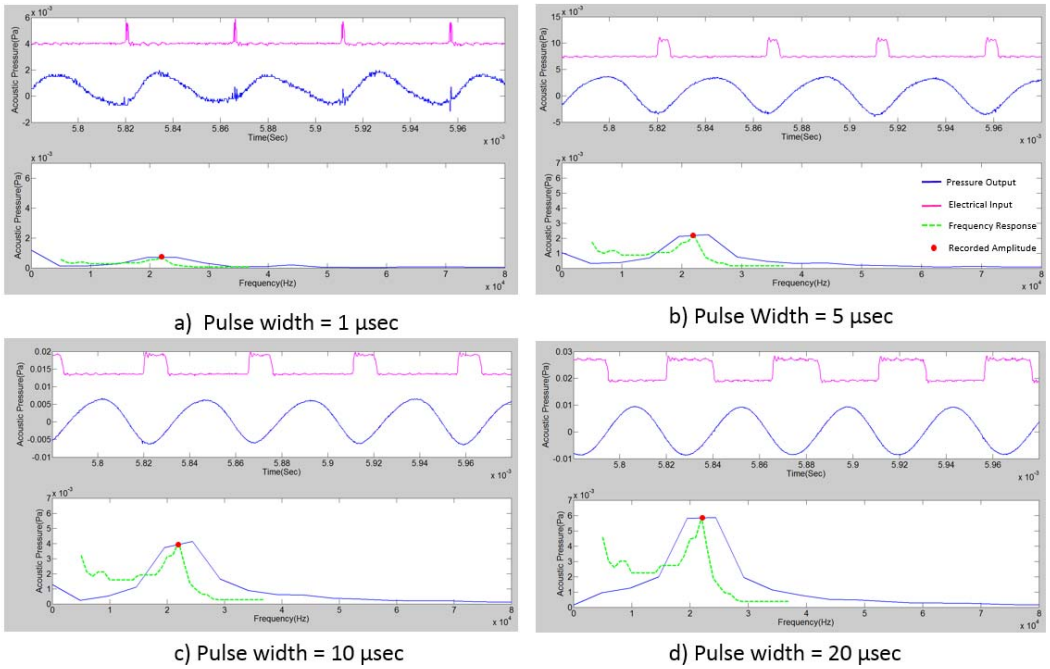

a) Pulse width = 1 µsec

b) Pulse Width = 5 µsec

c) Pulse width = 10 µsec

d) Pulse width = 20 µsec

Figure 4-7: The pressure output of a piezoelectric buzzer when feeding the digital pulse at 22 kHz and pulse width 1,5,10 and 20 µsec.

From Figure 4-8, it can be found that:

- Although the waveforms of the pressure output are not pure sine waves, the average frequency varies exactly according to the pulse rate of the electrical input.
- The amplitude of pressure output of different pulse rates depends on the frequency response of piezoelectric (dashed green line). The amplitude is at maximum when the pulse rate is equal to the resonant frequency of the buzzer (22 kHz).

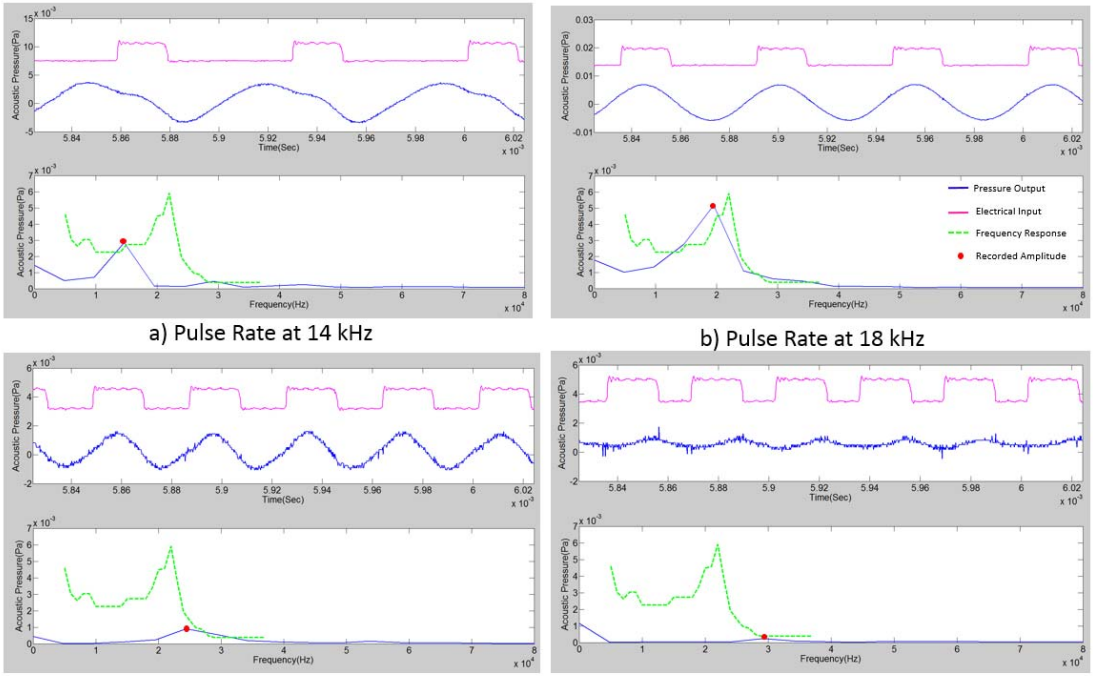

a) Pulse Rate at 14 kHz

b) Pulse Rate at 18 kHz

c) Pulse Rate at 26 kHz

d) Pulse Rate at 30 kHz

Figure 4-8: The pressure output of a piezoelectric buzzer when feeding the digital pulse with pulse width 20.µsec at 14, 18, 26 and 30 kHz.

Although different pulse rates cause different amplitudes of pressure output, the relationship between the amplitude and the pulse width is linear within a range of pulse widths between 1 and 20 µsec because the linear relationship (R^2) is greater than 0.95, as shown in Figure 4-9 and Table 4-3. However, the relationship between pulse rates 26 and 30 kHz is not linear because of noise in the system. The average pressure signal is small (less than 0.1 mPa), resulting in low signal-to-noise ratio.

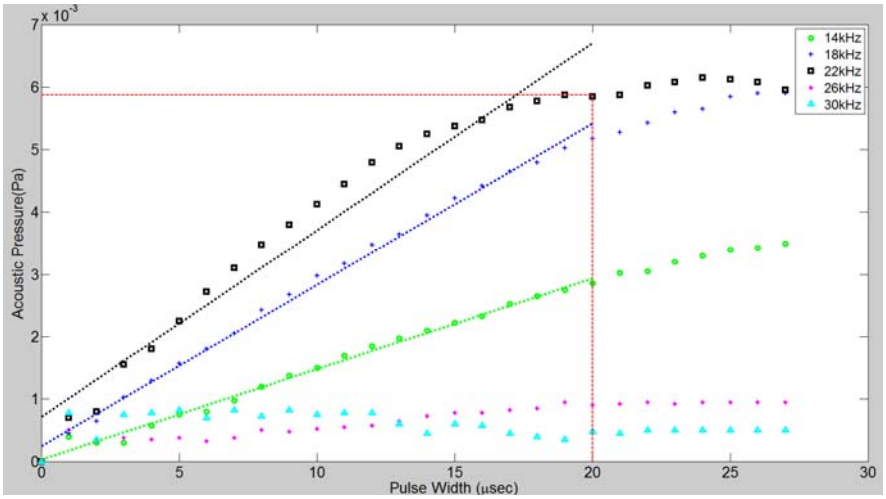

Figure 4-9: Relationship between the amplitude and the pulse width for pulse rate of 14, 18, 22, 26, 30 kHz.

Table 4-3: Results of linear regression of the piezoelectric buzzer with pulse width between1 and 20 µsec.

Pulse rate (kHz)	R^2	Linear equation y = ax+b	
		Slope(a) $x10^{-5}$	Y intercept (b)$x10^{-5}$
14	0.9912	1.45	0.38
18	0.9958	2.55	2.93
22	0.9522	2.88	8.68
26	0.8777	0.33	2.42
30	0.3411	-0.17	8.13

4.1.3.4.2 Ultrasonic Transducer

The results of the pressure output, the pulse rates and the pulse widths of the ultrasonic transducer correspond to the results of the buzzer, as shown in Figure 4-10 and Figure 4-11. The amplitude of the pressure output varies directly according to the pulse width of inputs from 1 to 12 µsec. The frequency of the output is equal to the pulse rate of the input, while the amplitude of the output depends on the frequency response of the transducer. The waveform of the output is similar to a pure sine wave because the frequency responses of the outputs have narrow widths, as shown in the frequency domain graphs.

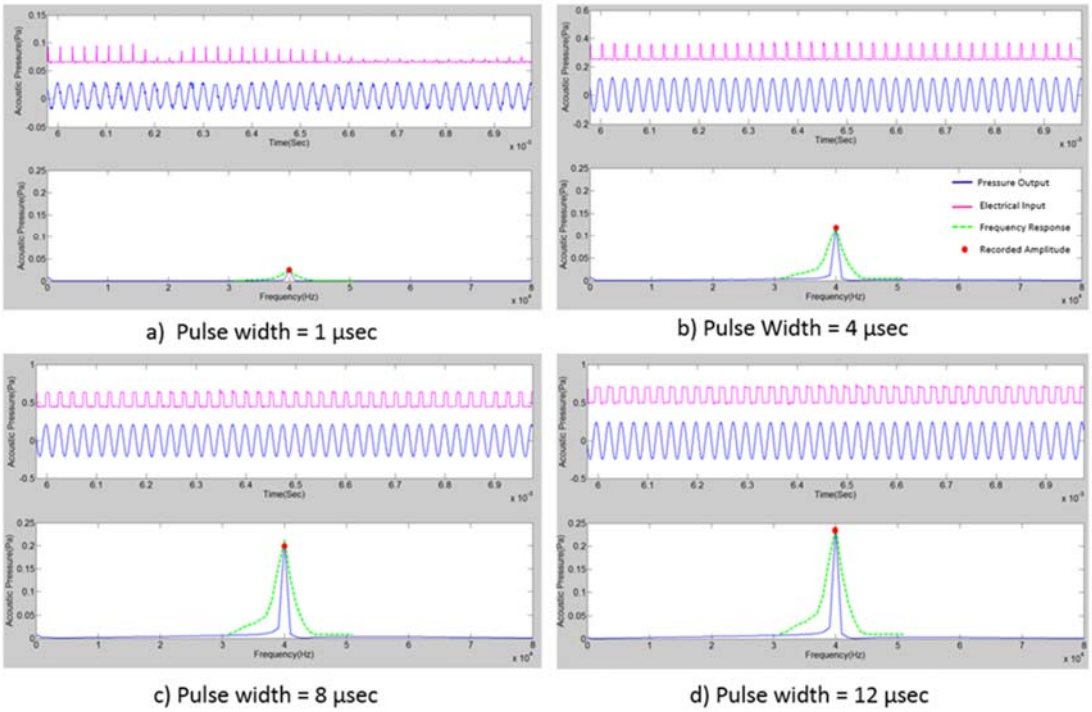

Figure 4-10: The pressure output of an ultrasonic transduce when feeding the digital pulse at 40 kHz and pulse width 1,4,8 and 12 µsec.

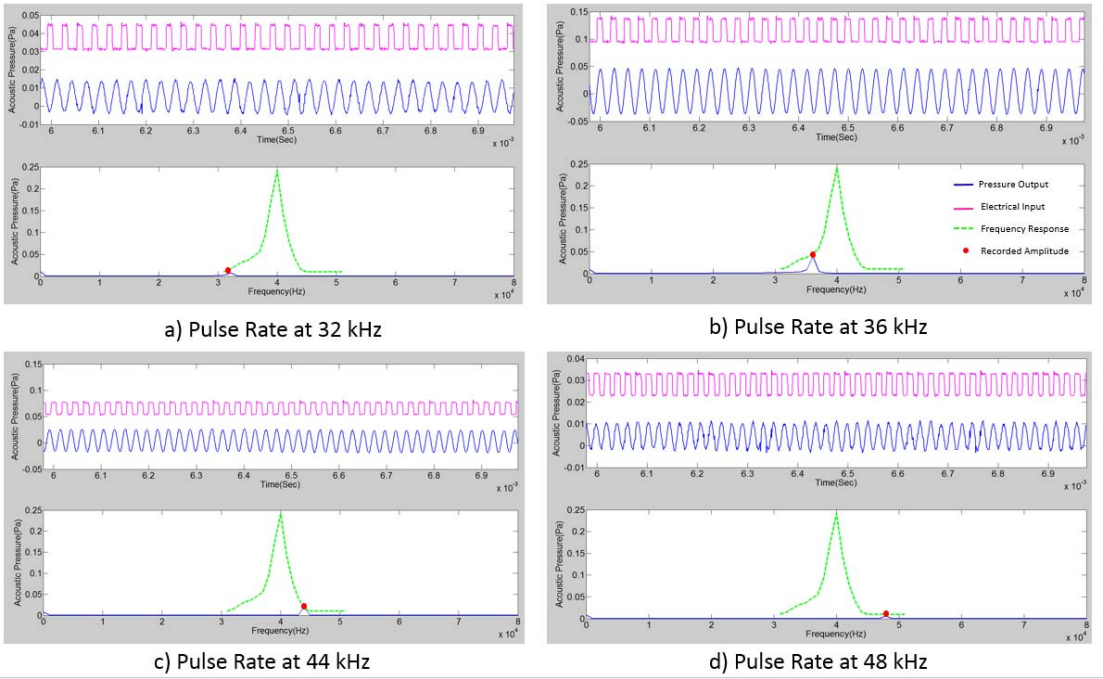

Figure 4-11: The pressure output of an ultrasonic transducer when feeding the digital pulse with pulse width 12.µsec at 32, 36, 44 and 48 kHz.

Similar to the results of the piezoelectric buzzer, the relationship between the amplitude and the pulse width is linear within a range of pulse widths between 1 and 10 µsec because the linear relationship (R^2) is greater than 0.95, as shown in Figure 4-12 and Table 4-4.

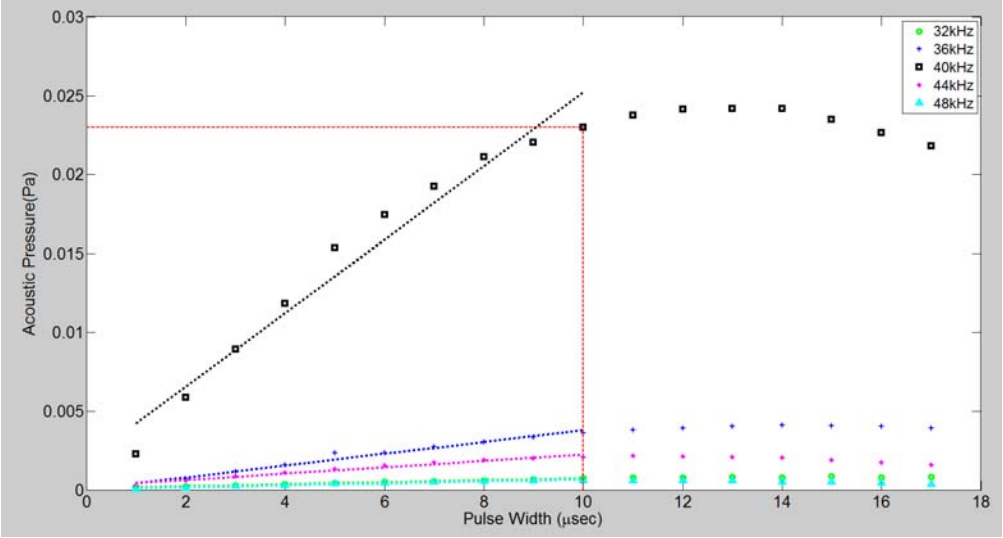

Figure 4-12: Relationship between the amplitude and the pulse width for pulse rate of 32, 36, 40, 44, 46 kHz.

Table 4-4: Results of linear regression of the ultrasonic transducer with pulse width between 1 and 10 µsec.

Pulse rate (kHz)	R^2	Linear equation y = ax+b	
		Slope(a) $x10^{-5}$	Y intercept (b)$x10^{-5}$
32	0.9919	6.30	10.8
36	0.9767	37.4	5.30
40	0.9626	230	190
44	0.9763	20.2	22.7
48	0.9635	6.17	4.07

4.1.3.5 Discussion

Although the relationship between the amplitude of pressure output and the pulse widths of electrical input of the speaklets is non-linear, the relationship can be linear in a certain range of pulse widths. The range of pulse widths is related to the period of the resonant frequency of the speaklets. The range is slightly greater than a quarter of the period of the resonant frequency of

the speaklets but less than half the period. From the experiments, the width ranges of 10 are greater than 6.25 μsec, which is a quarter of the period of the resonance at 40 kHz.

The amplitude of the pressure output of a speaklet can be maximized when the pulse rate of the electrical input is equal to the resonant frequency of the speaklet. In other words, the pulse rate of the digital driver of a speaklet works at the resonant frequency, or the natural frequency of the speaklet.

There is no test of a magnetic buzzer in this experiment because its results are not consistent. A growth in the pulse width of the electrical input has an effect not only on an increase in the pressure output, but also on a rise in temperature of the coil and magnet within the speaklet. The high temperature results in degradation in the conversion between electrical and mechanical energy. Therefore, when the pulse width increases, the pressure output is fuzzy.

4.1.4 Experiment of MDLA

A Multiple Level Digital Loudspeaker Array (MDLA) is the proposed method for increasing the quantizing level of digital reconstruction from applying the pulse width modulation (PWM) by representing the width of the pulses as the quantizing levels (for more details see Chapter 3.1). The MDLA concept imitates pulse generation from PWM but limits in a certain range of pulse width linearly related to magnitude of its output response.

From the previous experiment, it was found that in a certain range is approximately equal to a quarter of the period of the natural frequency of transducers. This experiment will demonstrate the reproduction of a pure tone with digital pulses with different widths.

4.1.4.1 Objective

- To study pressure response and its spectrum with different audio frequencies
- To investigate effects of the pulse rate of the electrical input on the pressure output
- To study efficiency of a MDLA and the different frequency responses of speaklets

4.1.4.2 Expectation of a MDLA

The pressure output of a MDLA should be similar to waveforms of rectified amplitude modulation (AM), as shown in . The spectrum of the waveforms consists of four components: baseband, carrier, lower sideband and upper sideband, as shown in Figure 4-13. The frequencies of the baseband, carrier, lower and upper sidebands should be equal to the audio frequency, pulse rate, pulse rate - audio frequency and pulse rate + audio frequency respectively. The amplitudes of the baseband, lower and upper sidebands should be the same.

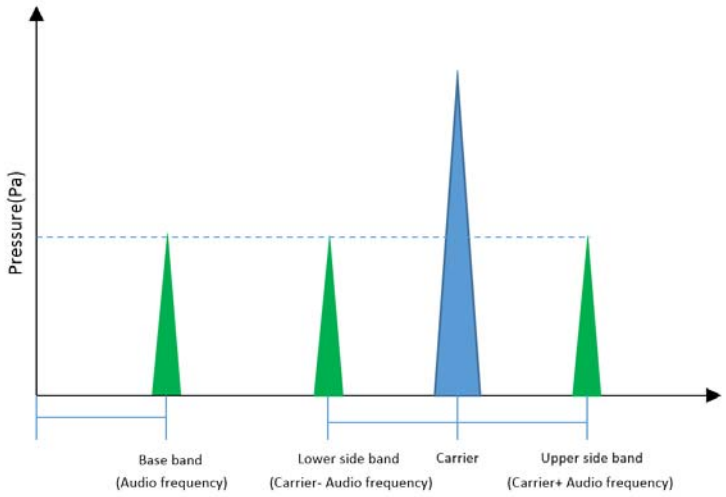

Figure 4-13: Frequency components of amplitude modulation from Section 3.4.1.

4.1.4.3 Procedure

Three speaklet types: ultrasonic transducer, piezoelectric buzzer and magnetic buzzer are tested for a MDLA by driving the speaklets with different pulse widths with a pure sine wave. The pulse generator is set at a pulse height of 10 V. The pure tones of frequencies at 1, 2, 4 and 7 kHz are reproduced in these experiments by different pulses modulated with PWM as parameters of pulse rates and pulse widths in Table 4-5. The resolution of audio is equal to the range of linearity of pressure response of the speaklets, divided by the clock period of the FPGA processor, which is 10 psec for 100 MHz.

Table 4-5: Parameters of pulse rate and pulse width

Experiment	Speaklet Type	Resonant Frequency(kHz)	Pulse Rates (kHz)	Pulse Width (µsec)		Resolution (level)
				Min	Max	
1	Piezoelectric buzzer	22	14,18,22,26 and 30	0	20	*2000
2	Ultrasonic transducer	40	36,40 and 44	0	10	*1000
3	Magnetic buzzer	22	18, 22 and 26	0	20	*2000

*Resolution is calculated from CPU speed at 100 MHz of the FPGA board

4.1.4.4 Results

The results are divided into three parts: piezoelectric buzzer, ultrasonic transducer and magnetic buzzer, which have different frequency responses.

4.1.4.4.1 Piezoelectric Buzzer

From the results in Figure 4-14 to Figure 4-16, it is found that:

- The pressure outputs are similar to the full wave AM signal rather than the half wave rectified AM signal. The output frequencies consist of carrier, lower sideband and upper sideband. The difference between successive components of the output frequencies are equal to the audio frequencies.
- The frequencies of the carrier are equal to the pulse rate of the input digital signals but the amplitude of the output depends on the frequency response of the speaklet. Therefore, in order to maximize the amplitude of the carrier, the pulse rate should be equal to the highest resonant frequencies, as shown in Figure 4-14.
- The lower and upper sidebands are not equal because of the frequency response of the speaklet. The common frequency responses are not flat or symmetric.
- In order to maximize the amplitude of the sidebands, the frequencies of the bands are within the bandwidth of the speaklet. From Figure 4-14, , Figure 4-15 and Figure 4-16, the amplitude of the sidebands of the 18 kHz pulse rate is greater than the amplitude of the sidebands of the pulse rates of 22k and 30k because the bandwidth is approximately between 4 and 25 kHz, as shown by the green dashed line. Therefore the frequency bands greater than 25 kHz will be dramatically attenuated.
- The resonant frequencies, or the peaks of the frequency response graph of the speaklets, might result in distortion of the output signals. Notably, when the output of the input pulse rate is not equal, but close to the highest resonant frequency, such as pulse rates of 26 and 18 kHz close to the resonant frequency at 22 kHz, there is the distorting frequency at 22 kHz within the pressure output, as shown in and Figure 4-15.
- A speaklet can produce audible sound when the audio frequencies are within the bandwidth of the speaklet, but the outputs are not formed as AM, as shown in graph c), 4 kHz and d), 7 kHz of the figures.

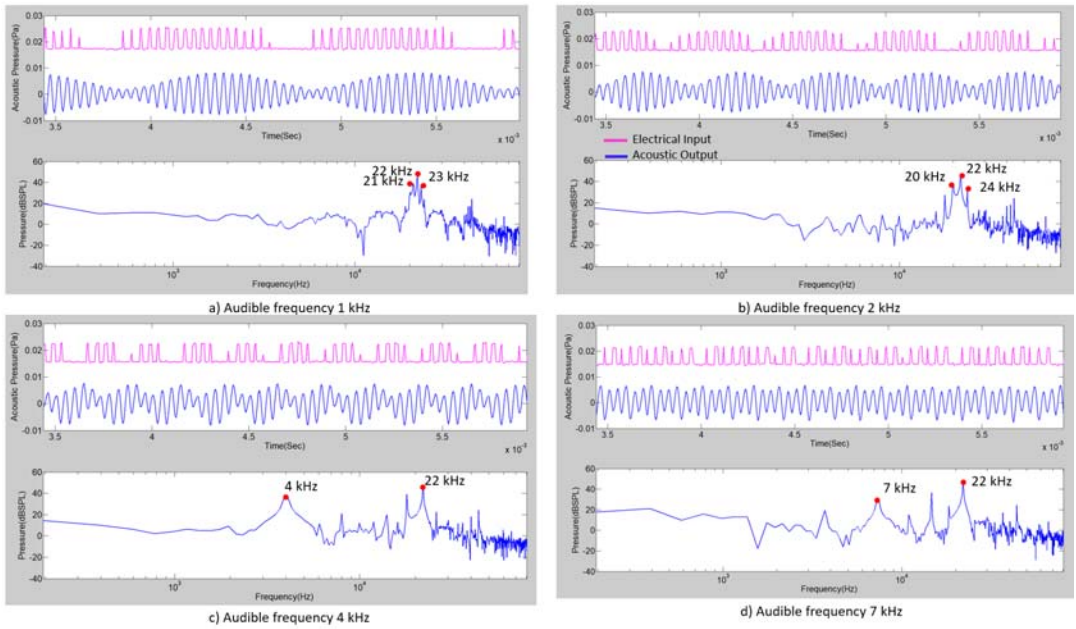

Figure 4-14: The pressure output of a piezoelectric buzzer when driving it with pulse rate at 22 kHz and audio frequency of 1, 2,4 and 7 kHz.

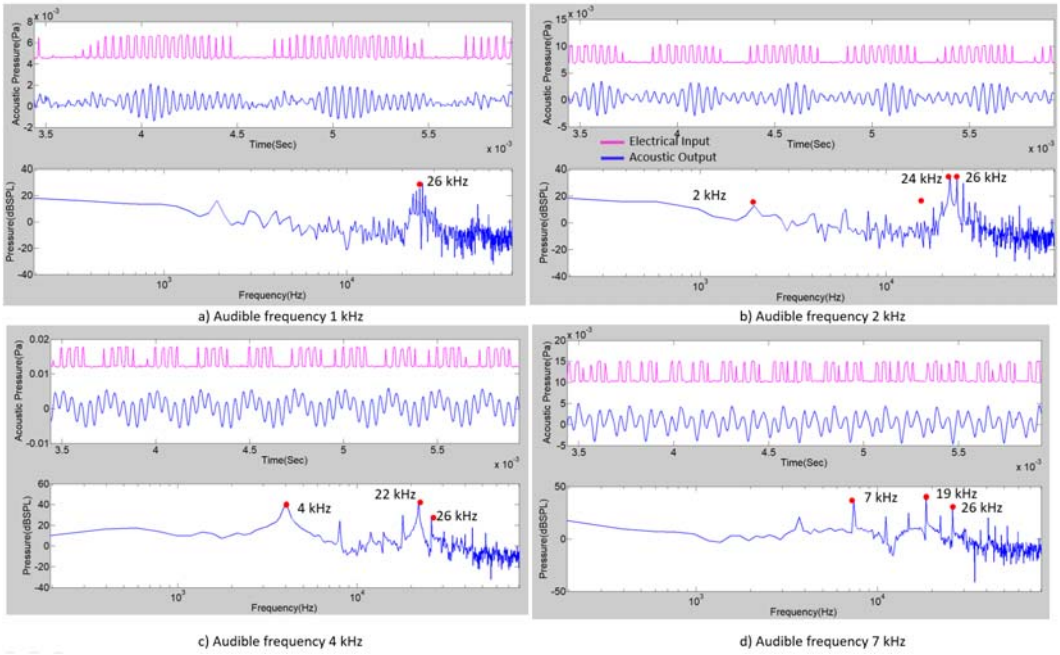

Figure 4-15: The pressure output of a piezoelectric buzzer when driving it with pulse rate at 26 kHz and audio frequency of 1, 2,4 and 7 kHz.

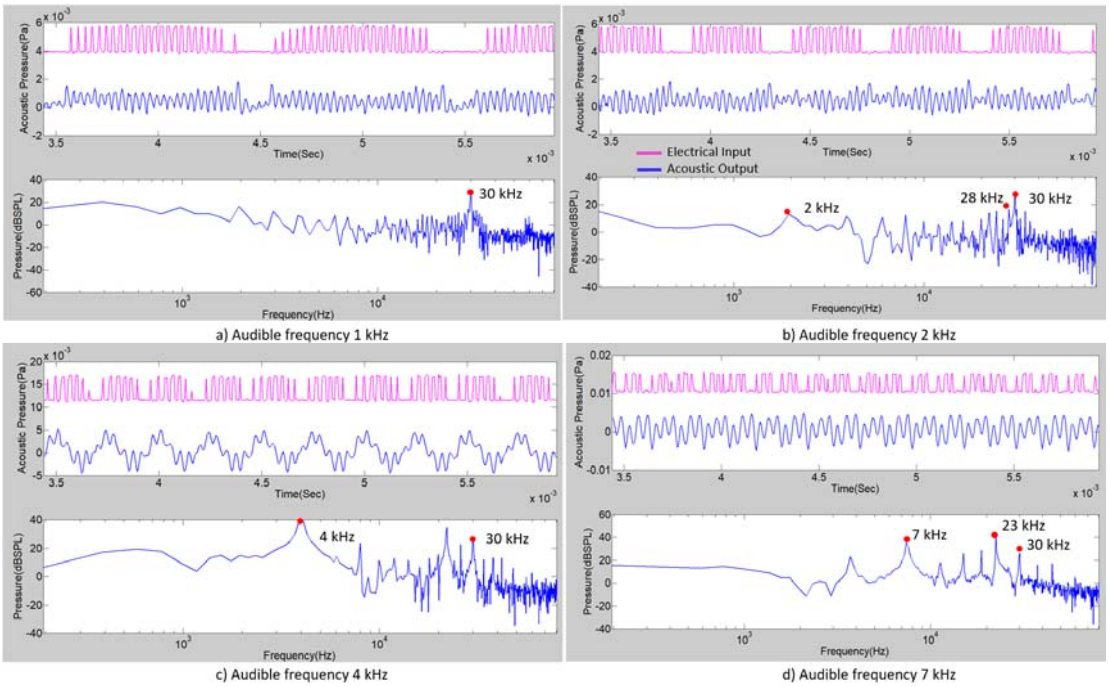

Figure 4-16: The pressure output of a piezoelectric buzzer when driving it with pulse rate at 30 kHz and audio frequency of 1, 2,4 and 7 kHz.

4.1.4.4.2 Ultrasonic Transducer

From the results in Figure 4-17 to Figure 4-19, it can be found that although the pressure outputs of the ultrasonic transducer have a single resonant frequency and a narrow bandwidth, the resulting signals are similar to the resulting signals of the buzzer, but they have a higher amplitude. The output signals have waveforms similar to amplitude modulation. The amplitude of output is the highest when the pulse rate of the digital input is equal to the resonant frequency. The amplitudes of the frequency bands vary according to the frequency response of the transducer.

However, there is a difference in the audible range (between 0 and 20 kHz) of the output of pulse rate at 40 kHz as shown in Figure 4-17. Due to the frequency response similar to the isosceles triangle with the top angle at 40 kHz, the responsive efficiency in a lower audio frequency is greater than in a higher audio frequency, which corresponds to the magnitude of the sidebands. However the amplitude of the sidebands is significantly higher than the audible frequency of the output. From graphs a), b), c) and d) of Figure 4-17 , which represent the audio frequencies of 1, 2, 4 and 8 kHz respectively, the amplitudes in the audible range are 5.6, 3.9, 2.3 and 0 mPa respectively, while the amplitudes of the lower sideband are 30.5, 19, 11.9 and 3.9 mPa respectively.

It is not effective to apply pulse rates outside or near the edge of the bandwidth of the transducer because the output amplitudes are significantly lower than the amplitude of the output with input pulse rates at the resonant frequency, as shown in Figure 4-18 and Figure 4-19. This results in no frequency component in the audible range.

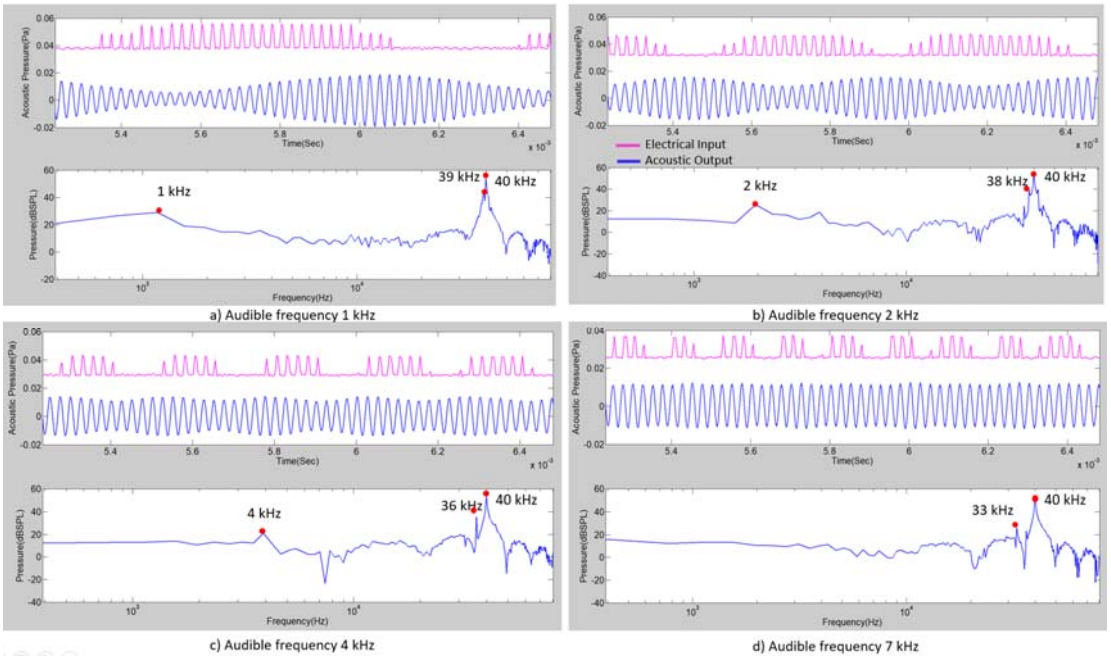

Figure 4-17: The pressure output of a ultrasonic transducer when driving it with pulse rate at 40 kHz and audio frequency of 1, 2,4 and 7 kHz.

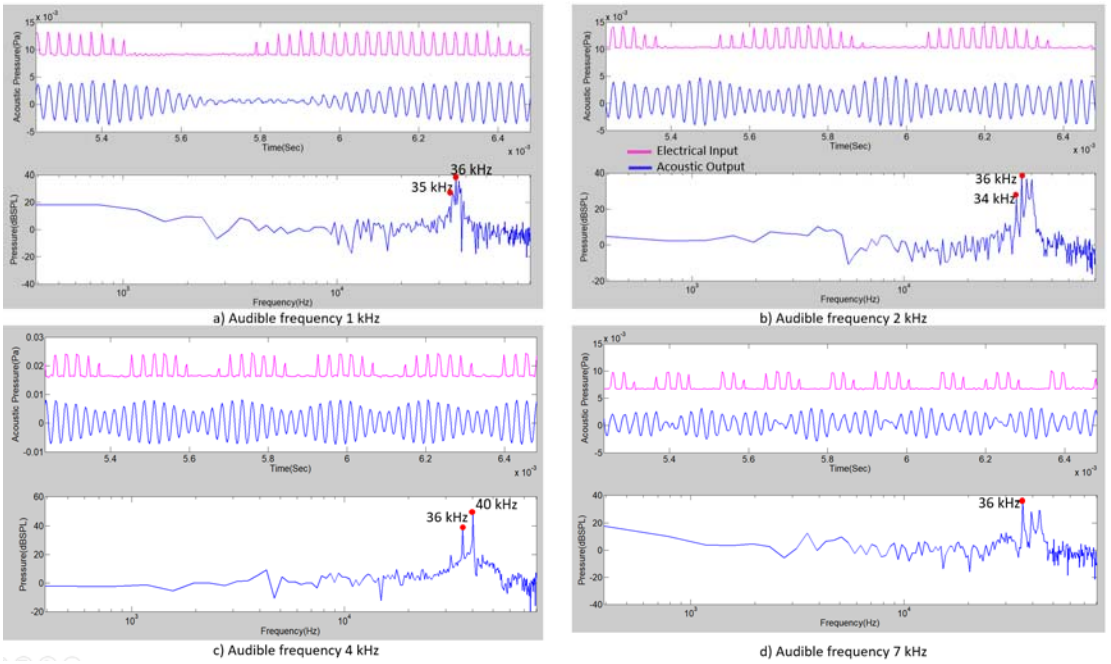

Figure 4-18: The pressure output of a ultrasonic transducer when driving it with pulse rate at 36 kHz and audio frequency of 1, 2,4 and 7 kHz.

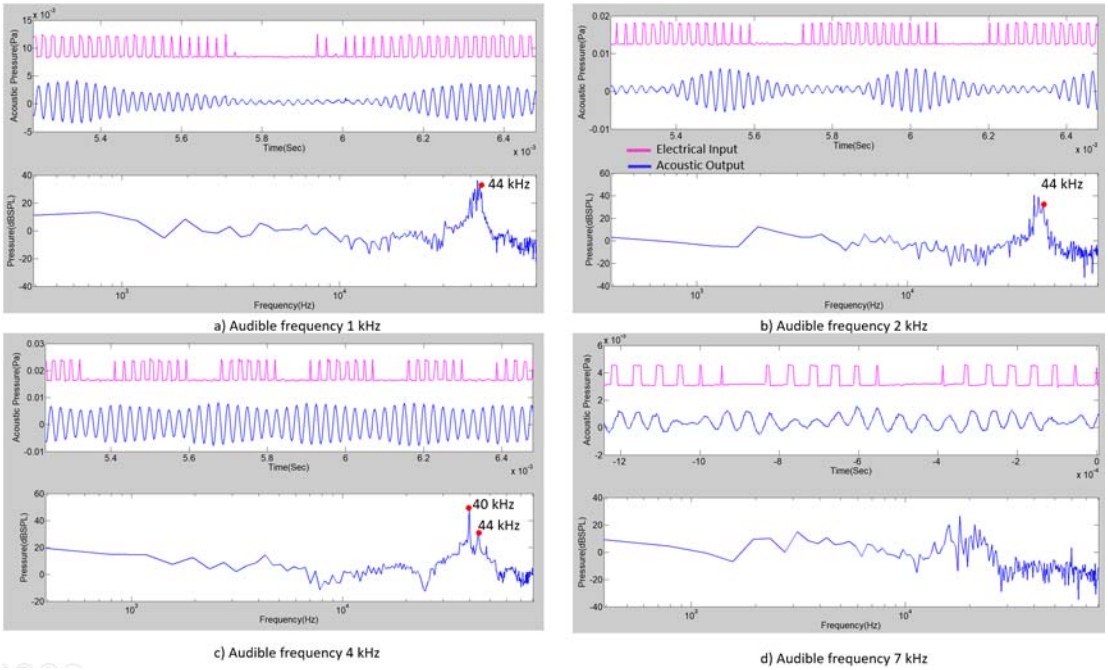

Figure 4-19: The pressure output of a ultrasonic transducer when driving it with pulse rate at 44 kHz and audio frequency of 1, 2,4 and 7 kHz.

4.1.4.4.3 Magnetic Buzzer

From the results in Figure 4-20 to Figure 4-22, it is shown that the outputs of the magnetic buzzer are weakly formed as amplitude modulated (AM) signals at low audio frequencies (1 and 2 kHz), as shown in graphs a) and b) while the outputs are not formed as AM signals at high audio frequencies (4 and 7 kHz), as shown in graphs c) and d). From the frequency domain graph, the four frequency components can be found but the amplitudes at low frequency are high, while the amplitudes at high frequency are low.

From the frequency response of the buzzer, there are multiple resonant frequencies, seen by peaks on the dashed green line. This causes signal distortion in the AM waveform.

Although the outputs of the magnetic buzzer do not conform to the AM waveform due to the low amplitude of the high frequency component, such as the lower and upper sidebands, the figures show that the speaklet can make sound at audio frequencies but the amplitudes at high frequencies (4 and 7 kHz) are higher than the amplitudes at low frequencies (1 and 2 kHz). There is sound distortion at the resonant frequencies.

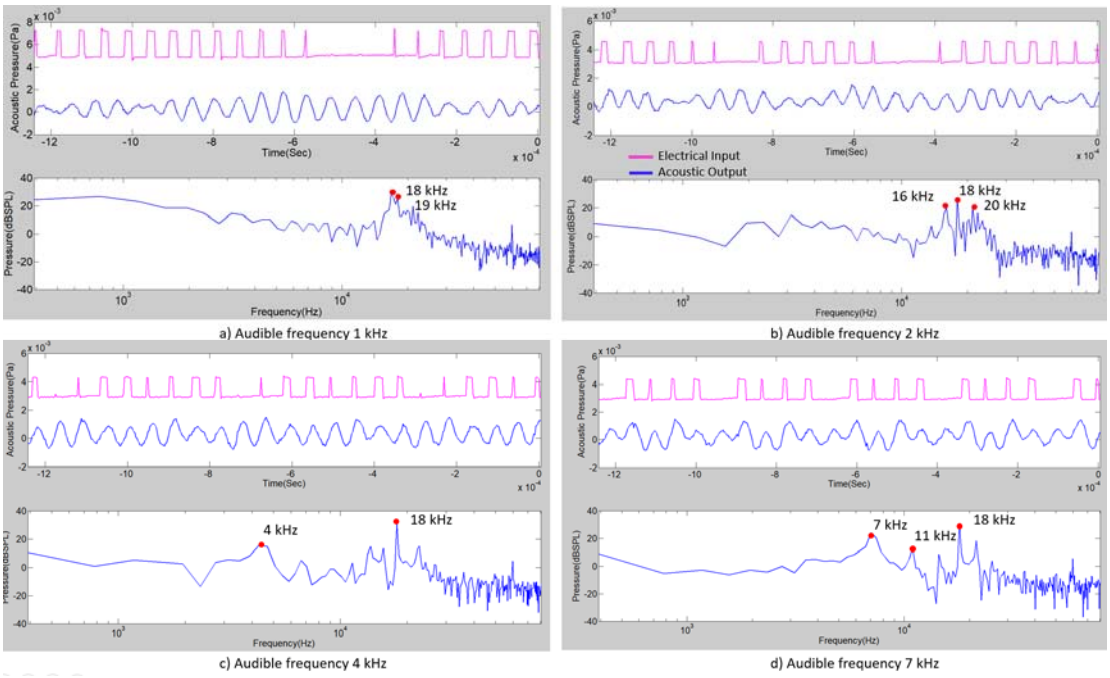

Figure 4-20: The pressure output of a magnetic buzzer when driving it with pulse rate at 18 kHz and audio frequency of 1, 2,4 and 7 kHz.

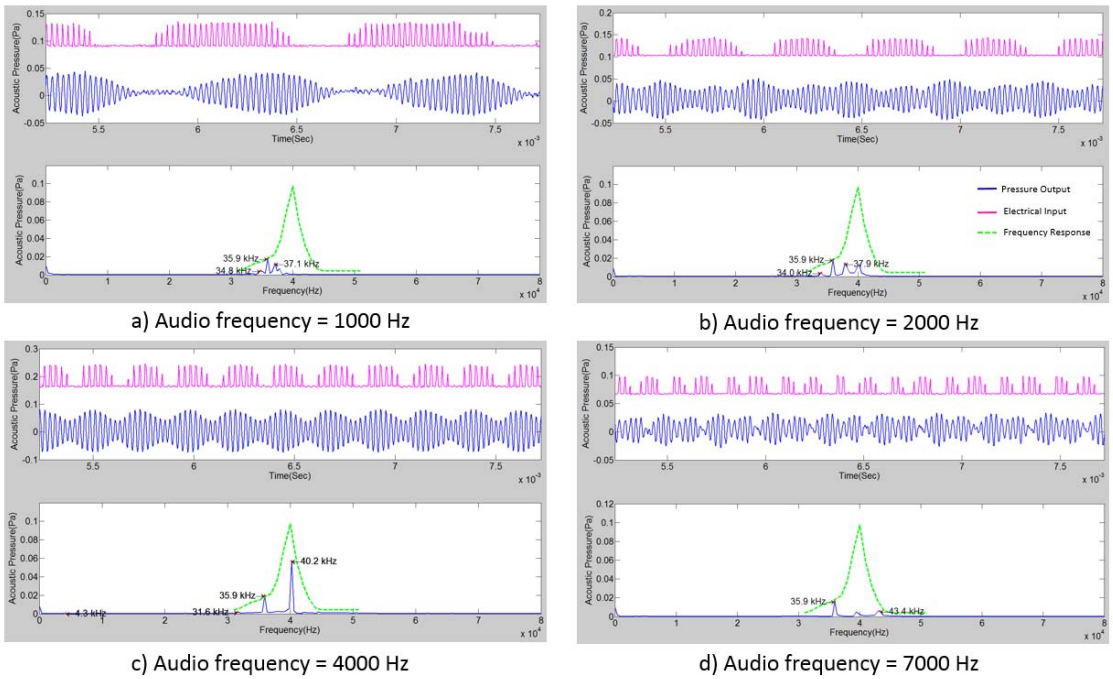

Figure 4-21: The pressure output of a magnetic buzzer when driving it with pulse rate at 22 kHz and audio frequency of 1, 2,4 and 7 kHz.

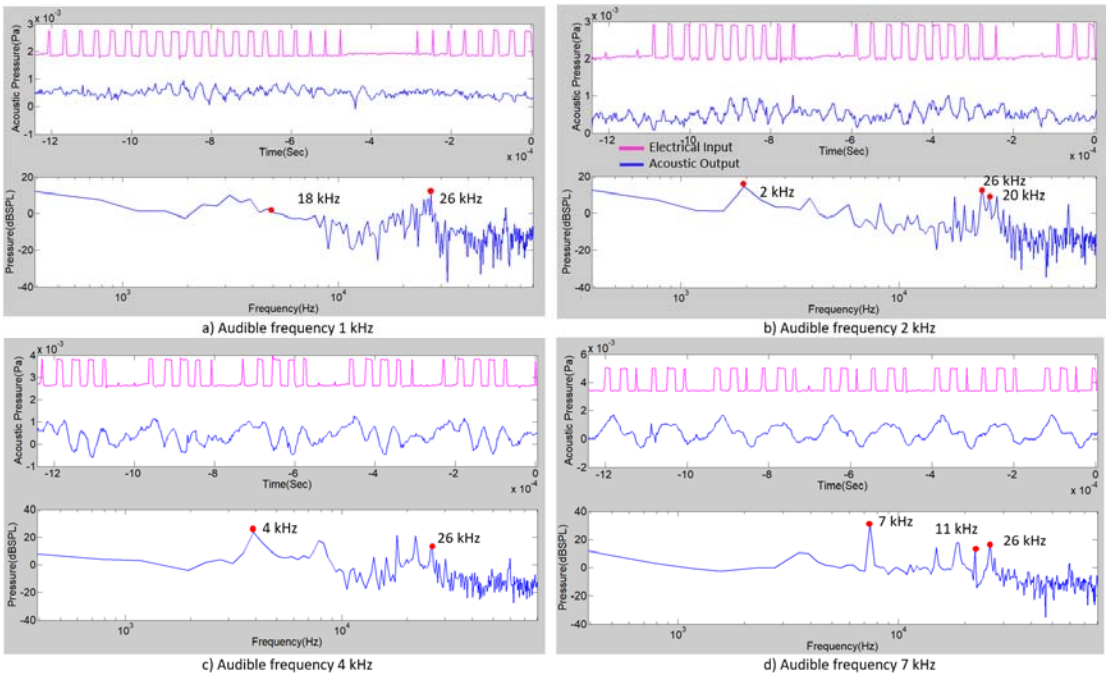

Figure 4-22: The pressure output of a magnetic buzzer when driving it with pulse rate at 26 kHz and audio frequency of 1, 2,4 and 7 kHz.

4.1.4.5 Discussion

Because it is impossible to stop pulses within a period of audio sampling rate, the pulse rate is defined by ignoring the first requirement of digital reconstruction. As a consequence, the amplitude of output frequencies depends on the frequency response of a speaklet. The pulse rate of a digital electrical input is equal to the resonant frequency in order to maximize the amplitude of the pressure output. This pulse rate acts like the carrier in an AM waveform.

The output waveform of a real electro-acoustic source, as a speaklet within a MDLA, is a full wave AM. This is similar to the sound reproduction of a parametric array, which is fed with the AM audio signal, as described in Section 2.2.3.

From the experiments, only the ultrasonic transducer can generate sound due to the beat frequency phenomenon sound be generated from ultrasound. Piezoelectric and magnetic buzzers can directly produce sound at some frequencies when the audio frequencies are within the bandwidth of the speaklets. The sound is mixed with ultrasound but it is not generated from ultrasound. In order to protect direct reproduction of sound, the bandwidth of the speaklets is in the ultrasonic range.

Efficiency of audio reproduction of a digitally driven speaklet can be identified by resolution, bandwidth and loudness of audio reproduction.

Resolution or quantizing levels of audio reproduction can be calculated from a clock period of FPGA and the range of linearity between the pulse width of the electrical input and the amplitude of the pressure output. The range of linearity is directly related to the input pulse period. An increase in the pulse rate results in reduction in the resolution.

The bandwidth of audio reproduction is less than, or equal to, a half of the bandwidth of the frequency response of a speaklet. The spectrum of an AM signal consists of carrier, lower and upper sidebands, which should be symmetric. The carrier is at the middle of the two sidebands. The reproduction bandwidth is equal to the width of the two sidebands. From the experiments, the bandwidth of the ultrasonic transducer is 8 kHz (from 36 to 44 kHz), but it can only reproduce sound with a bandwidth of 4 kHz. The narrow bandwidth of reproduction is enough for speech comprehension but is poor quality for music. The bandwidth is narrow due to the transducers being made from piezo ceramic. The bandwidth can be extended if the speaklet is made from piezo composite or PVDF similar to loudspeakers in audio spotlight technology, which claims that the sound quality is good for music, as described in Chapter 2.2.3.2.

Loudness of audible frequencies in AM sound from a MDLA relies on sharpness of curve of the relation between pressure and 1/density of the air medium. The relation results from asymmetry between compressing loop (positive pressure) and expanding loop (negative pressure) of the wave. The pressure of the ultrasound is high enough (60 dBSPL) to increase degree of asymmetry. The AM wave produces sound with reasonable loudness (30 dBSPL). Due to the shape of the frequency response not being flat but triangular, with the top angle above the middle of the base, as a result, the lower the frequency of the audio, the louder the sound from the speaklet. The speaklets conform to the human hearing contour, which shows that the sound level at low frequencies is higher than the sound level at high frequencies in order to have equivalent hearing (More detail in Chapter 2.1.4.1.).

4.2 Finite Element Model of a speaklet with DLA Based on PZT actuators

From the experiments, it can be found that the resonant frequency and amplitude (or sound level) of frequency response of the speaklets are key factors in audio reproduction. This section will examine the effects of the dimensions of PZT speaklets on their frequency responses in order to anticipate their specification for fabrication.

4.2.1 Objective

- To study the effect of change in dimensions of the transducer and diaphragm of a speaklet on the natural frequency and maximum magnitude of its vibration.

4.2.2 FEM Modelling and Parameters

Speaklets were modelled in Comsol Multiphysics in order to study the surface vibration response to a unit step pulse. The pulse had an amplitude of 5V and a 40 ns rise time. In order to study the maximum displacement of different sizes of speaklet diaphragm, which vibrate with different natural frequencies, a unit step is used rather than a rectangular pulse. Owing to the width of the electrical pulse corresponding to the frequency of the oscillation, a unit step allows a diaphragm to oscillate with maximum displacement. The structure of the speaklet is based on a typical piezo buzzer, which has a round disc as a diaphragm fixed around the edge. The diameters of the PZT and the bottom electrode are equal, as shown in Figure 4-23 (a)

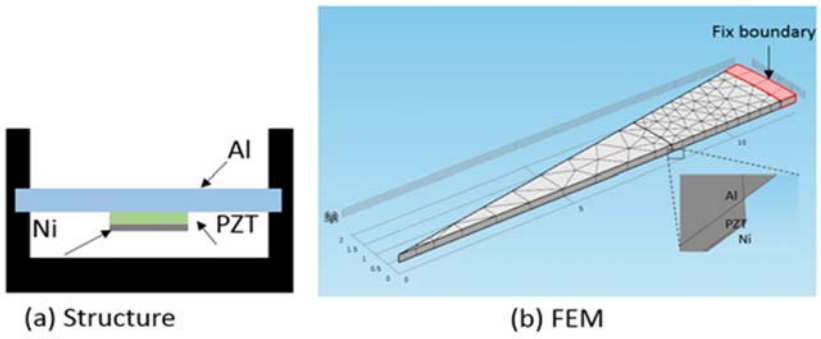

Figure 4-23: PZT speaklet cross section schematic view and FEM model

For the purpose of undertaking a Finite Element Model (FEM), a segment of 1/10 of the disc is simulated in order to reduce the simulation time and this is shown in Figure 4-23(b). The other parameters used are shown in Table 4-6

Table 4-6: Parameters in the FEM model

Layer	Function	Material	Thickness
1	Lower Electrode	Au	1.98 [μm]*
2	Active Layer	PZT-5H	20 [μm]*
3	Diaphragm and Upper Electrode	Al	50, 100, 150 and 200[μm]**

*The lower electrode and active layer are measured with a micrometre to be between 20 and 25 um and are estimated according to ratio of thickness between electrode and active layers in Bakke et al [28].

** The values of thickness of Aluminium are available in our experiment.

The simulation uses piezoelectric devices module which emulates movement of the diaphragm surface of the piezoelectric transducer when applying a voltage. The module consists of components as shown in Figure 4-24.

- Defining ground 1 component to upper electrode and Terminal 1 component as lower electrode;
- Defining voltage terminal in the Terminal 1 component with a discrete constant voltage pulse by using expression language as (t>=risingEdge && t<=fallingEdge)*volt, where volt is 5 voltage applying to the terminal. The values of risingEdge and fallingEdge are the rising edge at 22 ns and falling 60 ns of the discrete pulse;
- Defining fixed constraint on and under the area and symmetry 1 on both sides of the sector of circle as shown in Figure 4-23b

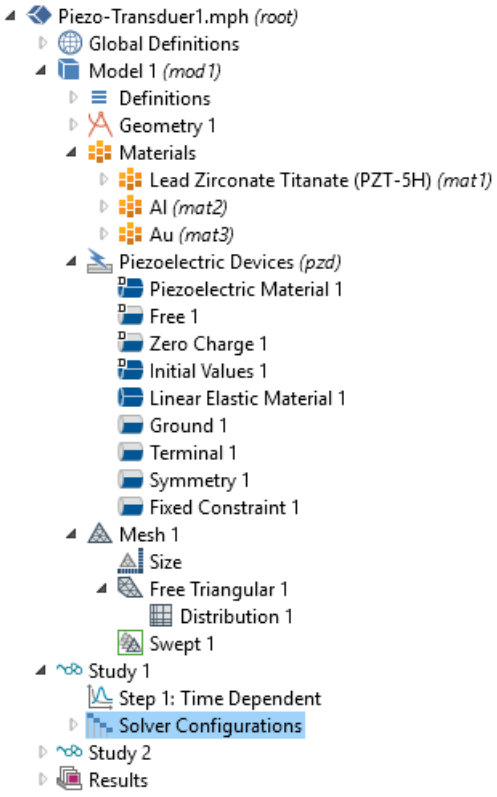

Figure 4-24: Components in piezoelectric devices module

To validate the model, the convergence of the maximum displacement at the centre of the diaphragm is plotted with the number of mesh points as shown in Figure 4-25. The curve starts to converge at 71037 mesh points

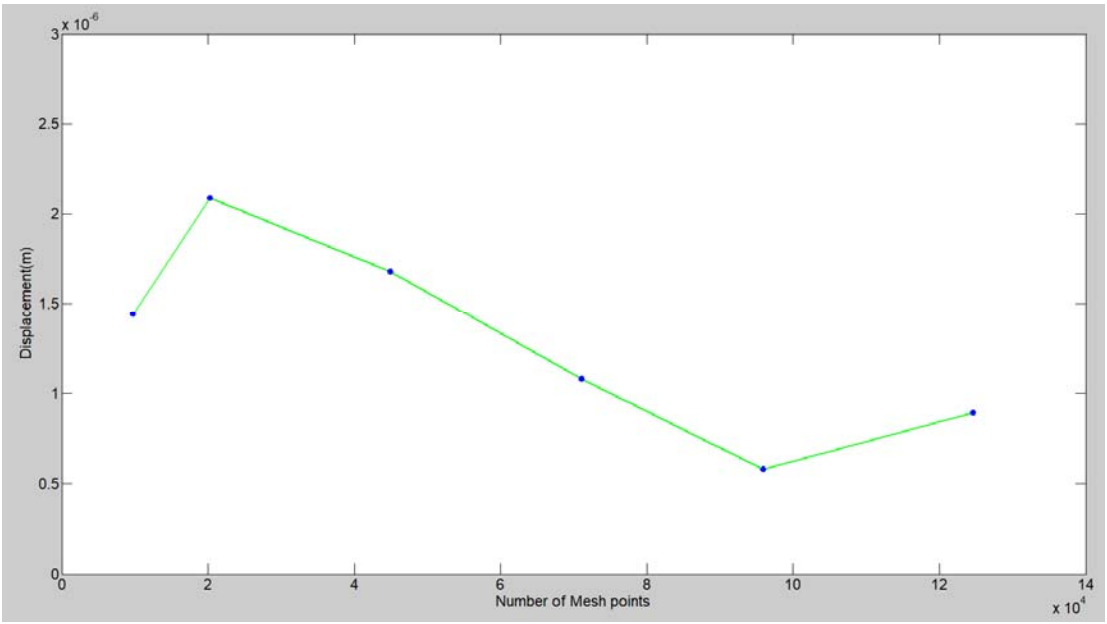

Figure 4-25: Convergence plot of maximum displacement of a speaklet VS the number of mesh points

4.2.3 Characterization of Diaphragm Vibration Response:

The FEM study of the membrane's response to a unit step allows the extraction of two important parameters for the DLA design. These are the fundamental resonant frequency (f_0) and the displacement amplitude of the first pulse of the response. Figure 4-26 shows an example response. Figure 4-26b is the frequency domain of the displacement response shown in Figure 4-26a. These parameters will affect the allowable driving pulse rate of the DLA and also the loudness of the reconstructed sound. For the following study, the diameter and thickness of the diaphragm and lower electrode are chosen as variable parameters.

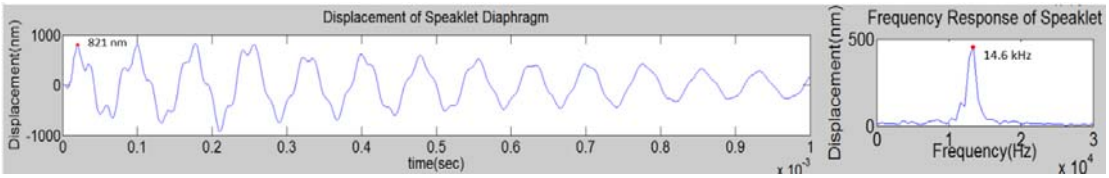

Figure 4-26: The displacement and frequency response of a speaklet with 12 mm, 0.2 mm and 9.1mm diameter, thickness of diaphragm and diameter of electrodes respectively.

The FEM results are divided into four categories as the following parameters are varied:

- radius of the diaphragm
- radius of the electrode
- thickness of the electrode
- thickness of the PZT layer

4.2.4 Results

A summary of these results is shown in graphs a), b), c) and d) respectively in Figure 3. The top row shows the effect on resonant frequency and the second row shows the effect on displacement. The individual curves in the graphs represent different thicknesses of diaphragm, as per the legends. For the study of the effect of the dimensions of the diaphragm, the lower electrode radius was fixed at 0.5mm in order that all speaklets with a diaphragm radius from 1 to 6 mm are exerted with the same force from the area of electrode. It can be seen that when reducing the diameter of the diaphragm or increasing its thickness, the resonant frequency increases (as shown in Figure 4-27(a).

1. This is expected as Eq.(2.32) shows the classical relationship between thickness (h), diameter (D) and the first resonant frequency or (f_0) of a diaphragm, showing a linear relationship with

thickness but a $1/D^2$ relationship with diameter.

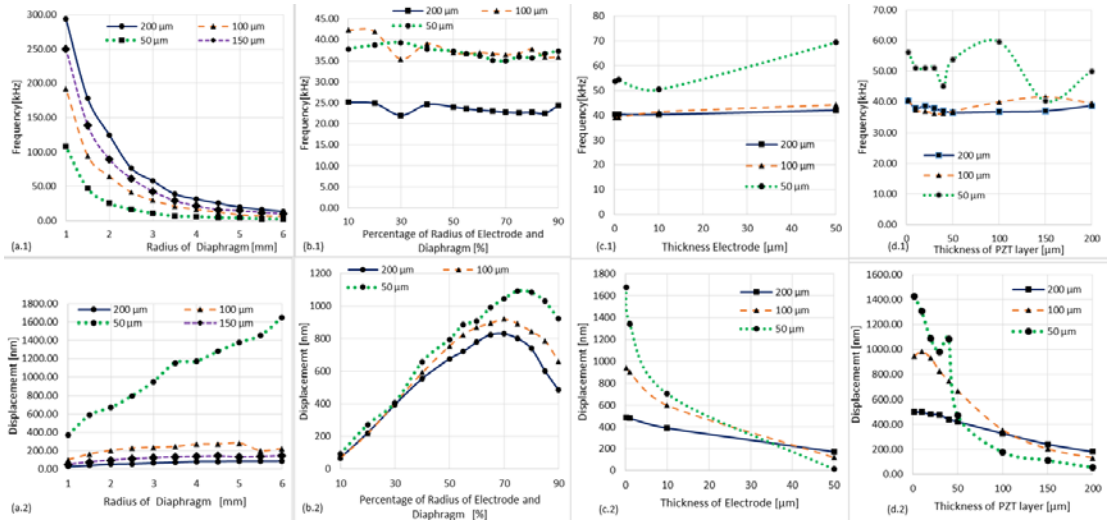

Figure 4-27: The result of the two main parameters: the displacement of oscillation and the first resonant frequency obtained from FEM

Considering displacement, an increase in thickness of the diaphragm will decrease the displacement, while a reduction in the diameter of the diaphragm decreases the displacement. The slope of the displacement change depends on the thickness of the diaphragm, as shown in Figure 4-27 (a).

2. When considering a constant dimension of diaphragm, but varying only the electrode diameter (as shown in Figure 4-27b), the relationship between displacement and electrode size is of the form of an inverted parabola having a peak of displacement at approximately three quarters of the diaphragm diameter because a bending moment is generated at the edge of the electrode. The peak of the relationship can be considered as an optimized diameter for the electrode and for a diaphragm. In Figure 4-27b.2, the position of the peak displacement with ratio of electrode to diaphragm diameter varies with the thickness of the diaphragm.

For example, a device with a diaphragm thickness of 50µm has a peak displacement that occurs at an electrode/diaphragm ratio of 75%, but this reduces to about 70% when the thickness is increased to 200µm. However, this ratio has very little effect on the device's resonant frequency, as shown in Figure 4-27b.1. Figure 4-27c shows that an increase in thickness of the bottom electrode has a slight effect on the frequency, while an increase in the electrode thickness can reduce the maximum displacement of the speaklet diaphragm. The degree of degradation depends on the thickness of the diaphragm. Similar results are found when the PZT layer is varied, as shown in Figure 4-27d. A constraint on the thickness of the PZT layer (other than mechanical construction issues) is that the breakdown field strength of the PZT cannot be exceeded, which will be the limiting factor in terms of electrical drive. This is typically in the order of 4 MV/m for

thick film PZT [52] and so a PZT thickness of 50 μm can withstand up to 200V. However this may be an issue if thin films of the order of a few microns are used, as the voltage would fall to a few volts or tens of volts.

Although this FEM study has concentrated on the mechanical dynamics rather than the acoustics, the acoustics follows because the displacement drives the air and they are linked by boundary conditions [51].

4.2.5 Discussion

The mechanism of sound reconstruction of a DLA relates to trains of pulses feeding the speaklets, the natural frequency and the amplitude of vibration of the speaklet diaphragm within the array. The resonant frequency linearly relates to the diaphragm thickness and hyperbolically to the diameter. The amplitude relates to the thickness and diameter of the diaphragm. The maximum value of the amplitude can be derived from the peak of the inverted-parabolic relationship between the size of the electrode and the maximum displacement. The applied voltage is limited by the thickness of the PZT layer, although the thinner the PZT and electrode layer are, the higher the potential amplitude is. For an applied voltage of 10 V, the thickness of the PZT layer is required to be 2 μm in order to produce an electric field strength of 4 MV/m. A potential enabling technology for the implementation of low voltage speaklets is thin or thick-film, which can produce PZT layers having high values of d33, typically being 300 pC/N estimated from the speaklet in the experiment. The thickness of the PZT and electrode layer degrade the amplitude and the degree of the reduction relates to the thickness of the diaphragm.

Although most of the results are based on FEM simulation, these allow us to understand the characterization of speaklets and this is a good approximation in the design of speaklets for a DLA. The thickness and diameter of diaphragm are the main variables in designing the resonant frequency of acoustic response of a speaklet. The thickness is the key parameter for the efficiency of a DLA because decrease in thickness makes a speaklet smaller in diameter and higher in amplitude of vibration for a required resonant frequency. The reduction in size of a speaklet results in not only an increase in the number of speaklets within a certain size of DLA but also expansion in directivity of sound radiation. An increase in the number of speaklets within the array causes an improvement in the bit resolution of sound reproduction. Although speaklets can be implemented with thin-film and thick-film technologies, the thin-film technology produces more efficient speaklets, especially for low voltage, due to the limitation of technologies in the production of the thickness of the layers of a transducer. Screen printing technology can produce speaklets with PZT and electrode layers with thicknesses in the order of tens of microns, while

thin-film technology can produce an electrode layer with thickness in the order of one-tenth of a micron and a PZT layer with thickness in the order of a micron, in order to obtain an electric field strength of 4 MV/m (10 V across 2.5 microns).

However, the response of a speaklet to a digital pulse from the FEM simulation is vibration on the surface of the diaphragm. It is sufficient to study the resonant frequency of the acoustic response because the frequencies of the vibrating surface and acoustic response are the same. In order to quantify the loudness and directivity of sound, the response has to transform the vibration on the diaphragm into radiation of the sound by using the wave equations. Therefore, the development of the FEM simulation would make interesting work in future.

4.3 Summary

The pressure response of speaklets was not demonstrated to be capable of meeting a key requirement for digital sound reconstruction, in that the response should stop before rising edge of the following pulse (more detail in Chapter 3.3.3.4). The responses of the speaklets have low damping ratios, which result in a long emitting time (in the order of milliseconds). The pulse rate which corresponds to the requirement is in the order of a hundred Hz, but the rate is too slow to reproduce sound from the audio stream, which has a sampling rate of 44.1 kHz.

The reduction of ringing of the response to a rectangular pulse by raising a second pulse, referred to as the double pulse technique, is not effective because of the multiple resonant frequencies of the response of the speaklets and the initial interval of the response, as described in Chapter 4.1.2.2. Because it is impossible to meet the first requirement, the first requirement is ignored and allows the response of consecutive pulses to overlap each other. As a consequence of the ignorance, the amplitude of the response of a speaklet to the pulse rate is related to the frequency response of the speaklet because the interference between successive pulses. The amplitude will maximize when the pulse rate is equal to the resonant frequency of the speaklet.

The relationship between the pulse width of the driving signal and the amplitude of the acoustic wave can be linear for a certain range of pulse widths. The range is directly related to the pulse period.

Driving a speaklet according to the concept of a MDLA produces the pressure response like an AM waveform. The frequency response of a speaklet should have a single resonance frequency in order to protect frequency distortion at the resonant frequency. The bandwidth of a MDLA speaklet requires twice the audio bandwidth. An 8 kHz bandwidth of a speaklet can only produce

a 4 kHz audio bandwidth. The loudness of a MDLA relies on the non-linear acoustic of the air medium, similar to a parametric array.

The relationship between the dimensions of a speaklet and its acoustic response when feeding a rectangle pulse shows that:

- Diameter of diaphragm of a speaklet is inversely related to the resonant frequency of the speaklet while the diameter is directly related to the amplitude of the response
- Thickness of diaphragm is directly related to the resonance frequency of the speaklet, while the thickness is inversely related to the amplitude of the response
- Change in diameter of transducer has a slight effect (less than 10 %)on variation in the resonance frequency, but an increase in diameter changes the amplitude of the response
- Change in thickness of the transducer has a slight effect (less than 10%)on variation in the resonance frequency and amplitude if the thickness is less than 50 μm

In conclusion, the pressure response of a MDLA with diaphragm based piezoelectric speaklets can generate sound with AM waveform by relying on non-linear acoustic medium but it is lower efficiency between loudness and the total transmitting wave enegy than the sound with half-wave rectified AM as the ideal case in Chapter 3. In the next chapter, a novel structure of a loudspeaker is introduced for sound generation with half-wave rectified AM waveform.

Chapter 5: A Potential Implementation for an Acoustic Rectifying Loudspeaker

5.1 Acoustic Rectifying Loudspeaker

This chapter will introduce the concept of a rectifying loudspeaker and perform the validation of the proposed conditions for acoustic rectification in Chapter 3. Pressure (p) is directly proportional to velocity (u), which is directly proportional to displacement (w) of the diaphragm, but only the proportional relationship between the displacement and the velocity is demonstrated in this chapter. Although this demonstration have not yet complete the validation, it is a good evidence that the loudspeaker has a potential for generating a rectified sound while the demonstration of the proportional relationship between pressure and velocity will be a further work, which is described in Chapter 6.1.1. The main reasons why AM sound requires a rectifier are addressed by consideration of sound in the frequency domain, and why a analogue loudspeaker or a transducer cannot produce the rectified sound is addressed by illustration in schematic diagrams of wave propagation. A proposed structure and mechanism for a rectifying loudspeaker is presented.

The validation of the condition is performed by a simplified structure. The advantages and efficiency are assessed and a practical structure is identified in the discussion section.

5.1.1 Principles

From the previous chapter, it was seen that a waveform of pressure output of multiple-level digital loudspeaker array (MDLA) is similar to a waveform of amplitude modulation. Although it can make sound, due to the non-linearity of the air medium between pressure and specific volume as described in Chapter 2.2.3.1, the efficiency of sound is low because the ratio of sound level to the magnitude of the side bands is low - approximately 1:10 as shown earlier in Figure 4-17

In order to increase the ratio to 1:1, the waveform of pressure output of the MDLA needs to be rectified, which can be achieved by demodulation of the modulated wave. The ratio will increase and the sound level will not only be indirectly affected by the non-linear acoustic medium, but the level is directly affected by the amplitude of the side band i.e. the modulated audio signal. As in the ideal case of the MDLA described in Chapter 3, the output waveform is half-wave rectified

waveform of amplitude modulation, which has an audible frequency component, although the acoustic linearization is assumed to be as shown in Figure 5-1.

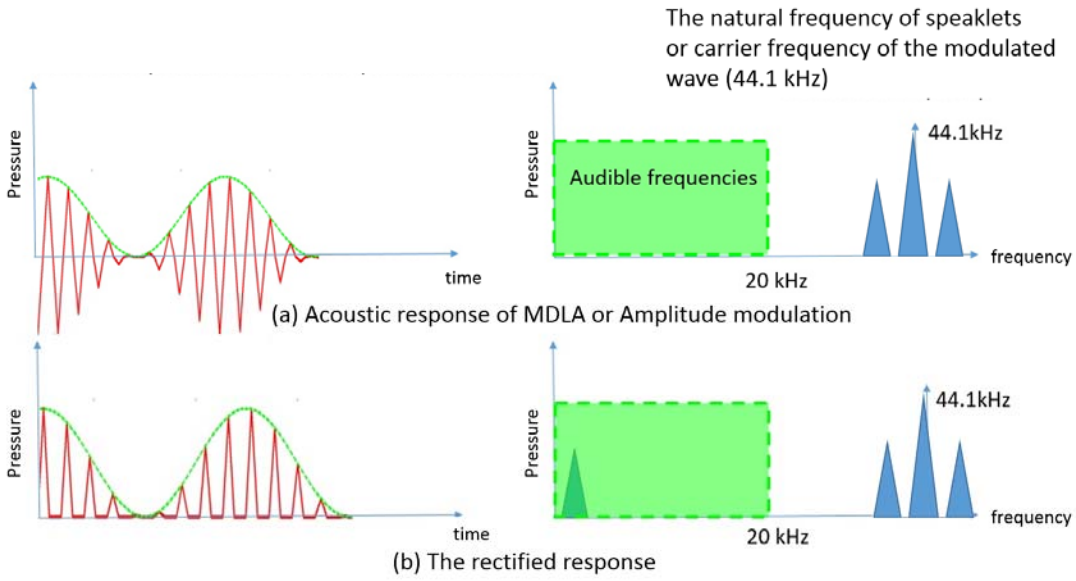

Figure 5-1: Frequency components of AM (a) and half-wave rectified AM (b)

The common structure of speaklets or tiny loudspeakers is based on a diaphragm as an acoustic generator. The sound propagation of a diaphragm or a piston can be illustrated as in Figure 5-2, based on assumption of air chunks and the direct proportion of air pressure to velocity of airflow as described in Chapter 2.1.1.

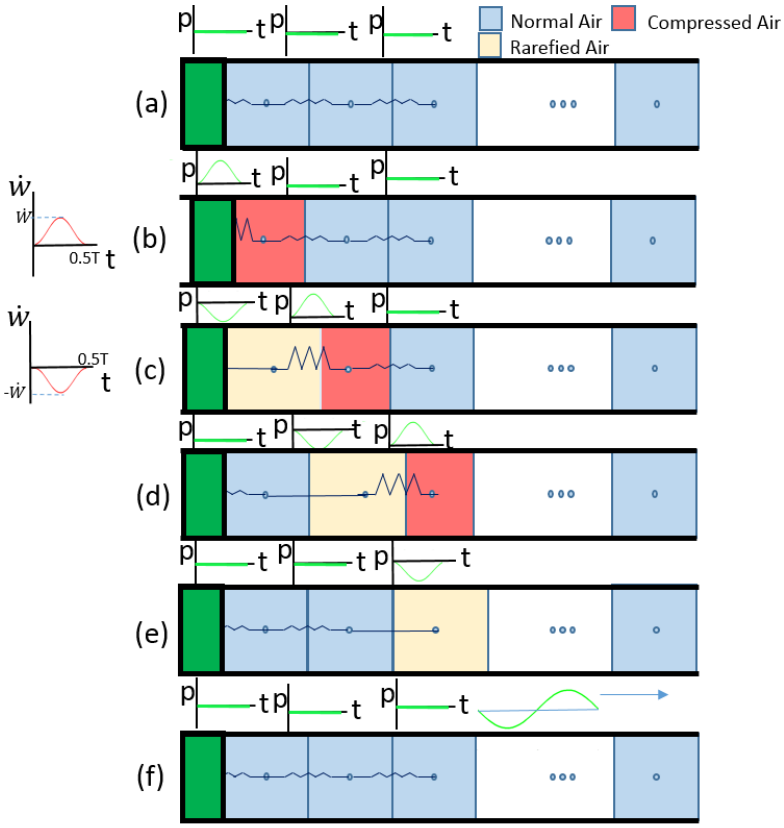

Figure 5-2: Schematic diagram of wave propagation of a piston or a diaphragm.

From the process of wave propagation shown in Figure 5-2, a piston produces compression and rarefaction. The compression results from forward movement of the piston, while the backward movement causes the rarefaction. Figure 5-2 (a)-(f) show the process of the wave-cycle. Figure 5-2(a) is the initial stage of the propagation. Figure 5-2 (b) shows the pressure and the velocity when the piston moves forward and stop with a simple harmonic motion. The first chuck is compressed and causes the pressure because the boundary between the surfaces of the piston and the first air block is shifted while the other side of its surface stays still. Figure 5-2 (c) shows the boundary between the first and the second chucks moving forward while the piston moves back. As a consequence, the first chunk is expanded while the second chuck is compressed. This starts to form a wave cycle. In Figure 5-2 (d) the boundary between the first and second blocks is pulled back because the first block reverts to the original shape with no expansion at the original position while the boundary between the second and the third blocks moves forward because the second chunk was compressed in the previous stage. As a result of the movements of the two boundaries, the second lump is expanded while the third lump is compressed. This starts to propagate the wave through a lump. Figure 5-2 (e) shows that the second chunk becomes the original shape at the original position. The wave propagates through another block. Figure 5-2 (e)

shows the wave propagate through air lumps by they not changing the position but moving forward and backward a cycle.

In order to produce a rectified wave, which has either compression or expansion, the diaphragm needs to move forward only or backward only. It is impossible for diaphragm-based loudspeakers to generate the rectified wave because the diaphragm vibrates forward and backward. Therefore, a new structure of a loudspeaker is introduced for rectified wave generation. This will be referred to as a rectifying loudspeaker.

5.1.1.1 Structure of a Rectifying Loudspeaker

An implementation of the rectifying loudspeaker is adapted from the human voice system, which is described in Chapter 2.2.4. There are three major components; air pump, air piston and diffuser as shown in Figure 5-3.

- Air pump acts like lungs. The pump pass the air though piston and diffusor with a constant pressure.
- Piston acts like a larynx. The air is injected into the piston through the edge of the piston and the air is discharged from the hole at the centre of piston, which are attached as diffusor. The air path is obstructed or permitted depending on vibration of a disc or a diaphragm, which acts like a vocal cord, within the piston. The vibration of a disc controls the velocity of the air flow. The vibrating force of the disc is different from the force of the vocal cord. The cord is vibrated by only Bernoulli' force while the force is the disc is vibrated by an electrical voltage.
- Diffuser acts like a vocal trace. The major function of the diffusor is to gather the airflow around the tube of piston into the single direction and to spread the air over a large area as the waveguide of sound. Humans use organs in the vocal trace such as a mouth and a tongue for different pronounce while different frequencies of sound is directly controlled by the vibrating disc.

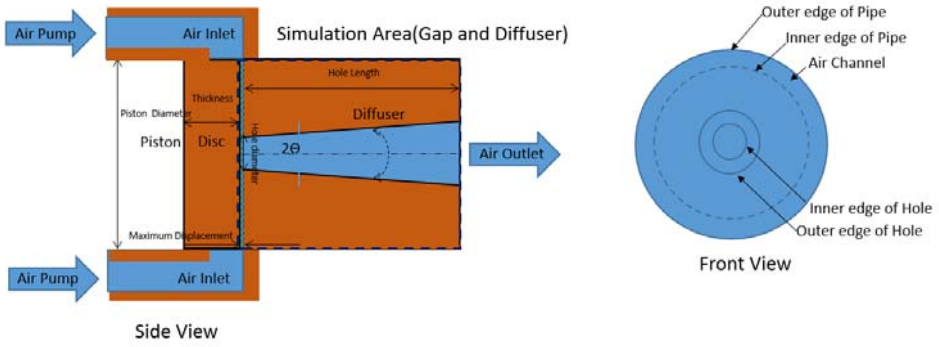

Figure 5-3: Structure of a Rectifying Loudspeaker

Operations of the rectifying loudspeaker are divided into two states as shown in Figure 5-4. Block state is when the air path is obstructed from the pump to the diffuser by a vibrating disc in a piston. The disc place on the equilibrium position in this stage is called the initial stage. Discharge state is when the air particles flow from the edge of the piston into a hole of a diffuser at the centre of the piston when the solid plate moves backward and forward in a cycle by an external force. While the channel between the disc and the diffuser is opening, air particles in the flow move and collide around the centre of the piston. As a result of the collision of a huge number of particles, the particles should be scattered omnidirectionally but there is merely a single channel out of the diffuser. The sudden change in direction or magnitude of velocity of the particle causes an acoustic- generating boundary as discussed in Chapter 2.1.3.2. When the moving plate returns to the original position, in which the disc blocks the air path, the state changes back to the block stage

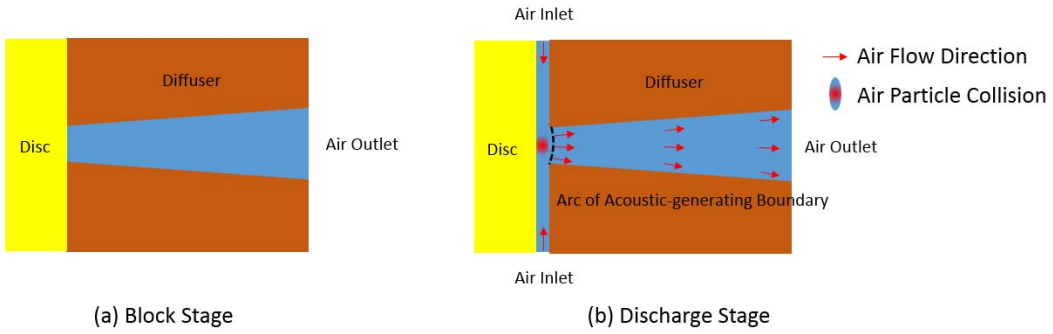

Figure 5-4: Operational stages of the rectifying loudspeaker

5.1.1.2 Propagation of a Rectifying Loudspeaker

The essential difference of the rectifying loudspeaker from a traditional loudspeaker is that the vibrational displacement of air particles at the boundary between air and sound source is never negative, that is, they move forward only, because the air particles at the neck of diffuser, which is next to the disc of the piston as the primary vibrating source, move in only one direction. The

rectifying loudspeaker produces sound from a secondary source, which is not a physical vibrating membrane but a virtual membrane of a rapidly changing velocity of air particles, similar to the phenomenon in a resonance tube of a sudden change in velocity of air particles between the inside and the outside of the tube at the opening. The sound propagation of the rectifying loudspeaker is illustrated at Figure 5-5, based on the assumption of air lumps and the direct proportion of air pressure to velocity of airflow as described in Chapter 2.1.1.

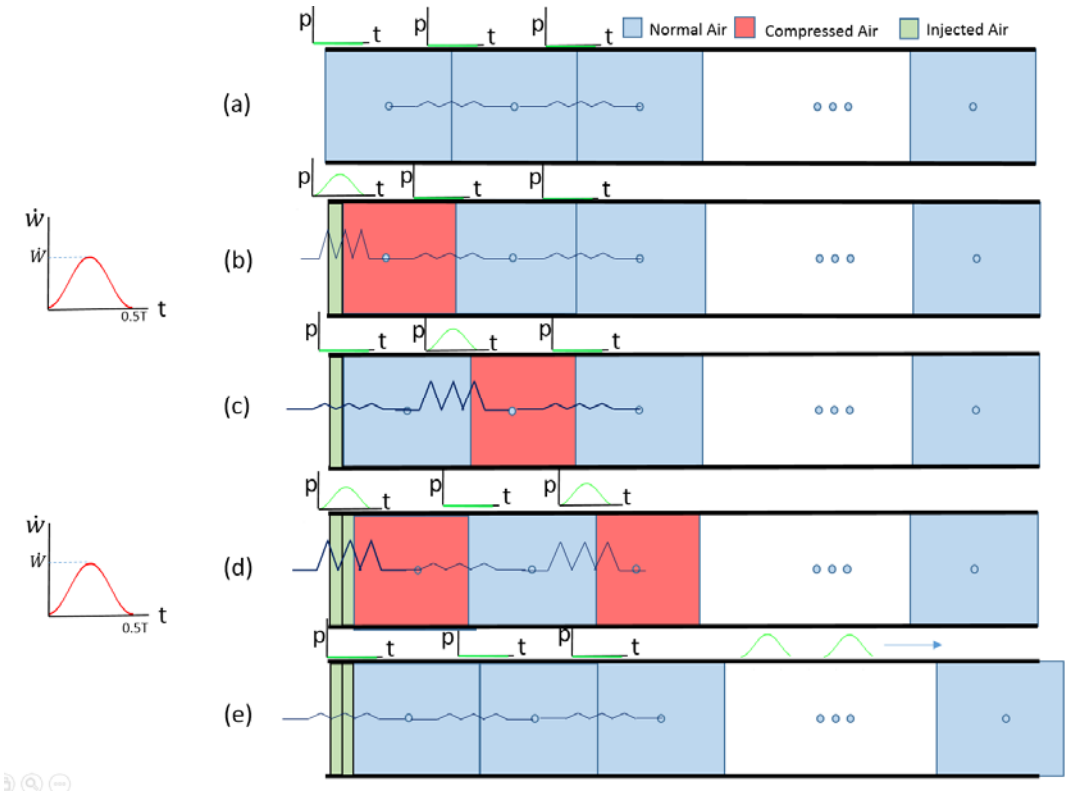

Figure 5-5: Schematic diagram of wave propagation of a rectifying loudspeaker.

From the process of wave propagation shown in Figure 5-5, a piston produces a rectified wave, which has a cycle with only a compression stage but no rarefaction stage. The compression results from rapid air injection. Figure 5-5 (a)-(e) show the process of propagation in two cycles of a wave. Figure 5-5 (a) is the initial stage of the propagation. Air particles are rapidly injected with simple harmonic motion as shown in the graph in front of Figure 5-5 (b) and blocked in the tube while the injected air presses and shifts the boundary of the first air lump. This causes the pressure in the first block to rise as shown in Figure 5-5 (b). Next, the first chuck returns to the original shape by pushing the boundary of the second lump and raising pressure in it as shown in Figure 5-5 (c).The first air mass changes position because the injected air replaces it. Figure 5-5 (d) shows that while the new air is injected in the tube, the second chucks revert to the original shape. Similarly, this results in the first and third chuck being compressed. Figure 5-5 (e) shows that the rectified wave propagates through air lumps within the piston block by block while the air

lumps change positions block by block. The displacements depend on the volume of the injected air.

5.1.1.3 Mathematical Model

From the structure of the rectifying loudspeaker, the MSD system is altered as shown in Figure 5-6. Two mechanical forces are introduced into the system; the lift force generated from Bernoulli's effect and a stopper, which enables the displacement of the mass to not be negative. The mass and the stopper represent the disc and the diffuser of a speaklet from Figure 5-6

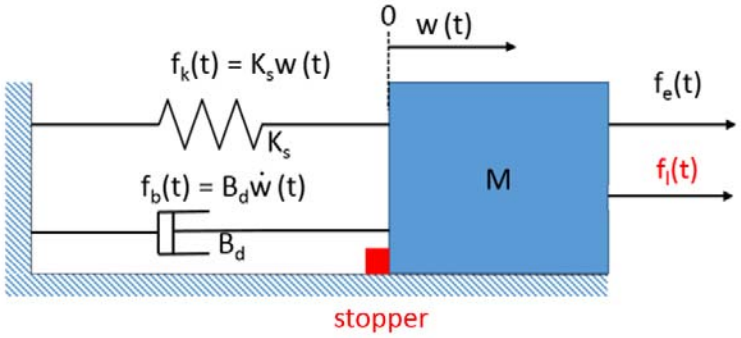

respectively

Figure 5-6: MSD model of the rectifying loudspeaker

When the airflow moves through the vibrating disc, it causes a lift force, which is the component of fluid force perpendicular to the fluid motion. The force can be expressed as [53]

$$f_l(t) = 0.5\rho C_L A_p u^2(t) \tag{5.1}$$

Where ρ, A_p and C_L are density of the air flow , the surface area of piston attached to the air flow and the lift force constant, respectively. The force is directly proportional to the square of the velocity (u(t)) of the flow, while the velocity is directly proportional to the displacement(w(t)) as shown Eq.(2.68). It can be rearranged as

$$Q(t) = A_h u(t) = \sqrt{\frac{2W_p^2}{\rho}}\sqrt{(P_1 - P_2)}w(t) \tag{5.2}$$

Where A_h is the area of the neck of the diffuser and W_p is the perimeter of the disc. P_1 and P_2 are the absolute pressure of the pump and pressure at atmosphere, respectively. Substituting u(t) of (5.2) into (5.1), the force can be expressed as:

$$f_l(t) = \frac{C_L A_p W_p^2 w^2(t) P_{pump}}{A_h} = C_{priton} w^2(t) P_{pump} \tag{5.3}$$

Where P_{pump} is the constant pressure of the air pump above the atmospheric pressure and $C_{priton} = \frac{C_L A_p W_p^2}{A_h}$ is a constant of the piston. The ratio of the area of the hole and the area of the piston have an effect on the force. An increase in A_p or decrease in A_h results in an increase in the force. The lift force is represented in the term of the square of the displacement and the constant pump pressure. The mathematical model of the rectifying loudspeaker can be expressed as

$$\ddot{w}(t) + 2\xi\omega_n\dot{w}(t) + \omega_n^2 w(t) = \frac{f_e(t) + f_l(t)}{M} = \frac{f_e(t) + C_{priton} w^2(t) P_{pump}}{M} \qquad (5.4)$$

This equation is a non-linear differential equation, which might be difficult to solve. The solution should be achievable using FEM software. However, it shows the lift force is involved with a free vibration because it is a term of displacement. Due to the term of square of displacement, the free vibration is not sinusoidal and its waveform might be similar to the air-flow pattern of a dark tone of the larynx as shown in Figure 2-20b. Therefore, the lift force generates a constant pattern of the wave while the external force ($f_e(t)$) will change the amplitude of the pattern in each wave cycle.

The stopper is designed as a fixed surface. When the mass vibrates, it hits the stopper. The movement of the diaphragm can be analysed by using collision of equations. The fundamental equations of the collision can be divided into two extreme cases of perfectly elastic and perfectly inelastic collision. The elastic collision is that the total kinetic energy is conserved as well as the total momentum of the disc and the fixed diffuser while the inelastic collision is that the total energy is lost or transferred into other energy[54]. In this model for the perfectly elastic collision, the velocity before and after collision are equal as with

$$U_a = U_b \qquad (5.5)$$

Where U_a and U_b are the velocity at a moment after and before the collision, respectively, under the assumption that the stopper does not move. For the perfectly inelastic collision the velocity after collision is equal to zero

$$U_a = 0 \qquad (5.6)$$

However, in the practical collision, the kinetic energy is partly lost depending on the elasticity of the material of the diaphragm and the diffuser. This will be studied as a part of the future work section in Chapter 6.2.1 .

5.1.2 FEM Modelling

From the ideal conditions for generation of rectified waves, the acoustic pressure is directly proportional to displacement of diaphragm as Eq.(3.17). This means that the acoustic pressure is directly proportional to velocity of air particles and the velocity is directly displacement of surface of diaphragm.

In this modelling, the relationship between the velocity of air particles at the neck of diffusers and the displacement of a disc is investigated. The structure of the model is based on the rectifying loudspeaker in Figure 5-3 but it is considered on only the diffuser and a gap between the disc and the diffuse as shown in the blue dashed rectangle in the figure.

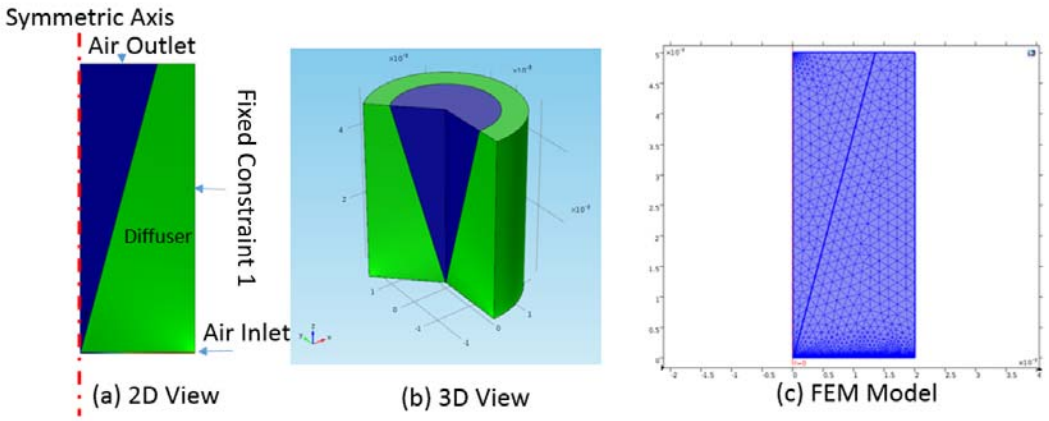

Figure 5-7: Schematic and FEM of diffuse and the gap between the disc and the diffuse.

From the model in Figure 5-7, the simulation is created with the Fluid-Structure Interaction (FSI) interface in comsol multiphysics. The model is divided in small elements with a free triangular mesh with a maximum size of elements of 2 µm. Air is defined as a compressible flow with the Mach number (the ratio of flow velocity to sound speed) less than 0.3. The condition of velocity at the boundary of the wall is 0 m/s or no slip at the wall. Inlet and outlet pressure are 20 and 0 Pa above the atmospheric pressure, respectively. The displacement is prescribed with motion of the vibrating disc as a half wave rectified AM define as Eq.2.60 where pressure is replaced with displacement from the equilibrium, which the disc is closed to the diffuser with the minimum gap of 2.5 µm, and displacement is not negative. The parameters are described in Table 5-1

Table 5-1: Parameters of modelling of the rectifying loudspeaker

Parameters	Value
Diffusor	
Angle(2Θ)	20°
Diameter of hole	20 µm
Length of hole	5 mm
Solid Disc	
Diameter	4 mm
Minimum gap between disc and diffuser	2.5 µm
Maximum gap between disc and diffuser	20 µm
Carrier frequency(f_c) and Amplitude (Ac)	40 kHz and 10 µm
Audio frequency (f_a)and Amplitude(Aa)	4 kHz and 10 µm
Air pressure	
Inlet Pressure	20 Pa
Outlet Pressure	0 Pa

As the simulation in the fluid structure interaction module, which emulates force interaction among the air flow and diffuse and the vibrating disc, it consists of components as shown in Figure 5-8.

- Prescribed Mesh Displacement 2 is defined for the vibration disc by r-displacement = 0 and z-displacement is defined with AM equation of Eq.(2.60) and wave parameters according to Table 5-1.;
- Prescribed Mesh Displacement 3 is defined for the gap between diffusor and the disc. The gap will be resized according to the displacement of the disc by unticking the checked box before z-displacement;
- Inlet, Outlet and fixed constant is defined at the edge as shown in Figure 5-7 and the value of pressure of inlet and outlet is defined according to Table 5-1. . The zero of outlet pressure means pressure is equal to the atmosphere pressure.

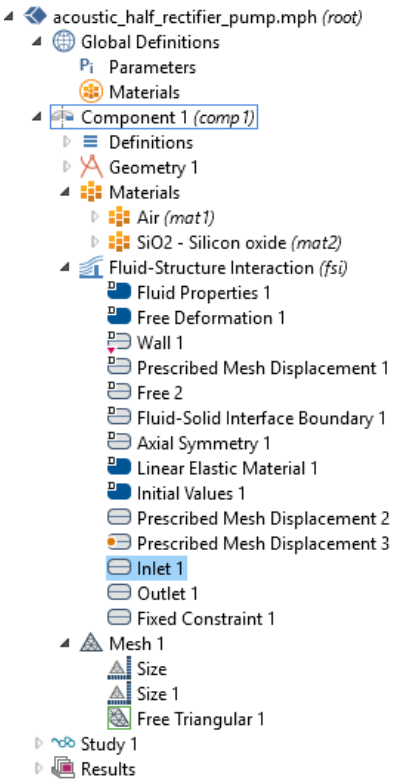

Figure 5-8: Components in fluid structure interaction module

To validate the model, the convergence of average velocity of airflow at the open inside the diffusor is plotted with the number of mesh points as shown in Figure 5-9. The curve starts to converge at 31600 points

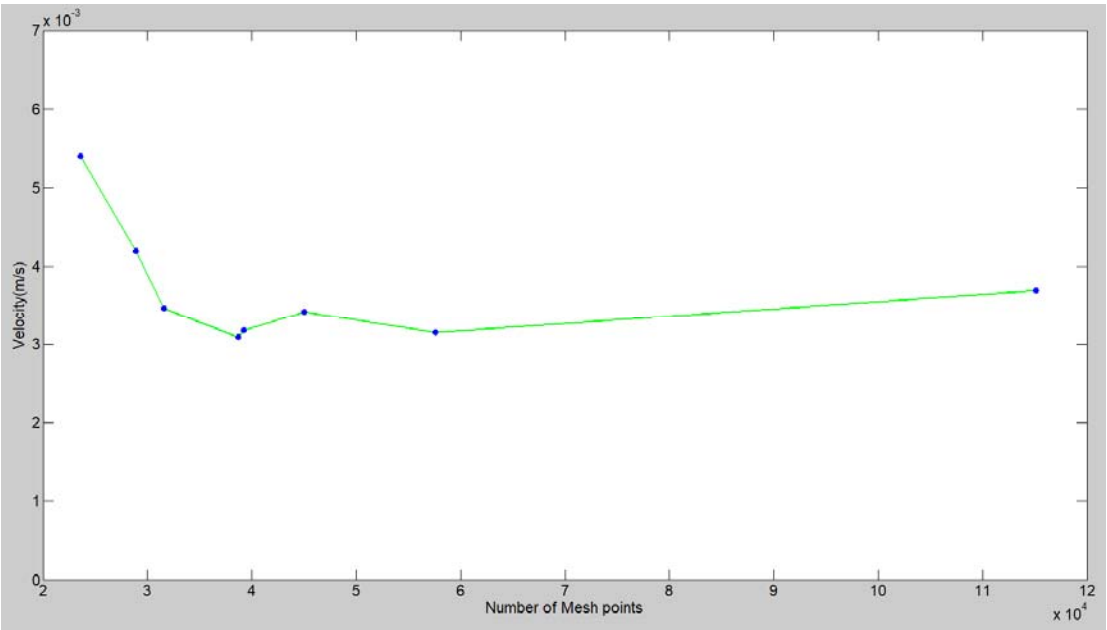

Figure 5-9: Convergence plot of velocity of the air flow in the front of the hole.

5.1.3 Results

From computation of time-dependent study, the average velocity is measured at the orifice or neck of the diffuser as shown in Figure 5-10 . The figure shows air particles flowing from the periphery of the piston through the gap between the rigid disc and the base of diffuser. At the centre, the flow changes rapidly from parallel with the disc surface to perpendicular to the surface. The air velocity is formed as semi-oval by the highest velocity at the middle of the hole. The direction of flow spreads according to the divergent part of the diffuser.

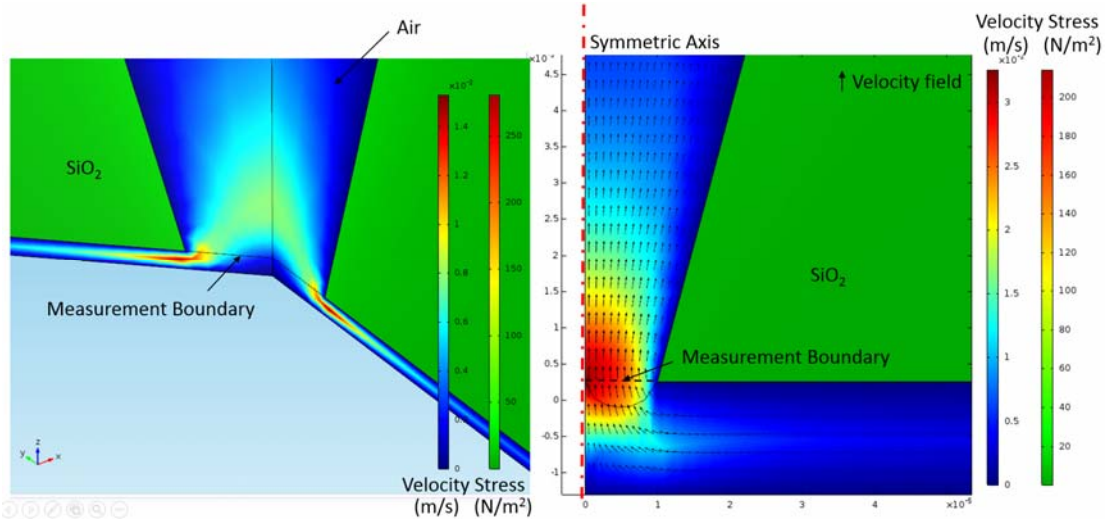

Figure 5-10: Air flow in the speaklet at the maximum displacement.

It is clearly seen that although the disc vibrates backward and forward, the average velocity of flow on the hole surface of the diffuser does not become negative. The vibration of the disc is pre-defined as a half-wave AM form because it is obstructed by the base of the diffusor. Although the movement of the disc and the velocity are not exactly proportional but the audible and the modulation frequency components of the half-wave AM vibration form of the displacement and velocity are equal as show in Figure 5-11a.

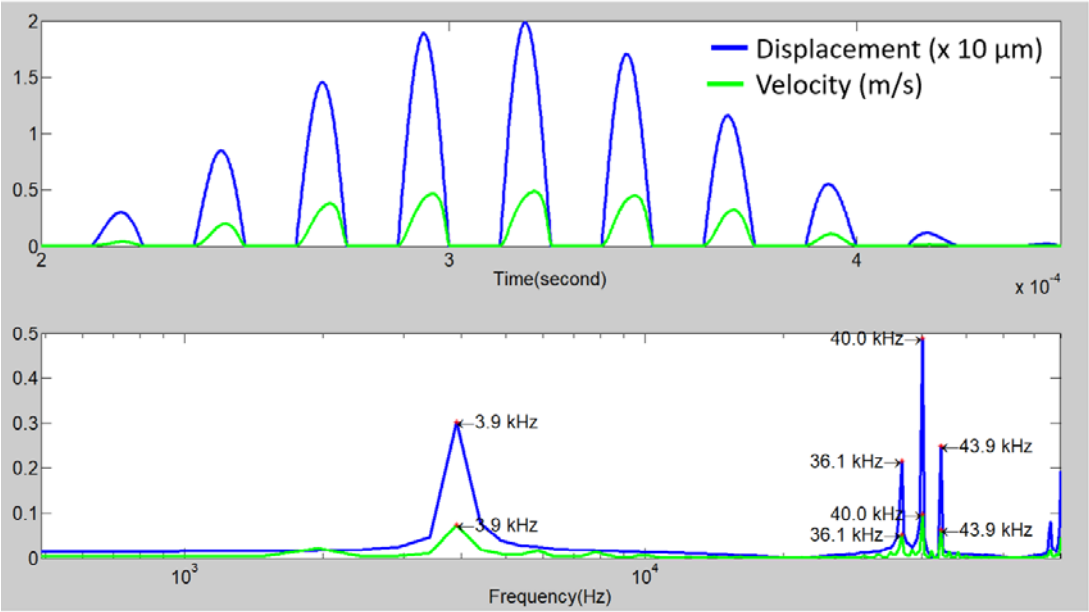

(a) Displacement VS Velocity

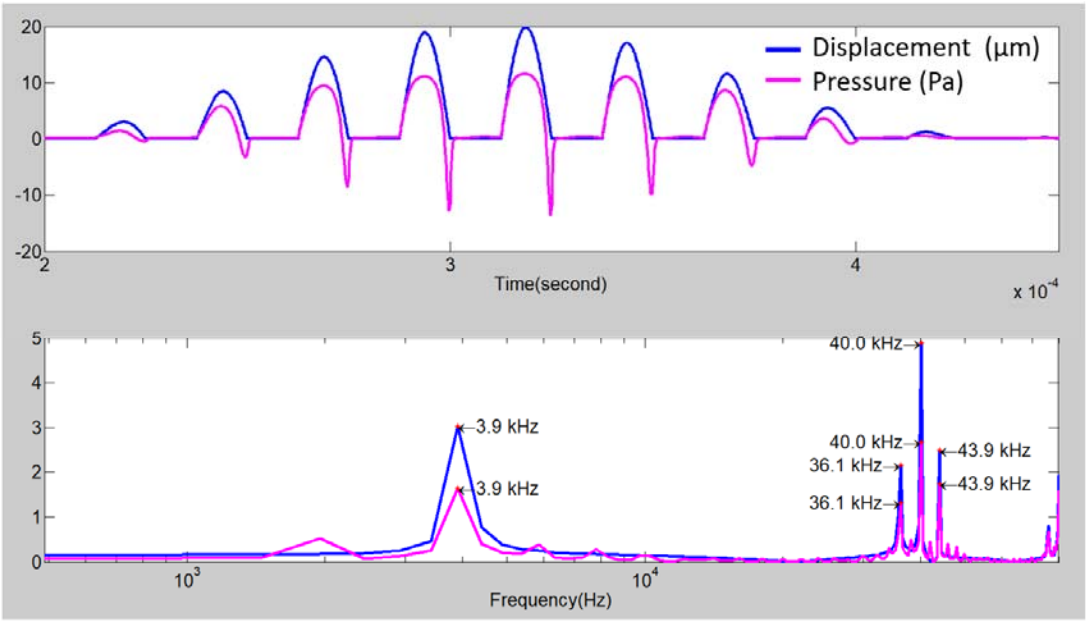

(b) Displacement VS Pressure

Figure 5-11: Comparison between displacement and velocity and between displacement of flow pressure.

In addition, flow pressure at the neck of the diffuser is not directly proportional to the displacement and the wave form of the pressure has short periods of negative pressure but their frequency components have the same frequency, similar to the velocity as shown in Figure 5-11b. The negative pressure results from the shifting phase of the rectified wave according to the polar

angle of acoustic impedance as described in Section 3.3.3.9. In addition, the amplitude of pressure is related to the pressure of the air supply (20 Pa).

5.1.4 Discussion

From the results, it is clearly seen that the velocity moves forward from the surface of the opening, which is designed for the secondary sound source. This implies that the displacement of air particles at the hole has one direction according to the direction of the velocity, while the disc moves forward and backward. The movement of the disc is the primary vibration sound, but acts like a valve, resulting in the velocity of airflow into the hole. Although air supply is introduced in the system, which increases in complexity, it rectifies direction of movement and velocity at the hole.

Although the model is designed for demonstration of direct proportion between the velocity and the displacement, the pressure flow at the velocity transition boundary is shown, but it is demonstrated that it is the acoustic pressure. Its waveform looks like the wave slightly shift phase, which reflects the wave equation of (2.132) . The wave equation is represented as the actual wave radiation of a spherical sound source and has a complex number term of kr-j , which identifies phase shift. This is different from the simplified wave of (2.139) in the ideal case, which is a real number. The variables k and r are the wave number and radius of sound source respectively. The real part of the complex number is significantly greater than the imaginary part, the wave is slightly shifted in its phase similar to the waveform of the flow pressure.

5.1.4.1 Advantages of Rectifying Loudspeakers

In addition to the waveform of the velocity being rectified, there are other benefits from introduction of an air pressure supply.

- Ultrasonic pressure depends not only on a force from a transducer attached to the diaphragm, but also pressure of the supply. Although the flow pressure has not yet been demonstrated to be the acoustic pressure, the acoustic pressure is proportional to the velocity of the air flow, which is proportional to the pressure of the air supply according to Bernoulli's equation, according to the wave equation. Therefore the air supply enables a small transducer to generate high ultrasonic pressure.
- The beam width is wider than the traditional ultrasonic transducer. Although the model didn't show directivity of the loudspeaker, there are two good pieces of evidence for the claim. The beam width is related to the ratio between diameter of diaphragm, which generate ultrasound, and the wavelength. In this model, the diameter of the hole of

diffuser, which emits 40 kHz-ultrasound, is 20 µm. From Eq.(2.30), the angle of the beam width of the loudspeaker model is 308° with the speed of sound(c =343 m/s). In addition, the shape of a sound source of an ultrasonic transducer is a flat diaphragm while the rectifying loudspeaker is the secondary source, which derives from collision of a huge number of air particles. The shape of the source would be alike spherical or elliptical as seen in Figure 5-10 . The magnitude of velocity is formed as spherical or elliptical at the middle of the hole. The flat surface of the source tends to radiate directionally while the arc surface is inclined to radiate with a wide angle.

5.1.4.2 Key Factor of Efficiency

A key factor of efficiency of the rectifying loudspeaker is ratio between a gap at the valve, which is the vibrating disc, closed, and the displacement at the valve opened to a maximum. The key, similar to the compression ratio(ϵ), is defined in a displacement micro-pump as [55]

$$\epsilon = \frac{\Delta Q}{Q_0} \tag{5.7}$$

Where ΔQ is the stroke value and Q_0 is the dead volume.

Therefore, in design, the closure of the hole is a more important feature of the loudspeaker than the displacement of the disc. Because the gap is very small or approaches to zero, the ratio increases.

From the modelling, the structure is simplified to test the relation between the displacement and the velocity but, in the practical loudspeaker, the structure should be altered to a diaphragm rather than a moving disc. Therefore, the base of the diffuser should be an arc as shown in Figure 5-12.

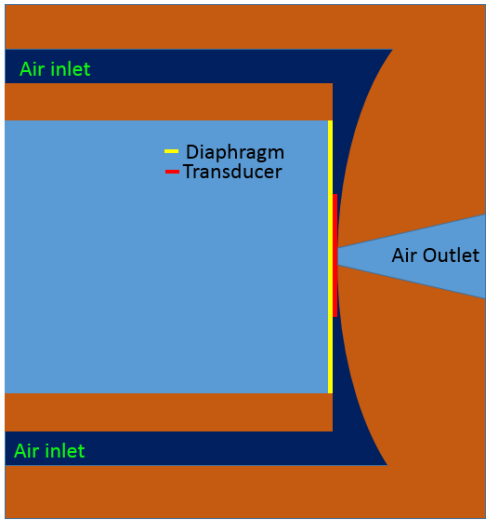

Figure 5-12: A practical structure of rectifying loudspeaker

5.2 Summary

Due to the fact that AM waveform is the output of sound generation from ultrasound, the rectification is the demodulation of AM signals. It is impossible for diaphragm-based loudspeakers to reproduce AM sound. A rectifying loudspeaker imitates a human voice system by introducing air pressure supply to it. The secondary source, which results from air-flow collision, is designed for sound generation. The lift force is introduced into the MSD model due to flow of air particles through the diaphragm while the vibration of the diaphragm is the rectified waveform because a stopper obstructs the movement of the diaphragm at the equilibrium point.

A FEM model of the rectifying loudspeaker is created to demonstrate the relationship between the velocity at the opening and the displacement of the disc, by pre-defining the disc with a half-wave AM with 4 kHz of audio frequency and 40 kHz of carrier frequency. It is found that the frequency components of the audio and their carrier are equal.

In additional to high efficiency in sound reproduction, the intensity of the rectified AM sound depends on the pressure of the air supply. The beam width of the loudspeaker is wide because of the very tiny diameter of the hole in the order of ten microns and because the shape of the sound source is similar to an oval. A key of successful implementation is the ratio between the closure of the hole and the maximum displacement of the moving disc or diaphragm.

Finally, a detailed design of the loudspeaker is not in the scope of this thesis but the next chapter will present a challenge to design the loudspeaker.

Chapter 6: Conclusion and Future Work

6.1 Conclusion

This chapter describes the coherence of the chapters in the body of the thesis, and summarises the essentials of the thesis. It is divided into three parts: illustration of the overall thesis, identification of the differences of DLA, and explanation of the challenges in design of a rectifying loudspeaker.

6.1.1 Landscape of Thesis

The main objective of this research is to investigate the possibility in the implementation of the MDLA. This study explores electro-acoustic transducer technologies and analyses their mechanical and electrical characteristics which affect the conversion from electrical energy to acoustic energy.

The exploration is performed by various methods – some with mathematical models, some with FEM software and some with experiments. A landscape is drawn to show the conversion from electrical energy to acoustic energy. It can be divided into three layers: conception, design and practical.

6.1.1.1 Conception Layer

The conception layer of this study refers to the study on the literature on the concepts of transducers in energy conversion to understand the mechanism of electro-acoustic transducers. The literature includes the studies on electrical and mechanical characteristics and on wave propagation of the ideal case of spherical source.

The studies on the electro-acoustic conversion of transducer can be divided into two conceptual transducers: electromechanical and acoustic transducers. Electromechanical transducers convert electrical energy into mechanical energy, while the acoustic transducers convert mechanical energy into acoustic energy. The electrical energy is in the form of voltage (v(t)). The mechanical energy can be in the form of external force $f_e(t)$ or movement (w(t)), while the acoustic energy is in the form of acoustic pressure(p(t)) as shown in Figure 6-1. From the figure, the red numbers indicate the section numbers and the green arrows show the paths of investigation.

From the conception layer, as shown in Figure 6-1,

- In Section 2.2.1, 2.2.2.2 and 2.2.2.4, the relationship between voltage and force of three potential enabling technologies for the electromechanical transducers - magnet, moving coil and piezoelectric - for the implementation of ultrasonic transducers was investigated. The parameters of the transducers are electrical characteristics, such as resistance, capacitance and inductance.
- In Section 2.4.2.2, mathematical analysis of wave propagation for an ideal spherical source in steady-state case was summarised. The relationship between vibration of the source in term of velocity $\dot{w}(t)$and its wave propagation according to the mathematical modelling of the acoustic pressure p(t). The investigated parameters are the radius of the source and the amplitude and the frequency of the vibration and the acoustic pressure.
- In Section 2.4.2.4, a mathematical model for the wave propagation in transient-state case or wave propagation of the impulse response was derived. The model for the transient-state case is based on the steady-state case but changes vibrating pattern from a pure sine wave form of $e^{-j\omega t}$to an impulse response wave form of $e^{-t(\delta+j\omega)}$. The investigated parameters are similar to the steady-state case; however it includes the damping ratio.
- Although these parameters do not describe the structure of a speaklet, such as thickness and diameter of a diaphragm of the speaklet, the model can be used to describe the effects of those parameters on the relationship between the voltage, force and acoustic pressure.

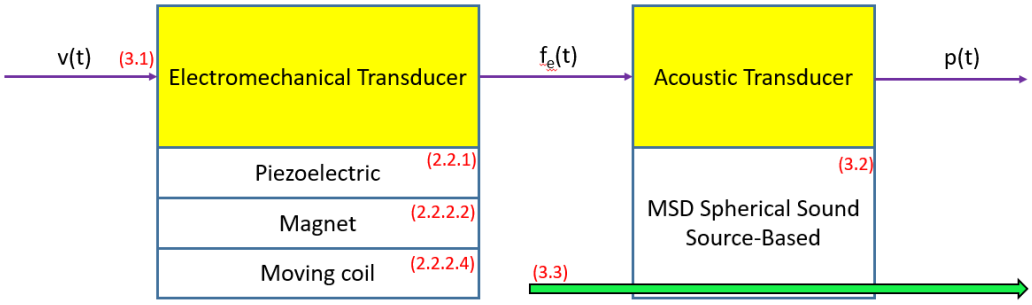

Figure 6-1: Conception layer of speaklets

In Chapter 3, an ideal electro-acoustic transducer is mathematically modelled for a MDLA.

- In Section 3.1, characteristics of electrical signals for driving speaklets were described. The signal is a series of rectangular pulses with different pulse widths but a constant pulse height by using the widths representing levels of sound amplitude. It is referred as a MDLA.

- In Section 3.2, a mathematical model of an ideal rectifying spherical source for a MDLA is mathematically modelled with vibrational parameters of natural frequency and damping ratio. For simplicity, the model assumes the linear relationship between the displacement of the pressure gate and the acoustic pressure traversing across the sound field as the proposed condition as shown in Figure 6-2 The assumption can be applied under two conditions as follows.
    1. The air flow in a pipe between the air outlet and pump is a steady laminar flow;
    2. The vibration of the gate in a valve between the air outlet and pump of the ideal rectifying source, and the propagating wave have high frequencies in an ultrasonic range.
- These conditions will enable speaklets to generate rectified AM sound.
- In Section 3.3, it was found that an ideal MDLA of speaklets generates rectified AM sound which consists of an audible frequency and ultrasonic frequencies. By assumed that speaklets are point sources, sound from the array propagates in all directions while ultrasound forms beam. The simulation in Section 3.3 is computed by the mathematical model from In Section 3.2
- Pressure response of the rectified AM wave contains a non-zero time integral. Hence, the air particles medium vibrates, and moves in direction of propagation. It differs from the air medium of common sound sources in that it vibrates and move from place to place.

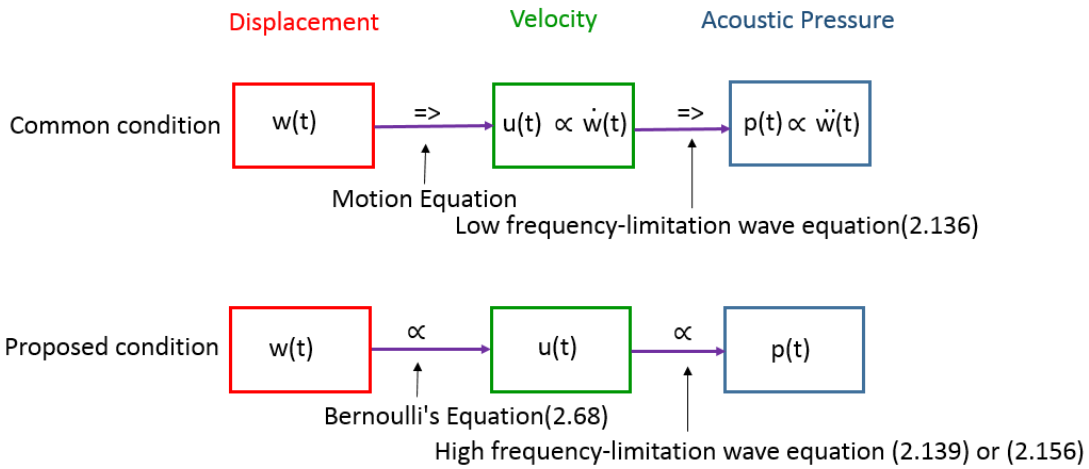

Figure 6-2: Common and proposed conditions of wave propagation

6.1.1.2 Design Layer

The study in design layer aims to investigate a structural model of a real speaklet with comsol, a FEM software. The speaklet as an electro-acoustic transducer is divided into three separated modules: electromechanical, fluid and acoustic; however, this thesis demonstrates only the first

two modules as shown in Figure 6-3. The electromechanical module shows the relationship between pulse voltage and displacement, and the fluid module shows the relationship between the displacement of the moving diaphragm and the velocity of the air particles in front of a rectifying speaklet. In this study, it found as follows:

- Casset, F. & Dejaeger, R. are only one active research group in the area of DLA. Their focus is on the relationship between pulse voltage and displacement.
- In Section 4.2, the effect of diameter and thickness of diaphragm and transducer on displacement and the natural frequency of the speaklet are presented. The thickness of a diaphragm is a key factor in the efficiency. These findings provide an idea for the design of a speaklet with the array.
- In Section 5.1, an FEM model was created by a fluid module for validation of the proposed condition of acoustic rectification only between displacement and velocity. The model was simulated by pre-definition of displacement as a rectified AM form. Although the waveforms of displacement (w(t)) and the velocity (u(t)) are slightly different as the FEM model is based on unsteady state flow while the conception model is based on steady state flow, the frequency components of displacement and velocity are similar.
- Although pressure response is similar to the rectified AM waveform but it has short periods of the negative pressure, its frequency components are similar to the components of the displacement. Phase angle of acoustic impedance causes the negative pressure periods.

Due to the incomplete validation of the condition of acoustic rectification and the structure of the model which uses a vibrating disc, it might not still be ready for the practice. Future work should consist of the realisation of the model by use of the diaphragm rather than a moving disc, and validation of the condition from voltage to acoustic pressure. This means a model of the rectified loudspeaker is composed of three modules:MEMS, microfluidics and acoustics. The detail of the model isdescribed in Section 6.1.2.

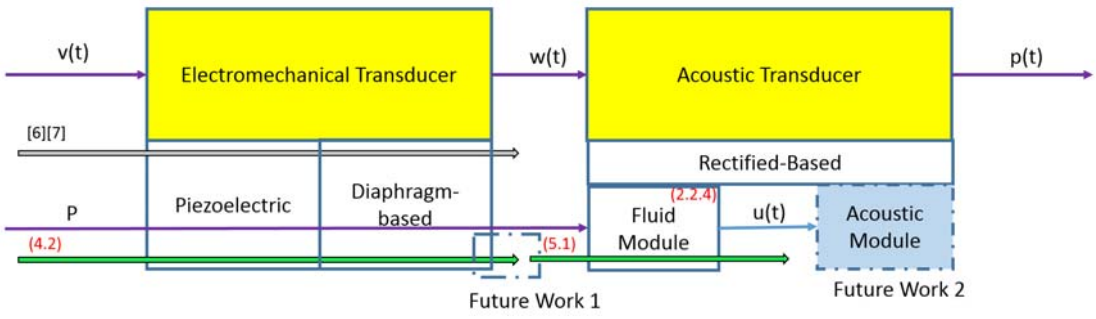

Figure 6-3: Design layer of speaklets

6.1.1.3 Practical Layer

In the practical layer, experiments are set up to validate AM sound generation of electro-acoustic transducer, such as ultrasonic transmitter, magnet and piezoelectric buzzers according to the MDLA concept as shown in Figure 6-4,

- Casset, F. & Dejaeger, R. fabricated a prototype of DLA with 256 speaklets by using MEMs. The diaphragms and transducers of the speaklets were produced from polysilicon and piezo-composite, respectively. The array can reproduce sound levels of 100 dB at 10cm from the speaklets. They focus on efficiency of their DLA
- From experiments in Section 4.1.2 and 4.1.3, it was found that acoustic pressure of the real transducers cannot satisfy the requirements of the digital sound reconstruction as demonstrated in Section 2.3.3. The relationship between the pulse widths of electrical pulses feeding into the transducers and their amplitude of acoustic pressure is linear. This satisfies the third requirement while the response time to an electrical pulse driving the real transducers do not meet the first requirement.
- From Section 4.1.4, the acoustic responses of real electroacoustic sources which represents speaklets within a MDLA are in the form of a full-wave AM acoustic signal. This is similar to that generated by a parametric array. However, Magnitudes in some frequencies are small and not stable, depending on the frequency response of the speaklets. The AM responses require high intensity of acoustic pressure for the sound in a range of audible frequencies.
- MDLA enables small transducers or loudspeaker to reproduce low frequency sound more efficient than high frequency sound.

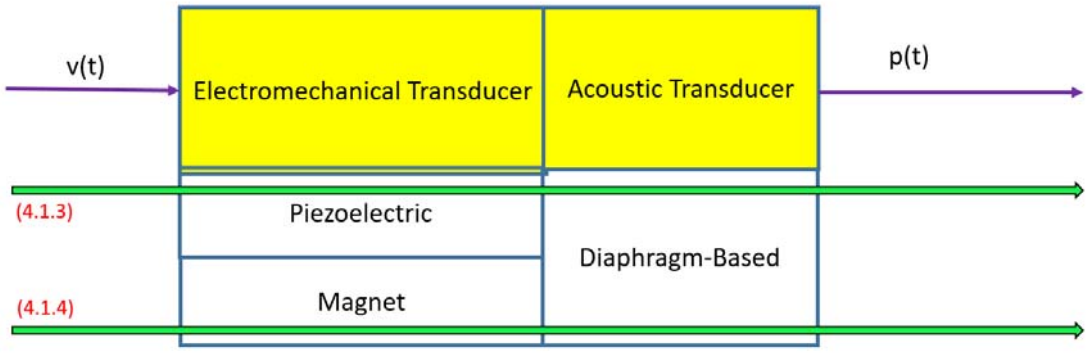

Figure 6-4: Practical layer of speaklets

6.1.2 Difference between DLA and Traditional Loudspeakers

This section distinguishes between a DLA and an analogue loudspeaker array, according to the characteristics in Table 6-1.

Table 6-1: A summary of differences between a DLA and a normal analogue array

Aspects	DLA	Analogue Loudspeaker Array
Electrical drive	Discrete signal	Continual signal
Wave propagation	Transient-state	Steady state
Working frequency	A resonant frequency	Avoidance of Resonant frequencies
Sound resolution	Resolution dependant on number of speaklets	Resolution dependant on resolution of ADC
Electrical circuit size	A switching circuit	ADC and analogue amplifier
Sound generation	Sound carried by ultrasound	Sound carried by itself
Frequency Response	Right triangular narrow band	Rectangular wide band
Attenuation	High	Low

The nature of drive in speaklets with digital or analogue signals are clearly different. The speaklet in a DLA is fed with a constant-voltage discrete signal. A DLA works at unsteady state or transient state. Owing to the necessity to drive with the discrete signals, the diaphragm of the speaklet vibrates freely at its natural frequency. In other words, the DLA works at the resonant frequency, which causes sound distortion in analogue loudspeakers. With a concept of MDLA, the resolution of audio of a speaklet depends on the clock speed of the pulse generation, and the range of linearity between the pulse width and amplitude of ultrasonic wave. The increase in resolution of a DLA depends on the number of speaklets, because the speaklets reproduce sound differently and independently, while the resolution of an analogue loudspeaker array does not increase because all speaklets in the array generate the same sound. The resolution of the system will depend on the resolution of the digital to analogue convertor (DAC). Amplification of digital signals is simple and the circuit is small because it is a switching circuit, the main component of which is a single transistor. In contrast to analogue application, the size of circuit of the DAC and the analogue amplifier is hundreds time larger than the digital amplifier. DLAs apply sound generation from ultrasound. In other words, a DLA generates ultrasound to carry a sound by modulation. Common ultrasonic transducers such as speaklets have a narrow bandwidth and a

triangular shape of frequency response. Due to the shape and the modulation, the shape of audible frequency response of the speaklets is a right triangle, which means that they can respond at low frequencies better than at high frequencies. The attenuation of sound depends on its frequency. Low frequencies of sound traverse the air further than high frequencies of sound or ultrasonic, because of their attenuation. Although the sound of a DLA might require more intensity due to high attenuation, the high attenuation enables a DLA to control the boundary of sound. This means the sound of a DLA traverses on the air a shorter distance than normal sound. This will protect sound disturbance from outside the target-listening area. However, this phenomenon remains to be demonstrated in further studies because it requires the measurement of sound generation of a prototype of a rectifying loudspeaker

6.2 Future Works

In addition to design of the rectifying loudspeaker, other topics are interested such as development of mathematical model and experiments about hazard of the AM sound.

6.2.1 Intellectual Challenge of Design

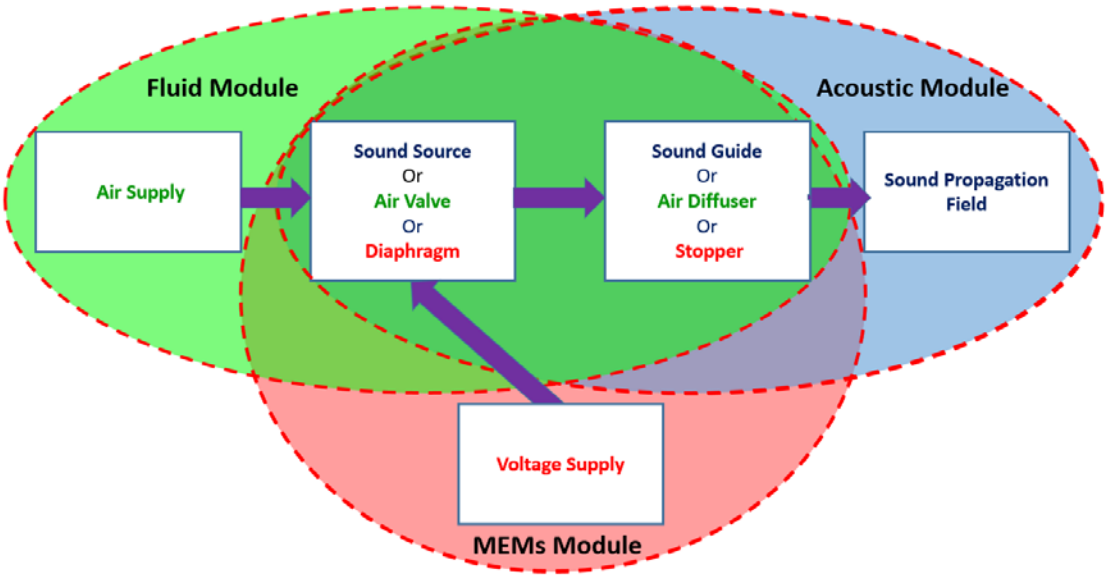

Figure 6-5: Perspectives of design of a rectifying loudspeaker.

The design of a rectifying loudspeaker involves the three different disciplinary sciences of MEMs, microfluidics and acoustics. Not only are these disciplines closely related in the design, as shown in Figure 6-5, but also the design requires advanced knowledge in these fields. This knowledge includes the unsteady state of microfluidics of compressible flows in fluid modules, the vibration of a diaphragm with obstruction, as a collision causes a partial loss of kinetic energy in MEMs

modules, and propagation of the rectified AM sound in acoustic modules in a waveguide. These areas of knowledge have not yet been researched in this thesis, especially the area of microfluidics.

The complexity of the loudspeaker increases when air pressure supply is introduced into it. A diaphragm of the loudspeaker is not directly used for a sound generation. When the diaphragm is vibrated by a transducer, its movement allows air flow from the air supply to the atmosphere through the diaphragm and a diffuser. While the air flow is moving through the diaphragm it induces a life force, which interacts with the vibration of the diaphragm. The vibration of the diaphragm is not independent, but the diaphragm and the surface of the base of the diffuser collide as a stopper in every cycle of the vibration.

As for the air flow, the velocity of the flow depends on pressure of the air supply, while the volume of the flow-out causes reduction in the pressure supply. Therefore, the mechanism of maintenance of pressure is important, because pressure has a direct effect on the acoustic pressure. If it is impossible to maintain the pressure, how it would affect sound or hearing is a further study.

In addition, the angle of the diffusor of the air flow causes differences in pressure and velocity between the neck and the opening, as shown in Figure 6-6d and e. The characteristics of the flow in the diffuser as a sound guide results in sound generation and sound propagation. This requires further study on the coherence between the air flow and sound field within the diffuser.

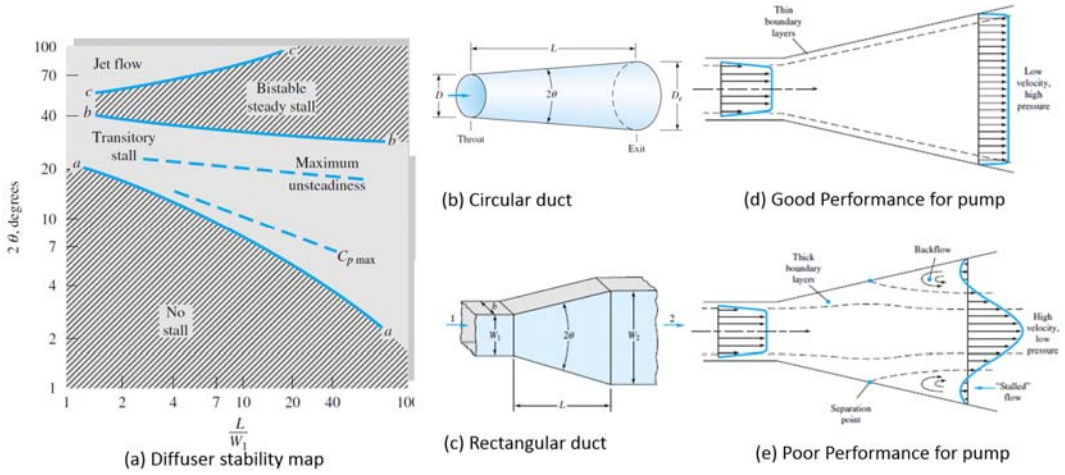

Figure 6-6: Performance of diffuser after White, F. [44]

Figure 6-6 d and e illustrate characteristics of the flow within the diffuser comparing good and poor performance of the diffuser, which is affected by the ratio between the angle of a diffuser and the proportion of the length to the width of diffuser. This is shown in the diagram (a), where

W in the diagram can represent the width of a rectangular duct or the diameter of the circular duct.

6.2.2 Realization of Mathematical Model

Since the purpose of the mathematical model is to understand the mechanism of sound generation from ultrasound of a DLA, especially frequencies of the generated sound, the model is simplified by ignoring some parameters relating to the amplitude of the wave. The wave equation in the model is Eq.(2.156), which is an estimated equation, for simplification.

In order to develop the mathematical model for estimation, further work would realize the model of a speaklet by using Eq.(2.153) which reflects the real wave propagation more than Eq. (2.156). Furthermore, the model starts from the mechanical force to the acoustic pressure. In order to realize it, the model should start from the input voltage. The literature provides the mathematical relation between the force and voltage, such as piezoelectric and magnet speaklets, as described in Chapter2.2.

In the ideal case, the speaklets in the array are also linearly aligned, while the array will be square in the practical implementation. In addition, studies on the effect of the interspacing of array to AM sound is useful to design of DLA. These topics are of interest because they will give ideas regarding sound beam form before FEM and implementation.

6.2.3 Ear Canal as a Biological Acoustic Low Pass Filter

Although ultrasound is widely used for radars, and industrial and medical detectors and cleaners, sound generation from ultrasound as a loudspeaker such as with Audio Spotlight is very limited because people are not familiar with it, and are scared of the danger of ultrasonic exposure. However, a high intensity of ultrasound will not damage health through the skin, even sensitive skin, because of a huge difference of acoustic impedance between the air and the tissue. On the other hand, the effect of pressure on the eardrums as biological pressure sensors is ambiguous, as described in 2.1.4.2 .

Should this ambiguity lead to further study, the characterization of acoustic waves at the eardrums would be of interest. Consideration of an ear canal as an acoustic low pass filter would be beneficial to the design of rectifying loudspeakers, for deciding on bandwidth and the intensity of ultrasound.

A precise idea of the configuration of the experiments is shown in Figure 6-7. AM sound will transmit to a human model using a microphone with a frequency response of 20 to 100 kHz

inside. The characteristics of acoustic waves at the eardrum can be analysed though the acoustic signal of the microphone.

It is hypothesised that if the acoustic wave of AM sound at the eardrum is similar to normal sound, which would mean that the ear canal functions as an acoustic low-pass filter, then AM sound would be no hazard for human ears.

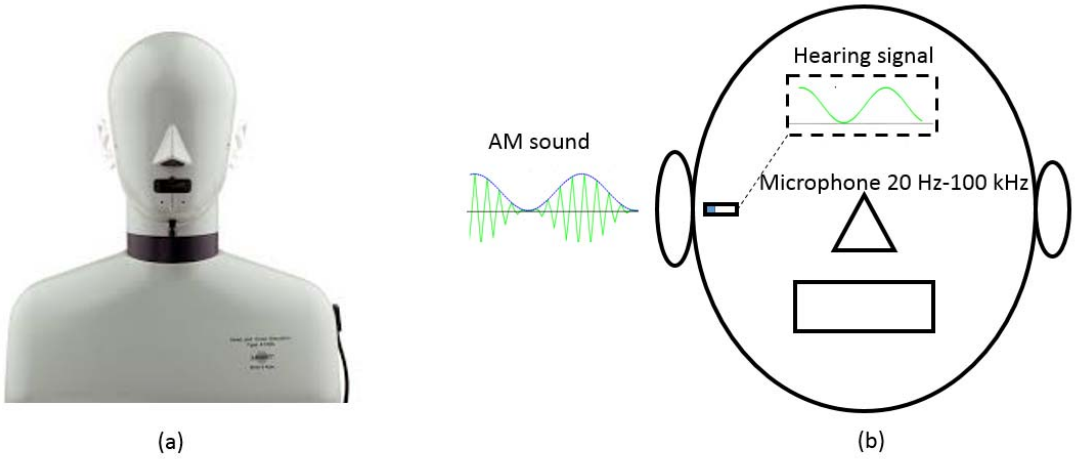

Figure 6-7: a) Head and Torso Simulator b) Positive scenarios of the hypothesis.

Appendices

Appendix A

Table A-1: Attenuation in dB/km of sound in the air[56]

Frequency	Relatively Humidity (%)								
(kHz)	10	20	30	40	50	60	70	80	90
1	14	6.5	5	4.7	4.7	4.8	5	5.1	5.3
2	45	22	14	11	9.9	9.3	9	9	9.1
4	110	75	49	36	30	26	23	21	20
5	130	110	74	55	44	38	33	31	28
10	190	280	240	190	160	130	120	100	95
20	260	510	600	580	520	470	420	380	350
31.5	360	670	890	990	1000	960	900	840	790
40	460	780	1100	1200	1300	1300	1300	1200	1200
50	600	940	1300	1500	1700	1700	1700	1700	1700
63	840	1200	1500	1800	2100	2200	2300	2300	2300
80	1200	1600	2000	2300	2600	2800	3000	3100	3100
100	1800	2200	2500	2900	3300	3600	3800	4000	4100

Appendix B

Table B-1: Frequency response of the A and AU weighting [24]

One-third octave band centre frequency (Hz)	A-weighing(dB)	AU weighing(dB)
20	-50.5	-50.5
25	-44.7	-44.7
31.5	-39.4	-39.4
40	-34.6	-34.6
50	-30.2	-30.2
63	-26.2	-26.2
80	-22.5	-22.5
100	-19.1	-19.1
125	-16.1	-16.1
160	-13.4	-13.4
200	-10.9	-10.9
250	-8.6	-8.6
315	-6.6	-6.6
400	-4.8	-4.8
500	-3.2	-3.2
630	-1.9	-1.9
800	-0.8	-0.8
1,000	0	0
1,250	+0.6	+0.6

Appendix B

One-third octave band centre frequency (Hz)	A-weighing(dB)	AU weighing(dB)
1,600	+1.0	+1.0
2,000	+1.2	+1.2
2,500	+1.3	+1.3
3,150	+1.2	+1.2
4,000	+1.0	+1.0
5,000	+0.5	+0.5
6,300	-0.1	-0.1
8,000	-1.1	-1.1
10,000	-2.5	-2.5
12,500	-4.3	-7.1
16,000	-6.6	-19.6
20,000	-9.3	-34.6
25,000	-	-50.0
31,500	-	-65.4
40,000	-	-81.1

Glossary of Terms

ADPCM	Adaptive differential pulse code modulation
AM	Amplitude modulation
AMPs	Digital audio amplifiers
ASICs	Application-specific integrated circuit system
DAC	Digital to analogue convertor
dB	Decibel
dBA	A-weighted decibels
dBSPL	Sound pressure level in decibel
DLA	Digital loudspeaker array
DSP	Digital signal processing
DTA	Digital transducer array
FEM	Finite element method
FFT	Fast fourier transform
FIR	Finite impulse response
FPGA	Field-programmable gate array
Hz	Hertz
IC	Integrated circuit
KCL	Kurchhoff's current law
LA	Loudspeaker array
LRAD	Long-range acoustic device
MDLA	Multiple-level digital loudspeaker array
MEMs	Microelectromechanical system
MP3	Moving picture expert group 1or 2 audio layer 3
MSD	Mass-spring dumper

NDFEB	Neodymium
Pa	Pascal
PCM	Pulse code modulation
PDMS	Polydimetylsiloxane
PMP	The parallel multimorph in parallel connection
PWM	Pulse width modulation
PZT	Lead zirconate titanate
SDM	Sigma-delta modulation
SLL	Sound loudness level
SMS	The serial multimorph in serial connection
SPL	Sound pressure level

List of References

[1] B. M. Diamond, J. J. Neumann, and K. J. Gabriel, “Digital Sound Reconstruction Using Arrays of CMOS-MEMS Microspeakers,” in *Fifteenth IEEE International Conference on Micro Electro Mechanical Systems*, 2002, no. 412, pp. 292–295.

[2] S. C. Busbridge, P. A. Fryer, and Y. Huang, “Digital Loudspeaker Technology: Current State and Future Developments,” in *AES 118th Convertion*, 2002.

[3] M. Klasco, “MEMS Microspeakers Are Truly Digital Transducers,” *audioxpress*, 2016. [Online]. Available: http://www.audioxpress.com/article/MEMS-Microspeakers-Are-Truly-Digital-Transducers.

[4] Yole, “Silicon speakers are ready for volume production,” *I-Micronews*, 2016. [Online]. Available: http://www.i-micronews.com/mems-sensors/7563-silicon-speakers-are-ready-for-volume-production-2.html. [Accessed: 15-Dec-2016].

[5] F. W. Kremkau, *Diagnostic Ultrasound: Principles and Instrument*, 6th ed. W.B. SAUNDERS COMPANY, 2006.

[6] R. Dejaeger, F. Casset, B. Desloges, G. Le Rhun, P. Robert, S. Fanget, Q. Leclère, K. Ege, and J.-L. Guyader, “Development and Characterization of a Piezoelectrically Actuated MEMS Digital Loudspeaker,” *Procedia Eng.*, vol. 47, pp. 184–187, Jan. 2012.

[7] F. Casset, R. Dejaeger, B. Laroche, B. Desloges, Q. Leclere, R. Morisson, Y. Bohard, J. P. Goglio, J. Escato, and S. Fanget, “A 256 MEMS Membrane Digital Loudspeaker Array Based on PZT Actuators,” *Procedia Eng.*, vol. 120, pp. 49–52, 2015.

[8] F. J. Pompei, “Sound From Ultrasound: The Parametric Array as an Audible Sound Source,” pp. 1–132, 2002.

[9] J. Croft, James and J. O. Norris, “Theory, History, and the Advancement of Parametric Loudspeakers,” 2003.

[10] N. A. Tatlas and J. Mourjopoulos, “Digital Loudspeaker Arrays driven by 1-bit signals,” in *Audio Eng. Soc.116th Convention*, 2004.

[11] Y. Cohen, “Digital Loudspeakers,” *audiopixels.*, 2011. [Online]. Available: http://www.audiopixels.com.au/index.cfm/news/videos/digital-loudspeakers-video/.

[12] P. Valoušek, “A Digital Loudspeaker : Experimental Construction,” vol. 46, no. 4, 2006.

[13] N. Tatlas, A. E. S. A. Member, and F. Kontomichos, “Design and Performance of a Sigma – Delta Digital Loudspeaker Array Prototype *,” vol. 57, no. 1, 2009.

[14] J. D. Turner and A. J. Pretlove, *Acoustics of Engineering*, 2nd ed. Macmillan Education LTD, 1991.

[15] E. F. Alton and K. C. Pohlmann, *Master Handbook of Acoustics*, 6th ed. 2015.

[16] Benade H. Arthur, *Fundamentals of Musical Acoustics*. 1976.

[17] W. M. Rubio, F. Buiochi, J. C. Adamowski, and E. C. N. Silva, “Modeling of functionally graded piezoelectric ultrasonic transducers,” *Ultrasonics*, vol. 49, no. 4–5, pp. 484–494, 2009.

[18] C. T. Crowe, D. F. Elger, B. C. Williams, and J. A. Roberson, *Engineering Fluid Mechanics*, 9th ed. John Willey & Sons, 2010.

[19] L. E. Kinsler, A. R. Frey, A. B. Coppens, and J. V Sanders, “Fundamentals of acoustics,” *Fundamentals of Acoustics, 4th Edition, by Lawrence E. Kinsler, Austin R. Frey, Alan B. Coppens, James V. Sanders, pp. 560. ISBN 0-471-84789-5. Wiley-VCH, December 1999.*, vol. 1. p. 560, 1999.

[20] S. A. Gelfand, *Hearing: An Introduction to Psychological and Physiological Acoustics*, 4th ed. Marcel Dekker, 2004.

[21] O. NDT, “Ultrasonic Transducers Technical Notes,” 2006.

[22] A. Vladišauskas, “Directivity characteristics of ultrasonic transducers for flow measurements,” *ULTRAGRASAS*, vol. 2, no. 2, pp. 2–5, 2001.

[23] S. A. Gelfand, *Hearing: An Introduction to Psychological and Physiological Acoustics*, 4th ed. Marcel Dekker, 2004.

[24] U. of S. B.W. Lawton (Institute of Sound and Vibration Research, “Damage to human hearing by airborne sound of very high frequency or ultrasonic frequency,” p. 86, 2001.

[25] C. H. Hansen, “Fundamentals of Acoustics,” in *Occupational exposure to noise: Evaluation, prevention and control*, 1994, pp. 23–52.

[26] H. Kuttruff, *Ultrasonics:Fundamentals and Applications*. Springer Netherlands, 1991.

[27] H. J. Kim, W. S. Yang, and K. S. No, “The vibrational characteristics of the triple-layered multimorph ceramics for high performance piezoelectric acoustic actuators,” *J.*

Electroceramics, May 2014.

[28] T. Bakke, A. Vogl, O. Żero, F. Tyholdt, I.-R. Johansen, and D. Wang, "A novel ultra-planar, long-stroke and low-voltage piezoelectric micromirror," *J. Micromechanics Microengineering*, vol. 20, no. 6, p. 64010, Jun. 2010.

[29] K. Uchino, "Introduction to Piezoelectric Actuators and Transducers," 2003.

[30] P. Gaucher, "Piezoelectric Micro-electro-mechanical Systems for Acoustic Applications."

[31] I. Henderson, *Piezoelectricx Ceramics: Principle and Application*, 2nd ed. APC International, Ltd, 2011.

[32] S. Senthilkumar and R. Vinothraj, "Design and study of ultrasound-based automatic patient movement monitoring device for quantifying the intrafraction motion during teletherapy treatment.," *J. Appl. Clin. Med. Phys.*, vol. 13, no. 6, p. 3709, 2012.

[33] E. O. Doebelin, *Measurement Systems Application and Design*, 4th ed. McGraw-Hill, 1990.

[34] F. A. E., C. J. Kingsley, and S. D. Uman, *Electric Machinery*. McGraw-Hill, 2003.

[35] C. Weber, Y. C. Chen, and Y. T. Cheng, "The Study of the Inductive Coil to the Acoustic Performance of Electromagnetic Driven Microspeaker," in *Eurosensors 2014 Conference Preceeding*, 2014, vol. 0, pp. 1–4.

[36] J. Chernof, "Principles of loudspeaker design and operation," *IRE Trans. Audio*, vol. 5, no. 5, pp. 117–127, 1957.

[37] P. J. Westervelt, "Parametric Acoustic Array," *Acoust. Soc. Am.*, vol. 35, no. 4, pp. 535–537, 1963.

[38] P. F. Joseph, "The Use of Airborne Ultrasonics for Generating Audible Sound Beam," *J. Audio Eng.*, vol. 47, no. 9, pp. 726–731, 1999.

[39] T. Wen-Kung, "Beam Width Control for a Dicectional Audible Sound System," *Int. J. Innov. Control*, vol. 9, no. 7, pp. 3061–3078, 2013.

[40] M. Yoneyama and J. Fujimoto, "The audio spotlight: An application of nonlinear interaction of Sound waves to a new type of loudspeaker design," *Audio*, vol. 73, no. May, pp. 1532–1536, 1983.

[41] T. Kamakura and K. Aoki, "A Highly Directional Audio System Using A Parametric Array In Air," *9th West. Pacific Acoust. Conf.*, vol. 0, 2006.

[42] C. Woodford, “Directional loudspeakers,” *explainthatstuff*, 2016. [Online]. Available: http://www.explainthatstuff.com/directional-loudspeakers.html.

[43] J. A. Thomas, C. F. Moss, and M. Vater, Eds., *Echolocation in Bats and Dolphins*. Saunder College, 2004.

[44] F. M. White, “Fluid Mechanics,” *McGraw-Hill*, p. 1024, 2009.

[45] B. M. Diamond, “Digital Sound Reconstruction Using Arrays of SMOD-MEMS Microspeakers,” 2002.

[46] F. Cohen, D. Lewin, S. Kaplan, A. Sromin, and B. Simon, “IMPROVED SPEAKER APPARATUS AND METHODS USEFUL IN CONJUNCTION THEREWITH.,” WO200966290A2, 2009.

[47] J. Mendoza-López, S. C. Busbridge, and P. A. Fryer, “Sound Field Characterisation in Audio Reproduction with the Bit-Grouped Digital,Transducer Array,” in *the 120th AES Convention*, 2009.

[48] M. O. J. Hawksford, “Smart Digital Loudspeaker Arrays,” in *110th Convention of the Audio-Engineering-Society*, 2003, vol. 51, no. 12, pp. 1133–1162.

[49] G. Ballou, *Electroacoustic Devices: Microphones and Loudspeakers*. Elsevier, 2009.

[50] G. Takács and B. Rohaľ-Ilkiv, *Model Predictive Vibration Control*. Springer, 2012.

[51] M. C. Junger and D. Feit, *Sound, Structures and Their Interaction*, 2nd ed. The MIT Press, 1972.

[52] N. R. Harris, M. Hill, N. M. White, and S. P. Beeby., “Acoustic power output measurements for thick-film PZT transducers,” *Electron. Lett.*, vol. 40, no. 10, pp. 636–637, 2004.

[53] P. J. Pritchard, *Fluid Machanics*, 8th ed. Wiley, 2012.

[54] N. OzKaya and Nordin Margareta, *Fundamentatals of Biomechanics, Equalibrium, Motion and deformation*, 2nd ed. Springer-Verlag New York Berlin Heidelberg, 1998.

[55] M. Richter, R. Linnemann, and P. Woias, “Robust design of gas and liquid micropumps,” *Sensors Actuators, A Phys.*, vol. 68, no. 1–3 pt 2, pp. 480–486, 1998.

[56] G. W. C. Kaye and T. H. Laby, “The speed and attenuation of sound,” *Natianal Physiccal Laboratory*, 1995. [Online]. Available: http://www.kayelaby.npl.co.uk/general_physics/2_4/2_4_1.html#speed_of_sound_in_air. [Accessed: 28-Jul-2016].